

# **Hydroxylamine-based inhibitors of auto-initiated styrene polymerization**

**Chiara Baldassarri**

PhD

University of York

Chemistry

September 2014

## Abstract

The object of this thesis was to investigate the inhibition mechanism of *N,N*-dibenzylhydroxylamine (DBHA) and 2,5-di-*tert*-butyl-1,4-benzoquinone (2,5-DTBBQ) mixture towards auto-initiated styrene polymerisation. This non-toxic composition represents a valid alternative to the quite efficient, but harmful 2,4-di-nitro-6-*sec*-butyl phenol.

A dilatometry study revealed that DBHA/2,5-DTBBQ mixture shows synergism, therefore in order to decipher its mechanism of inhibition, the inhibitors were first investigated individually and then together.

DBHA is a good inhibitor only in oxygenated systems. The main mechanism of inhibition of DBHA is the quenching of peroxy radicals at the end of the propagating chains by hydrogen abstraction. In the presence of oxygen *N,N*-dibenzyl nitroxide also contributes to the inhibition to some extent.

During the inhibition of styrene with DBHA/2,5-DTBBQ, 2,5-DTBBQ is reduced to 2,5-di-*tert*-butyl-hydroquinone (2,5-DTBHQ). Dilatometry study revealed that the 2,5-DTBHQ/2,5-DTBBQ mixture shows a limited retardation towards the styrene polymerisation. The ability of these compounds to stop propagation radicals by addition reactions was ruled out, since no addition products were detected.

Product analysis of the inhibition of styrene polymerization in the presence of DBHA and 2,5-DTBBQ allowed the detection of a few compounds, which were tested by dilatometry either singularly or as a mixture. This approach provides a way to rule out several molecules as responsible for the synergism of DBHA-2,5-DTBBQ. *N,N*-Dibenzyl nitroxide is formed during the inhibition, and a combination of dilatometry and EPR analyses revealed a correlation between its concentration in the mixture and inhibition time. *N,N*-Dibenzyl nitroxide is likely to be involved in the inhibition but not in the retardation. UV-Vis study confirmed that DBHA and 2,5-DTBBQ form a charge transfer complex, and its role in the inhibition and retardation cannot be excluded.

# Table of Contents

<b>Abstract.....</b>	<b>2</b>
<b>List of Figures .....</b>	<b>8</b>
<b>Acknowledgements .....</b>	<b>16</b>
<b>Declaration.....</b>	<b>17</b>
<b>1 Introduction.....</b>	<b>18</b>
1.1 Styrene.....	18
1.2 Mechanism of radical polymerisation .....	18
1.3 Auto-initiated styrene polymerisation .....	20
1.4 Inhibitors of polymerisation .....	22
1.4.1 Addition reaction .....	22
1.4.2 Hydrogen abstraction.....	24
1.4.3 Redox reaction .....	26
1.5 Inhibitors vs retarders .....	27
1.6 Synergistic effect .....	28
1.6.1 Restrictions about the use of nitrophenol compounds.....	30
1.7 Aim of the project.....	32
<b>2 N,N-Dibenzylhydroxylamine as an inhibitor of styrene polymerization.....</b>	<b>33</b>
2.1 Introduction.....	33
2.1.1 Background .....	33
2.1.2 Aim of the chapter .....	39
2.2 Inhibition efficiency of N,N-dibenzylhydroxylamine in the thermally initiated styrene polymerisation .....	40
2.2.1 Dilatometry .....	40
2.2.2 Results .....	41
2.3 N,N-Dibenzylnitroxide as inhibitor .....	44
2.3.1 Monitoring N,N-dibenzylnitroxide and oxygen evolution by EPR .....	44
2.3.2 Oxidation of N,N-dibenzylhydroxylamine by oxygen .....	52

2.3.3	N,N-DibenzylNitroxide as a radical trap .....	56
2.4	Conclusions.....	65
<b>3</b>	<b>2,5-Di-tert-butyl-hydroquinone as an inhibitor of the auto-initiated styrene polymerisation .....</b>	<b>67</b>
3.1	Introduction.....	67
3.1.1	Background .....	67
3.1.2	Aim of the chapter .....	73
3.2	Investigation of the antioxidant properties of 2,5-DTBHQ.....	74
3.3	Investigation of the inhibition properties of 2,5-DTBBQ .....	76
3.4	Reactivity of 2,5-di-tert-butyl-1,4-benzoquinone towards alkyl radicals .....	77
3.4.1	Reactivity of 2,6-di-tert-butyl-1,4-benzoquinone.....	81
3.5	Investigation of the reactivity of 2,5-di-tert-butyl-hydroquinone .....	84
3.6	Conclusions.....	90
<b>4</b>	<b>2,5-Di-tert-butyl-1,4-benzoquinone and N,N-dibenzylhydroxylamine: reaction in a non-polymerizable solvent.....</b>	<b>91</b>
4.1	Introduction.....	91
4.1.1	Background .....	91
4.1.2	Aim of the chapter .....	94
4.2	Investigation of charge transfer complexes.....	94
4.3	Investigation of N,N-dibenzylNitroxide formation by EPR spectroscopy .....	96
4.4	Investigation of intermediates and products by NMR spectroscopy.....	97
4.4.1	Reaction order and rate constant .....	97
4.4.2	Substituents effect .....	105
4.5	Reaction mechanism .....	109
4.6	Conclusions.....	111
4.7.....		91
<b>5</b>	<b>Products analysis of inhibition of the styrene polymerisation by DBHA/2,5-DTBBQ mixture.....</b>	<b>112</b>

5.1	Introduction.....	112
5.1.1	Background .....	112
5.1.2	Aim of the chapter .....	115
5.2	Investigation on a milligram-scale.....	115
5.2.1	Analysis of the styrene polymerisation inhibited by DBHA/2,5-DTBBQ.....	115
5.2.2	Products analysis in a non-polymerizable solvent.....	126
5.3	Investigation of the inhibition products in reactions carried out on a large scale	128
5.3.1	DBHA/2,5-DTBBQ mixture .....	128
5.3.2	Product analysis in the presence of either DBHA or N,N-benzylidenebenzylamine-N-oxide.....	148
5.3.3	Investigation of fluorine containing compounds.....	150
5.4	Conclusions.....	161
<b>6</b>	<b>A new inhibitor composition for the auto-initiated styrene polymerisation....</b>	<b>162</b>
6.1	Aim of the chapter.....	162
6.2	Inhibition efficiency of the DBHA/2,5-DTBBQ mixture .....	162
6.3	Concentrations monitoring by gas chromatography .....	164
6.4	Role of N,N-dibenzyl nitroxide in the inhibition mechanism.....	166
6.4.1	N,N-Dibenzyl nitroxide formation in the presence of DBHA and 2,5-DTBBQ/DBHA .....	166
6.4.2	Electronic effect of substituents in dibenzylhydroxylamines .....	169
6.4.3	Steric effect of substituents in dibenzylhydroxylamines .....	172
6.4.4	Varying reactants concentration.....	178
6.5	Other potential inhibitors of styrene polymerisation.....	182
6.5.1	N,N-Benzylidenebenzylamine-N-oxide .....	182
6.5.2	Isoxazolidine and isoxazoline .....	184
6.5.3	Mixture of N,N-benzylidenebenzylamine-N-oxide and 2,5-DTBHQ .....	185
6.6	Mechanism of inhibition .....	187
6.7	Conclusions.....	193

<b>7</b>	<b>General conclusion and future work .....</b>	<b>195</b>
<b>8</b>	<b>Experimental.....</b>	<b>198</b>
8.1	General materials and methodology.....	198
8.2	General procedure of EPR experiments .....	199
8.2.1	Sample preparation.....	199
8.2.2	Processing EPR data .....	200
8.3	General procedure of dilatometry experiments .....	201
8.3.1	Sample preparation.....	201
8.3.2	Processing data .....	202
8.4	General procedure of NMR experiments .....	203
8.4.1	Sample preparation.....	203
8.4.2	Processing NMR data .....	203
8.5	General procedures of gas chromatography and gas chromatography-mass spectrometry experiments.....	204
8.5.1	Qualitative analysis .....	204
8.5.2	Quantitative analysis.....	204
8.6	Procedure of IR experiment .....	205
8.7	Investigation of the reactivity of 2,5-DTBBQ and 2,5-DTBHQ (chapter 3).....	205
8.7.1	Reactivity of 2,5-DTBBQ in the presence of AIBN (Section 3.4) .....	205
8.7.2	Reactivity of 2,6-DTBBQ in the presence of AIBN.....	206
8.8	Charge transfer complex investigation (chapter 4).....	206
8.9	Reactions on a large scale .....	206
8.9.1	DBHA/2,5-DTBBQ mixture (Section 5.3.1) .....	206
8.9.2	DBHA (Section 5.3.2.1).....	207
8.9.3	N,N-Benzylidenebenzylamine-N-oxide (Section 5.3.2.2).....	207
8.9.4	Procedure of fluorine-containing compounds (Section 5.3.3) .....	208
8.10	Synthetic procedures .....	208
8.10.1	N,N-Dibenzylnitroxide generation (Chapter 2) .....	208

8.10.2	Synthesis of benzisoxazolidine.....	209
8.10.3	Synthesis of substituted hydroxylamines .....	209
8.10.4	Attempts to the synthesis of three rings hydroxylamine .....	214
8.10.5	Synthesis of three rings nitron (12) and its precursors.....	216
8.10.6	Synthesis of N-(1,2-diphenylpropyl)-N-[(Z)-phenylmethylidene]amine oxide	220
8.10.7	Synthesis of inhibition products.....	221
<b>List of abbreviations .....</b>		<b>226</b>
<b>References .....</b>		<b>228</b>

## List of Figures

Figure 1.1 Styrene synthesis .....	18
Figure 1.2 Second order initiation mechanisms .....	20
Figure 1.3 Flory mechanism .....	21
Figure 1.4 Mayo mechanism .....	21
Figure 1.5 Inhibition mechanism of nitrosobenzene .....	23
Figure 1.6 Mechanism of inhibition of TEMPO .....	23
Figure 1.7 Mechanism of inhibition of MEHQ .....	25
Figure 1.8 Inhibition mechanism of acrylic acid by PTZ .....	26
Figure 1.9 Difference between retardation and inhibition effect .....	27
Figure 1.10 Mechanism of action of nitrobenzene.....	28
Figure 1.11 Structure of 2,6-di-tert-butyl-substituted (19) and diphenylamine (20).....	29
Figure 1.12 Inhibition .....	31
Figure 2.1 Dilatometer .....	41
Figure 2.2 Dilatometry traces for the inhibition of the auto-initiated styrene polymerisation by DBHA .....	41
Figure 2.3 Enlargement of the chart in Figure 2.2 .....	42
Figure 2.4 Non-linear relationship between the inhibition time and DBHA concentration.....	43
Figure 2.5 Zeeman effect .....	46
Figure 2.6 EPR experiment.....	47
Figure 2.7 EPR spectrum of TEMPO .....	48
Figure 2.8 Hyperfine splitting of $^1\text{H}$ .....	48
Figure 2.9 EPR spectrum of N,N-dibenzyl nitroxide.....	50
Figure 2.10 Evolution of N,N-dibenzyl nitroxide and oxygen concentrations in 2000 ppm DBHA in styrene at 110 °C.....	51
Figure 2.11 Evolution of nitroxide concentration for a 3000 ppm DBHA in diphenyl ether under nitrogen and air atmosphere .....	53
Figure 2.12 Oxidation mechanism of DBHA.....	53
Figure 2.13 Nitroxide evolution during the oxidation of 3000 ppm DBHA in DPE at 110 °C .....	54



Figure 2.14 Simulation of the consumption of 3000 ppm DBHA in DPE at 110 °C by molecular oxygen .....	54
Figure 2.15 Nitroxide evolution in 3000 ppm DBHA in styrene and 2000 ppm DBHA in diphenyl ether .....	55
Figure 2.16 Examples of stable nitroxides with a hydrogen atom on the carbon $\alpha$ to the nitrogen atom .....	57
Figure 2.17 N,N-dibenzyl nitroxide decay at 25 °C, generated by the oxidation of 3000 ppm DBHA at 110 °C. ....	59
Figure 2.18 Simulation of the N,N-dibenzyl nitroxide decay using the rate constant reported by Ingold, 41000 M <sup>-1</sup> s <sup>-1</sup> . ....	60
Figure 2.19 Formation of the alkoxyamine 11 from the reaction between N,N-dibenzyl nitroxide (2) and styrene radical (10) .....	64
Figure 3.1 Possible reactions of 2,5-di-tert-butyl-hydroquinone .....	68
Figure 3.2 Possible reactions of 2,5-di-tert-butyl-1,4-benzoquinone.....	70
Figure 3.3 Reversible redox equilibrium between 2,5-DTBBQ and 2,5-DTBHQ .....	72
Figure 3.4 Reaction pathway of 2,5-di-tert-butyl-1,4-benzoquinone .....	72
Figure 3.5 Dilatometry trace for the inhibition of the thermal styrene polymerisation by 2,5-DTBHQ (4.5 mM).....	74
Figure 3.6 Dilatometry trace for the inhibition of the thermal styrene polymerisation by 2,5-DTBBQ (4.5 mM) .....	76
Figure 3.7 GC chromatogram of the reaction between 2,5-DTBBQ in styrene at time zero.....	77
Figure 3.8 GC chromatogram of the reaction of 2,5-DTBBQ in styrene after 3 h at 110 °C .....	78
Figure 3.9 GC-EI chromatogram of 2,5-DTBBQ in styrene after 3 h .....	79
Figure 3.10 ESI mass spectrum of 2,5-DTBBQ in styrene after 3 h heating.....	80
Figure 3.11 Addition products of 2,5-DTBBQ and styrene radicals .....	82
Figure 3.12 ESI mass spectrum of an isolated product from the reaction between 2,6-DTBBQ and AIBN .....	82
Figure 3.13 <sup>1</sup> H-NMR of compound 14.....	83
Figure 3.15 GC -Chromatogram of 2,5-DTBHQ in styrene after being heated at 110 °C for 5 h.....	85

Figure 3.16 GC chromatogram of a solution of 2,5-DTBHQ and AIBN in styrene at time = 0.....	86
Figure 3.17 Field ionization-mass spectrometry chromatogram of a solution of 2,5-DTBHQ and AIBN in toluene after 19 h heating.....	87
Figure 3.18 Mechanism of hydrogen abstraction from 2,5-DTBHQ by 2-cyano-propyl-2-radicals .....	89
Figure 4.1 Charge transfer complex diagram.....	93
Figure 4.2 UV-Vis spectrum of DBHA/2,5-DTBBQ mixture in acetonitrile.....	95
Figure 4.3 Evolution of N,N-dibenzyl nitroxide concentration during the oxidation of DBHA by 2,5-DTBBQ at 90 °C .....	96
Figure 4.4 <sup>1</sup> H-NMR spectrum of the DBHA/2,5-DTBBQ solution in toluene-d <sub>8</sub> , recorded at time 0 min using a 400 MHz spectrometer at 25 °C.....	98
Figure 4.5 Structures of reagents.....	98
Figure 4.6 <sup>1</sup> H-NMR spectrum of 2,5-DTBBQ/DBHA in toluene-d <sub>8</sub> , recorded using a 400 MHz NMR spectrometer at 25 °C after 11 h of heating.....	99
Figure 4.7 Products structures .....	99
Figure 4.8 DBHA, 2,5-DTBBQ, 2,5-DTBHQ and N,N-benzylidenebenzylamine-N-oxide concentrations evolution in toluene-d <sub>8</sub> at 90 °C .....	100
Figure 4.9 Fitting of Dynafit data to experimental data for the reaction between 2,5-DTBBQ and DBHA in toluene-d <sub>8</sub> at 90 °C .....	100
Figure 4.10 DBHA 2,5-DTBBQ, 2,5-DTBHQ and N,N-benzylidenebenzylamine-N-oxide concentrations evolution in toluene-d <sub>8</sub> at 90 °C.....	101
Figure 4.11 Fitting of Dynafit data to experimental data for the reaction between 2,5-DTBBQ and DBHA in toluene-d <sub>8</sub> at 80 °C .....	102
Figure 4.12 Fitting of Dynafit data to experimental data for the reaction between 2,5-DTBBQ and DBHA in toluene-d <sub>8</sub> at 70 °C .....	103
Figure 4.13 Arrhenius plot. The logarithm of the rate constant is plotted vs the reciprocal of the temperature .....	104
Figure 4.14 Eyring plot .....	105
Figure 4.15 General scheme for the synthesis of p-substituted hydroxylamines .....	107
Figure 4.16 Fitting of Dynafit data to experimental data for the reaction between 2,5-DTBBQ and DBHA-Cl in toluene-d <sub>8</sub> at 70 °C .....	107

Figure 4.17 Fitting of Dynafit data to experimental data for the reaction between 2,5-DTBBQ and DBHA-CH <sub>3</sub> in toluene-d <sub>8</sub> at 70 °C .....	108
Figure 4.18 Fitting of Dynafit data to experimental data for the reaction between 2,5-DTBBQ and DBHA-CF <sub>3</sub> in toluene-d <sub>8</sub> at 70 °C.....	108
Figure 4.19 Mechanism proposed by Hassan for the oxidation of N-benzyl-N-methylhydroxylamine by benzoquinone .....	110
Figure 4.20 Schematic mechanism of DBHA oxidation by 2,5-DTBBQ .....	110
Figure 5.1 Basic mechanism of nitroxide mediated polymerisation .....	112
Figure 5.2 Interaction scheme of nitron (4) with an electron rich dipolarophile (styrene) and electron poor dipolarophile (2,5-DTBBQ) .....	114
Figure 5.3 Representation of the exo and endo addition of styrene to the nitron 4.	114
Figure 5.4 GC chromatogram of 2,5-DTBBQ/DBHA in styrene after 15 h at 110 °C.....	116
Figure 5.5 Reaction scheme of the 1,3-dipolar cycloaddition between N,N-benzylidenebenzylamine-N-oxide (4) and styrene (5) leading to isoxazolidines (cis-7) and (trans-7).....	117
Figure 5.6 Tandem MS-MS spectrum for the mixture 2,5-DTBBQ/DBHA in styrene after 15 h at 110 °C .....	118
Figure 5.7 Fragmentation pattern of isoxazolidine (7) .....	118
Figure 5.8 Hypothesised mechanism of formation of N-(1,2-diphenylpropyl)-N-[(Z)-phenylmethylidene]amine oxide (12).....	119
Figure 5.9 General scheme of the attempts for the synthesis of nitron (12) .....	120
Figure 5.10 Synthetic route to N-(1,2-diphenylpropyl)-N-[(Z)-phenylmethylidene]amine oxide (12) .....	121
Figure 5.11 <sup>1</sup> H-NMR of N-benzyl-N-hydroxy-1,2-diphenylpropane-1-amine (13) recorded on a 700 MHz spectrometer and using CDCl <sub>3</sub> as a solvent. ....	122
Figure 5.12 <sup>1</sup> H-NMR spectra of N-benzyl-N-hydroxy-1,2-diphenylpropane-1-amine (13) recorded in a 400 MHz spectrometer, in DMSO-d <sub>6</sub> , at 25 °C (a), 30 °C (b), 50 °C (c) and 80 °C (d).....	123
Figure 5.13 <sup>1</sup> H-NMR of N-benzyl-N-hydroxy-1,2-diphenylpropane-1-amine (13) in CDCl <sub>3</sub> , at 25 °C and -30 °C.....	124
Figure 5.14 EPR spectrum of nitroxide (10) .....	124
Figure 5.15 Oxidation 3 rings hydroxylamine (13) to 3 rings nitron (12).....	125

Figure 5.16 Chromatogram of DBHA/2,5-DTBBQ and di-tert-butyl-benzoquinone in toluene at time 0.....	127
Figure 5.17 GC-chromatogram of DBHA/2,5-DTBBQ and di-tert-butyl peroxide in toluene after 24 h at 110 °C.....	127
Figure 5.18 Top MS spectrum: fragmentation of compound at retention time 9.1 min. Bottom MS spectrum: fragmentation of diphenyl ethane found in NIST .....	128
Figure 5.19 <sup>1</sup> H-NMR spectrum of cis-1,2-diphenylcyclobutane .....	130
Figure 5.20 <sup>1</sup> H-NMR spectrum of the trans 1,2-diphenylcyclobutane .....	130
Figure 5.21 <sup>1</sup> H-NMR spectrum of the fraction 1 .....	131
Figure 5.22 ESI mass spectrum of Fraction 1 .....	132
Figure 5.23 Possible fragment present in Fraction 1 .....	133
Figure 5.24 <sup>1</sup> H-NMR of Fraction 2 .....	133
Figure 5.25 Fragment of DBHA .....	134
Figure 5.26 Proposed fragment of Fraction 2 .....	134
Figure 5.27 MS-ESI spectrum of Fraction 2.....	135
Figure 5.28 <sup>1</sup> H-NMR of Fraction 3 .....	135
Figure 5.29 MS-ESI spectrum of Fraction 3.....	136
Figure 5.30 MS-ESI spectrum of Fraction 4.....	137
Figure 5.31 <sup>1</sup> H-NMR of Fraction 4 .....	138
Figure 5.32 Possible fragments present in Fraction 4.....	138
Figure 5.33 IR spectrum of CO <sub>2</sub> in the air.....	140
Figure 5.34 IR spectra of the head space of the styrene polymerisation inhibition by DBHA-2,5-DTBBQ .....	141
Figure 5.35 MALDI-MS spectrum of the polymer .....	143
Figure 5.36 Enlargement of the MALDI-MS spectrum in Figure 5.35.....	144
Figure 5.37 Mechanism of fragmentation during pyrolysis degradation .....	145
Figure 5.38 Pyrogram of the polymer .....	146
Figure 5.39 Top spectrum: fragmentation of our sample. Bottom spectrum: spectrum of benzonitrile found in the NIST library.....	147
Figure 5.40 Fragment of DBHA found in the polymer. Formation of benzonitrile fragment.....	148

Figure 5.41 Expected products of DBHA-CF <sub>3</sub> (22)/2,5-DTBBQ inhibited styrene polymerisation .....	151
Figure 5.42 <sup>19</sup> F-NMR spectrum of DBHA-CF <sub>3</sub> (22) in styrene at 110 °C .....	152
Figure 5.43 <sup>19</sup> F-NMR spectrum of nitron-CF <sub>3</sub> (23) recorded at 110 °C in styrene .....	153
Figure 5.44 <sup>19</sup> F-NMR spectrum of isoxazolidine-CF <sub>3</sub> (24) recorded at 110 °C in styrene .....	154
Figure 5.45 <sup>19</sup> F-NMR spectrum of the alkoxyamine-CF <sub>3</sub> (25) recorded at 110 °C in styrene.....	155
Figure 5.46 <sup>19</sup> F-NMR spectrum of the polymer recorded in styrene at 110 °C .....	156
Figure 5.47 <sup>19</sup> F-NMR spectra of the styrene polymerisation inhibited by DBHA-CF <sub>3</sub> (22)/2,5-DTBBQ at 110 °C .....	157
Figure 5.48 <sup>19</sup> F-NMR spectra recorded after 5 h and 24 h (the spectra were recorded at 25 °C, in a 400 MHz spectrometer) of styrene polymerisation inhibited with DBHA-CF <sub>3</sub> (22)/2,5-DTBBQ.....	158
Figure 5.49 Comparison of the spectrum of the reaction mixture carried out in the NMR tube and the spectrum recorded after 72 hours of the large scale reaction. The spectra were recorded at 110 °C, at a 400 MHz spectrometer .....	159
Figure 5.50 <sup>19</sup> F-NMR spectra recorded at 110 °C during the styrene polymerisation inhibited by DBHA-CF <sub>3</sub> .....	160
Figure 6.1 Dilatometry traces for the inhibition of the auto-initiated styrene polymerisation by DBHA, 2,5-DTBBQ and DBHA/2,5-DTBBQ mixture .....	163
Figure 6.2 Enlargement of Figure 6.1.....	163
Figure 6.3 Reagents concentrations trend during the styrene polymerisation inhibited by 2,5-DTBBQ and DBHA at 110 °C .....	165
Figure 6.4 Hydrogen abstraction mechanism .....	165
Figure 6.5 Evolution of N,N-dibenzyl nitroxide in the inhibition of styrene polymerisation with DBHA and 2,5-DTBBQ/DBHA mixture.....	167
Figure 6.6 Oxygen consumption in the inhibition of styrene polymerisation with DBHA and 2,5-DTBBQ/DBHA mixture .....	168
Figure 6.7 p-Substituted N,N-dibenzylhydroxylamines synthesised and the corresponding nitroxides .....	170

Figure 6.8 Evolution of nitroxide concentration during the inhibition of styrene using p-substituted hydroxylamines and 2,5-DTBBQ.....	170
Figure 6.9 Dilatometry trace of p-substituted hydroxylamines and 2,5-DTBBQ mixture during the inhibition of styrene polymerisation at 110 °C .....	171
Figure 6.10 Enlargement of Figure 6.9.....	172
Figure 6.11 Mechanism proposed by Ingold and co-workers for the N,N-dibenzyl nitroxide decomposition .....	173
Figure 6.12 Mechanism proposed by Nilsen and co-workers for nitroxide decomposition .....	173
Figure 6.13 Hydroxylamines synthesised and the corresponding nitroxides.....	174
Figure 6.14 Evolution of nitroxide concentration during the inhibition of styrene at 110 °C using hindered hydroxylamines/2,5-DTBBQ mixture.....	174
Figure 6.15 Dilatometry trace of hindered hydroxylamines/2,5-DTBBQ mixture during the inhibition of styrene polymerisation at 110 °C.....	175
Figure 6.16 Enlargement of Figure 6.15.....	176
Figure 6.17 Mechanism of inhibition of TEMPOH and AD-hydroxylamine .....	177
Figure 6.18 Evolution of N,N-dibenzyl nitroxide concentration for a series of DBHA/2,5-DTBBQ ratios during the inhibition of styrene polymerisation at 110 °C.....	178
Figure 6.19 Dilatometry traces for the inhibition of the auto-initiated styrene polymerisation in the presence of different DBHA/2,5-DTBBQ ratios .....	179
Figure 6.20 Evolution of N,N-dibenzyl nitroxide concentration during the inhibition of styrene polymerisation in the presence of different ratios of DBHA/2,5-DTBBQ.....	180
Figure 6.21 Dilatometry trace of the inhibition of styrene polymerisation using different concentrations of DBHA and constant 2,5-DTBBQ concentration. ....	181
Figure 6.22 Dilatometry trace of DBHA/2,5-DTBBQ 50/200 ppm and 250/200 ppm, for the inhibition of the styrene polymerisation at 110 °C .....	181
Figure 6.23 Benzisoxazolidine formation.....	183
Figure 6.24 Dilatometry trace for the inhibition of the styrene polymerisation at 110 °C by N,N-benzylidenebenzylamine-N-oxide/2,5-DTBBQ mixture and N,N-benzylidenebenzylamine-N-oxide. ....	183
Figure 6.25 Isoxazolidine and isoxazoline formation.....	184

Figure 6.26 Dilatometry trace for the inhibition of the styrene polymerisation at 110 °C by isoxazolidine and isoxazolidine/2,5-DTBBQ mixture. ....	185
Figure 6.27 Dilatometry trace for the inhibition of the styrene polymerisation at 110 °C by N,N-benzylidenebenzylamine-N-oxide and N,N-benzylidenebenzylamine-N-oxide/2,5-DTBHQ mixture.....	186
Figure 6.28 Overall mechanism of reaction .....	188
Figure 6.29 Inhibition of styrene polymerization by N,N-dimethylaniline/chloranil charge transfer complex .....	192
Figure 8.1 Sample for EPR experiment .....	200
Figure 8.2 Height of a peak of a sharp N,N-dibenzyl nitroxide.....	201
Figure 8.3 Sample preparation and analysis in dilatometry experiments.....	202

## Acknowledgements

I would like to thank my supervisor Victor Chechik for giving me the opportunity to do my PhD in his group, but also for his constant support and providing useful ideas for my project. A particular thank to Nufarm Ltd. for funding this project.

Thank you to all the people who have helped me during these four years in York. Thanks to Karl Heaton for providing mass spectra and precious advices. Thanks to Heather Fish for running the NMR studies.

Big thanks go to members of VC group: Rob Smith, Thomas Newby, Rob Thatcher and Kazim Raza Naqvi. As special thanks to Zhou Lu for teaching me how to run a “flash column” and for making my life in York more enjoyable.

Thanks to Sindhu Krishna, Luisa Ciano and Danielle Jowett for reading my chapters. A special thanks to Sindhu for being always so nice and helpful.

Thanks to Tessa and Julia for been part of the “Chiara has to finish her PhD” team! Heartfelt thanks to Tessa for your help, I really appreciated it.

Thanks to my family for supporting me in the decision to come to UK. I would not have been able to survive here without their help!

The last thanks, but not the least to Matteo, for listening my complaints and for never letting me feel alone!



## **Declaration**

I declare that this thesis submitted for the degree of Doctor of Philosophy at University of York has not been presented to any other university for examination.

This thesis is entirely my own work except where indicated by specific references.

# 1 Introduction

This introduction aims to provide background about auto-initiated styrene polymerisation and its control by the use of additives.

## 1.1 Styrene

Styrene is a major industrial monomer<sup>1, 2</sup>. Around 90% of styrene is produced by dehydrogenation of ethyl benzene in the presence of steam over iron oxide as a catalyst (Figure 1.1). The reaction is carried out in either adiabatic or tubular isothermal reactors<sup>2</sup>.

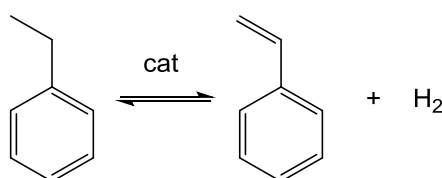


**Figure 1.1 Styrene synthesis**

This industrial production of styrene is a multi-tonne process, and fractional distillation is usually used for its purification. During this process, styrene is heated to its boiling point which can trigger spontaneous free radical polymerisation.

## 1.2 Mechanism of radical polymerisation

Free radical polymerisation<sup>1</sup> involves three main steps: Initiation, propagation and termination.

### *Initiation*

Initiation is a process leading to the formation of a free radical by an initiator ( $I_2$ ) (Equation 1), followed by the addition of this radical to a molecule of monomer (M) (Equation 2).



There are different ways to initiate polymerisation, such as thermal decomposition of initiators<sup>3</sup>, redox initiation<sup>4</sup>, photochemical initiation<sup>5</sup> and pure thermal initiation<sup>6,7</sup>.

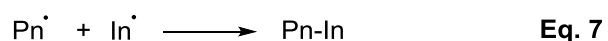
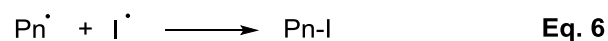
### *Propagation*

The radical formed during initiation reacts with another monomer by addition reaction, during propagation polymer chain grows. The chain propagates until termination occurs (Equation 3).

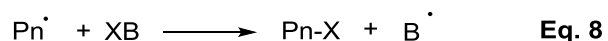


### *Termination*

There are different ways to terminate the polymer growth: coupling between two chains (Equation 4), disproportionation (Equation 5), combination of a growing chain with free radical initiator (Equation 6), or an inhibitor (Equation 7).



A particular case of termination occurs via chain transfer (Equation 8). Hydrogen or another atom, or species (X), is transferred from a monomer or another compound (XB), to a growing chain causing its termination. However, a new radical is formed (B·), which may re-initiate the polymerisation.



In the presence of heat, styrene undergoes spontaneous polymerisation without the addition of initiators. The mechanism of the auto-initiated polymerisation has been a matter of a long debate, which is discussed in the next section.

### 1.3 Auto-initiated styrene polymerisation

The auto-initiated styrene polymerisation at high temperatures has been studied by many researchers and several mechanisms have been proposed<sup>8</sup>. An early study, attributed the initiation of styrene polymerisation to the formation of a biradical, which undergoes biradical propagation through the addition of monomers on both active centres (Figure 1.2, Mechanism 1). Another mechanism, involves the formation of monoradicals by the interaction of two styrene monomers (Figure 1.2, Mechanism 2). However, both mechanisms are not consistent with the established third order initiation process.

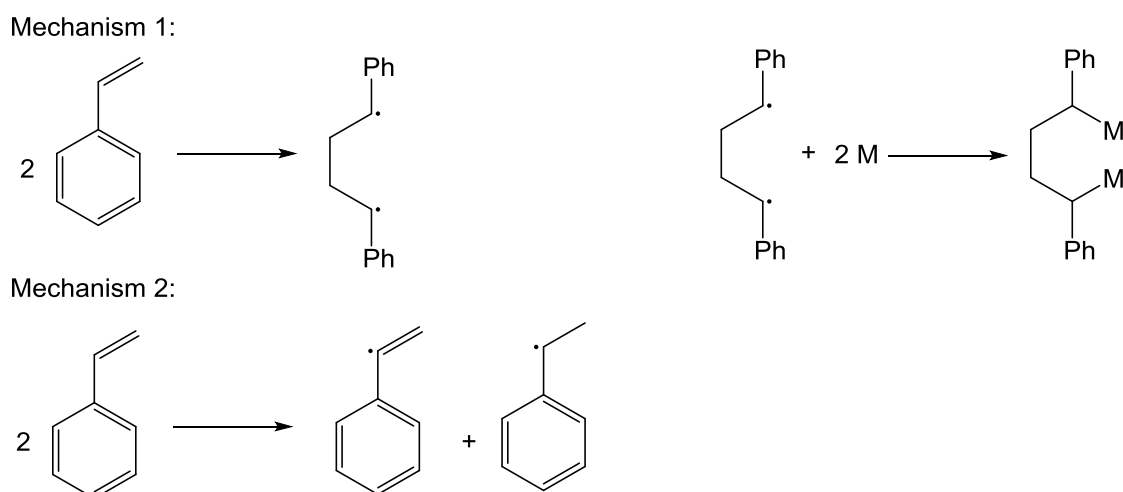


**Figure 1.2** Second order initiation mechanisms

Later, Flory proposed<sup>9</sup> an innovative mechanism (Figure 1.3), which agrees with the kinetics finding. The first step is similar to mechanism 1, in which two molecules of styrene dimerize leading to a diradical. Then, a third molecule of styrene removes one of the two radical centres by chain transfer reaction, leading to monoradical propagation. According to Flory, the diradical can abstract a hydrogen atom from monomers leading to diradical propagation, but can also cyclize to give either 1,2-diphenylcyclobutane or Diels Alder dimer. The latter, then undergoes polymerisation following the Mayo mechanism (Mayo mechanism is reported in the next section). Further studies established that the diradical life-time is too short to allow any of the above reactions. Therefore, even this mechanism has been excluded.

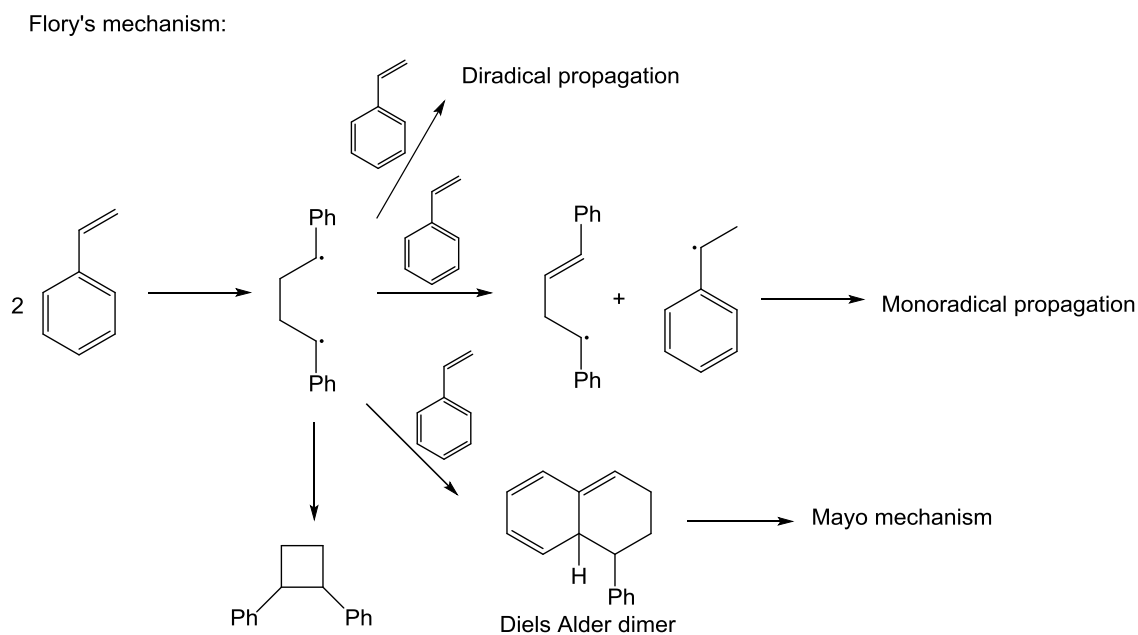


**Figure 1.3 Flory mechanism**

The mechanism proposed by Mayo<sup>6,7</sup> is the one commonly accepted (Figure 1.4).

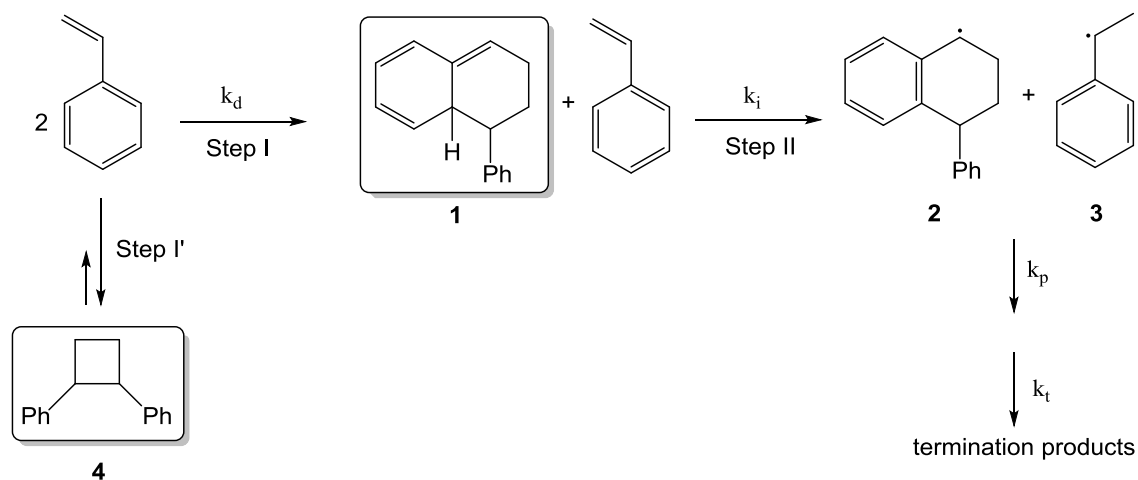


**Figure 1.4 Mayo mechanism**

The mechanism involves Diels-Alder dimerization of styrene with the formation of cycloadduct (**1**) characterised by a weak C-H bond ( $k_d = 3 \times 10^{-8} \text{ M}^{-1} \text{ s}^{-1}$  at  $120^\circ \text{C}$ )<sup>10</sup> (Step I), which in the presence of another styrene molecule generates radicals (**2**) and (**3**) (Step II) ( $k_i = 5 \times 10^{-8} \text{ M}^{-1} \text{ s}^{-1}$  at  $120^\circ \text{C}$ ). Radicals (**2**) and (**3**) are able to initiate polymerisation, which proceeds as a normal free radical polymerisation. This mechanism is consistent with the observed overall 5/2 order mechanism, where

propagation ( $k_p = 2 \times 10^3 \text{ M}^{-1}\text{s}^{-1}$  at 120 °C) and termination ( $k_t = 10^7 \text{ M}^{-1}\text{s}^{-1}$  at 120 °C) occur via a second-order process, while initiation is via a third-order mechanism<sup>6</sup>. Despite long chains being generated via a third-order process, dimers such as 1-phenyltetralin (derived by termination of **(2)**) and 1,2-diphenylcyclobutane **(4)** are formed via bimolecular and non-chain reactions<sup>7</sup>. In addition, product analysis of the polymerisation mixture reveals that dimer **(4)** is the major dimeric product, beside the higher molecular weight polymers. However, product distribution is dependent on reaction conditions (e.g., presence of additive)<sup>11</sup>. Thermal styrene polymerisation occurs at a rate of 2% per hour at 100 °C<sup>11</sup>, and to stop it additives are usually added to the monomer, as discussed in the next section.

## 1.4 Inhibitors of polymerisation

The ability to control spontaneous styrene polymerisation is essential, safety is one of the main reasons. Styrene polymerisation is an exothermic reaction ( $\Delta H = 17.8 \text{ kcal/mol}$ <sup>12</sup>), hence if heat is not removed, the reaction may self-accelerate leading, in extreme cases, to thermal explosion. Furthermore, purification of styrene in industry leads to economic loss due to a reduced monomer yield and a purification process that is not very efficient (increasing of viscosity may induce to a partial or total equipment blockage)<sup>13</sup>. To avoid polymerisation, substances which can intercept propagation radicals are added to the monomer. These compounds are called inhibitors. Based on their mechanism of action, inhibitors are divided into three main classes, addition reaction, hydrogen abstraction, or redox.

### 1.4.1 Addition reaction

These types of inhibitors usually have a multiple bond and they combine with the radical to form a bigger molecule (RHI·). The product has a low tendency to initiate polymerisation (Equation 9).



## Nitrosobenzene

Nitrosobenzene efficiently inhibits styrene polymerisation due to the rapid addition of radicals to the N=O bond. The following is the inhibition mechanism proposed<sup>14, 15</sup> by Kende and co-workers and commonly accepted (Figure 1.5).

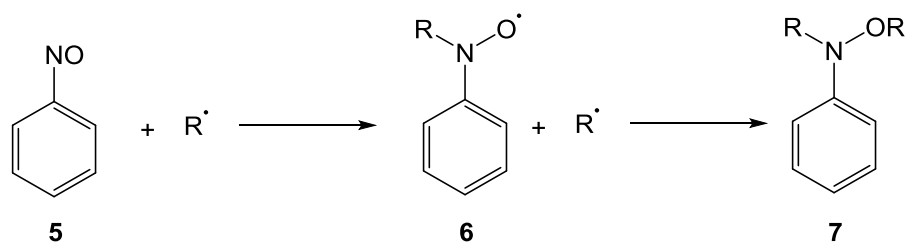


**Figure 1.5 Inhibition mechanism of nitrosobenzene**

A combination of dilatometry and EPR analyses, reported in the literature<sup>14</sup>, suggest that nitrosobenzene reacts efficiently with styrene radicals. This interaction leads to intermediate nitroxide (**6**), which is capable of adding to a new carbon-centred radical leading to (**7**). Alkoxyamine (**7**) was synthesised in laboratory to confirm its presence in the reaction mixture.

## TEMPO

2,2,6,6-Tetramethylpiperidine-1-oxyl (TEMPO) is a stable radical (long lived) capable of stopping propagation chains by an addition reaction (Figure 1.6).

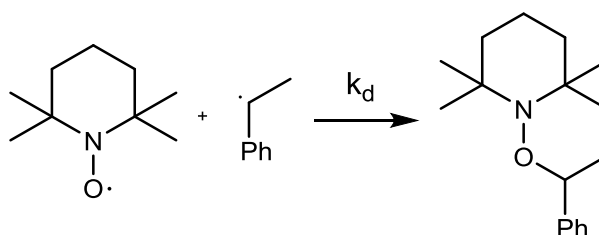


**Figure 1.6 Mechanism of inhibition of TEMPO**

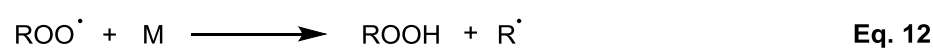
The fast coupling reaction with carbon-centred radical ( $k_d = 1.6 \times 10^8 \text{ M}^{-1}\text{s}^{-1}$  at  $18^\circ\text{C}$ <sup>16</sup>), allows TEMPO to act as an inhibitor of polymerisation<sup>17</sup>. This reaction, however, may be reversible due to the low R-O BDE (86 kJ/mol, at  $393 \text{ K}$ <sup>18</sup>), with a consequent releasing of TEMPO and alkyl radical.

## Oxygen

Another inhibitor operating by an addition reaction is oxygen, which is considered as one of the strongest free radical inhibitors. Oxygen dissolved in styrene solution rapidly reacts with propagation radicals leading to peroxy radicals  $\text{ROO}\cdot$  ( $10^9 \text{ M}^{-1}\text{s}^{-1}$ )<sup>19</sup> (Equation 10).



Peroxy radicals can react with styrene monomers either by addition (Equation 11) or hydrogen abstraction (Equation 12) and the rate constants at 120 °C are approximately the same order of magnitude ( $10^1 \text{ M}^{-1}\text{s}^{-1}$ )<sup>20</sup>. Both reactions are much slower than styrene propagation chain ( $2 \times 10^3 \text{ M}^{-1}\text{s}^{-1}$ )<sup>10</sup> (Equation 13), hence polymerisation is controlled.



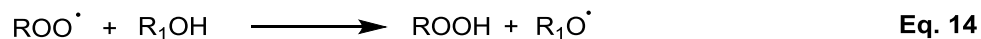
Fast reaction between oxygen and carbon-centred radical however, leads to rapid oxygen consumption. In addition, peroxy radicals can react to give other products that re-initiate polymerisation<sup>21-23</sup> and hence oxygen is quite often used in combination with another inhibitor (e.g., antioxidant).

### 1.4.2 Hydrogen abstraction

As anticipated in the previous paragraph, oxygen is commonly used in combination with antioxidants. Antioxidant is a substance (e.g., hydroxylamines, phenols, etc.), capable of stopping propagation chains by donating a hydrogen atom (Equation 14). Unlike oxygen, the antioxidant does not react rapidly with alkyl radicals<sup>24</sup>, therefore, when both oxygen and antioxidants are in solution there is an initial build-up of peroxy radicals, followed by the antioxidant-peroxy radical interaction. In a general inhibition process, a peroxy radical ( $\text{ROO}\cdot$ ) is quenched, while the antioxidant ( $\text{R}_1\text{OH}$ )



loses a hydrogen atom and forms ( $R_1O\cdot$ ) (e.g., alkoxy or aminoxyl radical) and hydroperoxide (ROOH) (Equation 14).



The efficiency of the antioxidant in controlling polymerisation depends on the reactivity of  $R_1O\cdot$  and the bond dissociation energies (BDE) of both  $R_1OH$  and ROOH. Indeed,  $R_1O\cdot$  should be rather unreactive so that it can only combine with another radical or lose a hydrogen atom to form a double bond. In addition, BDE of  $R_1O-H$  bond has to be low enough to allow a rapid hydrogen abstraction by peroxy radical. On the contrary, BDE of ROO-H has to be rather high to avoid re-initiation of polymerisation (BDE for antioxidants and hydroperoxide is reported in Chapter 2).

### ***p*-Methoxy phenol (MEHQ)**

MEHQ (**8**)<sup>25</sup>, as other antioxidants requires oxygen to work. Hence, at a normal oxygen level<sup>26</sup> in solution, a carbon-centred radical reacts first with oxygen to give peroxy radical ( $ROO\cdot$ ), then MEHQ stops the intermediate  $ROO\cdot$  by hydrogen abstraction leading to (**9**) and hydroperoxide. The presence of oxygen is essential, as otherwise hydrogen abstraction from MEHQ by carbon-centred radical would be too slow to efficiently stop propagation chains<sup>27, 28</sup>.

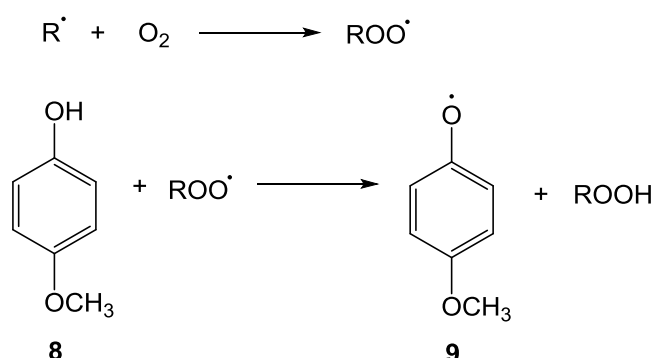
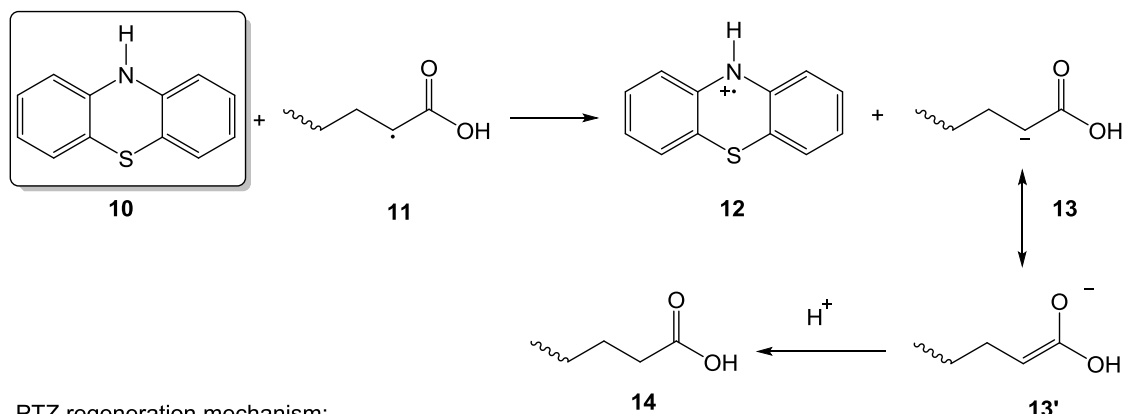


**Figure 1.7 Mechanism of inhibition of MEHQ**

### 1.4.3 Redox reaction

This kind of inhibitor works by a single electron transfer. Phenothiazine (PTZ) is an example of commercially available inhibitor commonly used to stop acrylic acid polymerization. Leny investigated the action mechanism<sup>29</sup> as reported in Figure 1.8.

PTZ inhibition mechanism:



PTZ regeneration mechanism:

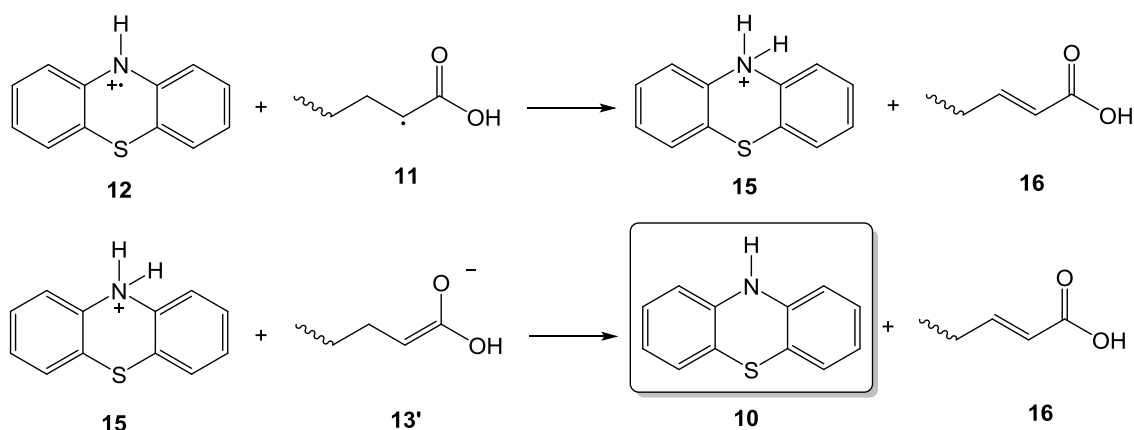
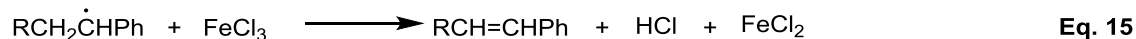


**Figure 1.8 Inhibition mechanism of acrylic acid by PTZ**

PTZ (10) efficacy is not dependent on oxygen concentration, as it reacts with propagation chains faster than oxygen<sup>30</sup>. PTZ is oxidized to a radical cation (12), while carbon-centred radical (11) is converted to carbanion (13). (13) is then neutralized to (14). The ability of PTZ to inhibit polymerisation for a long time is due to the regeneration of the inhibitor during the inhibition. Radical cation (12) abstracts a hydrogen atom from (11) leading to an acrylic acid derivative (16) and protonated PTZ (15). (15) eventually loses the proton by interacting with the anionic intermediate (13'), re-forming PTZ.

$\text{FeCl}_3$  is another example of a redox inhibitor used to stop styrene polymerization<sup>4</sup> as shown by Equation 15.



The above classification is based only on the mechanism of action, however a further distinction needs to be made in terms of efficiency of an additive in stopping propagation reaction.

## 1.5 Inhibitors vs retarders

Inhibitor is a substance capable of completely suppressing polymerisation for a certain time, called inhibition time (Figure 1.9, inhibitor). However, if a substance can only stop a proportion of the propagation chains then it is called retarder (Figure 1.9, retarder). The distinction is based on their effectiveness to stop polymerisation.

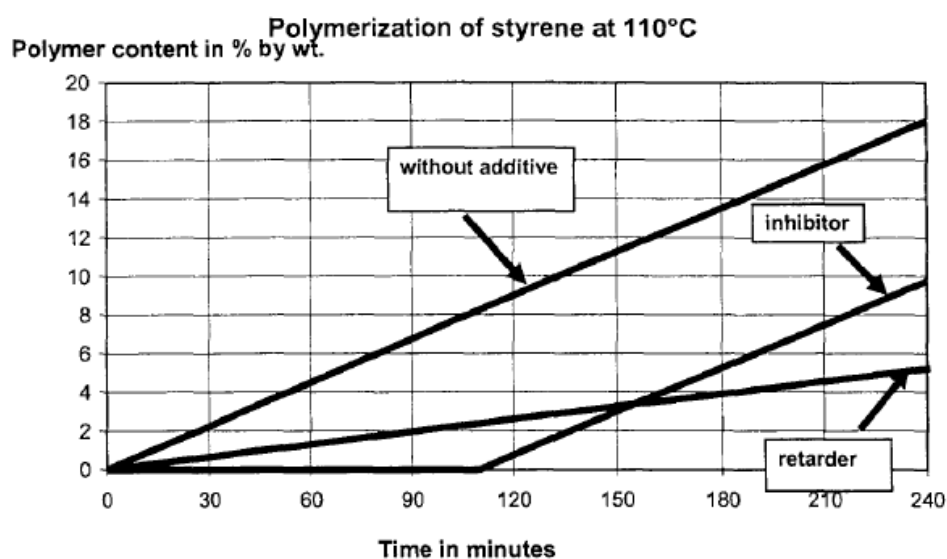


**Figure 1.9 Difference between retardation and inhibition effect<sup>31</sup>**

Tudos<sup>15</sup> gave a more quantitative distinction between inhibitors and retarders by assuming that  $k_p$  is the rate constant of propagation and  $k_i$  is rate constant of inhibition. If  $k_i/k_p$  ratio is  $> 10$  true inhibition occurs, and if  $k_i/k_p$  ratio is  $< 10$  the effect is retardation. However, the distinction is not always so clear, for example a strong inhibitor could generate a product which affects the rate of polymerisation, but to a

different extent. Hence, at the point when inhibitor concentration becomes too low and the product concentration is dominant, polymerisation would be retarded rather than inhibited.

Nitrobenzene represents an example of a retarder of styrene polymerisation and the following is its mechanism of action (Figure 1.10).

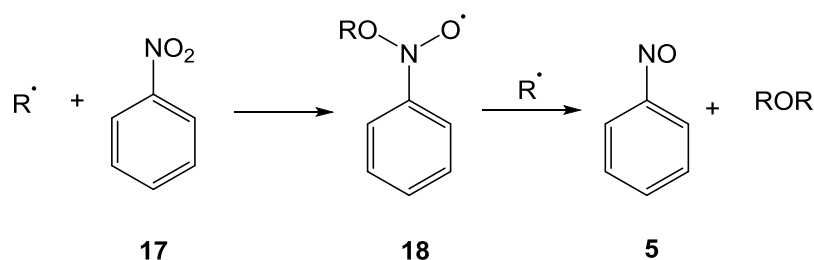


**Figure 1.10 Mechanism of action of nitrobenzene**

A previous work established<sup>15</sup> that retardation occurs through the addition of a carbon-centred radical to the oxygen atom of the nitro group, with generation of **(18)**. **(18)** then experiences the attack of a second propagation chain leading to nitrosobenzene **(5)**, which reacts further as seen in Figure 1.5.

The choice to use an inhibitor instead of a retarder depends on the application<sup>15</sup>. For instance, if the function of the additive is to stop the polymerisation rapidly and efficiently, an inhibitor is preferred. Indeed, during monomer storage, inhibitors in low concentration are used. On the other hand if a long protection of the polymerisation is required (e.g., during distillation), a retarder is added. They are less reactive and their consumption is slower than that of an inhibitor, hence their effect lasts for longer. Quite often, to obtain longer protection, a mixture of inhibitors/retarders is used.

## 1.6 Synergistic effect

There are particular situations, during industrial processes where it is necessary to control the polymerisation for a long time. To achieve this result, there are two possibilities, increasing retarder concentration or using a mixture of retarders/inhibitors. Usually the inhibition time depends on inhibitor concentration<sup>15</sup>, thus in many cases a higher concentration corresponds to a longer inhibition time,

however the main disadvantages are costs (inhibitors are quite expensive), solubility of the additive in the monomer and removal of the additives from the monomer. To keep these disadvantages to a minimum, quite often rather than increasing inhibitor concentration a mixture of two or three components is used. It is well documented<sup>32-34</sup> that a combination of the right components may give an effect which is significantly better than the sum of the effects of the single compounds. This effect is called synergism. Literature reports describe the synergistic effect between 2,6-di-tert-butyl-substituted phenols (**19**) and diphenylamine (**20**)<sup>35,36</sup> towards styrene radicals (Figure 1.11).

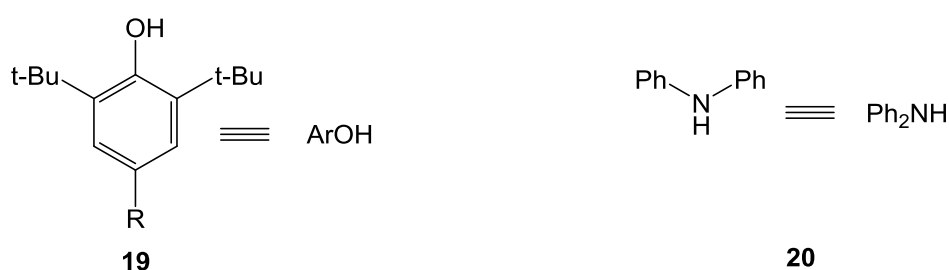
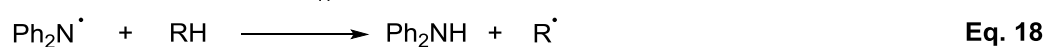
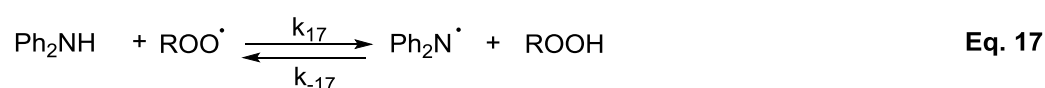


**Figure 1.11 Structure of 2,6-di-tert-butyl-substituted (**19**) and diphenylamine (**20**)**

Diphenylamine acts as an antioxidant towards peroxy radical, and hence stops propagation chains by donating a hydrogen atom, so that a diphenylaminyl radical and hydroperoxide are generated ( $k_{17} = 3.4 \times 10^5 \text{ M}^{-1} \text{ s}^{-1}$ )<sup>35</sup> (Equation 17).



However, Equation 17 is reversible, so diphenylaminyl radical re-abstracts a hydrogen from the hydroperoxide ( $k_{-17} = 1 \times 10^5 \text{ M}^{-1} \text{ s}^{-1}$ ) diminishing the positive effect of diphenylamine as an inhibitor. Carbon-centred radicals are also formed by Equation 18 ( $k_{18} = 0.7 \text{ M}^{-1} \text{ s}^{-1}$ ). Instead, in the presence of 2,6-di-tert-butyl-substituted phenols (**19**), unfavourable reactions are suppressed as diphenylaminyl radical is consumed through Equation 19.



Alkoxy radical ( $\text{ArO}^\cdot$ ) can either react<sup>20</sup> with hydroperoxide (Equation 20) or terminate by a coupling reaction (Equation 21).



In this example, cooperation between the two components is due to the removal of an intermediate which is able to re-initiate the polymerisation. Other combinations show synergism, such as 2,4-dinitro-ortho-sec-butyl-phenol (DNBP) with hydroxylamine<sup>34</sup> or a stable nitroxide<sup>31</sup>. Efficacy of the inhibitor/retarder is not the only aspect to consider, regulations which have been introduced to protect human health and the environment, prohibit the use of some common inhibitors.

### 1.6.1 Restrictions about the use of nitrophenol compounds

Nitrophenol compounds, such as 2,4-dinitro-ortho-cresol, 2,6-dinitro-para-cresol, 2,4-dinitrophenol and 2,4-dinitro-ortho-sec-butyl-phenol (DNBP) are the most used retarders to control polymerisation either on their own or in a composition<sup>32</sup>, however these compounds are quite toxic for both humans and environment<sup>37</sup>. For instance, it has been established that 2,4-dinitro-ortho-sec-butyl-phenol (DNBP) may cause cancer, sterility and damage to the immune system. The use of DNBP and all chemical compounds is, hence, regulated by national and international authorities. European Chemical Agency (ECHA) was founded in 2007<sup>38</sup> and regulates the use of chemicals with the introduction of legislations. They aim to ensure safe use of chemicals and find replacement for the chemicals found to be extremely dangerous for humans and environment<sup>39</sup>. To increase safety, ECHA unified classification and labelling of chemicals with CLP<sup>40</sup>(Classification, Labelling and Packaging regulation). Regulation (EC) No 1272/2008 classifies nitrophenols, such as DNBP and 2,4-dinitro-ortho-cresol as toxic for reproduction while (EC) No 552/2009 restricts their sale or use above a

certain concentration. Before being placed on the market, the package has to be marked visibly as “restricted to professional users”. In addition, companies have to agree to REACH regulation (Registration Evaluation, Authorisation and Restriction of Chemicals)<sup>41</sup>, which declares that information on the hazards and safe use of the chemicals have to be provided. If the substance cannot be safely handled, it has to be removed from the market and replaced with a less dangerous one. Under these regulations, the use of nitrophenols will be soon prohibited completely and new efficient inhibitors/retarders as an alternative have to be introduced.

The possibility that DNBP will be soon banned from the market, pushed Nufarm UK Ltd to start an extensive screening of new potential retarders of styrene polymerisation. They observed that *N,N*-dibenzylhydroxylamine (DBHA) and 2,5-di-*tert*-butyl-1,4-benzoquinone (2,5-DTBBQ) in a 2:1 ratio represents an effective and harmless alternative to DNBP, DBHA/2,5-DTBBQ shows synergism. An initial study revealed that DBHA and 2,5-DTBBQ is not a stable composition, but is converted to 2,5-di-*tert*-butylhydroquinone (2,5-DTBHQ) and *N,N*-benzylidenebenzylamine-*N*-oxide (nitron) (Figure 1.12).

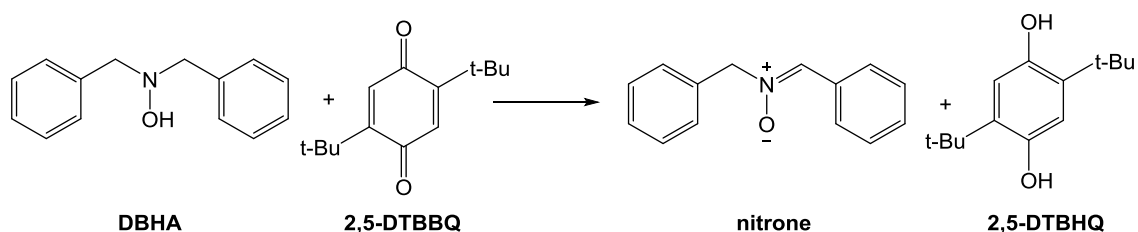


**Figure 1.12 Inhibition**

Therefore starting with an initial 2:1 ratio DBHA/2,5-DTBBQ mixture, the final composition is *N,N*-benzylidenebenzylamine-*N*-oxide (1 part), DBHA (1 part) and 2,5-DTBHQ (1 part). This mixture shows a similar inhibition efficacy to DBHA/2,5-DTBBQ, and a further study revealed that *N,N*-benzylidenebenzylamine-*N*-oxide is not essential for the inhibition properties of the mixture. Structure-activity effect was also investigated using a series of hydroxylamines (e.g., bis-hydropropylhydroxylamine) and benzoquinones (e.g., 2,5-di-methyl benzoquinone, 2,6 and tetra substituted benzoquinones). Those results suggest that there is a benefit from having some steric

hindrance around oxygen atoms in benzoquinone, but having both ortho position substituted reduced the efficacy of the mixture. On the other hand, replacing DBHA with bis-hydropropylhydroxylamine causes inhibition rather than retardation.

In order to place this new retarder composition on the market for the protection of styrene from unwanted polymerisation, Nufarm Ltd needs to determine the mechanism of action of DBHA/2,5-DTBBQ. However, the above information are not sufficient to unravel the complex mechanism of inhibition, thus an extensive study was carried out.

## 1.7 Aim of the project

DBHA/2,5-DTBBQ represents a valid alternative to the toxic DNBP, however unravelling its mechanism of action is quite challenging, as the system is quite complex and multiple reactions can occur to stop polymerisation. In order to simplify this system the inhibitors were initially studied singularly. The idea was to understand the inhibition mechanism of the single components, to rule out some plausible reactions during the inhibition by DBHA/2,5-DTBBQ. Using Nufarm UK Ltd. results as a starting point, it was known that 2,5-DTBBQ/DBHA was converted to *N,N*-benzylidenebenzylamine-*N*-oxide and 2,5-DTBHQ, but in the final mixture DBHA was still present. Therefore the inhibition properties and the mechanism of 2,5-DTBHQ, *N,N*-benzylidenebenzylamine-*N*-oxide and DBHA were investigated. Furthermore, Nufarm UK Ltd. observed that changing substituents on the benzoquinone ring seems to affect inhibition properties of the mixture. Hence, we needed to understand if this behaviour was due to the ability of the substituents to hamper or facilitate the addition reaction of propagation chains on 2,5-DTBBQ. The next step was the investigation of the mixture DBHA/2,5-DTBBQ. Product analysis and efficacy tests of products (or mixture of them) were carried out in order to establish what component (or components) is responsible for the synergism.



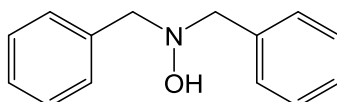
## 2 *N,N*-Dibenzylhydroxylamine as an inhibitor of styrene polymerization

### 2.1 Introduction

The hydrogen abstraction from *N,N*-dibenzylhydroxylamine by peroxy radicals stops the propagation reaction. However, in deoxygenated systems the inhibition ability drops as the hydrogen abstraction from DBHA by the styrene radicals is not efficient. This chapter describes a detailed study of this complex system of reactions with particular emphasis on the role of both oxygen and *N,N*-dibenzylhydroxylamine on the inhibition mechanism. The chapter starts with a review of relevant literature and then proceeds with the description of experimental results, which should give some insight into the mechanism of inhibition of DBHA.

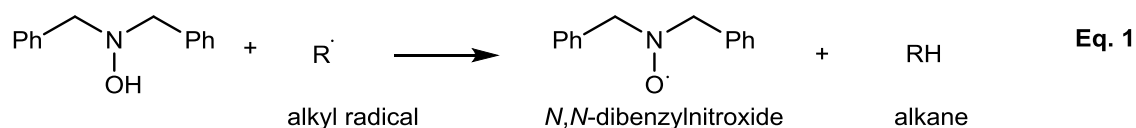
#### 2.1.1 Background

*N,N*-Dibenzylhydroxylamine (DBHA) is a common less toxic inhibitor<sup>42, 43</sup> of styrene polymerisation.



*N,N*-Dibenzylhydroxylamine

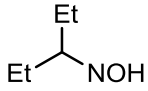
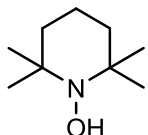
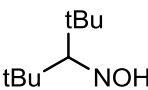
Due to relatively weak RNO-H bond, the hydroxylamine inhibitors can stop propagation of radicals by hydrogen abstraction. The homolytic scission of the O-H bond of the hydroxylamine leads to the formation of compounds that cannot propagate the polymerisation, such as nitroxides (RNO $\cdot$ ) and alkanes (RH) (Equation 1).



The strength of the O-H bond is expressed as Bond Dissociation Energy (BDE) in kcal/mol. Though the BDE of the O-H bond in DBHA is not available, it is expected to be

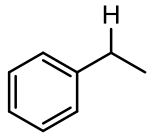
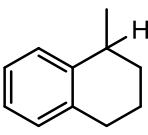
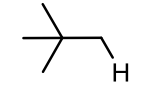
in the range between 68-75 kcal/mol, as the majority of the hydroxylamines<sup>44-46</sup>, Table 2.1.

**Table 2.1 O-H Bond Dissociation Energies in hydroxylamines<sup>45</sup>**

Hydroxylamine	BDE (kcal/mol)
	69.5
	71.58 <sup>46</sup>
	68.2

These BDE values are lower than those of alkanes (Table 2.2)<sup>45</sup> which are within the range 85-100 kcal/mol (Table 2.2).

**Table 2.2 C-H Bond Dissociation Energies in hydrocarbons**

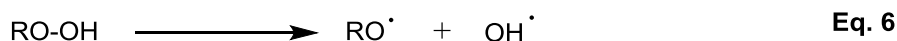
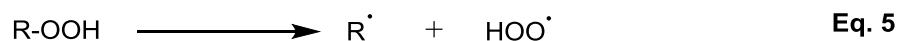
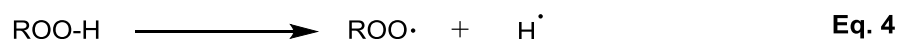
Hydrocarbon	BDE C-H (kcal/mol)
	84.6
	79.3
	95.6

The difference in BDE explains why hydroxylamine readily reacts with alkyl radicals, while the reverse reaction is unlikely to happen. The alkane formed does not react further, either (Equation 1).

In oxygenated systems, alkyl radicals react with oxygen at a rate constant of about  $10^9 \text{ M}^{-1}\text{s}^{-1}$  to give peroxy radicals (Equation 2)<sup>19</sup>. Thus, for oxygen concentration above  $10^{-4} \text{ M}$  (oxygen concentration in styrene at 25 °C is  $1.6 \times 10^{-3} \text{ M}$ <sup>26</sup>),  $[\text{ROO}\cdot] \gg [\text{R}\cdot]$ <sup>35</sup>. Moreover, it has been demonstrated that the hydrogen abstraction from hydroxylamines by peroxy radicals (Equation 3) is more efficient than the reaction of hydroxylamines with alkyl radicals (Equation 1)<sup>24, 44</sup>. Indeed, the rate constant ( $k_1$ ) for the hydrogen abstraction from TEMPO hydroxylamine (TEMPOH)<sup>24</sup> by styrene radicals at 90°C is only  $35 \text{ M}^{-1}\text{s}^{-1}$ , but that for the reaction of *N*-hydroxyphthalimide<sup>44</sup> with peroxy radical at 30°C  $k_3$  is  $7.2 \times 10^3 \text{ M}^{-1}\text{s}^{-1}$ . So, in oxygenated conditions the main reaction in the polymerising mixture of air-saturated monomer with a hydroxylamine is the hydrogen abstraction from the hydroxylamine by a peroxy radical to give hydroperoxide and nitroxide<sup>19</sup> (Equation 3).



Due to the low BDE values, hydroperoxides (ROOH) can further decompose at high temperature and initiate the polymerisation. BDE values of O-H bond in ROO-H are close to 84 kcal/mol, as reported by Blanksby<sup>47</sup> (Equation 4), whereas the homolysis of the R-OOH bond is much easier to occur (BDE of  $(\text{CH}_3)_3\text{C-OOH}$  is 38 kcal/mol)<sup>47</sup> (Equation 5). RO-OH cleavage is also possible due to the low BDE of this bond (BDE of  $(\text{CH}_3)_3\text{CO-OH}$  is 47 kcal/mol)<sup>47</sup> (Equation 6).



Peroxy radicals ( $\text{ROO}\cdot$ ) undergo decomposition by different pathways, the main one is by coupling with another peroxy radical to give a tetroxide as an intermediate (Equation 7)<sup>21</sup>. They can also add to styrene monomers and initiate the polymerisation<sup>22</sup> (Equation 8).

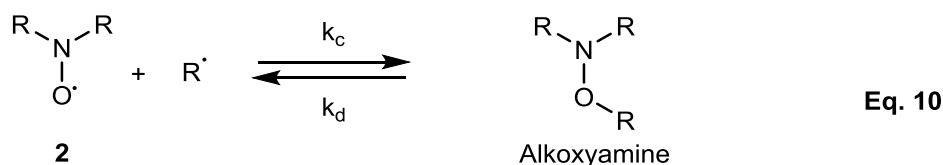


The further decomposition of tetroxide may lead to either non-radical products such as ketones, alcohols and oxygen or to alkoxy radicals (Equation 9)<sup>20</sup>.



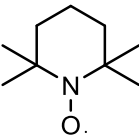
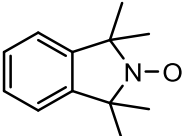
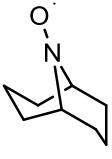
The alkoxy radicals (RO·) formed in Equations 6 and 9 are able to initiate the styrene polymerisation. Stepin and Dikusar reported<sup>23</sup> that the rate constant for the initiation of styrene polymerisation at 110 °C by a series of alkoxy radical is within the range 9-27x10<sup>6</sup> s<sup>-1</sup>.

The hydrogen abstraction from a hydroxylamine by oligostyryl (Equation 1) or peroxy radicals (Equation 3) leads to the formation of a nitroxide radical. The role of nitroxides in polymerisation has been widely studied in Nitroxide Mediated Polymerisation, as they react reversibly with alkyl radicals to form alkoxyamines (Equation 10)<sup>48</sup>.



The rate constants for the reaction between nitroxide and styrene radical ( $k_c$ ) (1.6-8.6x10<sup>8</sup> M<sup>-1</sup>s<sup>-1</sup>) are available in the literature<sup>16</sup>, Table 2.3.

**Table 2.3** Rate constant for the reaction between nitroxides and styrene radical<sup>a</sup> at 18°C

Nitroxide	$k_c$ ( $M^{-1}s^{-1}$ )
 (TEMPO)	$1.6 \times 10^8$
 (TMIO)	$3 \times 10^8$
 (ABNO)	$8.6 \times 10^8$

a

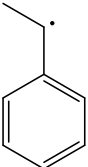
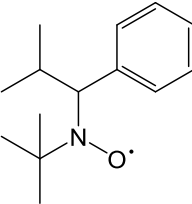
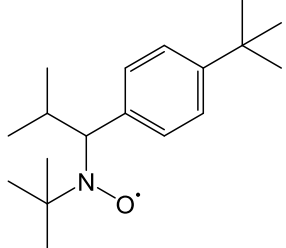
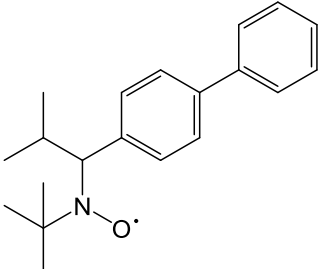


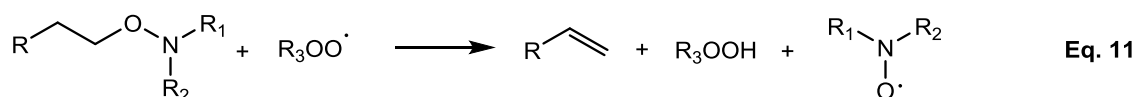
Table 2.3 shows that for a given alkyl structure, variation in nitroxide structure affects the  $k_c$  value, so it is hard to predict the  $k_c$  value for DBHA. However, similarly to *N,N*-dibenzylnitroxide, 9-azabicyclo[3.3.1]nonane-*N*-oxyl (ABNO) bears hydrogen on the  $\alpha$  carbon with respect to the nitrogen, so the  $k_c$  values for these two nitroxides are likely to be similar.

On the other hand, the rate of dissociation of alkoxyamines ( $k_d$ )<sup>49</sup> to reform nitroxide and alkyl radical is much smaller than  $k_c$ , but still dependent on the structures of the nitroxide radical, as shown in Table 2.4.

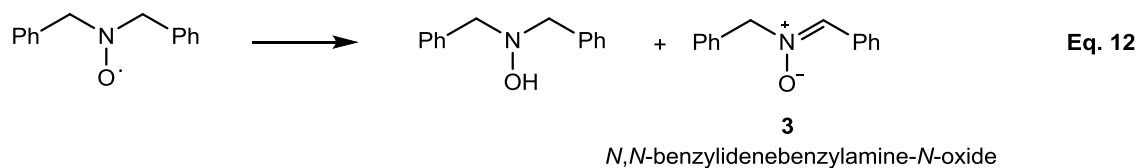
Table 2.4  $k_d$  values for a series of alkoxyamines at 120 °C in which the alkyl part is always styrene radical and the nitroxide part is varied<sup>49</sup>

Nitroxide	$k_d$ (s <sup>-1</sup> )
	1.32x10 <sup>-3</sup>
	2.85x10 <sup>-3</sup>
	1.32x10 <sup>-3</sup>

The rate of combination of nitroxides with alkyl radicals (Equation 10) is much smaller than the rate of reaction of oxygen with alkyl radicals (Equation 2). Moreover, in the presence of oxygen, nitroxide is regenerated by the reaction of alkoxyamines with peroxy radicals (Equation 11)<sup>20</sup>. For those reasons, nitroxide consumption in oxygenated systems is quite small compared to the consumption of nitroxide in the absence of oxygen.



*N,N*-dibenzylnitroxide is a relatively unstable radical due to the presence of four hydrogen atoms on the carbons  $\alpha$  to the nitrogen atom<sup>50</sup>. Unlike TEMPO, which can be stored at room temperature for a long time, the life-time of this kind of nitroxide is much shorter as it rapidly disproportionates to the corresponding hydroxylamine and nitrene (Equation 12).



The rate of disproportionation varies significantly for different nitroxides. Thus, the presence of bulky substituents or electron donating group next to the N-O moiety stabilises the radical and slows the decomposition rate. On the contrary, the disproportionation is accelerated with small or electron withdrawing substituents<sup>16,51</sup>.

## 2.1.2 Aim of the chapter

The above review shows that whilst the benefit of using DBHA as an antioxidant of the thermal styrene polymerisation is well documented, the information regarding the mechanism of inhibition is quite limited and always lacking of kinetic data. It is commonly accepted that DBHA stops propagation radicals by hydrogen abstraction by peroxide radicals, leading to *N,N*-dibenzyl nitroxide formation. However in oxygenated systems, *N,N*-dibenzyl nitroxide could be also generated by the oxidation of DBHA by molecular oxygen and the contribution of the latter process to the overall amount of nitroxide formed is unknown. One of the aims of this chapter is to provide the absolute concentrations of nitroxide in inhibited styrene polymerisations in the presence and absence of oxygen, in order to determine which chemical reactions control the nitroxide concentration. In addition, the estimation of the kinetic data for the oxidation of DBHA by oxygen at 110 °C is presented, as they are not available in the literature. As no literature data related to the reactivity of *N,N*-dibenzyl nitroxide towards styrene radical and its efficiency as a radical trap is available, a study on the possible role of *N,N*-dibenzyl nitroxide is presented. Although *N,N*-dibenzyl nitroxide is recognised as an unstable radical, the rate of decomposition proposed in the literature seems too high compared to our experimental results. The second part of this chapter therefore is dedicated to the investigation of the stability of this nitroxide, providing the kinetic parameters for the decomposition reaction at room temperature and 110 °C. We also tried to elucidate the reactivity of nitroxide and its contribution to the inhibition of the thermal styrene polymerisation and the data are shown herein.

## **2.2 Inhibition efficiency of *N,N*-dibenzylhydroxylamine in the thermally initiated styrene polymerisation**

Even though *N,N*-dibenzylhydroxylamine is commonly used as an inhibitor of the thermal styrene polymerisation in the presence of oxygen<sup>42, 43</sup>, the mechanism of inhibition is still not fully understood. In addition, most of the information regarding the use and the efficacy of this compound is reported in patents, which do not provide any mechanistic information. For those reasons, we decided to clarify the inhibition mechanism; our first concern was to prove the actual efficacy of DBHA in the inhibition of the thermal polymerisation of an air saturated solution of styrene. The inhibition was monitored by dilatometry, which is briefly introduced before the discussion of our results, dilatometry technique is introduced.

### **2.2.1 Dilatometry**

Dilatometry is a thermo-analytical method for monitoring the contraction or expansion of a liquid due to a change of temperature or progress of a chemical reaction. The latter is the reason for the use of this technique in this report. Due to the higher density of the polymer compared to monomer, a change of volume is observed when polymerisation occurs. Taking advantage of this property, dilatometry is often applied to monitor the inhibition properties of an additive. Indeed, if polymerisation is completely suppressed, no volume change is observed, if polymerisation occurs, volume is reduced. The time in which volume remains constant equals the inhibition time. In our experiments the polymerisation was monitored in sealed capillary tubes, which were affixed to a rigid sample rack. The sample rack was immersed in a beaker filled with paraffin. To control the temperature of the oil a thermocouple was used. Baffles helped to ensure good mixing essential for maintaining constant temperature (Figure.2.1). The entire procedure for estimating volume changes during the experiment and data processing is reported in detail in the experimental section.



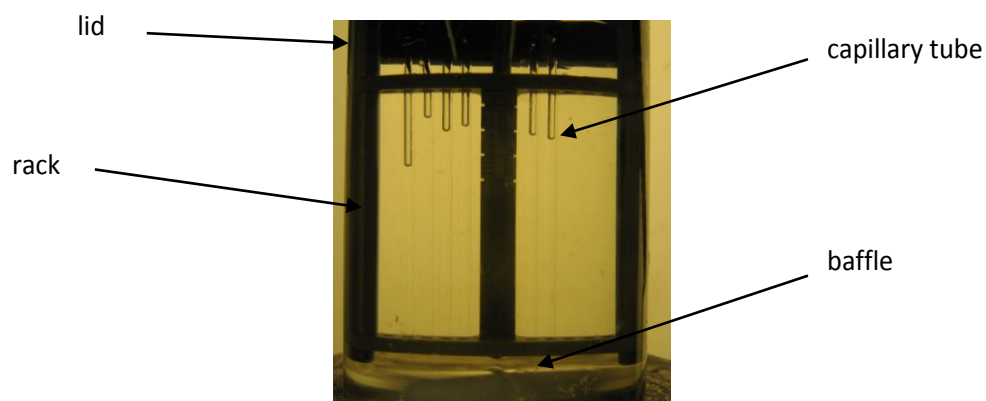


Figure 2.1 Dilatometer

## 2.2.2 Results

As reported in more detail in the experimental part (Section 5.3), different concentrations of DBHA in styrene were sealed in capillary tubes and immersed in an oil bath at 110 °C for 6.5 h. The % of conversion is plotted against time (Figure 2.2).

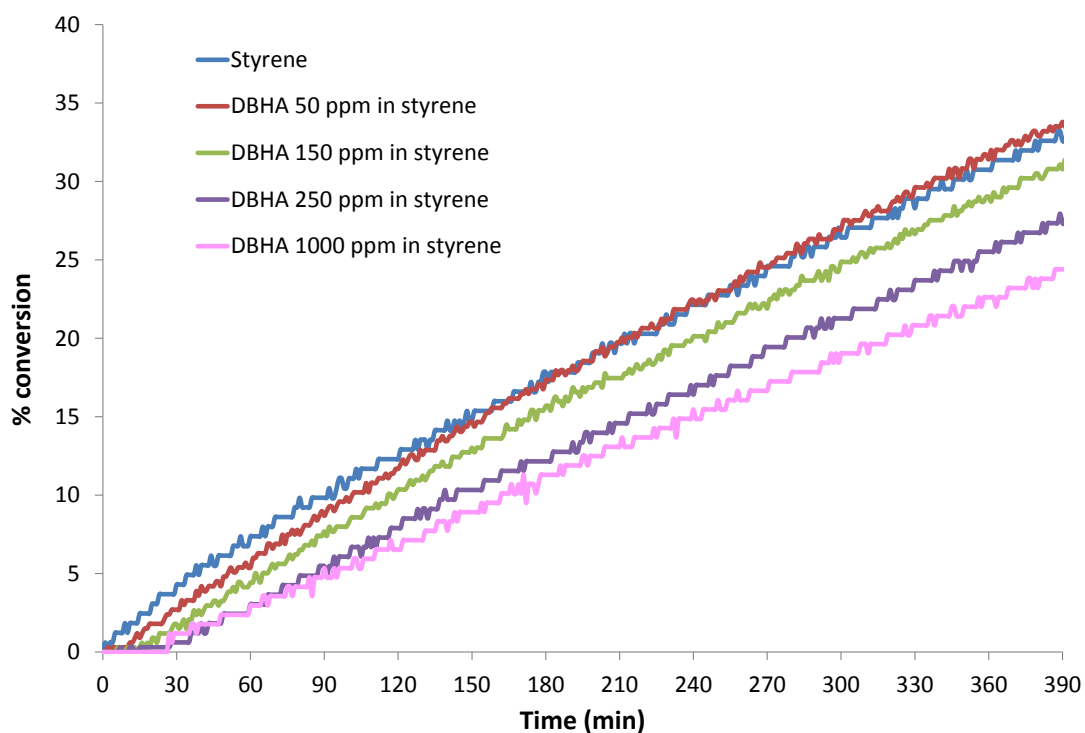
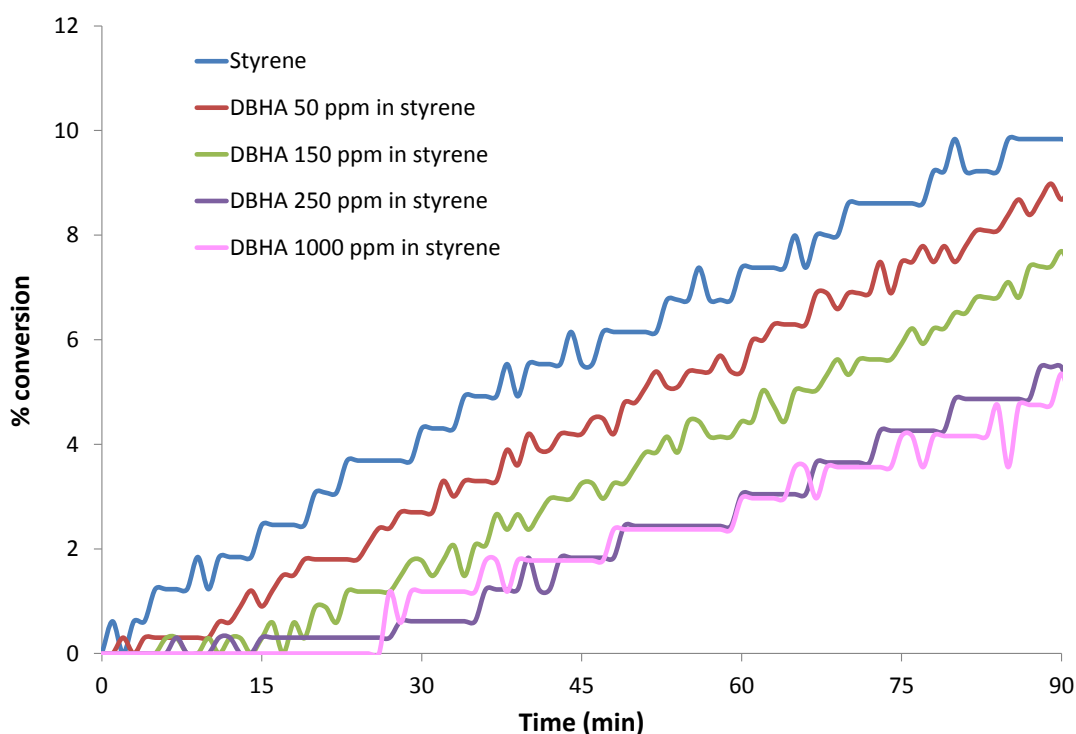


Figure 2.2 Dilatometry traces for the inhibition of the auto-initiated styrene polymerisation by DBHA

Figure 2.2 shows an initial flat line which correspond to the inhibition period. During the inhibition time the inhibitor works efficiently capturing most of the alkyl radicals formed and thus breaking the chain polymerisation. This period is generally followed by a retardation period in which only a portion of the propagation/initiation radicals is stopped. In case of retardation the line is not flat, but the slope is smaller than the reference (neat styrene). In this case the retardation is evident for 250 ppm and 1000 ppm.

An enlargement of Figure 2.2 is given in Figure 2.3. It is clear that there is an enhancement of the inhibition period with the increased concentration of the hydroxylamine.



**Figure 2.3 Enlargement of the chart in Figure 2.2**

By plotting the inhibition time vs the concentration of the inhibitor, a non-linear relationship was obtained (Figure 2.4). An increase of the DBHA concentration from 50 ppm to 250 ppm gives an increase of the inhibition time from  $11 \pm 3$  to  $28 \pm 3$  min, but no difference was shown between 250 ppm and 1000 ppm solutions.

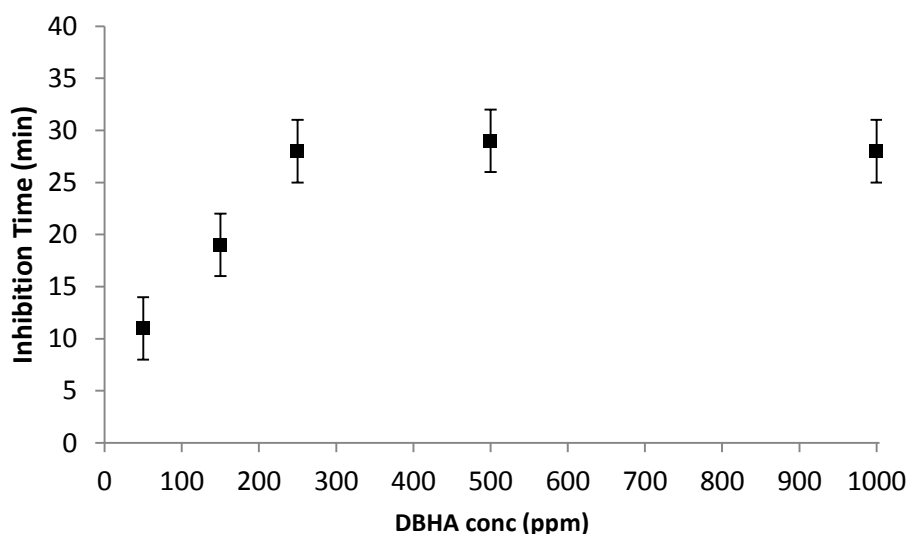
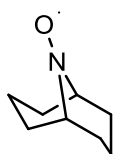


**Figure 2.4 Non-linear relationship between the inhibition time and DBHA concentration**

This behaviour suggests that for concentrations up to 250 ppm, DBHA is the limiting reagent compared to the oxygen dissolved in solution. Thus, the length of the inhibition period depends on DBHA concentration, and once all DBHA is consumed, the polymerisation proceeds unchecked. Indeed, the amount of oxygen dissolved in styrene at 35 °C is 45 ppm ( $3 \times 10^{-3}$  M)<sup>12</sup>, so it is reasonable to assume that at 110 °C oxygen is still in excess with respect to DBHA (250 ppm DBHA corresponds to  $1 \times 10^{-3}$  M). On the contrary, for DBHA concentrations above 250 ppm, oxygen becomes the limiting reagent, so the inhibition is now limited by the amount of oxygen dissolved in solution. Although this experiment does not allow any conclusions to be drawn about the mechanism of action of DBHA, we can expect oxygen to be crucial for the efficiency of DBHA inhibition, as already reported for similar hydroxylamines on the inhibition of styrene polymerisation<sup>52</sup>. Because our experiment was carried out in sealed capillary tubes, the system becomes quickly deoxygenated as oxygen is consumed during the polymerisation. Indeed, oxygen can either react with propagation radicals<sup>19</sup> or oxidise DBHA<sup>50</sup>. The inhibition period in Figure 2.2 for higher concentrations of DBHA probably corresponds to the complete consumption of oxygen during inhibited polymerisation. In the presence of dissolved oxygen, DBHA thus effectively inhibits polymerisation. However, in the absence of oxygen, the inhibition by hydrogen abstraction from DBHA becomes inefficient as the concentration of alkyl

radicals becomes higher than that of peroxy radicals. The hydrogen abstraction from DBHA by alkyl radical is slow<sup>24</sup> compared to the propagation rate of styrene polymerisation<sup>10</sup>. So in the absence of oxygen, the only reaction which could stop the polymerisation is the cross coupling between nitroxide and propagation radicals, but apparently this reaction cannot inhibit the polymerisation either. Although, the rate constant of reaction for *N,N*-dibenzyl nitroxide and propagation radical is unknown it is likely to be similar to that of ABNO ( $k_c \text{ ABNO} = 8.6 \times 10^8 \text{ M}^{-1} \text{ s}^{-1}$ ) as both bear hydrogen on the  $\alpha$  carbon with respect to the nitrogen<sup>16</sup>.



9-Azabicyclo[3.3.1]nonane *N*-oxyl (ABNO)

Thus, the inefficiency as inhibitor in deoxygenated systems could be attributed to the low concentration of nitroxide in solution that does not stop all propagation chains. This hypothesis is investigated and described in the next section.

## 2.3 *N,N*-Dibenzyl nitroxide as inhibitor

### 2.3.1 Monitoring *N,N*-dibenzyl nitroxide and oxygen evolution by EPR

As already anticipated in the previous paragraph, in deoxygenated systems the main inhibition process should be the coupling reaction between *N,N*-dibenzyl nitroxide and carbon-centred radical, and this reaction should have a rate constant close to  $10^8 \text{ M}^{-1} \text{ s}^{-1}$ <sup>16</sup>. However, in the absence of oxygen there is no inhibition, but only a slightly retardation at concentration of DBHA above 500 ppm (Figure 2.2). We moved therefore to investigate if in the absence of oxygen the concentration of *N,N*-dibenzyl nitroxide is too low to trap all the propagation chains. Thus, a parallel detection of both nitroxide and oxygen evolution during the inhibition was monitored by EPR. Before the discussion of results, EPR technique is introduced.

### **2.3.1.1 Electron Paramagnetic Resonance (EPR)**

Electron Paramagnetic Resonance is a suitable technique for the study of free radicals and all chemical species with one or more unpaired electrons<sup>53</sup>.

An electron is characterised by spin angular momentum  $S = 1/2$  and a spin quantum number  $m_s = \pm 1/2$ , therefore the electron spin can be in two states. In the absence of an external magnetic field these states have equal energy, and they are said to be *degenerate*. However, in the presence of an external magnetic field ( $B_0$ ) there is a splitting of the states. To explain this effect, it needs to be considered that the electron spin angular momentum  $S$  is correlated to a magnetic moment  $\mu_e$ :

$$\mu_e = g_e \mu_B S$$

Where  $g_e$  is  $g$  factor of electron ( $g_e = 2.002319$ ),  $\mu_e$  is the Bohr magneton.

The energy of a magnetic moment depends by the scalar product between  $\mu_e$  and  $B$ , hence the electron spin energy is correlated to the orientation of the magnetic moment with respect to  $B$ . Choosing the  $z$  axis as the arbitrary to represent  $B$ , the energy is expressed by the following equation:

$$E = -\mu_e \cdot B = g|\mu_B| m_s B_0$$

$B_0$  equals the magnetic field intensity. The electron spin can align either parallel ( $m_s = 1/2$ ) or antiparallel ( $m_s = -1/2$ ) to the magnetic field  $B_0$ , hence there is a splitting of the energy states (Figure 2.5). This effect is called Zeeman effect.

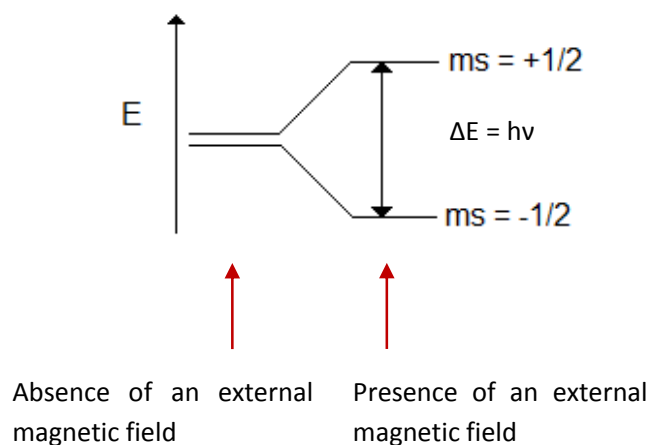


**Figure 2.5 Zeeman effect**

Hence, the energy difference between the two states can be described as:

$$\Delta E = g_e |\mu_B| B_0 = h\nu$$

When electromagnetic radiation, with energy equal to  $\Delta E$ , is absorbed by the sample the electron flips from the lower to the higher energy state.  $\Delta E$  depends on the magnetic field ( $B_0$ ) and the frequency of the electromagnetic radiation ( $\nu$ ). In EPR experiments, the frequency is kept constant while the magnetic field is swept. At a resonance condition the output signal corresponds to an absorption curve (Figure 2.6), however to improve the signal-noise ratio a second frequency (modulation frequency) with amplitude  $H_m$  is applied. The output amplitude, hence, corresponds to the slope of the absorbance curve and the observed spectrum would be its 1<sup>st</sup> derivative (Figure 2.6).

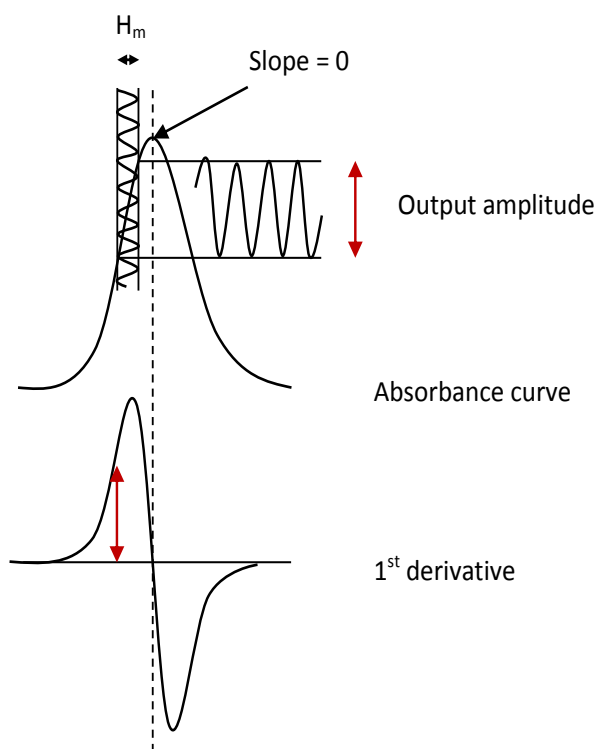


**Figure 2.6 EPR experiment**

Two important parameters in EPR are  $g$ -factor and hyperfine constant. The  $g$ -factor corresponds to the line position, in other words it is similar to chemical shift in nuclear magnetic resonance. Hyperfine constant represents the splitting of the signal due to the interaction of the electron with nearby nuclei with spin angular momentum  $I \neq 0$  (eg.  $^1\text{H}$ ,  $^{13}\text{C}$ ,  $^{14}\text{N}$ ) (Figure 2.7). Nuclear spin quantum number would be  $m_I = I, I-1, I-2, \dots$ , hence in the presence of an external magnetic field  $B_0$  the number of lines in the EPR spectrum is  $2I+1$ .

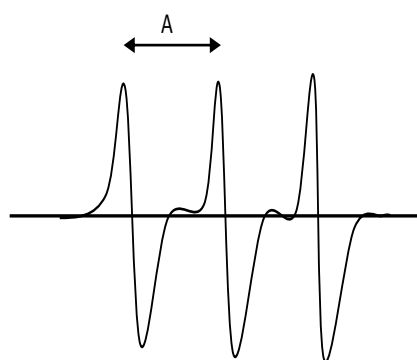


**Figure 2.7 EPR spectrum of TEMPO**

For instance, the interaction between proton ( $I=1/2$ ) and electron splits the two states of the electron (Zeeman splitting) in four states. Based on selection rules, transition occurs only with  $\Delta m_S = \pm 1$  and  $\Delta m_I = 0$ , hence here only two transitions are allowed and the resulting signal is a doublet (Figure 2.8).

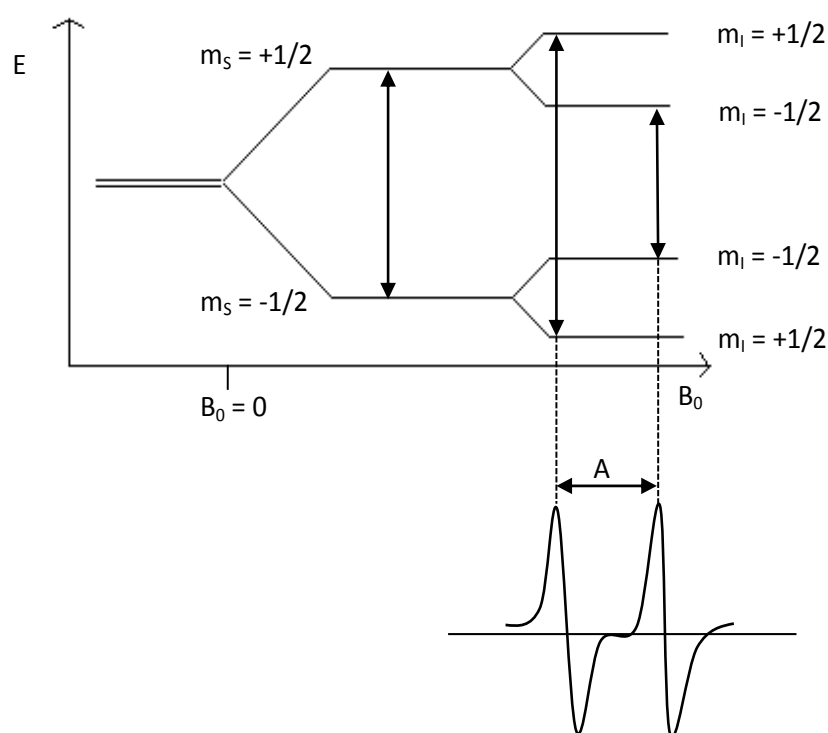


**Figure 2.8 Hyperfine splitting of  $^1\text{H}$**

Ideally line shape of EPR spectrum should be infinitely sharp, however broadening is caused by two different mechanisms, homogeneous and inhomogeneous<sup>54, 55</sup>. Homogeneous broadening is caused by spin-lattice, spin-spin and Heisenberg



interactions, which give a Lorentzian lineshape. Lorentzian broadening is related to the spin life time, the shorter the life time, the larger the linewidth. Gaussian broadening (inhomogeneous broadening), instead, maybe due to magnetic field non-uniformities, unresolved fine or hyperfine structures, electron-electron dipolar interactions<sup>56,57</sup>. The EPR spectrum results in a distribution of individual resonant lines into one overall line.

In systems with high concentration of radicals and rapid tumbling (e.g., fluid solutions), Heisenberg interaction leads to significant line broadening. Oxygen is a paramagnetic molecule, but it cannot be directly detected by EPR due to its fast relaxation, however oxygen can broaden EPR spectra of another paramagnetic electron spin (e.g., nitroxide). Broadening is proportional to oxygen concentration, thus for a series of EPR spectra with different oxygen concentration it is possible to estimate the relative oxygen concentration. Smirnov developed<sup>58, 59</sup> a convolution based fitting method (EWVoigt), which allows the extraction of the broadening function. Assuming that in dilute solution lineshape is determined by homogeneous interaction, this method allows the simultaneous estimation of oxygen and the other paramagnetic substance concentration<sup>13</sup>.

### **2.3.1.2 Results**

A solution of 2000 ppm DBHA in styrene was analysed at 110 °C as described in detail in the experimental part. The EPR spectrum of *N,N*-dibenzyl nitroxide is illustrated in Figure 2.9.

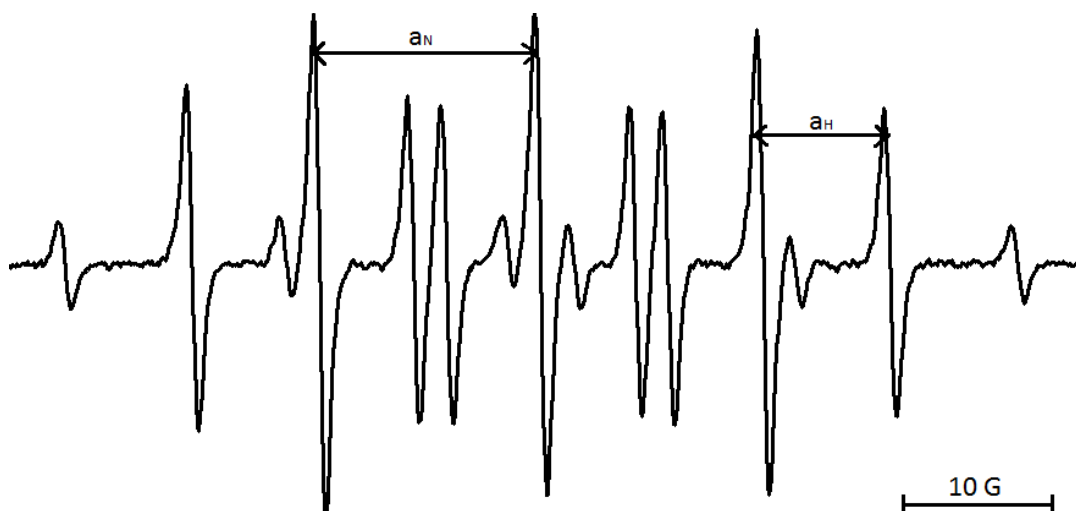


**Figure 2.9 EPR spectrum of *N,N*-dibenzylhydroxylamine**

The spectrum of *N,N*-dibenzylhydroxylamine in Figure 2.4 is characterised by 15 lines, a triplet of quintet with hyperfine values  $a_N$  17.0 G and  $a_H$  10.0 G.

EPR spectra were recorded for a sealed solution of 2000 ppm DBHA in styrene every 2.7 min at 110 °C for 2 h. A sharpening of the EPR spectra was observed due to the oxygen consumption during the polymerisation. The concentration of oxygen is reduced due to the reaction of oxygen with either alkyl radicals to form peroxy radicals, or *N,N*-dibenzylhydroxylamine. Using a convolution-based fitting method (EWVoigt software<sup>60</sup>), oxygen concentrations were estimated and plotted against the absolute nitroxide concentration, as shown in Figure 2.10.

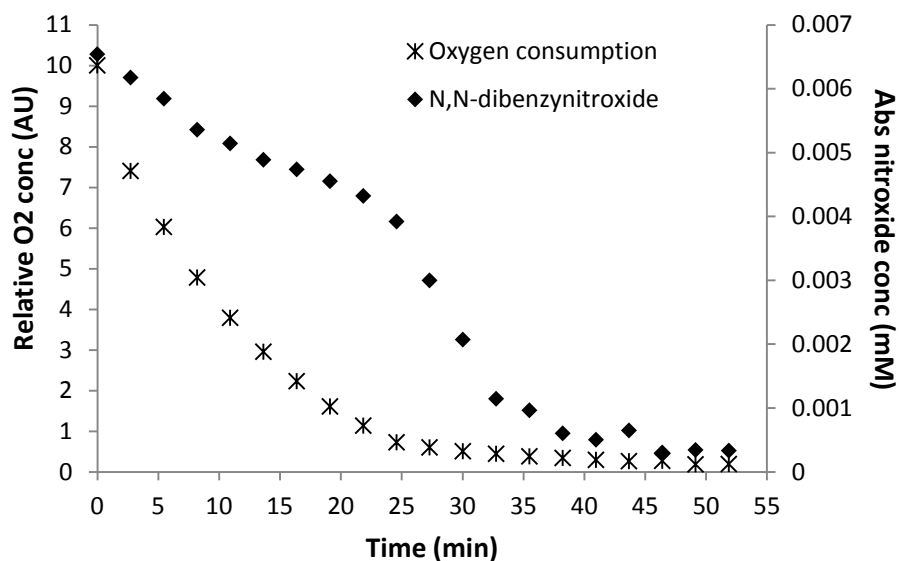


**Figure 2.10** Evolution of *N,N*-dibenzylnitroxide and oxygen concentrations in 2000 ppm DBHA in styrene at 110 °C

The data in Figure 2.10 represent the oxygen consumption (stars) and the *N,N*-dibenzylnitroxide concentration (diamonds). The arbitrary initial value on the Y axis (10) was chosen for the initial concentration of oxygen in the sample, as it was easy to compare the data with those of nitroxide on the same axis. In addition, the absolute *N,N*-dibenzylnitroxide concentration was estimated comparing the area of each nitroxide EPR signal to the area of a signal produced by a 1 mM TEMPO standard solution in toluene. The analysis of Figure 2.10 shows that nitroxide is rapidly formed and reaches the maximum concentration of  $6.5 \times 10^{-3}$  mM before the first measurement is taken. The kinetic profile shows the relationship between nitroxide and oxygen consumption, both are consumed simultaneously, in particular, when the system becomes totally deoxygenated, nitroxide concentration is close to zero.

By comparing the data in Figure 2.10 with those in Figure 2.3, some conclusions can be drawn. After approximately 30 min, DBHA becomes inefficient as inhibitor regardless of the initial DBHA concentration (Figure 2.3), which corresponds to the point in time when the system becomes completely deoxygenated and nitroxide concentration is below  $1 \times 10^{-3}$  mM (Figure 2.5). This implies that the absence of oxygen is responsible for the inefficiency of DBHA and consequently for the disappearance of nitroxide in solution.

A combination of EPR and dilatometry analyses shows that in the presence of oxygen DBHA stops the polymerisation by hydrogen abstraction. In deoxygenated systems DBHA stops working as an inhibitor. Furthermore, EPR experiment reveals the presence of nitroxide only when oxygen is dissolved in solution. The next section considers the mechanism of nitroxide formation.

### **2.3.2 Oxidation of *N,N*-dibenzylhydroxylamine by oxygen**

As mentioned in the previous paragraph, we have demonstrated that during the inhibition of the thermally initiated styrene polymerisation by DBHA, *N,N*-dibenzyl nitroxide is only formed in the presence of oxygen. Thus, we needed to understand if the nitroxide is originated from the oxidation of DBHA by molecular oxygen or if it is the product of the hydrogen abstraction from DBHA by peroxy radicals.

In order to estimate the rate of DBHA oxidation with molecular oxygen, EPR analysis of DBHA solution in a non-polymerizable system was carried out in air and under nitrogen atmosphere. In the first case, approximately 70  $\mu\text{L}$  of 3000 ppm DBHA in diphenyl ether were introduced in a capillary tube, which was sealed at both ends. For the analysis under nitrogen atmosphere, instead, the solution was analysed in a Pasteur pipette sealed on the top with a plastic cap to allow the degassing of the solution by purging nitrogen gas for 15 min. The samples were heated at 110  $^{\circ}\text{C}$  in the EPR cavity and the spectra were recorded every 2.7 min for 6 h (Figure 2.11).

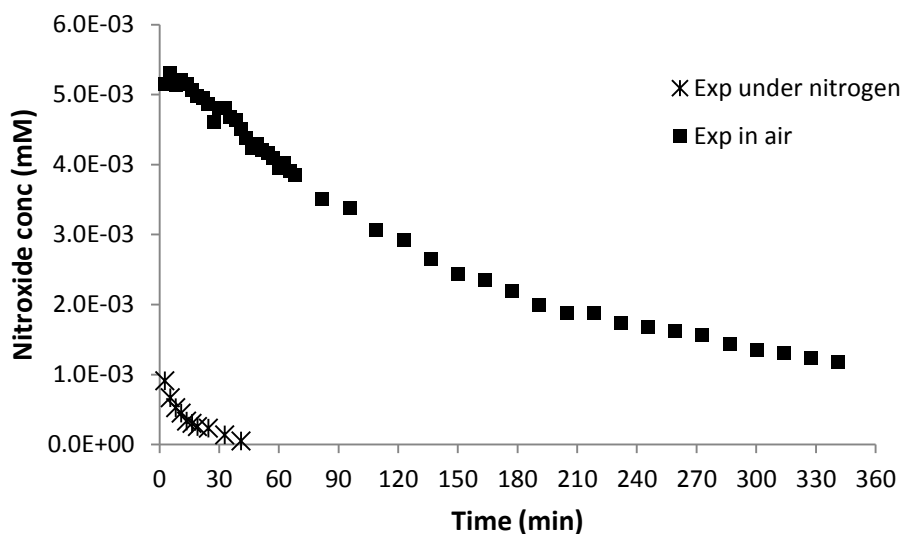


**Figure 2.11** Evolution of nitroxide concentration for a 3000 ppm DBHA in diphenyl ether under nitrogen (stars) and air atmosphere (squares)

The analysis of Figure 2.11 shows that DBHA can be oxidised by the oxygen present in solution as *N,N*-dibenzyl nitroxide is only formed in air. In a nitrogen atmosphere the amount of nitroxide is negligible, there is a weak signal, and it is reasonable to assume that it is largely due to the residual oxygen in the sample.

The kinetic parameters were estimated by using Dynafit, assuming a two steps mechanism as shown in Figure 2.12. DBHA is oxidized by the molecular oxygen in the first step leading to *N,N*-dibenzyl nitroxide formation. This step is followed by the disproportionation of nitroxide to *N,N*-benzylidenebenzylamine-*N*-oxide and DBHA.

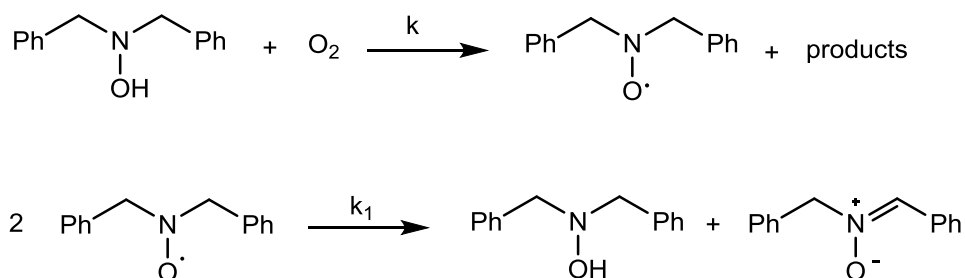


**Figure 2.12** Oxidation mechanism of DBHA

The oxygen concentration dissolved in solution was assumed to be  $1 \times 10^{-3}$  mol/L. The data for the oxygen solubility at high temperature in DPE were not available, however combining the solubility of oxygen in different organic solvents<sup>26</sup> with the solubility

curves at different temperatures<sup>61</sup>, could be extrapolated that this concentration is quite reasonable. The fitting of the experimental *N,N*-dibenzylnitroxide concentrations with the theoretical concentrations is reported in Figure 2.13, and the evolution of DBHA concentration estimated by Dynafit<sup>62</sup> is reported in Figure 2.14.

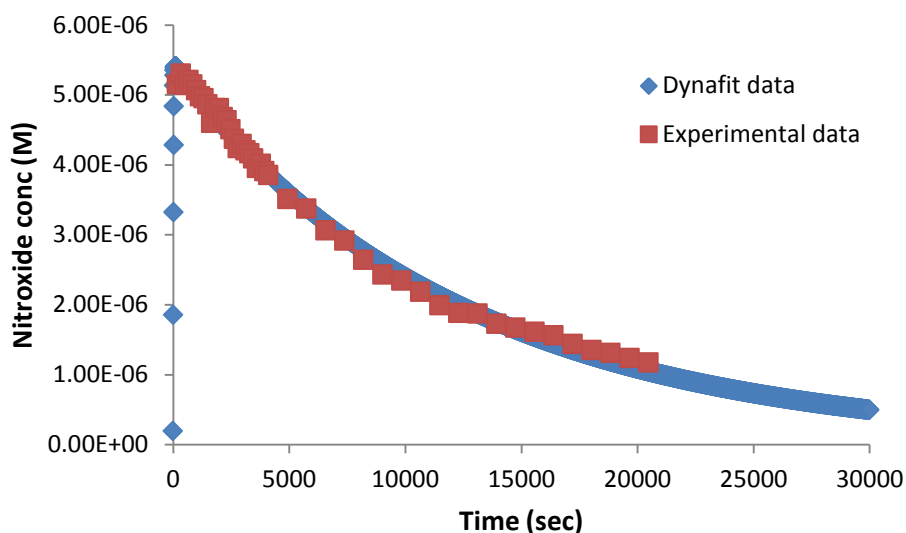


**Figure 2.13 Nitroxide evolution during the oxidation of 3000 ppm DBHA in DPE at 110 °C: Experimental data (squares), Dynafit data (diamonds)**

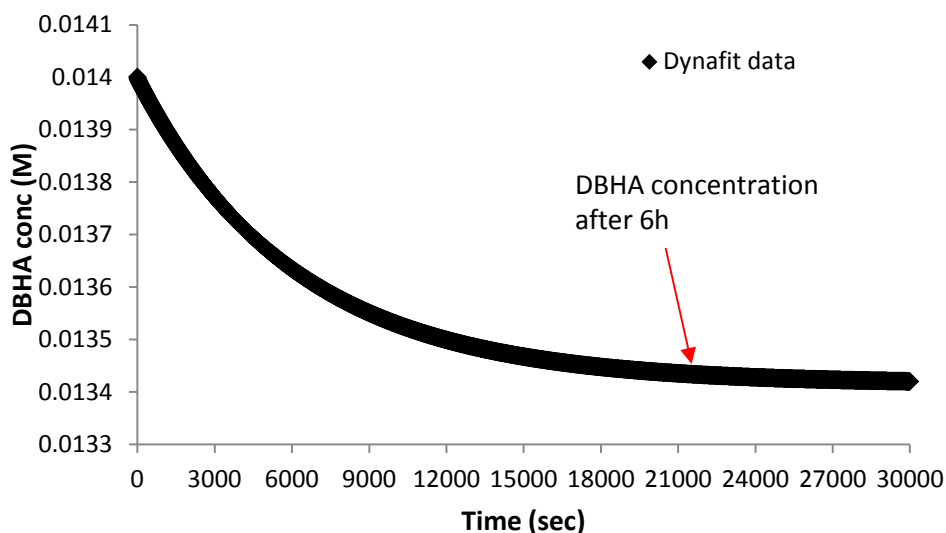


**Figure 2.14 Simulation of the consumption of 3000 ppm DBHA in DPE at 110 °C by molecular oxygen**

The oxidation of DBHA by oxygen is extremely fast, and the rate constant cannot be determined, however the rate constant of *N,N*-dibenzylnitroxide disproportionation

( $k_1$ ) is  $3245 \pm 33 \text{ M}^{-1}\text{s}^{-1}$ . Figure 2.13 shows a good agreement between the experimental and theoretical data. In addition, Figure 2.14 shows that after 6 h most of DBHA is still unreacted and the concentration of the hydroxylamine in solution is approximately 0.0135 M. Subtracting this value from the initial concentration, we can estimate the amount of DBHA reacted and calculate the amount of oxygen consumed after 6 h, which is  $5 \times 10^{-4} \text{ M}$ . This means that after 6 h half of the initial amount of oxygen is still unreacted.

Comparison of the initial nitroxide intensity in 3000 ppm DBHA air saturated solutions in styrene and in diphenyl ether (DPE) shows that there is a slightly higher nitroxide formation in styrene with respect to the solution in DPE (Figure 2.15). In DPE, the nitroxide is formed only by DBHA oxidation, but in styrene the nitroxide can also be formed by the hydrogen abstraction from DBHA by peroxy radicals. On the other hand, the nitroxide signal in DPE is more persistent than in styrene. In DPE, the nitroxide is consumed only by a disproportionation reaction, but in styrene the consumption of nitroxide is more complex.

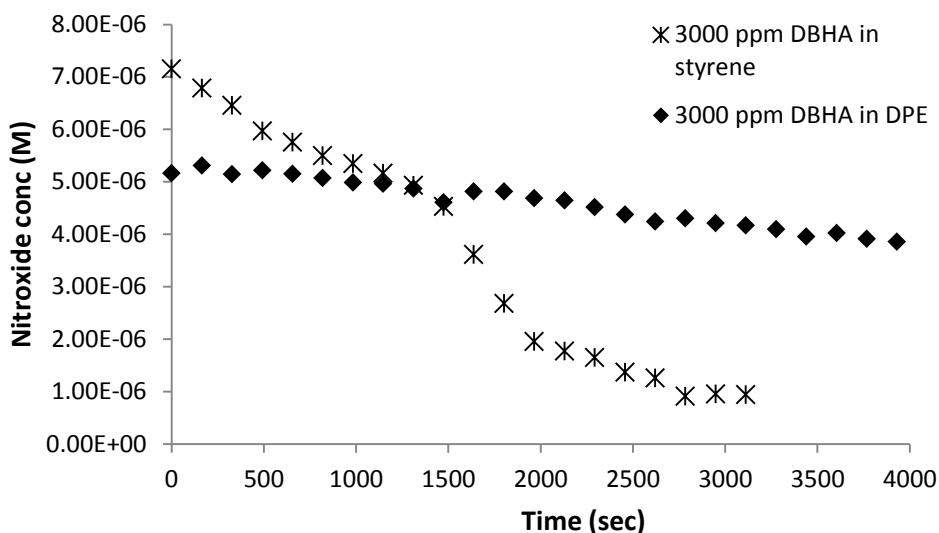


**Figure 2.15 Nitroxide evolution in 3000 ppm DBHA in styrene (stars) and 2000 ppm DBHA in diphenyl ether (diamonds)**

Looking at the data in Figure 2.15, it is clear that during the inhibition of styrene polymerisation by DBHA, most of the nitroxide in solution comes from the oxidation of

DBHA by dissolved molecular oxygen and not from the reaction of DBHA with peroxy radicals.

Based on the results obtained so far, we can conclude that DBHA shows a good inhibition of the air-saturated auto-initiated styrene polymerisation due to the effective hydrogen abstraction from DBHA by peroxy radicals. If oxygen is in excess compared to DBHA, the inhibition time depends on the concentration of the latter. Indeed in the absence of oxygen, DBHA stops working since the number of oligostyryl radicals outnumbers peroxy radicals and the hydrogen abstraction from hydroxylamine by propagation radicals is not efficient. The EPR data show that in the presence of oxygen, a small amount of *N,N*-dibenzyl nitroxide is formed. As confirmed by previous experiments, most of this nitroxide is originated from the oxidation of DBHA by the molecular oxygen dissolved in solution. The rate constant of *N,N*-dibenzyl nitroxide disproportionation at 110 °C was estimated as  $3245 \pm 33 \text{ M}^{-1} \text{ s}^{-1}$ , which suggests that for an averaged concentration of  $2.5 \times 10^{-6} \text{ M}$  (Figure 2.13), the half-life at this temperature is approximately 125 s. This finding was quite unexpected as from the information available in the literature this nitroxide should have been substantially more unstable<sup>5</sup>. The following sections describe a study of the stability of *N,N*-dibenzyl nitroxide and the attempts to investigate its properties as a radical trap.

### 2.3.3 *N,N*-Dibenzyl nitroxide as a radical trap

In order to investigate the role of nitroxide in the inhibition of styrene polymerisation, the isolation of a relative pure solution of *N,N*-dibenzyl nitroxide was needed. As evidenced by the results presented in the previous section, the rate constant for *N,N*-dibenzyl nitroxide disproportionation, generated by the oxidation of DBHA by the oxygen in a diphenyl ether solution at 110 °C, is  $3245 \pm 33 \text{ M}^{-1} \text{ s}^{-1}$ , with a life-time of about 125 s at  $2.5 \times 10^{-6} \text{ M}^{-1} \text{ s}^{-1}$  concentration (Figure 2.13). This suggests that the half-life time of *N,N*-dibenzyl nitroxide at room temperature would be much larger, approximately  $10^4$  times if we consider that the rate constant triples with the increase in temperature by 10 °C. Although this is a big approximation, we were confident that *N,N*-dibenzyl nitroxide was more stable than what was reported in the literature<sup>5</sup>. By generating *N,N*-dibenzyl nitroxide from the photolysis of DBHA in the presence of di-



*tert*-butyl peroxide, the rate constant for the disproportionation at 25 °C was reported as  $9.1 \times 10^3 \text{ M}^{-1} \text{ s}^{-1}$  in benzene and  $41 \times 10^3 \text{ M}^{-1} \text{ s}^{-1}$  in isopentane. These data seemed quite inconsistent with our results and thus, in order to confirm the feasibility of synthesising solutions of nitroxide, we estimated the kinetic data for the nitroxide decomposition at room temperature. This section is thus divided into two main sections, the first one discusses the stability of nitroxide at room temperature and the second one reports the attempted synthesis of *N,N*-dibenzylnitroxide. The followings are example of stable nitroxides present in the literature.

As reported in the review published by Nilsen and Braslau<sup>50</sup>, nitroxides with at least one hydrogen atom on the carbon  $\alpha$  to the nitrogen atom disproportionate to the corresponding hydroxylamine and nitrene. However, the stability of these nitroxides is strongly dependent on the polar and steric factors<sup>63</sup>. Thus, if the molecule is stabilised enough, even a nitroxide bearing  $\alpha$  hydrogen atoms can be stable for an unlimited period of time. Indeed, there are several examples of stable nitroxides with hydrogen atom on the carbon next to the nitrogen<sup>64,65</sup>, as shown in Figure 2.16.

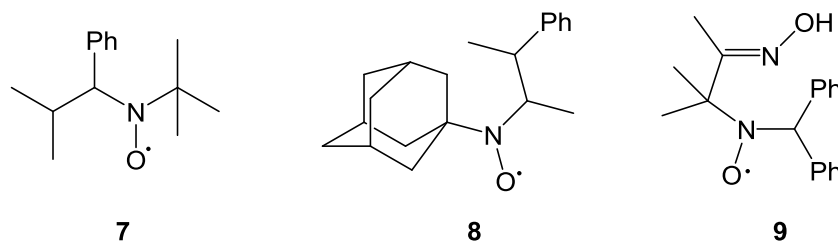
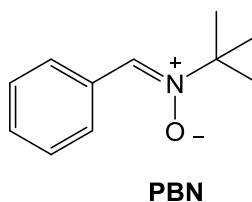


**Figure 2.16** Examples of stable nitroxides with a hydrogen atom on the carbon  $\alpha$  to the nitrogen atom

Less stable nitroxides, but with a structure more similar to *N,N*-dibenzylnitroxide are the adducts of the phenyl-*tert*-butyl nitrene (PBN).



PBN is a common spin trap and a wide range of radicals have been captured by this nitron and their decay monitored by EPR. One example is the phenylsilyl adduct generated by the photochemical activation of di-*tert*-butyl peroxide in the presence of silane and PBN<sup>66</sup>. The adduct shows a half-life of about 5 s at 25 °C.

The above discussion suggests that the stability of nitroxide is strongly dependent on the structure and also nitroxides with  $\alpha$  hydrogen may have a reasonable life-time. Hence, an investigation of the stability of *N,N*-dibenzyl nitroxide at room temperature was carried out.

### **2.3.3.1 A study of the stability of *N,N*-dibenzyl nitroxide at room temperature**

We needed to be sure that the life-time of nitroxide at room temperature was long enough before attempting any isolation of this compound. To assess its stability, the nitroxide was generated and its decay monitored by EPR.

3000 ppm DBHA solution was prepared and ca. 0.5 mL of this solution were transferred in an EPR tube. The solution was heated at 110 °C for three minutes, to allow the formation of a reasonable concentration of nitroxide. After this time the solution was quickly cooled down to room temperature and deoxygenated by purging nitrogen gas through it for 1 min, to stop the further oxidation of DBHA. The EPR tube was sealed with a plastic cap and EPR spectra were recorded at 25 °C every 18 min. The rate constant of disproportionation was estimated using Dynafit<sup>62</sup> (Figure 2.17).

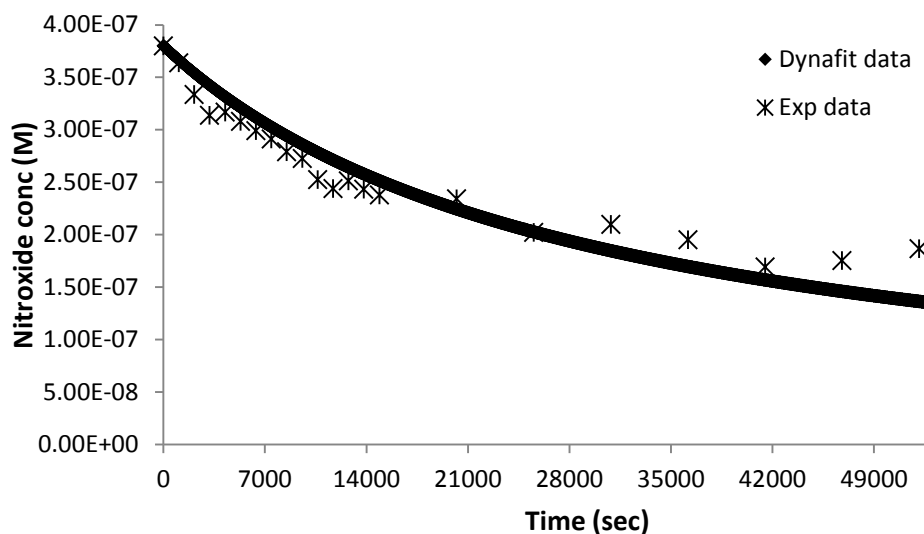


**Figure 2.17** *N,N*-dibenzylnitroxide decay at 25 °C, generated by the oxidation of 3000 ppm DBHA at 110 °C. The stars represent the experimental data and the diamonds corresponds to the data simulated by Dynafit

Figure 2.17 shows the comparison between the simulated data. The simulation was carried out assuming that *N,N*-dibenzylnitroxide decays as a second order process. One can see that there is not a perfect match between the experimental and the semi-empirical data. In order to exclude the possibility of a reverse reaction, comproportionation, the sample was analysed again after a day and the EPR signal almost disappeared. Hence, we can rule out the equilibrium process. The rate constant for the second order decay, estimated using Dynafit software, is  $45 \text{ M}^{-1}\text{s}^{-1}$ , so for a concentration of  $2.5 \times 10^{-7} \text{ M}$  the half life time of *N,N*-dibenzylnitroxide at 25 °C is about 24 h. Assuming that the rate constant was  $41000 \text{ M}^{-1} \text{ s}^{-1}$ , as reported by Ingold<sup>5</sup>, the half-life would have been only 97 s. The simulation of the nitroxide decay using our data and those reported in the literature, are shown in Figure 2.18.

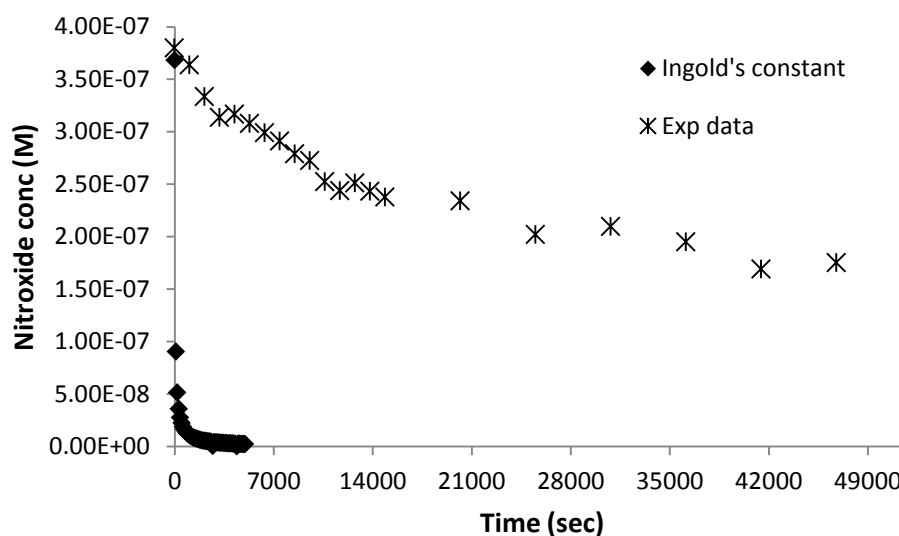


**Figure 2.18** Simulation of the *N,N*-dibenzylnitroxide decay using the rate constant reported by Ingold, 41000 M-1s-1 (diamonds). The experimental data are reported as a comparison (stars)

Figure 2.18 shows that there is a significant discrepancy between our experimental data and those simulated using the rate constant reported in the literature.

In view of these encouraging results we decided to embark on the synthesis of *N,N*-dibenzylnitroxide. However, conscious of the poor stability of *N,N*-dibenzylnitroxide we were not expecting to isolate this compound, but we thought that the generation of a relative pure solution of *N,N*-dibenzylnitroxide in a reasonable concentration was a realistic possibility. Indeed, the half-life time of a  $1 \times 10^{-4}$  M solution of *N,N*-dibenzylnitroxide would be approximately 4 min, and this time is long enough to carry out some investigations of the *N,N*-dibenzylnitroxide reactivity.

In the next section a comprehensive work on the synthesis of *N,N*-dibenzylnitroxide is described.

### **2.3.3.2 Synthesis of *N,N*-dibenzylnitroxide**

The first part of this section describes the efforts to synthesise *N,N*-dibenzylnitroxide using the procedures reported in literature. Although in most of these papers the aim was the isolation of pure nitroxide, in our case this was probably not possible due to limited stability of the nitroxide. Our main objective was the generation of a

reasonable pure solution of nitroxide with high enough concentration to allow the study of the reactivity of *N,N*-dibenzyl nitroxide.

Nitroxides such as TEMPO are commonly prepared by the treatment of the corresponding hydroxylamines with mild oxidants, with or without catalyst<sup>50</sup>. Alewood and co-workers<sup>67</sup> synthesised and isolated a series of acyl nitroxides from hydroxamic acid. They used nickel peroxide (or silver oxide) in the presence of sodium sulphate as the oxidising agent. An alternative oxidation was carried out by Sen *et al.*<sup>68</sup> in aqueous alkaline  $K_3Fe(CN)_6$ . They also conducted an interesting study of the catalytic oxidation of 1-hydroxypiperidines by  $K_2WO_4$  and  $H_2O_2$  at room temperature. Kirilyuk's group, in a recent paper in 2004<sup>69</sup>, isolated several 2,2,5,5-tetraethylimidazole nitroxides using  $MnO_2$  in chloroform to oxidise the corresponding hydroxylamines. Other nitroxides were formed by the oxidation of the parent amines using Kirilyuk's method, an example is the work of Couet *et al.*<sup>70</sup>. They prepared and isolated piperidine and pyrrolidine nitroxides. Hydrogen peroxide and sodium tungstate were used at 0°C in aqueous methanol. Ingold and co-worker<sup>5</sup> generated *N,N*-dibenzyl nitroxide by photolysis of *N,N*-dibenzylhydroxylamine in the presence of di-*tert*-butyl peroxide. However, they could not isolate the final products. Pedulli *et al.* generated<sup>71</sup> *tert*-butyl nitroxide by mixing the corresponding amine with a solution of magnesium monoperoxyphthalate. In order to achieve high enough concentration of the nitroxide, they generated the radical by continuous-flow experiments. The same flow technique was used by Gutch and Waters<sup>72</sup>. They oxidized hydroxylamine and *N*-substituted hydroxylamine, with ferricyanide in alkaline conditions. Both Serianz and Cowley's research groups generated *N,N*-dibenzyl nitroxide and characterised it *in situ*. Serianz<sup>73</sup> used *tert*-butyl-hydroperoxide in a saturated solution of DBHA in benzene. Cowley<sup>74</sup> produced nitroxide in basic conditions using copper (II) as an oxidizing agent. Finally, Reznikov and Volodarsky<sup>65</sup> synthesised and isolated the acyclic nitroxide (compound **(9)**, Figure 2.16) by oxidation of the corresponding hydroxylamine with  $MnO_2$ .

The synthesis proved more challenging than we expected and despite a wide range of oxidising agents and conditions tested, the yields of reactions were always rather low, as reported in Table 2.5. It needs to be clarified that in this case the yield is not

referred to the amount of *N,N*-dibenzyl nitroxide isolated, but to the estimation of the nitroxide formed in solution by comparing the intensity of EPR signal of the product with that of a standard solution of TEMPO.

**Table 2.5 Reaction conditions for the synthesis of *N,N*-dibenzyl nitroxide**

	DBHA (mmol)	Oxidant	Oxidant (mmol)	Solvent	V (mL)	T (°C)	Time (min)	Yield (%)
1	$2 \times 10^{-2}$	O <sub>2</sub>	sat <sup>a</sup>	Tol <sup>b</sup>	2.5	80	1200	/
2	0.4	(CH <sub>3</sub> ) <sub>3</sub> C-OOH <sup>c</sup>	0.8	Tol <sup>b</sup>	1	RT	6	/
3	0.4	(CH <sub>3</sub> ) <sub>3</sub> C-OOH	0.8	H <sub>2</sub> O/DCM <sup>d</sup>	5	RT	10	$7 \times 10^{-3}$
4	1	H <sub>2</sub> O <sub>2</sub> <sup>e</sup>	5	H <sub>2</sub> O/DCM <sup>d</sup>	15	RT	10	$7 \times 10^{-2}$
5	0.8	H <sub>2</sub> O <sub>2</sub> <sup>f</sup>	0.9	CH <sub>3</sub> OH	0.8	RT	180	/
6	$4 \times 10^{-2g}$	MMPP <sup>h</sup>	$4 \times 10^{-2}$	H <sub>2</sub> O	50	RT	240	$2 \times 10^{-2}$
7	$2 \times 10^{-2g}$	MMPP <sup>h</sup>	$2 \times 10^{-2}$	H <sub>2</sub> O	50	60	2	/
8	0.5	Pd/C	$4 \times 10^{-2}$	Tol <sup>b</sup>	2.5	110	2	$1 \times 10^{-2}$
9	1.4	Pd/C	0.1	Tol <sup>b</sup>	7.5	40	10	$4 \times 10^{-2}$
10	0.5	Pd/C	0.2	Tol <sup>b</sup>	250	RT	180	0.4
11	0.5	NiO <sub>2</sub>	0.2	DCM	25	RT	10	$5 \times 10^{-2}$
12	0.5	ZnO	0.3	DCM	25	RT	20	$5 \times 10^{-2}$
13	0.5	Ag <sub>2</sub> O	0.1	DCM	25	RT	8	0.7
14	0.5	Ag <sub>2</sub> O <sup>i</sup>	0.1	DCM	25	RT	15	1.2

a) The solution was saturated with pure oxygen, purging the gas through the solution for 15 s; b) toluene; c) tert-butyl peroxide; d) H<sub>2</sub>O/DCM 1:1; e) To a solution of DBHA in DCM (5 mL), a solution of H<sub>2</sub>O<sub>2</sub> in water (10 mL) was added. Then, under vigorous stirring, copper sulphate ( $6 \times 10^{-3}$  mmol) was added; f) to a solution of DBHA and H<sub>2</sub>O<sub>2</sub> in methanol (45% in water), Na<sub>2</sub>WO<sub>4</sub>·2H<sub>2</sub>O ( $3 \times 10^{-2}$  mmol) was added; g) *N,N*-dibenzylamine was used rather than *N,N*-dibenzylhydroxylamine; h) Magnesium monoperoxyphthalate; i) MgSO<sub>4</sub> ( $2 \times 10^{-2}$  mmol) was added to the solution to remove the water produced.

The best conditions for the nitroxide formation were obtained using silver oxide as an oxidant. DBHA, Ag<sub>2</sub>O and MgSO<sub>4</sub> were mixed in dichloromethane and left under

vigorous stirring at room temperature for 15 min (Detailed conditions in the experimental section). An aliquot of the reaction mixture (ca. 0.1 mL) was injected in a bottom sealed Pasteur pipette and transferred to the EPR cavity. The amount of nitroxide produced was estimated by comparing the double integral of *N,N*-dibenzyl nitroxide signal with that of a standard solution of 1 mM TEMPO. The amount of nitroxide formed in solution was approximately  $6 \times 10^{-3}$  mmol, corresponding to 1.2% yield.

Using the best conditions for the generation of nitroxide, we carried out a few attempts to remove the excess of DBHA and nitron from the solution in order to obtain a reasonable pure solution of *N,N*-dibenzyl nitroxide. In all these cases silver oxide was removed by filtration before starting the purification process.

In the first attempt, a pH 4.65 buffer solution sodium acetate/acetic acid was added to the reaction mixture to protonate DBHA and the mixture extracted. We hoped that the hydroxylamine would transfer to the aqueous phase leaving nitroxide and nitron in the organic phase. After the acidification the solution was neutralized with water and then dried over  $\text{MgSO}_4$  and filtered. TLC showed that DBHA was not removed from the organic phase.

A silver-loaded sulfonic acid resin (Dowex<sup>®</sup> DR 2030) was used to purify the reaction mixture. The resin was prepared following the literature procedure<sup>75</sup> and loaded into a Pasteur pipette. The ion exchange resin surface has silver sulfite functional groups. The rationale was that the nitroxide would form a silver complex and thus get retained by the column, allowing the separation from the hydroxylamine and nitron. However, an EPR analysis of the solution after column, confirmed that nitroxide was still in the reaction mixture.

To summarise, we have optimised the conditions to make *N,N*-dibenzyl nitroxide from the oxidation of the corresponding *N,N*-dibenzyl hydroxylamine. The aim of the synthesis was the generation of a solution of relatively pure *N,N*-dibenzyl nitroxide in order to explore the reactivity of this nitroxide towards styrene radicals. However, attempts of purify *N,N*-dibenzyl nitroxide were unsuccessful. Thus, we had to find an

alternative way to explore the reactivity of *N,N*-dibenzyl nitroxide towards styrene radicals. In order to probe the involvement of *N,N*-dibenzyl nitroxide in the inhibition, we carried out product analysis. In the next section trapping of styrene radicals by *N,N*-dibenzyl nitroxide is demonstrated by the isolation of the coupling product from the reaction mixture.

### 2.3.3.3 Isolation of the alkoxyamine from the reaction mixture

The combination of dilatometry and EPR experiments revealed that in the absence of oxygen the concentration of nitroxide in solution is close to zero and in these conditions DBHA does not show any inhibition of the thermal styrene polymerisation. We therefore needed to clarify if the inefficiency of DBHA in deoxygenated systems is due to the low concentration of nitroxide in solution or the inability of nitroxide to trap any radicals. As the isolation of *N,N*-dibenzyl nitroxide proved to be challenging, we had to find another method of testing its reactivity towards oligostyryl radicals. Thus, we decided to analyse the DBHA inhibition products in the thermal styrene polymerisation. The presence of alkoxyamines such as the alkoxyamine (**11**) in Figure 2.19 would be the evidence that *N,N*-dibenzyl nitroxide can trap propagation radicals.

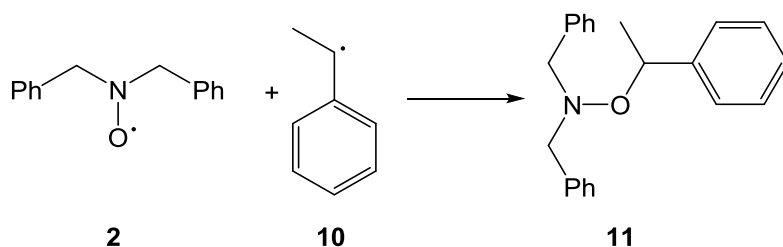


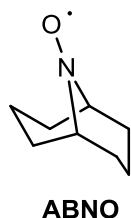
**Figure 2.19** Formation of the alkoxyamine **11** from the reaction between *N,N*-dibenzyl nitroxide (**2**) and styrene radical (**10**)

A complete description of the reaction conditions and the full characterisation of the inhibition products are reported in Chapter 5. For the discussion in this section it is only important to know that from the scale-up of the inhibition of the styrene polymerisation by DBHA under nitrogen atmosphere we have isolated the alkoxyamine (**11**) with 13% yield (the yield is based on the initial amount of DBHA used).

The presence of the alkoxyamine (**11**) in the reaction mixture proves that *N,N*-dibenzyl nitroxide can trap styrene radicals. Although this experiment does not give any



kinetic information about the coupling reaction between styrene radicals and nitroxide we can assume that the rate constant is similar to that of 9-azabicyclo[3.3.1]nonane-*N*-oxyl ABNO ( $9 \times 10^8 \text{ M}^{-1}\text{s}^{-1}$ ), as both structures bear  $\alpha$  hydrogen atoms.



In addition, our previous experiments showed that the rate constant of disproportionation of nitroxide at 110 °C is  $3245 \pm 33 \text{ M}^{-1}\text{s}^{-1}$ , which is significantly smaller than the rate constant of coupling reaction. This is a further confirmation that *N,N*-dibenzylnitroxide is stable enough to allow the trapping of propagation chains. The combination of our previous dilatometry and EPR experiments suggests that in the absence of oxygen there is no inhibition and the absolute nitroxide concentration is close to zero. The isolation of the alkoxyamine (**11**) proves that in the absence of oxygen DBHA stops working because the amount of nitroxide in solution is too small to stop all propagation chains. On the other hand during the inhibition in the presence of oxygen, although still extremely low, the concentration of nitroxide is significantly higher than in the absence of oxygen. The absolute nitroxide concentration in the presence of 2000 ppm DBHA is approximately  $6 \times 10^{-6} \text{ M}$ .

In conclusion, the isolation of the hydroxylamine (**11**) from the reaction mixture confirms that *N,N*-dibenzylnitroxide can trap styrene radical. However, in deoxygenated systems, the amount of nitroxide in solution is too small to contribute to the inhibition mechanism.

## 2.4 Conclusions

*N,N*-dibenzylhydroxylamine is a good inhibitor for the thermally-initiated styrene polymerisation only in the presence of oxygen. The hydrogen abstraction from DBHA by peroxy radicals efficiently breaks the propagation chains. However, in the absence of oxygen the inhibition by hydrogen abstraction becomes inefficient as the number of

oligostyryl radical increases. The hydrogen abstraction from DBHA by carbon centred radical is slow compared to the rate of propagation.

EPR spectroscopy detected the formation of *N,N*-dibenzyl nitroxide during the inhibition, however in the absence of oxygen nitroxide concentration is below  $1 \times 10^{-6}$  M. A comparison between the absolute nitroxide concentration formed in air-saturated solutions of styrene and diphenyl ether respectively shows that most of nitroxide is formed by the oxidation of DBHA by the oxygen.

In the absence of oxygen the only reaction that could stop the propagation chains is the coupling reaction between styrene and nitroxide radical. The isolation from the reaction mixture of the alkoxyamine proved that nitroxide can trap the styrene radicals, but due to its extremely low concentration in solution it cannot stop all propagation chains.

## 3 2,5-Di-*tert*-butyl-hydroquinone as an inhibitor of the auto-initiated styrene polymerisation

### 3.1 Introduction

Despite a number of reports on the hydroquinone inhibition of styrene polymerisation, the role of individual reactions in the overall inhibition of the auto initiated styrene polymerisation by 2,5-di-*tert*-butyl-hydroquinone (2,5-DTBHQ) remains unclear. It is generally accepted that 2,5-DTBHQ stops propagation predominantly by hydrogen abstraction, however it is not clear if this is the only pathway. Furthermore, 2,5-di-*tert*-butyl-1,4-benzoquinone (2,5-DTBBQ) is also rapidly formed during the inhibition, and dilatometry experiments carried out in our laboratories revealed a retardation of the polymerisation in the presence of this compound. Thus, in order to understand if 2,5-DTBHQ and 2,5-DTBBQ contributes to the inhibition/retardation of styrene polymerization by reacting with propagation chains by addition reaction, an analysis of the inhibition products was carried out. The following section reviews the pertinent literature.

#### 3.1.1 Background

##### 3.1.1.1 2,5-Di-*tert*-butyl-hydroquinone

2,5-Di-*tert*-butyl-hydroquinone (**1**) (2,5-DTBHQ) is an excellent antioxidant for styrene polymerisation and for this reason it is widely used in industrial processes. However, the mechanism of its action is still not clear. Antioxidants often work in the presence of oxygen and stop the propagation by providing hydrogen atoms to quench peroxy radicals (Reaction I, Figure 3.1). The high reactivity of hydroquinones towards peroxy radicals is due to their low BDE(O-H) (BDEs for 2,5-DTBHQ and 2,5-di-*tert*-butyl semiquinone (**2**) are 81.2 and 59.1 kcal/mol, respectively)<sup>76</sup>. However, the stoichiometric factor (the number of peroxy radicals trapped by a molecule of hydroquinone) of 2,5-DTBHQ for the inhibition of styrene polymerisation initiated by 2,2'-azobis-(2,4-dimethylvaleronitrile) in chlorobenzene is only 0.3<sup>77</sup>. This suggests that

the overall number of peroxy radicals trapped is quite small, especially if compared to phenols which have commonly a stoichiometric factor of 2<sup>77</sup>. The mechanism proposed by Amorati and co-workers<sup>77</sup> involves the reaction of semiquinone (**2**) with molecular oxygen (Reaction III, Figure 3.1). In particular, 2,5-DTBHQ reacts with a peroxy radical ( $k_1 = (1.6 \pm 0.4) \times 10^6 \text{ M}^{-1} \text{ s}^{-1}$  at 303 K) leading to semiquinone (**2**) which then undergoes the attack by oxygen ( $k_5 = (2.0 \pm 0.9) \times 10^6 \text{ M}^{-1} \text{ s}^{-1}$ ) to give 2,5-DTBBQ and hydroperoxyl radical (HOO·), but the latter can also initiate the polymerisation. The addition of oxygen to semiquinone (**2**) occurs in the para-position with respect to the oxygen radical followed by a one-step hydrogen atom transfer – elimination reaction.

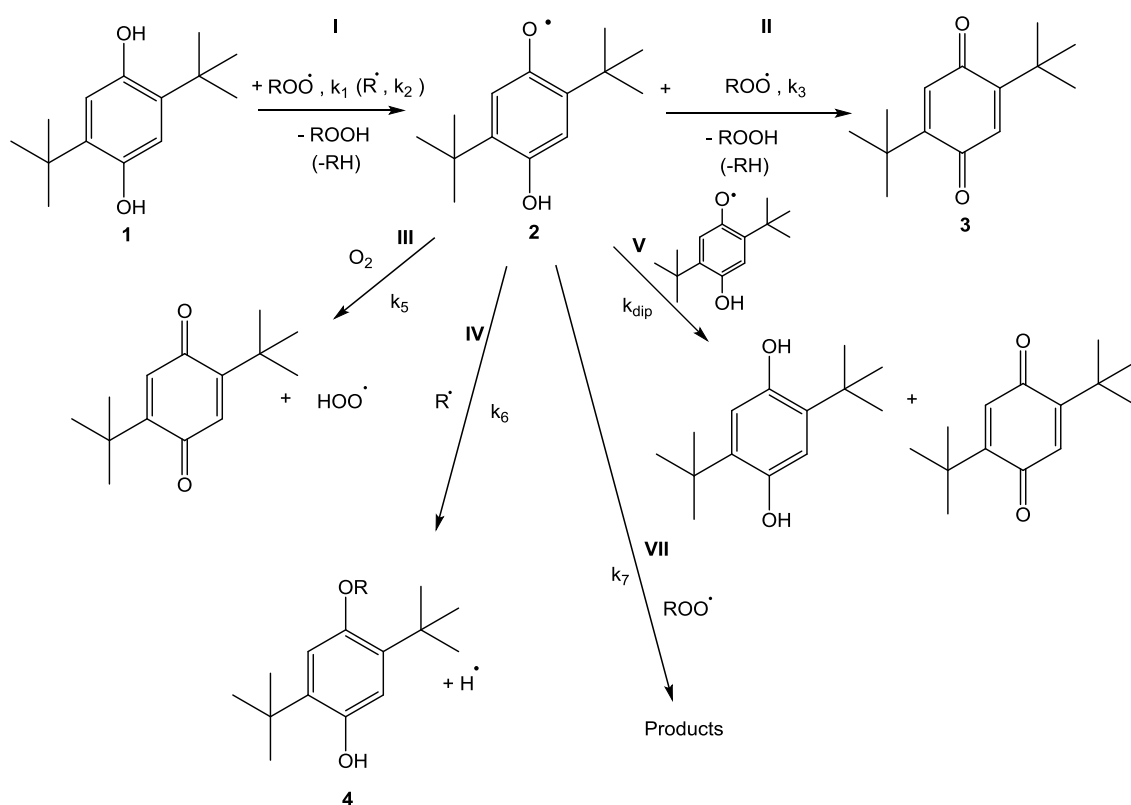


**Figure 3.1 Possible reactions of 2,5-di-*tert*-butylhydroquinone**

The ability of semiquinone (**2**) to stop a second propagation chain, either by hydrogen abstraction (Reaction II) or addition reaction (Reaction IV), is crucial during the inhibition process. The semiquinone (**2**) can disproportionate to 2,5-DTBHQ and 2,5-di-*tert*-butyl-1,4-benzoquinone (2,5-DTBBQ) (**3**) (Reaction V), without trapping any further peroxy radical. The rate constant of disproportionation ( $k_{dis}$ ) is  $5 \times 10^9 \text{ M}^{-1} \text{ s}^{-1}$  at

303 K. This process seems to be predominant compared to that proposed by Amorati<sup>77</sup> and although semiquinone rapidly disproportionates, it regenerate 2,5-DTBHQ which could react further. Another possibility is the addition reaction of semiquinone (**2**) by another peroxy radical (Reaction **VII**). Although  $k_7$  is not available, it is reasonable to assume that it is similar to that for the reaction of peroxy radical with phenoxy radicals ( $\text{PhO}\cdot$ ), as semiquinone and  $\text{PhO}\cdot$  have similar structures. Also, it has been demonstrated that this rate constant is almost independent of the phenoxy radical structure<sup>78</sup>. Thus, we can assume that the rate constant of semiquinone reaction with peroxy radical ( $k_7$ ) is close to  $2 \times 10^8 \text{ M}^{-1}\text{s}^{-1}$ . The addition of a carbon centred-radical on the oxygen of semiquinone has also been proposed (Reaction **IV**). Indeed, a study published by Maslovskaya on the radical reactions of 2,5-DTBHQ and hexane under  $\gamma$ -irradiation shows the formation of the mono-alkyl ether (**4**)<sup>79</sup> in the reaction mixture (Figure 3.1). However, this reaction is only relevant at low oxygen level as under these conditions the concentration of alkyl radicals is much higher than that of peroxy radicals<sup>35</sup>. Furthermore, at low oxygen level the hydrogen abstraction from 2,5-DTBHQ by carbon-centred radicals may also become effective for the inhibition ( $k_2$ ) (Reaction **I**). Although the rate constant is not available for the reaction of 2,5-DTBHQ with alkyl radicals, we can assume that it is close to that of a reaction of phenol with alkyl radicals. The rate constant proposed by Pedulli and co-workers<sup>27</sup> for the hydrogen abstraction from a series of phenols by primary alkyl radicals at room temperature is within the range  $1\text{-}70 \times 10^{-4} \text{ M}^{-1}\text{s}^{-1}$ .

The inhibition mechanism of 2,5-DTBHQ predominantly involves the hydrogen abstraction from 2,5-DTBHQ by peroxy radicals, leading to semiquinone (**2**). Although the disproportionation reaction of (**2**) seems to be the main process, other reactions may occur which can affect the rate of propagation, such as the addition or the hydrogen abstraction by alkyl radicals.

### **3.1.1.2 2,5-Di-*tert*-butyl-1,4-benzoquinone**

*p*-Benzoquinones and their derivatives are an important class of inhibitors of styrene polymerisation<sup>1</sup>. The mechanism of inhibition is quite complex and strongly dependent

on the benzoquinone structure<sup>80, 81</sup>. 2,5-Di-*tert*-butyl benzoquinone (**3**) has two positions for the attack of propagation radicals: the oxygen and the C=C double bond (Figure 3.2).

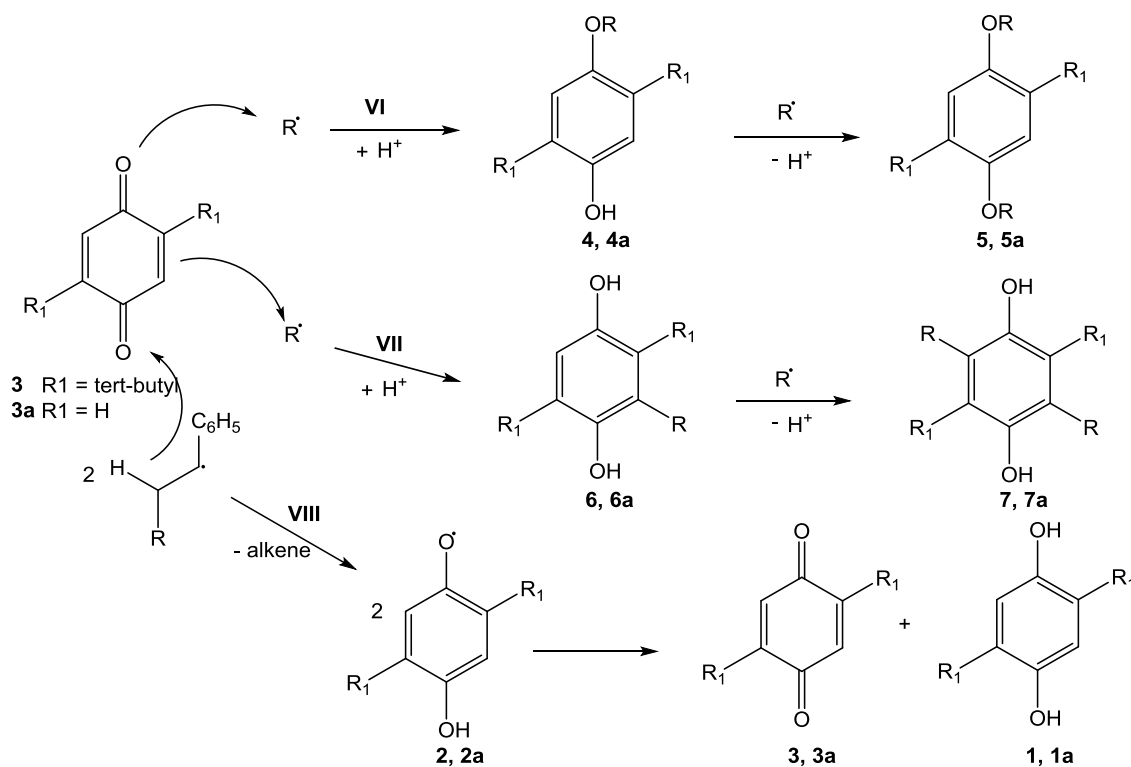


**Figure 3.2** Possible reactions of 2,5-di-*tert*-butyl-1,4-benzoquinone

The addition of alkyl radicals to the carbonyl oxygen atoms of (**3**) produces hydroquinone ethers (**4**) and (**5**) (Reaction **VI**). The addition of alkyl radicals to the C=C bonds leads to hydroquinones (**6**) and (**7**) (Reaction **VII**). An interesting work published by Cohen reveals<sup>82</sup> that the inhibition properties of *p*-benzoquinone (**3a**) are connected with the formation of hydroquinone (**1a**) and its derivatives (**4a**), (**6a**) and (**7a**) which act as retarders. He assumed that alkyl radicals can undergo hydrogen abstraction by *p*-benzoquinone (**3a**) with the consequent formation of alkene and semiquinone (**2a**) (Reaction **VIII**), the latter then disproportionates to hydroquinone (**1a**) and benzoquinone (**3a**) as shown in Figure 3.2. Furthermore, a test using 2,5-DTBBQ as an inhibitor for the peroxide initiated styrene polymerisation revealed its poor inhibitor behaviour<sup>82</sup>. The rather low reactivity of 2,5-DTBBQ was also observed by Hageman<sup>83</sup> during the thermal decomposition of 2,2'-azobis-(2-methylpropionitrile)

in the presence of 2,5-DTBBQ. The 2-cyano-2-propyl-radicals formed by the decomposition of the azo compound did not show any addition to 2,5-DTBBQ, which was fully recovered from the reaction mixture. The influence of the *tert*-butyl groups on the reactivity of 2,5-DTBBQ was rationalised by Simandi and Tudos<sup>84</sup>. They postulated that the reactivity of benzoquinones depends on both the redox potential and the steric effect of the substituents. The correlation between redox potential and reactivity is given by the following equation:

$$\log \frac{k_7}{k_8} = \frac{nF}{RT} \times E^0 + \text{constant}$$

Here  $k_7$  is the rate constant for the addition reaction of an alkyl radical to a benzoquinone molecule, and  $k_8$  is the rate constant of the propagation reaction,  $n$  is the number of electrons transferred,  $F$  is the Faraday constant,  $E^0$  is the redox potential and  $R$  is the gas constant. The correlation between redox potential and reactivity in systems with no hindered substituents gives a straight line, thus any deviation from the straight line represents the steric effect. These authors also calculated the percentage of shielding exerted by a substituent next to a reactive centre, in other words they quantified the coverage, in terms of space, imposed by a group on the attack position. In this case they calculate the shielding exerted by the *tert*-butyl group on the oxygen (they assumed that the addition of the alkyl radical occurs only on the oxygen) which is 9.81. This percentage of shielding for *tert*-butyl is much bigger than methyl and hydrogen, which are 2.02 and 0 respectively.

The above reports agree on the poor inhibition property of 2,5-DTBBQ mainly due to the presence of highly demanding substituents in position 2 and 5, which hamper the addition of propagation chains on the carbonyl oxygen atoms.

### 3.1.1.3 *Quinone/hydroquinone redox couple*

The quinone/hydroquinone redox couple is well known in electrochemistry<sup>85</sup>. In aprotic solvents the reduction of 2,5-DTBBQ occurs via two successive one-electron steps which produce the radical anion and the hydroquinone dianion (Figure 3.3). The reduction of 2,5-DTBBQ is a reversible reaction as demonstrated by Parker<sup>86</sup> and

Eggs<sup>87</sup> who carried out electrochemical studies of the 2,5-DTBBQ/2,5-DTBHQ couple in acetonitrile.

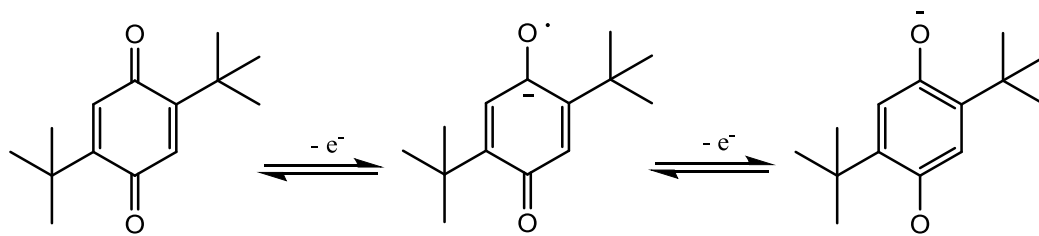


**Figure 3.3 Reversible redox equilibrium between 2,5-DTBBQ and 2,5-DTBHQ**

In the presence of protic solvents or other proton donors, things become a bit more confusing and complex. There are three main mechanisms for the oxidation of 2,5-DTBHQ and reduction of 2,5-DTBBQ. Several ways can be found in literature to name these mechanisms but in this thesis the nomenclature of Mayer will be used<sup>88</sup> (Figure 3.4).

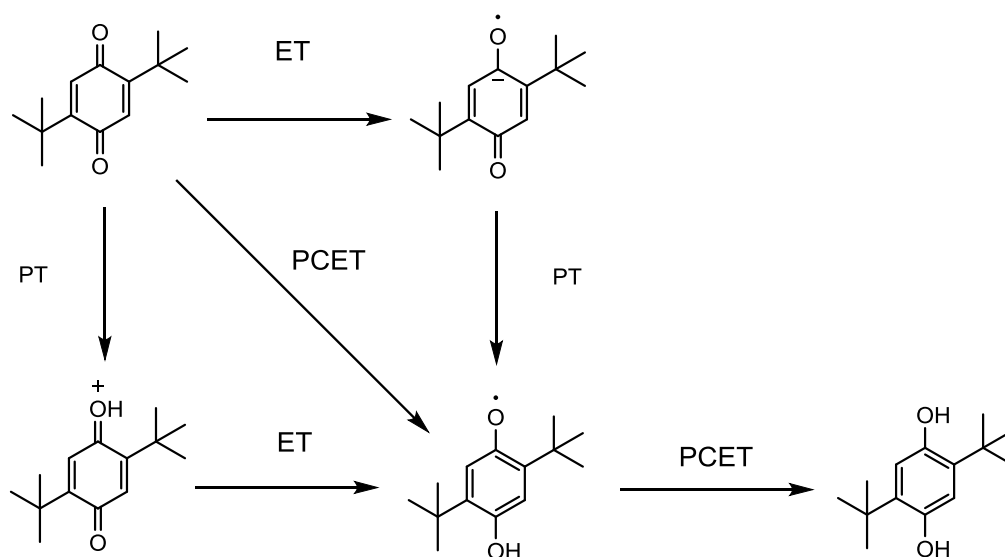


**Figure 3.4 Reaction pathway of 2,5-di-*tert*-butyl-1,4-benzoquinone**

The concerted proton and electron transfer (Figure 3.4, diagonal) is named Proton Coupled Electron Transfer (PCET); the transfer in two steps is called PT/ET if there is an initial transferring of the proton followed by the electron transfer. Otherwise, if the electron transfer takes place before the proton transfer the mechanism is ET/PT. Several researchers investigated the mechanism of the interconversions in the



benzoquinone/hydroquinone redox couple. Song *et al.* studied<sup>89</sup> the interconversion of hydroquinone and benzoquinone at different pH by the redox couple  $\text{Os}(\text{dmb})_3^{3+/2+}$  (dmb = 4-4'-dimethyl-2,2'-bipyridine). They concluded that the two steps mechanisms (ET/PT and PT/ET) are catalysed in the presence of acids. The same conclusion was proposed by Graige and co-workers<sup>90</sup> after a study of the reduction of benzoquinone in organic systems. So, in polar systems the two step mechanism is favoured compared to the concerted mechanism. On the other hand, it is commonly accepted that in apolar solvents the concerted mechanism (PCET) is thermodynamically favoured. Contrary, other authors correlate the predominance of PCET, in apolar solvents, to the BDE of the O-H bond. Due to the low BDE of the O-H of hydroquinones, it is likely that the oxidation process goes through the PCET mechanism, supported by the fact that hydroquinones are good antioxidants<sup>91, 92</sup>.

Although different reasons are proposed to explain the predominance of one mechanism over the other in the interconversion of hydroquinone/benzoquinone redox couple, they all agree that in aprotic organic solvents the reaction is likely to occur via a PCET mechanism.

### 3.1.2 Aim of the chapter

The above review shows that the inhibition mechanism of 2,5-DTBHQ could be quite complex and it is not clear whether the hydrogen abstraction mechanism is the only pathway responsible for the inhibition. The only information available in the literature about 2,5-DTBHQ as an inhibitor only refers to systems containing high levels of oxygen and in which hydrogen abstraction by peroxy radicals is the predominant mechanism. However, we wanted to understand if other reactions could contribute to the process. 2,5-DTBBQ is formed in high concentrations during the inhibition of styrene polymerisation, but 2,5-DTBBQ is known to be inert towards propagation radicals due to the presence of hindering substituents. As we found that 2,5-DTBBQ retards the polymerisation, a study on the reactivity of 2,5-DTBBQ will be detailed in order to understand if the addition reaction of carbon-centred radicals onto 2,5-DTBBQ occurs at a reasonable level that causes retardation. In conjunction, a

comparison between the reactivity of 2,5-DTBBQ and 2,6-DTBBQ is included to confirm what is reported in previous works. In particular, they suggest that in 2,6-DTBBQ the strategic position of the *tert*-butyl groups allows this molecule to react with styrene radical. To conclude this work a product analysis of the reaction between 2,5-DTBHQ with styrene and 2-cyano-2-propyl radicals will be detailed. The experiment will give information on the reactivity of 2,5-DTBHQ in deoxygenated conditions.

### 3.2 Investigation of the antioxidant properties of 2,5-di-*tert*-butyl-hydroquinone

The literature reviewed in the introduction describes 2,5-DTBHQ as an inhibitor of the styrene polymerisation. Thus, before attempting any investigation of the inhibition products, we decided to confirm the inhibition properties of 2,5-DTBHQ regarding the auto-initiated styrene polymerisation by dilatometry.

A 4.5 mM solution of 2,5-DTBHQ in styrene was analysed at 110 °C for 4 h. The results are reported in Figure 3.5.

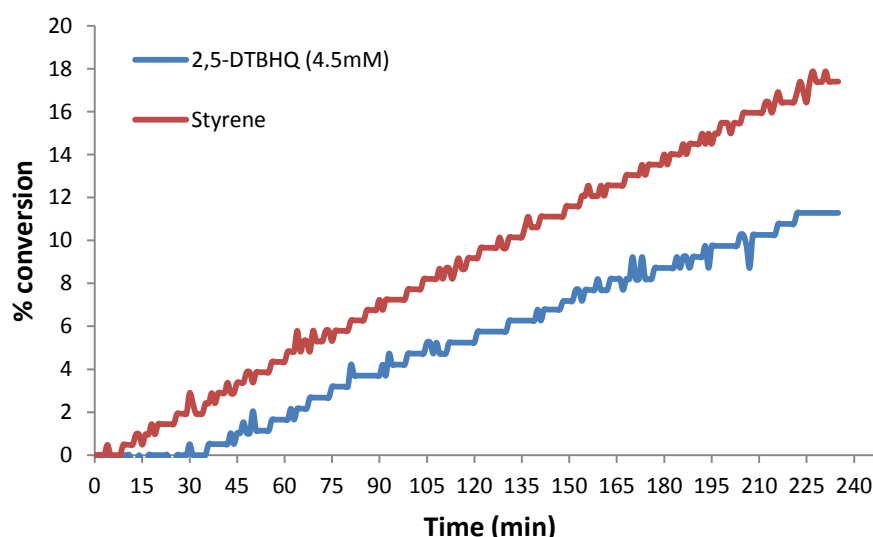


**Figure 3.5 Dilatometry trace for the inhibition of the thermal styrene polymerisation by 2,5-DTBHQ (4.5 mM)**

Figure 3.5 shows an inhibition time of 36 min for the inhibition of styrene polymerisation by 2,5-DTBHQ, which appears rather poor considering the high

concentration of the inhibitor. We can assume that 2,5-DTBHQ stops working in the absence of oxygen and that the length of the inhibition time corresponds to the time that is taken by the system to become deoxygenated. Indeed, the inhibition time is similar to that shown by the antioxidant *N,N*-dibenzylhydroxylamine as reported in chapter 2, section 2.2. So, the dilatometry trace suggests that 2,5-DTBHQ shows good inhibition only in the presence of oxygen and hence its efficiency is due to breaking propagation chains by hydrogen abstraction. However, the inhibition is followed by a slight retardation of the styrene polymerisation (e.g., the slope of the dilatometry trace in Fig 3.5 is smaller than that for uninhibited styrene) and a few reactions may be involved in this step. In particular, 2,5-DTBBQ may react with carbon-centred radicals by addition reaction and stop some propagation chains<sup>80</sup>. This compound is rapidly formed as the hydrogen abstraction from 2,5-DTBHQ by peroxy radicals leads to semiquinone radicals which are likely to disproportionate giving 2,5-di-*tert*-butyl-1,4-benzoquinone (2,5-DTBBQ) as one of the products<sup>77</sup>. Although, the reactivity of 2,5-DTBBQ seems quite limited due to the presence of hindering groups in position 2 and 5, the reaction could still occur at a reasonable level that causes retardation. Another possibility is that in the deoxygenated system the hydrogen abstraction from 2,5-DTBHQ by oligostyryl radical contributes to the retardation<sup>27</sup>. But we cannot exclude also that the addition of alkyl radicals to semiquinone (**2**) can be effective to some extent<sup>79</sup>.

The dilatometry trace for the inhibition of the auto-initiated styrene polymerisation confirmed the excellent ability of 2,5-DTBHQ to stop propagation chains in oxygenated systems. In addition, at a low oxygen level 2,5-DTBHQ slightly retards the polymerisation. As far as we know the role of 2,5-DTBHQ as a retarder is not reported in any paper, as it is commonly studied under oxygenated conditions in which 2,5-DTBHQ acts as an inhibitor. Thus, there is a limited amount of information related to the reactivity of either 2,5-DTBHQ or its intermediate (**2**) with carbon-centred radicals, especially correlated to the inhibition of the styrene polymerisation. Furthermore, 2,5-DTBBQ could also stop propagation chains and actively participate in the

retardation/inhibition processes. Thus, to verify this hypothesis, inhibition properties of 2,5-DTBBQ by dilatometry is explored in the next section.

### 3.3 Investigation of the inhibition properties of 2,5-di-*tert*-butyl-1,4-benzoquinone

2,5-DTBHQ shows retardation in deoxygenated conditions, and this effect may be due to the contribution of 2,5-DTBBQ, which is likely to be formed in a reasonable amount during the inhibition. Thus, the inhibition properties of 2,5-DTBBQ was investigated by dilatometry.

A 4.5 mM solution of 2,5-DTBBQ in styrene was analysed at 110 °C for 4 h. The data are reported in Figure 3.6.

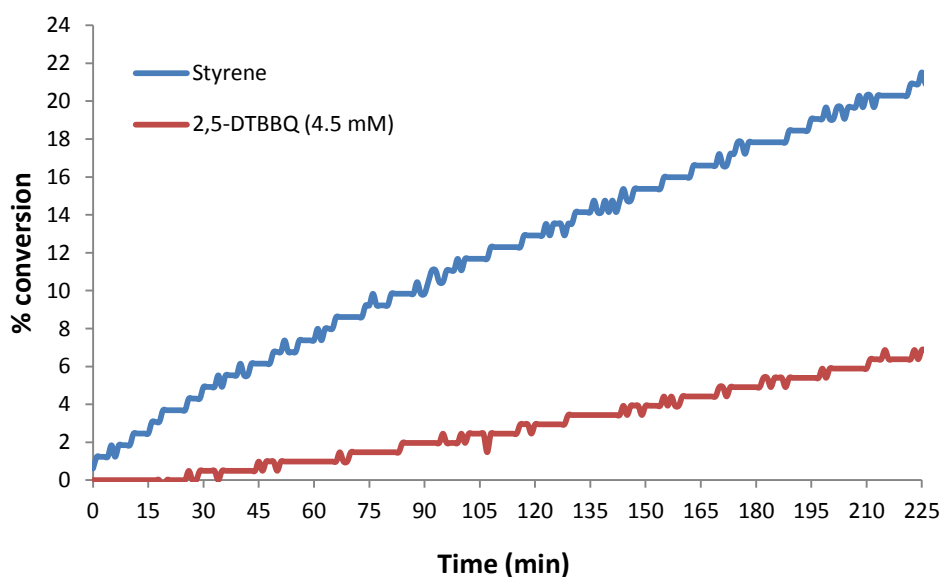


**Figure 3.6 Dilatometry trace for the inhibition of the thermal styrene polymerisation by 2,5-DTBBQ (4.5 mM)**

The kinetic profile in Figure 3.6 shows that 2,5-DTBBQ acts only as a retarder, as there is no evidence of an initial flat line, corresponding to lack of polymerisation, on the dilatometry trace. Combining this result with the data for 2,5-DTBHQ (Figure 3.5), it is not unreasonable to suggest that the inhibition properties of 2,5-DTBHQ include a contribution of 2,5-DTBBQ. Essentially, 2,5-DTBHQ shows inhibition, but poor

retardation, on the other hand 2,5-DTBBQ does not show any inhibitor properties, but is a retarder to some extent.

In order to gain a better understanding of the extent of the contribution of the addition reaction to the retardation mechanism of 2,5-DTBBQ, a detailed study of the reactivity of 2,5-DTBBQ towards carbon-centred radicals was carried out.

### 3.4 Reactivity of 2,5-di-*tert*-butyl-1,4-benzoquinone towards alkyl radicals

The addition of carbon-centred radicals is the main mechanism of inhibition of benzoquinones<sup>80, 81</sup> so we decided to investigate this reaction and its products in order to gain a better understanding of the mechanism of retardation of 2,5-DTBBQ. We also investigated the reactivity of 2,6-DTBBQ, as it has similar chemical properties but a substantial difference in steric hindrance, compared to 2,5-DTBBQ, as previously reported by other researchers<sup>83, 84</sup>.

2,5-DTBBQ (4.6 mM) was dissolved in styrene and the solution was left stirring at 110 °C for 3 h. Gas chromatograms at time zero (Figure 3.7) and after 3 h (Figure 3.8) were recorded.

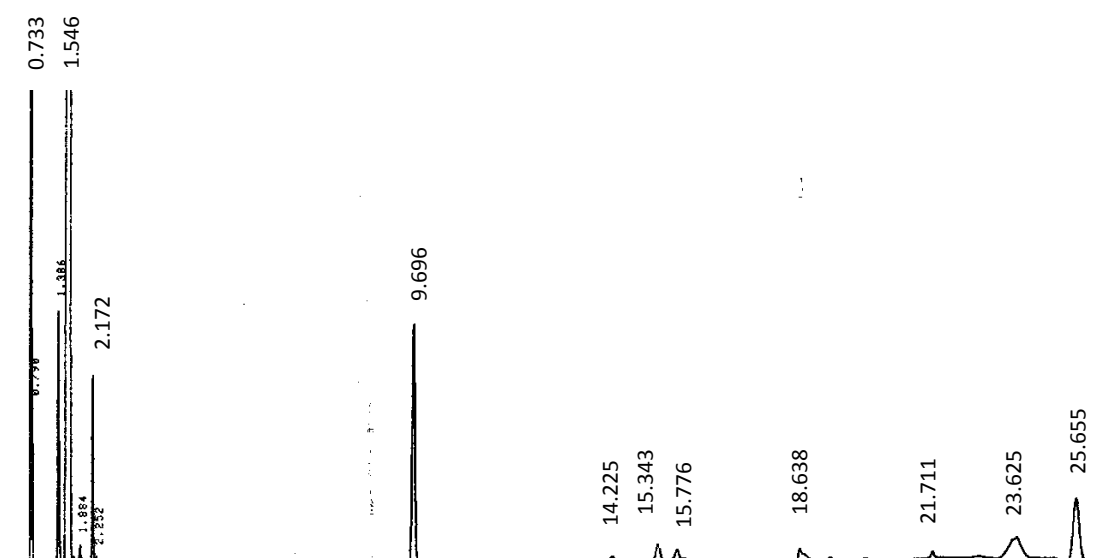
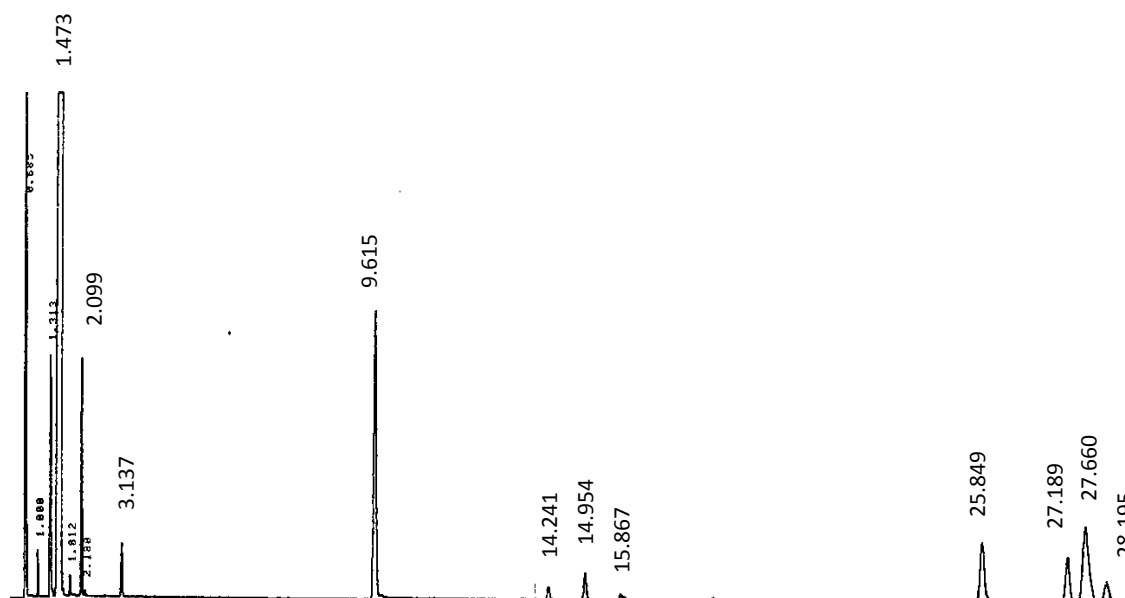


Figure 3.7 GC chromatogram of the reaction between 2,5-DTBBQ in styrene at time zero

In Figure 3.7 the peaks at 1.55 and 9.70 min correspond to styrene and 2,5-DTBBQ respectively. All the other peaks (e.g., those around 14 min (14.22, 15.34 and 15.78 min) and between 18-28 min (18.73, 21.71, 23.62, and 25.05 min)) are derived from styrene oxidation, as will be confirmed later by the gas chromatography with electron impact mass spectrometry (GC-EI) (Figure 3.9). During the analysis the solution is exposed to temperatures between 100-250 °C which causes a partial polymerisation and oxidation of styrene.

GC chromatogram after 3 h is reported in Figure 3.8.



**Figure 3.8 GC chromatogram of the reaction of 2,5-DTBBQ in styrene after 3 h at 110 °C**

Figures 3.7 and 3.8 match almost perfectly, there is no evidence of the formation of new products, but only an enhancement of the peaks already present in the first chromatogram, which correspond to styrene oxidation products. The assignment of the main peaks has been possible by comparison of the fragmentation for each compound from the GC-EI analysis (Figure 3.9) with the data for known compounds formed in the styrene polymerisation/oxidation<sup>7, 93, 94</sup> (Table 3.1).

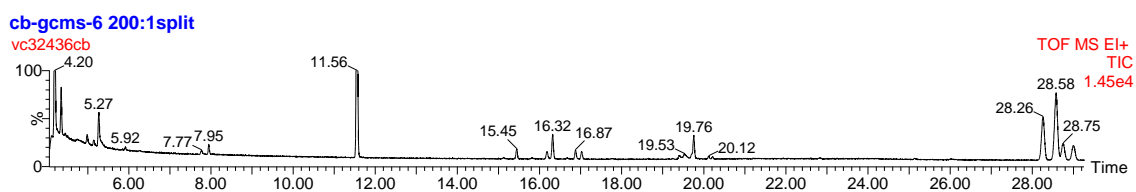
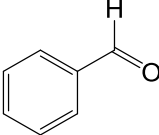
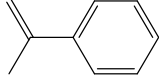
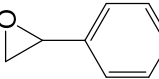
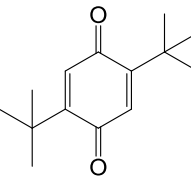
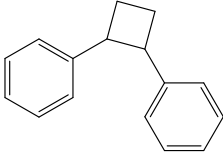
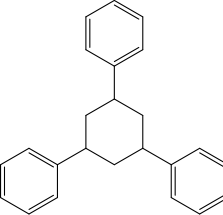
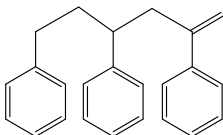


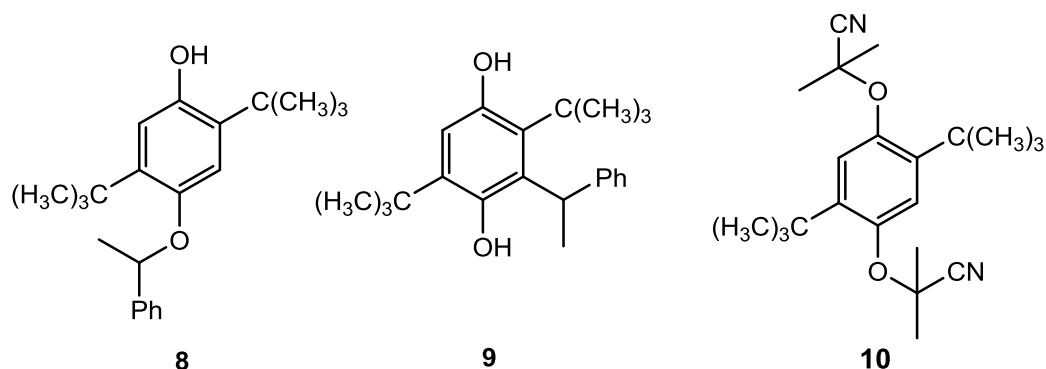
Figure 3.9 GC-El chromatogram of 2,5-DTBBQ in styrene after 3 h

Table 3.1 Products of styrene polymerisation/dimerisation

Retention Time	Mass	Structure <sup>a</sup>
4.20	106.04	
4.35	118.08	
5.27	120.06	
11.56	120.15	
16.32	208.13	
28.26	312.16	
28.58	312.16	

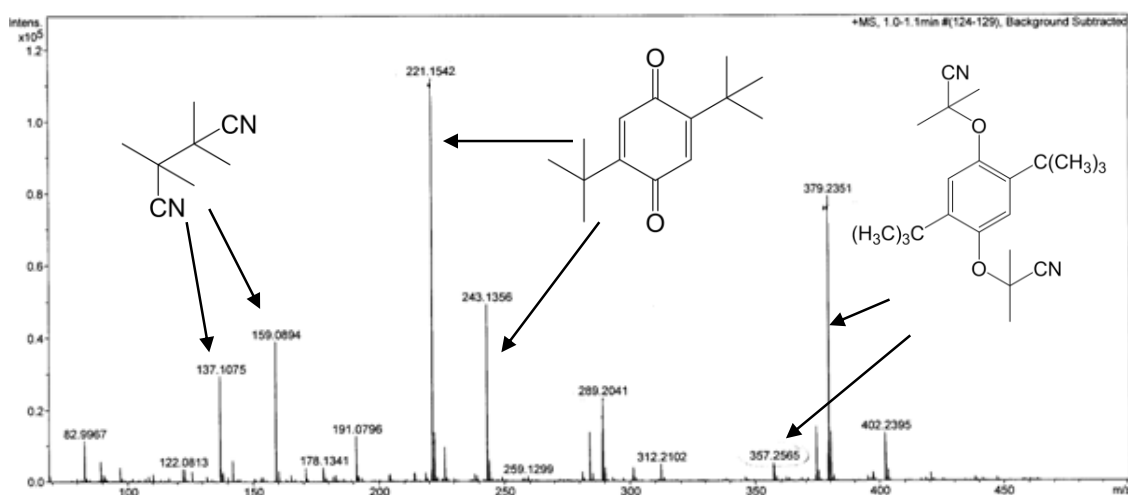
a) in some cases the structure reported is representative of a series of possible structural isomers.

The analysis of the reaction mixture by GC and GC-EI does not show any evidence of the quinone addition products such as **(8)**, **(9)** or their derivatives.



Before concluding that 2,5-DTBBQ is inert towards alkyl radicals, it was decided to repeat the reaction in a non polymerizable solvent using AIBN as a source of alkyl radicals. Indeed, auto-initiated polymerisation of styrene gives rise to a complex reaction mixture which can make the detection of any products difficult.

2,5-DTBBQ and AIBN were dissolved in toluene. The reaction was left stirring at reflux for 4.5 h. Only the presence of 2,5-DTBBQ was observed. However, the analysis of the reaction mixture by mass spectrometer with positive electrospray ion source (ESI) evidenced the presence of compound **(10)** (or structural isomers).

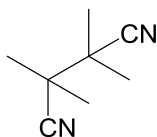


**Figure 3.10** ESI mass spectrum of 2,5-DTBBQ in styrene after 3 h heating

The peak at  $m/z$  137.5075 corresponds to the  $[M+H]^+$  ion of one of the decomposition products of AIBN and the peak at  $m/z$  159.0894 is  $[M+Na]^+$ . The thermal



decomposition of AIBN liberates nitrogen gas and 2-cyano-2-propyl radicals, and the latter tend to combine leading to (**11**)<sup>95</sup>. The peaks at  $m/z$  221.2542 and 243.1356 are the  $[M+H]^+$  and  $[M+Na]^+$  ions of 2,5-DTBBQ. The peak at  $m/z$  357.2565 corresponds to the  $[M+H]^+$  ion arising from (**10**) and the peak at  $m/z$  379.2351 is the same product, but associated with a sodium cation  $[M+Na]^+$ .

**11**

In order to isolate and characterise the product detected by ESI spectrometry, the reaction was scaled up using 2,5-DTBBQ, AIBN and toluene in the same conditions as before. However, only the presence of the starting materials was observed, and despite several attempts aimed at the optimisation of the reaction conditions, 2,5-DTBBQ was always recovered quantitatively.

2,5-DTBBQ thus showed a rather limited reactivity towards carbon-centred radicals. Although there was some evidence of the formation of the addition products, the characterisation of these compounds was not possible. These results suggest that the contribution of addition reaction to the retardation must be quite limited. On the other hand, the oxidation of propagation radicals by 2,5-DTBBQ to stable alkenes, could explain the retardation and the absence of new products in the reaction mixture. Indeed, Cohen already reported<sup>82</sup> the hydrogen abstraction from alkyl radicals by benzoquinone during the inhibition of styrene polymerisation. In the next paragraph the reactivity of 2,6-DTBBQ is investigated.

### 3.4.1 Reactivity of 2,6-di-*tert*-butyl-1,4-benzoquinone

Several papers discuss the differences in reactivity between 2,5-DTBBQ and 2,6-DTBBQ<sup>83, 84</sup>. Engel and co-workers characterised<sup>80</sup> (**12**) and (**13**) from the reaction between 2,6-DTBBQ and styrene radicals (Figure 3.11).

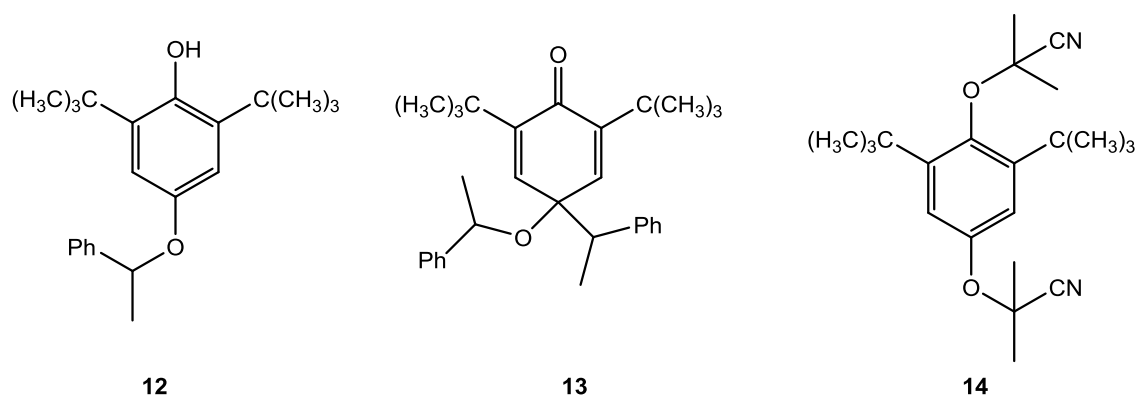


**Figure 3.11** Addition products of 2,5-DTBBQ and styrene radicals

90% of (**14**) was instead isolated by Hageman<sup>83</sup> from the reaction of 2,6-DTBBQ with 2-cyano-2-propyl radicals.

Repeating the reaction conditions reported in the literature, we could not isolate any of the expected products. By optimising the temperature and reactant concentrations, one product was isolated, although the reactivity of 2,6-DTBBQ appeared rather poor (95% of starting material recovered). After purification, the product was analysed by ESI mass spectrometry (Figure 3.12) and <sup>1</sup>H-NMR (Figure 3.13).

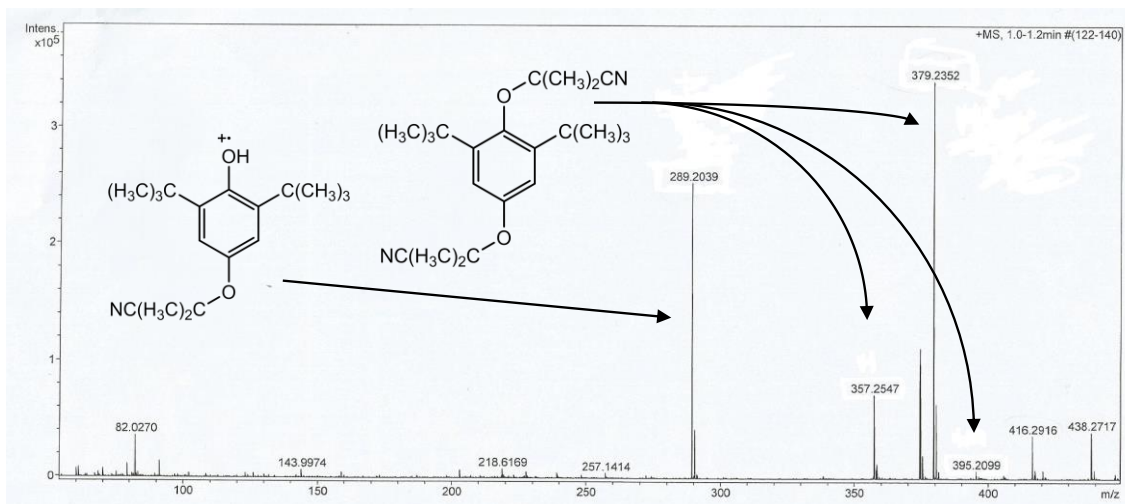


**Figure 3.12** ESI mass spectrum of an isolated product from the reaction between 2,6-DTBBQ and AIBN

The peak at  $m/z$  357.2547 corresponds to the  $[M+H]^+$  ion of (**14**), the peaks at  $m/z$  379.2352 and at  $m/z$  395.2099 are the sodium  $[M+Na]^+$  and the potassium  $[M+K]^+$  ions,

respectively. The peak at  $m/z$  289.2039 could be associated to the radical cation of compound (**15**).

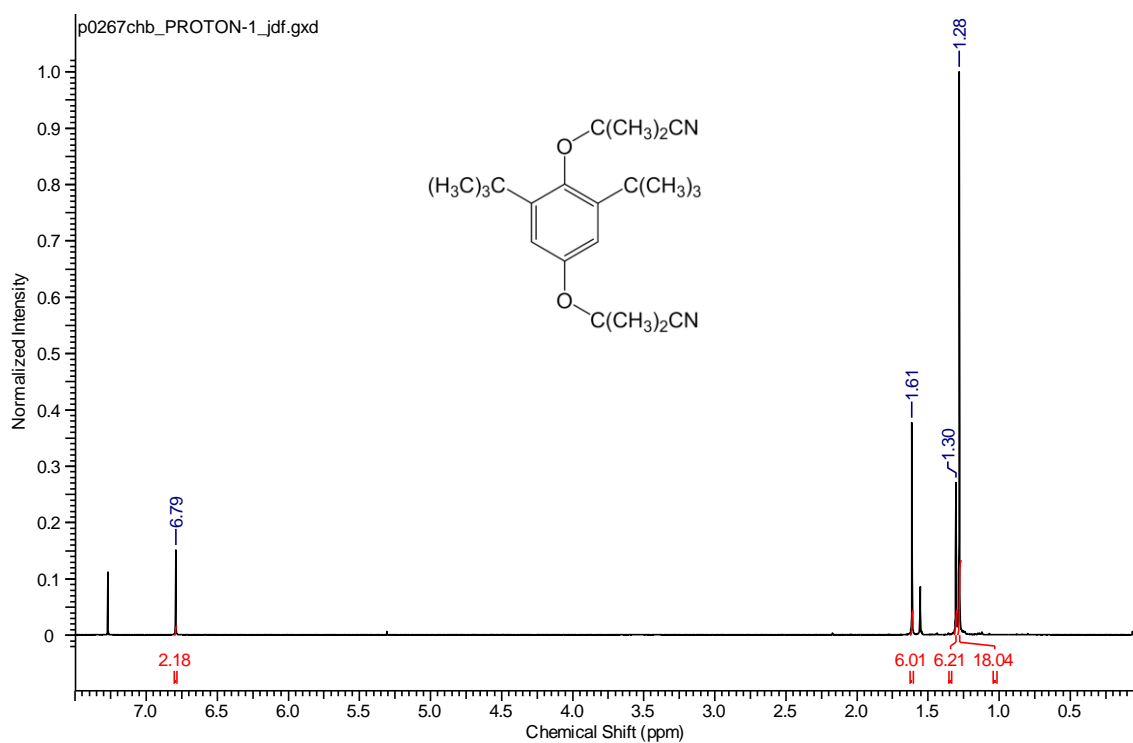
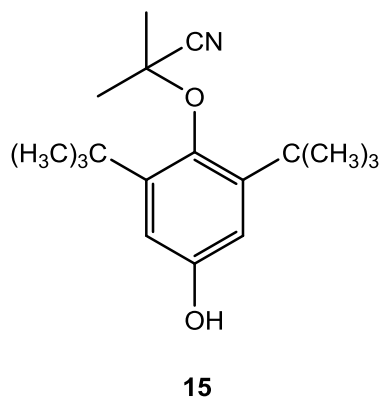


**Figure 3.13**  $^1\text{H-NMR}$  of compound **14**

The  $^1\text{H-NMR}$  spectrum in Figure 3.13 confirms that the isolated compound is (**14**). The spectrum was compared to that one reported in the literature<sup>83</sup> and the signals perfectly match. The singlet at 1.28 ppm corresponds to the *tert*-butylic protons (18 H), the proton atoms of 2-cyano-2-propyl groups show two singlets at 1.30 and 1.60 ppm respectively, and each signal integrates to 6, the singlet of the aromatic protons (2 H) instead falls at 6.79 ppm.

Even though compound (**14**) was isolated, it has to be pointed out that almost 95% of the starting material was recovered unreacted. Although, a significant effort was spent on optimising the reaction conditions, similar results were obtained every time, therefore our results suggest poor reactivity of 2,6-DTBBQ.

In conclusion, the reactivity of both 2,5-DTBBQ and 2,6-DTBBQ towards carbon-centred radicals seemed rather poor.

### **3.5 Investigation of the reactivity of 2,5-di-*tert*-butyl-hydroquinone**

Dilatometry experiments confirmed that 2,5-DTBHQ shows inhibition for the auto-initiated styrene polymerisation in the presence of oxygen dissolved in solution and only retardation in deoxygenated systems. We have also demonstrated that 2,5-DTBBQ cannot contribute by addition reaction to propagation chains. Thus, in this section, a product analysis is carried out to determine if 2,5-DTBHQ acts only as an antioxidant or if it can also trap propagation chains.

A 72 mM solution of 2,5-DTBHQ in styrene was heated at 110 °C for 5 h. GC chromatograms of the reaction at time zero (Figure 3.14) and after 5 h (Figure 3.15) were recorded.

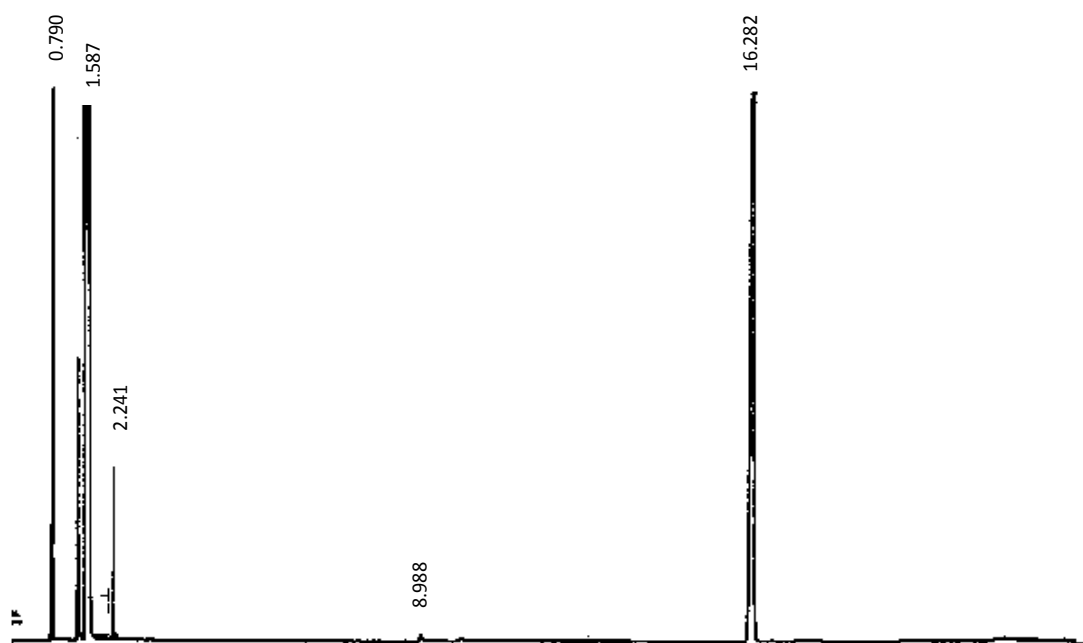


Figure 3.14 GC Chromatogram of 2,5-DTBHQ in styrene at  $t = 0$

Figure 3.14 represents the GC chromatogram of the solution before being heated. The main peaks correspond to styrene at 1.59 min and 2,5-DTBHQ at 16.28 min. The peaks between 0.79-2.32 min are correlated to the styrene oxidation products as reported in Table 3.1. Figure 3.14 does not show all polymerization that come out after 20 min (Figure 3.7) as the time of the run in this case was 20 min.

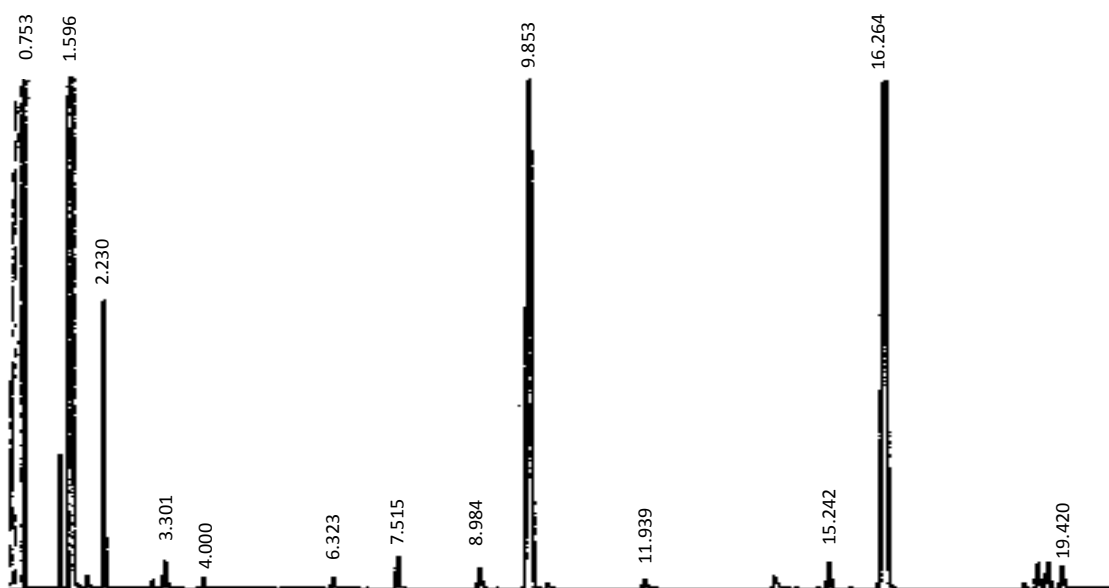
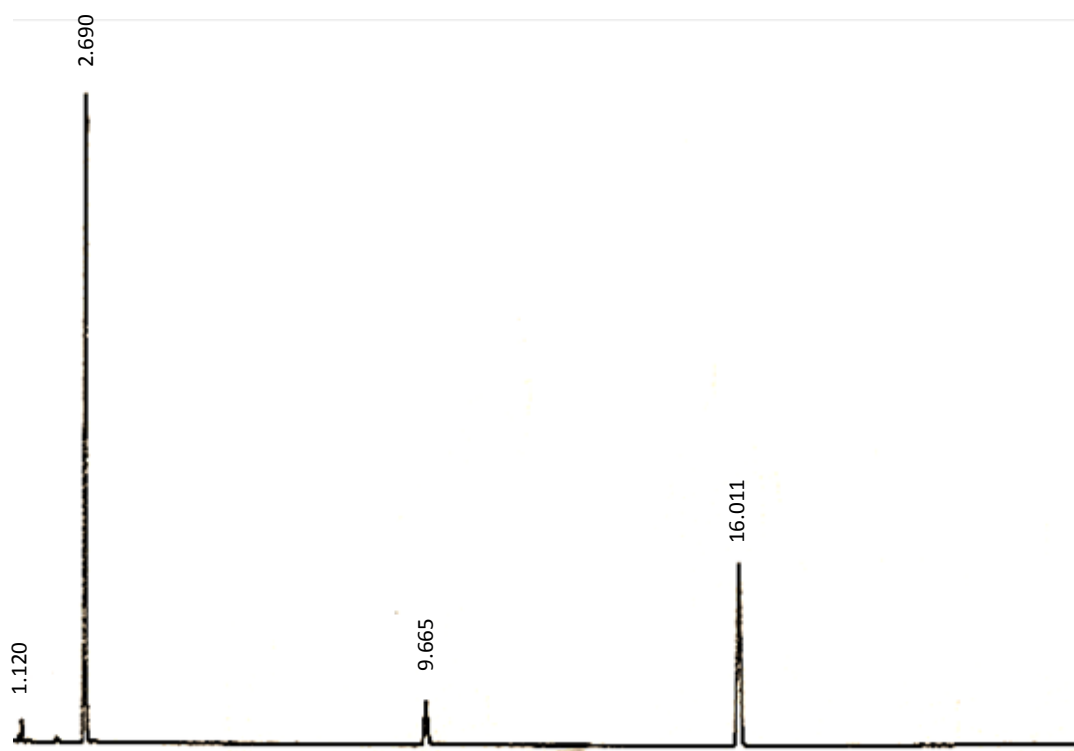


Figure 3.15 GC -Chromatogram of 2,5-DTBHQ in styrene after being heated at 110 °C for 5 h

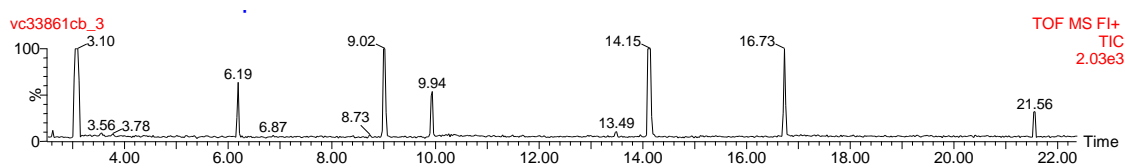
The GC chromatogram in Figure 3.15 reveals the predominant formation of 2,5-DTBBQ with a retention time of 9.85 min. In addition, several small peaks appear on the chromatogram, but they were too small to be assigned. To avoid all the products derived from styrene polymerisation we decided to work in a non-polymerizable solvent and use AIBN as a source of alkyl radicals.

2,5 DTBHQ ( $7.5 \times 10^{-2}$  mmol) and AIBN (0.45 mmol) were dissolved in toluene (7.5 mL). The solution was left at 80 °C for 19 h under nitrogen atmosphere. The solution was monitored by gas chromatography (Figure 3.16) and gas chromatography with field ionization mass spectrometry (GC-FI) (Figure 3.17).



**Figure 3.16 GC chromatogram of a solution of 2,5-DTBHQ and AIBN in styrene at time = 0**

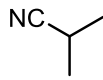
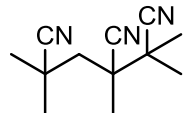
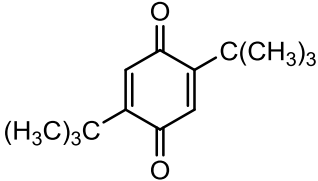
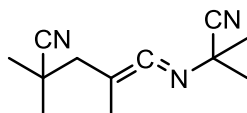
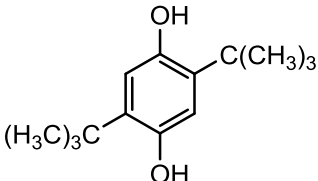
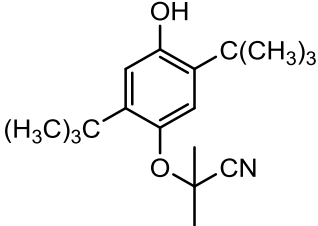
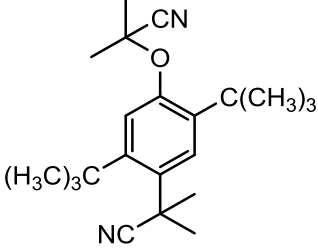
In Figure 3.16 the peak at 1.02 min is toluene and at 2.69 min is the peak of AIBN. Also, the peaks at 9.66 and 16.01 min are 2,5-DTBBQ and 2,5-DTBHQ, respectively. 2,5-DTBBQ comes from the partial oxidation of 2,5-DTBHQ during the analysis.



**Figure 3.17** Field ionization-mass spectrometry chromatogram of a solution of 2,5-DTBHQ and AIBN in toluene after 19 h heating

The GC-FI chromatogram after 19 h at 80 °C (Figure 3.17) shows the predominant peak of 2,5-DTBHQ (14.15 min) suggesting the poor reactivity of hydroquinone with alkyl radicals. Indeed, after 19 h all AIBN should be decomposed (half-life at 70 °C is 6 h)<sup>96</sup>. The assignment of the peaks is given in Table 3.2.

Table 3.2 List of the structures for the GC-FI chromatogram

Retation Time (min)	Mass (g/mol)	Structure <sup>a</sup>
3.10	69.06	
6.19	203.96	
9.02	220.15	
9.94	203.96	
14.15	222.17	
16.73	289.23	
21.56	340.26	

a) in some cases the structure reported is representative of a series of possible structural isomers.

Looking at the Table 3.2 the peaks at 3.10 min, 6.19 min and 9.94 min come from the AIBN decomposition<sup>95</sup> and the peak at 9.02 corresponds to 2,5-DTBBQ. It is reasonable to assume that 2,5-DTBBQ is generated by the disproportionation of semiquinone (**2**),



which is formed by the hydrogen abstraction of 2,5-DTBHQ (**1**) by 2-cyano-2-propyl radicals (Figure 3.18)<sup>27, 79</sup>. However, it must be noted that some 2,5-DTBBQ is produced during the GC analysis.

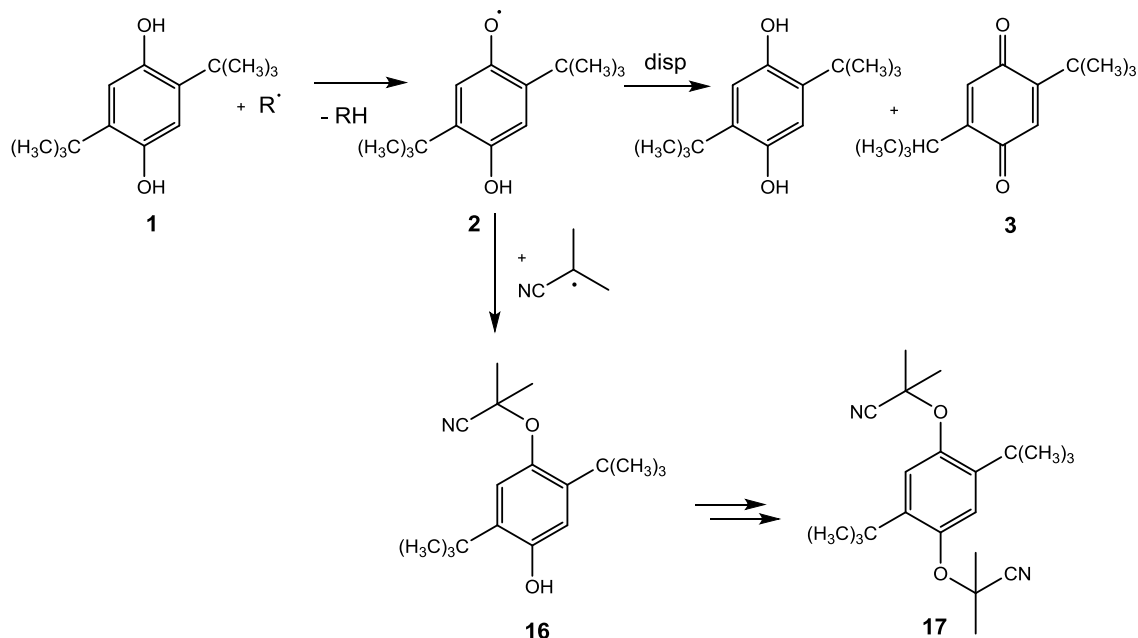


**Figure 3.18 Mechanism of hydrogen abstraction from 2,5-DTBHQ by 2-cyano-propyl-2-radicals**

In addition, semiquinone (**2**) could eventually trap a 2-cyano-2-propyl radical as confirmed by the presence of (**16**) in the reaction mixture. Compound (**16**) could then keep reacting with more alkyl radicals, however there was no evidence of (**17**) in the chromatogram. For the last compound in Table 3.2 with mass 340.26 it is really hard to find a plausible explanation of the mechanism of formation.

The study of the reactivity of 2,5-DTBHQ revealed the predominant antioxidant behaviour of this compound in an air saturated styrene solution. The high concentration of 2,5-DTBBQ in the reaction mixture indicates that the hydrogen abstraction by peroxy radicals with the formation of semiquinone radical (**2**) and rapid disproportionation to 2,5-DTBBQ and 2,5-DTBHQ is the key mechanism. However, in deoxygenated systems and in the presence of 2-cyano-2-propyl radicals, traces of the product (**16**) appear on the chromatogram.

### 3.6 Conclusions

The ability of 2,5-DTBHQ to stop propagation radicals by hydrogen abstraction, in oxygenated conditions, is well documented and has been confirmed in our laboratory carrying out dilatometry experiments. Furthermore, our studies revealed, for the same mixture, a retardation of the polymerisation at low oxygen level, meaning that other reactions may contribute to stop the propagation chains. A dilatometry trace of the auto-initiated styrene polymerisation in the presence of 2,5-DTBBQ (2,5-DTBBQ is the main product formed during the inhibition by 2,5-DTBHQ) showed a slight retardation of the polymerisation. Previous studies describe 2,5-DTBBQ as inert towards the addition reaction of carbon centred radicals, thus we repeated the experiments in order to see whether or not the addition reaction occurs to give retardation. Analysis of the reaction mixture by mass spectrometry revealed the presence of the expected addition products; however the concentration in solution was too small to allow the isolation of those products. These results suggest a limited contribution of the addition reaction to the mechanism. Correlated to this, we compared the reactivity of 2,5-DTBBQ to that of 2,6-DTBBQ, as previous works attributed the difference in reactivity between them to the position of the *tert*-butyl groups. Hence, 2,6-DTBBQ was reacted with either styrene or 2-cyano-2-propyl radicals, however we found that there is not a significant difference in reactivity between those two molecules. As a final work, we also investigated the reactivity of 2,5-DTBHQ with carbon-centred radicals. Although 2,5-DTBHQ is reluctant to react in deoxygenated conditions, we found in the reaction mixture the presence of a few compounds which suggest that carbon-centred radicals abstract the hydrogen atom from 2,5-DTBHQ leading to the semiquinone (**2**). This intermediate then reacts further with other propagation chains. We can conclude by saying that beside the hydrogen abstraction, the inhibition of the auto-initiated styrene polymerisation by 2,5-DTBHQ involves other reactions, but their contribution to the overall process seems rather limited.

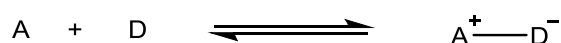
## 4 2,5-Di-*tert*-butyl-1,4-benzoquinone and *N,N*-dibenzylhydroxylamine: reaction in a non-polymerizable solvent

### 4.1 Introduction

2,5-Di-*tert*-butyl-1,4-benzoquinone (2,5-DTBBQ) and *N,N*-dibenzylhydroxylamine (DBHA) show synergism towards the inhibition of the auto-initiated styrene polymerisation. In other words, the inhibition efficiency of the mixture of these two compounds is significantly enhanced with respect to the single components. This improvement could be attributed to the reaction between DBHA and 2,5-DTBBQ yielding new inhibitors. This chapter aims to detect these compounds and investigate the mechanism of their formation.

#### 4.1.1 Background

Benzoquinones are electron poor molecules which often interact with electron donors, such as amines and hydroxylamines, via charge transfer complex formation<sup>97, 98</sup>. The term “charge-transfer complex” refers to substances containing one or more components which interact by charge transfer forces<sup>99, 100</sup>. The nature of the interaction is mainly non-covalent in the ground state, but characterized by London dispersion, dipole-dipole, induced dipole or hydrogen bond forces. The almost complete absence of the covalent bond ensures that the complex is in equilibrium with its dissociated components and the position of the equilibrium depends on the strength of both electron donor and acceptor.



Using the valence-bond theory the interaction at the ground state between donor (D) and acceptor (A) can be described by the following wave function<sup>99, 100</sup>:

$$\psi_G(AD) = a\psi_0(A, D) + b\psi_1(A^- - D^+)$$

$\psi_0$  corresponds to the “no bound” function, in which the bonding results from non-covalent interaction.

$\psi_1$  is the “dative” function and it corresponds to the ionic structure in which the electron has been shifted from the donor to the acceptor.

a and b are coefficients.

In terms of energy (Figure 4.1), the ground state ( $W_G$ ) will be related to the energy of the two independent components ( $W_\infty$ ) modified by the “no bound” energy ( $G_0$ ) ( $G_0$  can be positive or negative), and by the resonance energy ( $X_0$ ) between the complex and the two individual compounds as shown by the following equation:

$$W_G = W_\infty + G_0 - X_0$$

The irradiation of the complex with a suitable light (usually in visible region) produces a transition from the ground state to the excited state; the wave function of the excited state ( $\psi_E$ ) is described as:

$$\psi_E(AD) = a\psi_1(A^- - D^+) - b\psi_0(A, D)$$

and the energy related to the excited state would be:

$$W_E = W_1 + X_1$$

Here,  $W_1$  is the energy of dative state and  $X_1$  is the resonance energy between the complex and the separated components (Figure 4.1).

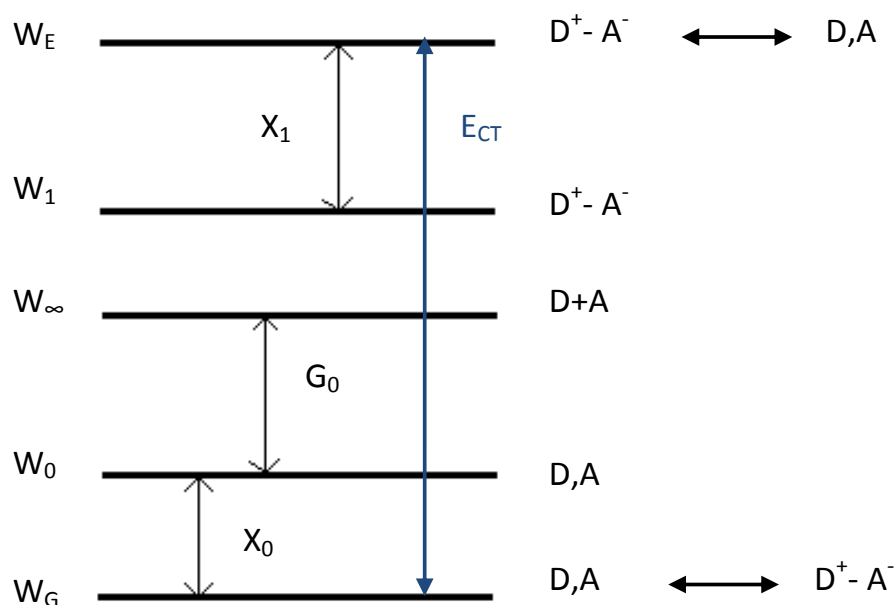


**Figure 4.1 Charge transfer complex diagram**

The  $W_G$  and  $W_E$  energies depend on the overlapping between  $\psi_0$  and  $\psi_1$  in the ground and excited state, respectively, hence,  $\psi_0$  and  $\psi_1$  have to belong to the same group theory to overlap at least to some extent. Therefore, the strength of the interaction will be dependent on the extent of the overlapping between molecular orbital of the donor and the acceptor<sup>99, 100</sup>.

In the simplest case only a single transition occurs from the ground to the excited state in the complex, this transition is called intermolecular charge transfer transition and the energy ( $E_{CT}$ ) is

$$E_{CT} = h\nu_{CT}$$

$\nu_{CT}$  is the frequency characteristic of the intermolecular charge-transfer transition (Figure 4.1). The electronic spectrum of a charge transfer complex will be characterized by the absorption band of the separated components and by at least one extra band characteristic of the complex. This extra band would be at a frequency corresponding to the intramolecular charge-transfer transition. However, in solution it may not be easy to observe the band relative to the CTC, especially with a weak donor and acceptor. In this case, the complex has similar UV spectrum to the separated components with a consequent overlapping between the band of the complex and

that of the individual components. Strong donors and acceptors however, will have a complete transfer of the electron with a consequent band of the CTC shifted to a considerably longer wavelength with respect to the individual compounds. Al-Ahmary details<sup>101</sup> the characterization and the investigation of the thermodynamic properties of a charge transfer complex formed by 2-aminopyridine and 2,5-dihydroxy-*p*-benzoquinone. The charge transfer complex is stable enough to be isolated as violet crystals. Strong colour is typical of charge transfer complexes. The electronic absorption spectrum shows a band at a longer wavelength, with respect to the single components, which has been attributed to the complete transfer of charge from 2-aminopyridine to 2,5-dihydroxy-*p*-benzoquinone.

The above literature review suggests that benzoquinones are likely to form charge transfer complexes with hydroxylamines and the charge transfer may be responsible for polymerisation inhibition.

### **4.1.2 Aim of the chapter**

Observing the formation of a charge transfer complex between DBHA and 2,5-DTBBQ is one of the main aims of the chapter. In addition, combination of analytical techniques was used to detect the formation of products and intermediates. Moreover, information regarding the reaction between DBHA and 2,5-DTBBQ was obtained from kinetic analyses and by monitoring the substituent effect.

## **4.2 Investigation of charge transfer complexes**

As mentioned in the introduction, it is common for benzoquinones to form charge transfer complexes with amines or hydroxylamines<sup>98, 101</sup>. Hence, ultraviolet-visible spectroscopy (UV-Vis) was used to detect the potential band characteristic of the intramolecular charge transfer transition of DBHA/2,5-DTBBQ complex.

Solutions of DBHA, 2,5-DTBBQ and 2,5-DTBBQ/DBHA (1:1) in acetonitrile were prepared. Similarly, a solution of *N,N*-benzylidenebenzylamine-*N*-oxide and 2,5-DTBHQ were prepared. Those two compounds are the products of the reaction between DBHA and 2,5-DTBBQ. Styrene could not be used as a solvent because it absorbs the

ultraviolet radiation in the same region as the substances under analysis. For each solution, the electronic absorption spectra were recorded at room temperature (Figure 4.2). Although the inhibition of styrene polymerisation is carried out at 110 °C, we decided to investigate the charge transfer complex formation at room temperature as the lower temperature favours the CTC formation and increases the chance of observing the CTC band.

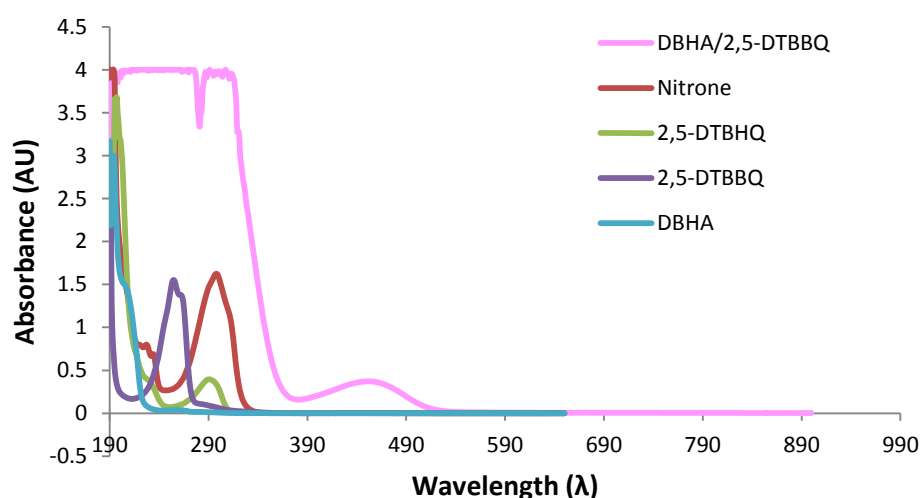


**Figure 4.2 UV-Vis spectrum of DBHA/2,5-DTBBQ mixture in acetonitrile**

Figure 4.2 shows that in the electronic spectrum of the DBHA/2,5-DTBBQ mixture an extra band appears compared to that of the separated components. This extra band can be associated with the intramolecular charge transfer transition, confirming that 2,5-DTBBQ and DBHA form a charge transfer complex. Even though molar extinction coefficient was not estimated, it is possible that the charge transfer complex in solution is not negligible. Indeed, previous studies reported the molar extinction coefficient for stable charge transfer complexes between benzoquinones and a series of compounds (e.g., 4-aminopyridine<sup>101</sup>, biphenyl, naphthalene, acetanilide, p-acetotoluidine<sup>102</sup>), the values are between 1000-6000 L·mol<sup>-1</sup>·cm<sup>-1</sup>. Assuming that the molar extinction coefficient of the DBHA/2,5-DTBBQ charge transfer complex is in that range, the concentration would be between 10<sup>-5</sup>-10<sup>-4</sup> M. These values are not accurate, but

suggest that in spite of the weak band (Figure 4.2), the CTC concentration could be sufficiently high to affect inhibition.

Although we confirmed that DBHA and 2,5-DTBBQ combine via non-covalent interactions, the formation of other intermediates was explored, in particular radical intermediates by using EPR spectroscopy.

### 4.3 Investigation of *N,N*-dibenzyl nitroxide formation by EPR spectroscopy

*N,N*-dibenzyl nitroxide, as we have already seen in Chapter 2, traps propagation radicals, thus it was decided to investigate the formation of this nitroxide during the reaction between DBHA and 2,5-DTBBQ, as a potential inhibitor.

A 0.1 M solution of DBHA and 2,5-DTBBQ (1:1 ratio) in toluene was prepared. The analysis was carried out under nitrogen atmosphere, in the EPR cavity at 90 °C. EPR spectra were recorded every 2.7 min for 3 h (Figure 4.3).

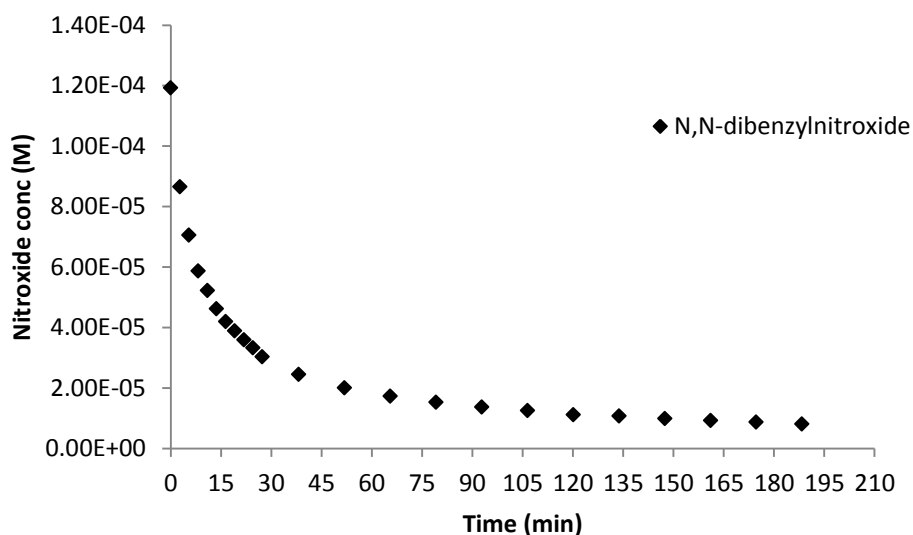


**Figure 4.3** Evolution of *N,N*-dibenzyl nitroxide concentration during the oxidation of DBHA by 2,5-DTBBQ at 90 °C

Figure 4.3 reports the absolute *N,N*-dibenzyl nitroxide concentration produced during the reaction. Nitroxide concentration was estimated by comparing the double integral



of each signal to that of 1 mM solution of TEMPO. It is evident from the above chart that the maximum *N,N*-dibenzyl nitroxide concentration is reached before the first scan, but even though its concentration is relatively low, the signal persists in all scans.

*N,N*-dibenzyl nitroxide is a good candidate to be tested as inhibitor of the styrene polymerisation, however the end products of DBHA/2,5-DTBBQ reaction have to be identified. <sup>1</sup>H-NMR spectroscopy is the next technique to be used.

## 4.4 Investigation of intermediates and products by NMR spectroscopy

A kinetic study of the reaction between 2,5-DTBBQ and DBHA was carried out in a suitable non-polymerizable solvent. This approach has a double advantage of giving information on the reaction kinetics, and the structure of intermediates and products. In particular, it was important to establish if the reaction is an irreversible or an equilibrium process, as equilibrium between reagents and products could be responsible for the synergism of DBHA/2,5-DTBBQ. A parallel investigation of substituent effect was also carried out to gain more information about the mechanism of reaction.

### 4.4.1 Reaction order and rate constant

The reaction of 2,5-DTBBQ with DBHA was carried out in toluene-d<sub>8</sub>, which is a non-polymerizable solvent with similar properties to styrene. *N,N*-Dibenzylhydroxylamine (0.25 mmol) and 2,5-di-*tert*-butyl-1,4-benzoquinone (0.25 mmol) were dissolved in toluene-d<sub>8</sub> (2.5 mL) and 1,4-dioxane (0.41 mmol) was added as an internal standard. The reaction was monitored by NMR under nitrogen atmosphere at 90 °C for 11 h, recording a spectrum every 17 min (Figure 4.7). Sample preparation is reported in the experimental part. The following are the <sup>1</sup>H-NMR spectra recorded at time zero (Figure 4.4) and after 11 hours (Figure 4.6).

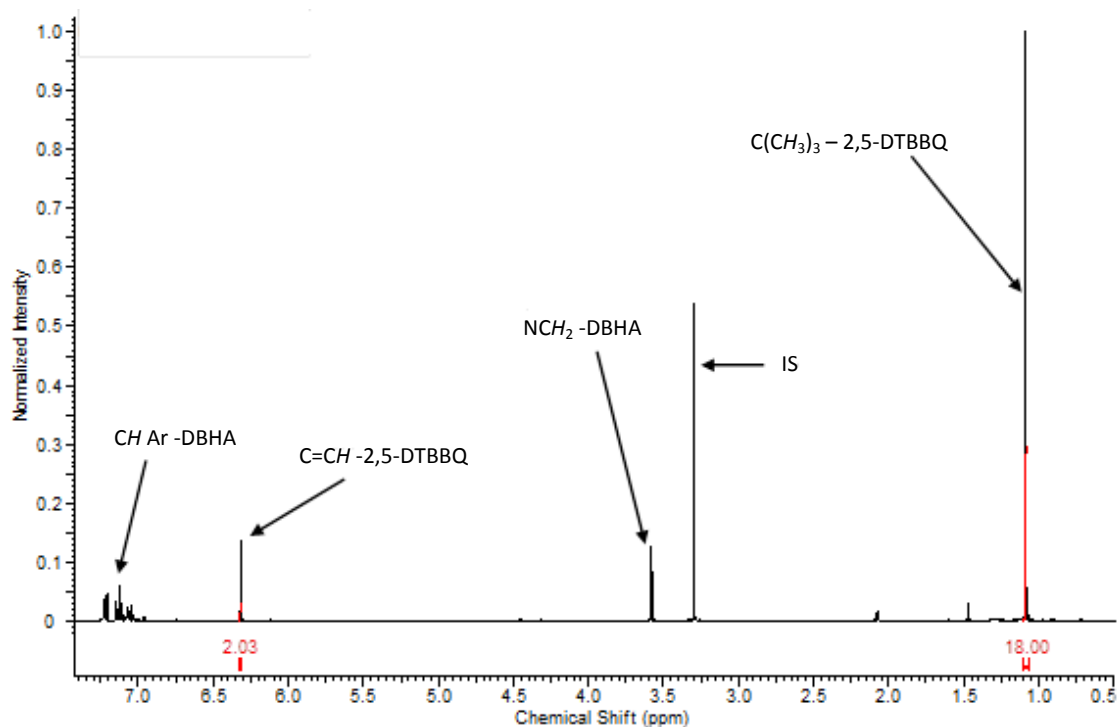


Figure 4.4  $^1\text{H-NMR}$  spectrum of the DBHA/2,5-DTBBQ solution in toluene- $d_8$ , recorded at time 0 min using a 400 MHz spectrometer at 25 °C

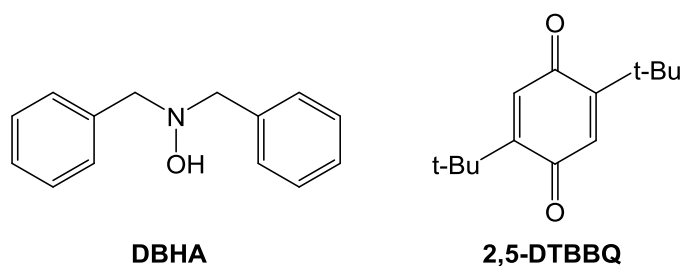


Figure 4.5 Structures of reagents

Figure 4.4 shows the  $^1\text{H-NMR}$  spectrum of the reaction mixture recorded at time zero at room temperature while Figure 4.5 presents the corresponding reagents structures. The signals of *N,N*-dibenzylhydroxylamine are  $\delta$  7.3-6.9 (m, 10H, *CH Ar* x 10) and 3.4 (s, 4H, *NCH*<sub>2</sub> x 2) and the signals of 2,5-DTBBQ are  $\delta$  1.1 (s, 18H, *C(CH*<sub>3</sub>)<sub>3</sub> x 2), 6.3 (s, 2H, *C=CH* x 2).

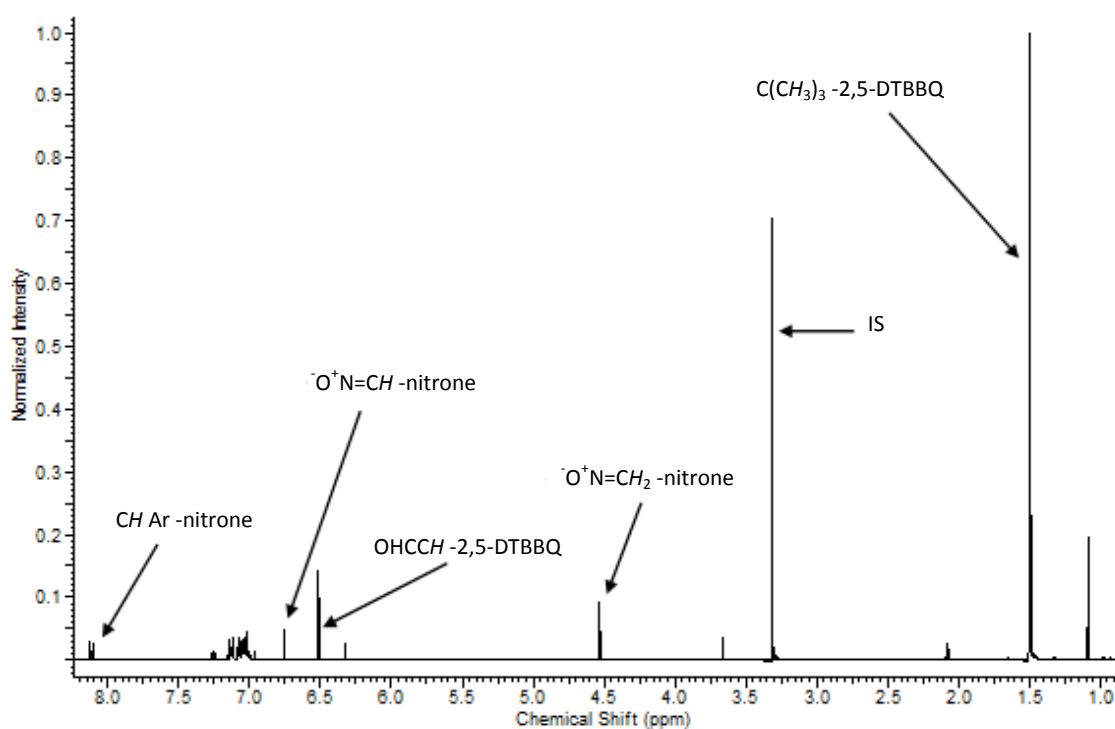


Figure 4.6  $^1\text{H-NMR}$  spectrum of 2,5-DTBBQ/DBHA in toluene- $d_8$ , recorded using a 400 MHz NMR spectrometer at 25 °C after 11 h of heating

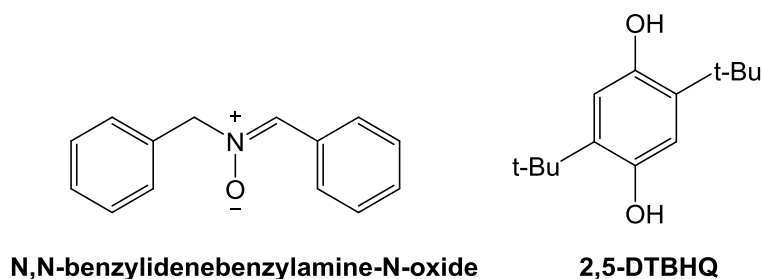


Figure 4.7 Products structures

The spectrum in Figure 4.6 clearly shows that most of the starting material has been consumed. The structures of the products are reported in Figure 4.7. NMR signals of *N,N*-benzylidenebenzylamine-*N*-oxide are  $\delta$  8.2-8.1 (m, 2H, CH Ar x 2), 7.3-6.9 (m, 8H, CH Ar x 8), 6.7 (s, 1H,  $\text{O}^+\text{N}=\text{CH}$ ), 4.5 (s, 2H,  $\text{O}^+\text{NCH}_2$ ), while NMR signals of 2,5-DTBHQ are  $\delta$  6.5 (s, 2H, OHCCH x 2), 1.5 (s, 18H,  $\text{C}(\text{CH}_3)_3$  x 2).

Reactants and products concentrations calculated from each  $^1\text{H-NMR}$  spectrum (calculation is reported in the experimental section) were plotted against time as shown in Figure 4.8.

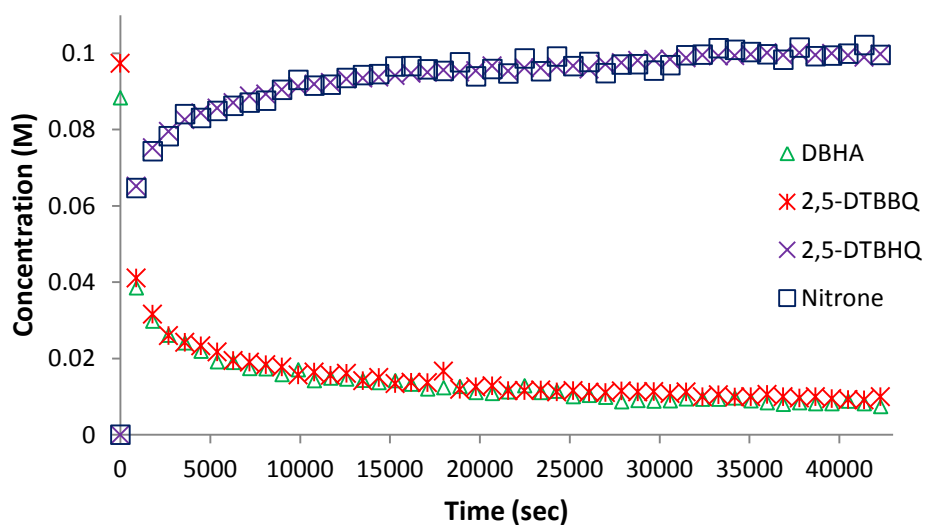


Figure 4.8 DBHA (green triangles), 2,5-DTBBQ (red stars), 2,5-DTBHQ (purple crosses) and *N,N*-benzylidenebenzylamine-*N*-oxide (blue squares) concentrations evolution in toluene- $d_8$  at 90 °C

Figure 4.8 shows that 2,5-DTBBQ is reduced to 2,5-DTBHQ while DBHA is oxidised to *N,N*-benzylidenebenzylamine-*N*-oxide with no evidence of formation of intermediates.

The experimental data were then fitted to a second order mechanism using Dynafit<sup>62</sup> to estimate kinetics parameters (Figure 4.9).

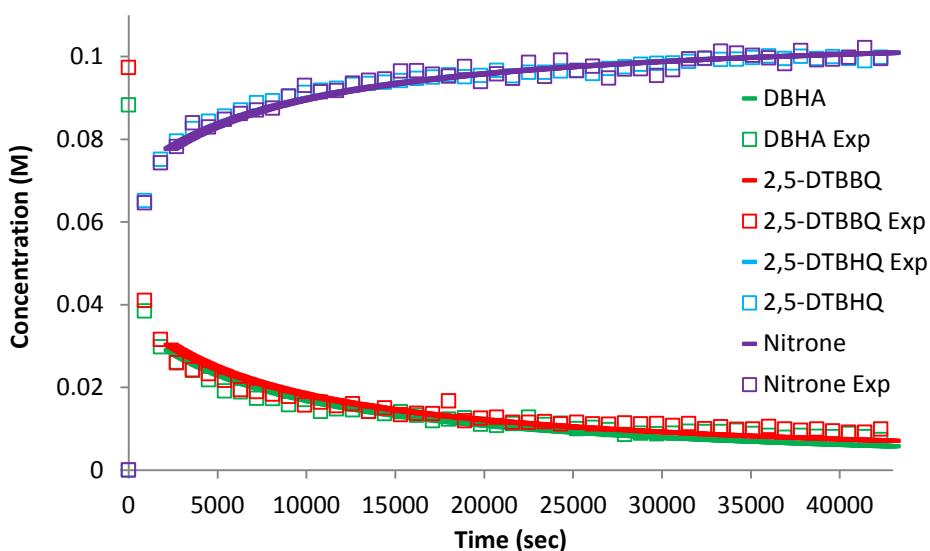
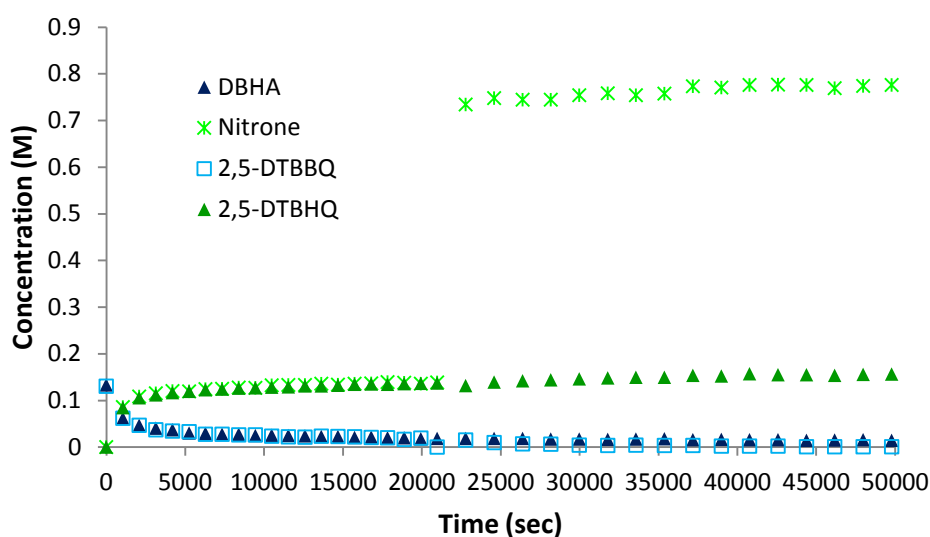


Figure 4.9 Fitting of Dynafit data (lines) to experimental data (empty squares) for the reaction between 2,5-DTBBQ and DBHA in toluene- $d_8$  at 90 °C

In Figure 4.9, the experimental concentrations (empty squares) are compared to theoretical data generated by Dynafit (lines) for a second order process. The experimental data nicely fit the second order mechanism and the estimated rate constant is  $(3.02 \pm 0.09) \times 10^{-3} \text{ M}^{-1} \text{ s}^{-1}$ .

In order to test if this reaction is reversible, *N,N*-benzylidenebenzylamine-*N*-oxide was added at the end of reaction to see if there is any change in reactant concentrations. Variation of the concentrations would have been an indication of a reverse reaction.

*N,N*-Dibenzylhydroxylamine (0.25 mmol), 2,5-di-*tert*-butyl-1,4-benzoquinone (0.25 mmol) and 1,4-dioxane (0.41 mmol) in toluene- $d_8$  (2.5 mL) were degassed and  $^1\text{H}$ -NMR spectra were recorded at 90°C every 17 min for 6 h. At this point the solution was cooled down and *N,N*-benzylidenebenzylamine-*N*-oxide (0.25 mmol) was added. After the addition the solution was filled with nitrogen and heated again at 90 °C in the NMR cavity. Spectra were recorded every 17 min for 7.5 h (Figure 4.10).



**Figure 4.10** DBHA (purple triangles) 2,5-DTBBQ (blue squares), 2,5-DTBHQ (green triangles) and *N,N*-benzylidenebenzylamine-*N*-oxide (green stars) concentrations evolution in toluene- $d_8$  at 90 °C

Figure 4.10 shows that the addition of *N,N*-benzylidenebenzylamine-*N*-oxide does not affect the reactants concentration, confirming that DBHA and 2,5-DTBBQ react via an irreversible mechanism.

The use of toluene as a solvent allowed us to monitor the reaction at a maximum temperature of 90 °C (boiling point of toluene is 110 °C). However, we needed to estimate the value of the rate constant at 110 °C, as that is the temperature at which the inhibition of styrene polymerisation is normally carried out. The problem was solved by using the Arrhenius equation, which correlates the change of rate constant to the change of temperature. The kinetics of 2,5-DTBBQ/DBHA reaction was monitored at 80 (Figure 4.11) and 70 °C (Figure 4.12).

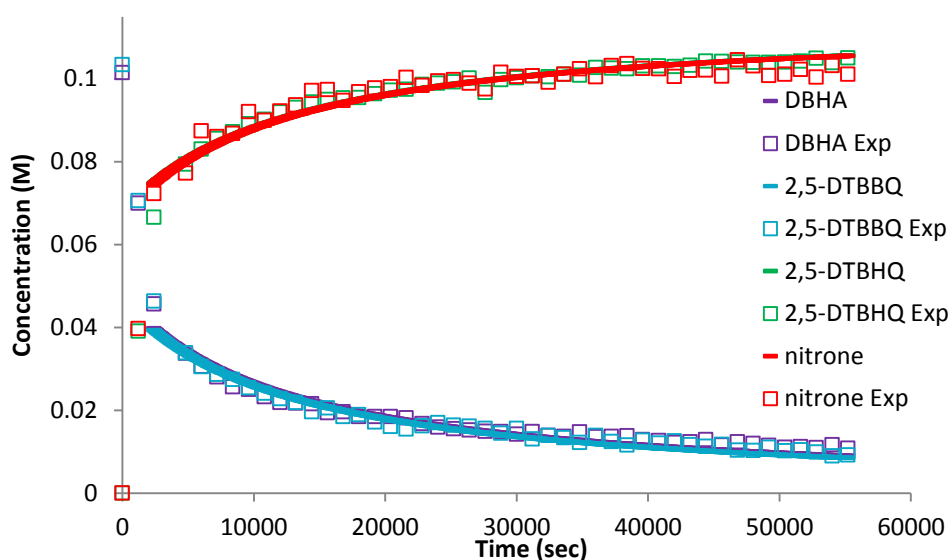


**Figure 4.11** Fitting of Dynafit data (lines) to experimental data (empty squares) for the reaction between 2,5-DTBBQ and DBHA in toluene- $d_8$  at 80 °C

In Figure 4.11 a comparison between the experimental (empty squares) and the Dynafit data (lines) is reported for the reaction at 80 °C. The rate constant for the process is  $(1.70 \pm 0.04) \times 10^{-3} \text{ M}^{-1} \text{ s}^{-1}$ .

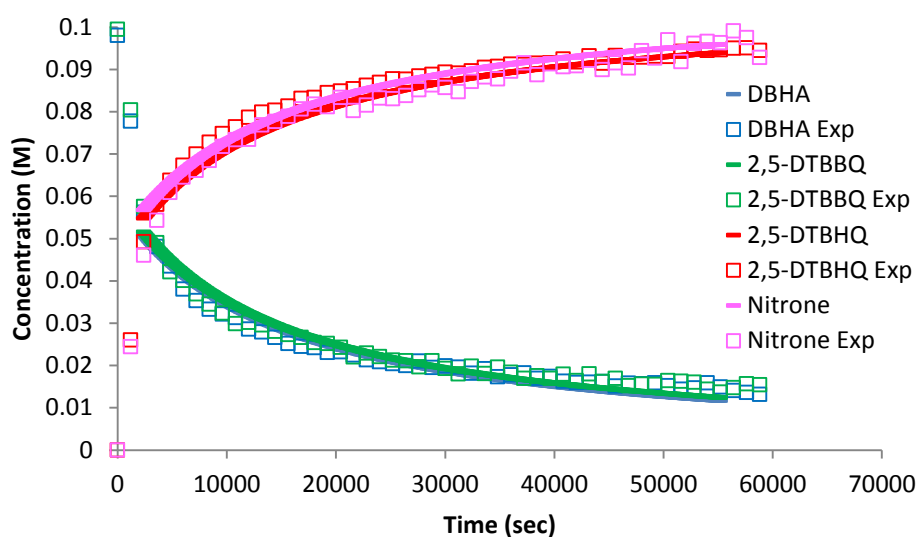


**Figure 4.12** Fitting of Dynafit data (lines) to experimental data (empty squares) for the reaction between 2,5-DTBBQ and DBHA in toluene- $d_8$  at 70 °C

Figure 4.12 reports the comparison between experimental data (empty squares) and Dynafit data (lines) for the process at 70 °C. The rate constant is  $(1.20 \pm 0.03) \times 10^{-3} \text{ M}^{-1} \text{ s}^{-1}$ .

The activation energy is extrapolated by using the following equation:

$$\ln k = -\frac{E_a}{R \times T} + \ln A \quad \text{Slope} = -\frac{E_a}{R}$$

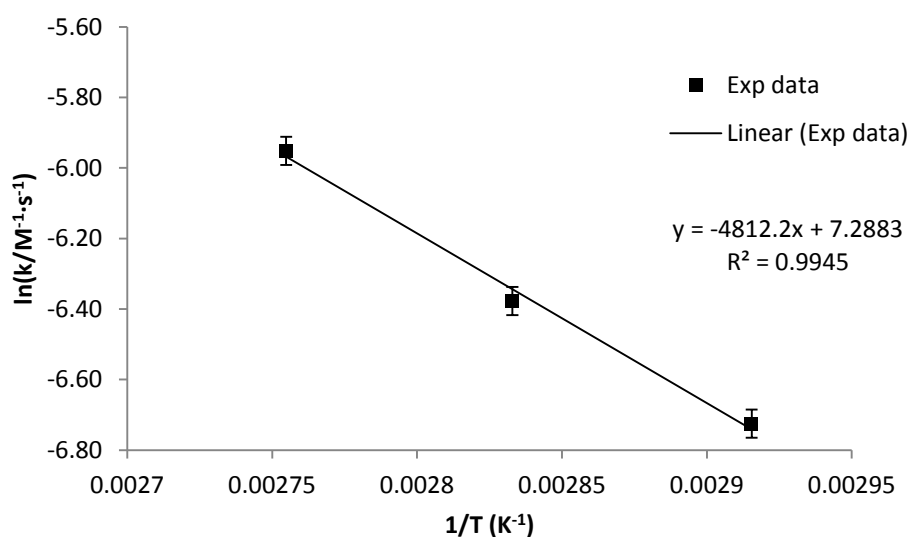


**Figure 4.13 Arrhenius plot. The logarithm of the rate constant is plotted vs the reciprocal of the temperature**

The activation energy for the reaction is 39.9 kJ/mol. By using the following equation the rate constant at 110 °C was estimated:

$$\ln\left(\frac{k_{343\text{ K}}}{k_{383\text{ K}}}\right) = -E_a \times \left(\frac{1}{383} - \frac{1}{343}\right)$$

Rate constant at 110 °C is 0.0051 M<sup>-1</sup>s<sup>-1</sup>. By knowing the rate constant we were also able to estimate the half-life:

$$-\frac{1}{2} \frac{d[A]}{dt} = k[A]^2$$

$$t_{1/2} = \frac{1}{kA_0}$$

The half-life at 110 °C is 32 min.

Activation parameters were calculated from Eyring plot (Figure 4.14).

$$k = \left(\frac{k_B T}{h}\right) e^{\left(\frac{-\Delta G^\ddagger}{RT}\right)} = \left(\frac{k_B T}{h}\right) e^{\left(\frac{\Delta S^\ddagger}{R}\right)} e^{\left(\frac{-\Delta H^\ddagger}{RT}\right)}$$

$$\text{Intercept} = \left(\ln \frac{k_B}{h}\right) + \frac{\Delta S^\ddagger}{R} \quad \text{Slope} = -\frac{\Delta H^\ddagger}{R}$$



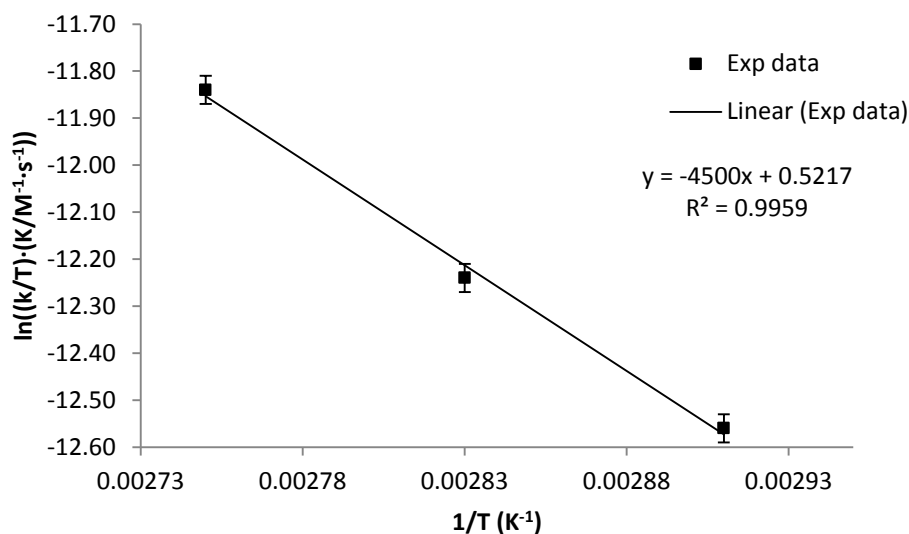


**Figure 4.14 Eyring plot**

The activation entropy ( $\Delta S^\ddagger$ ) was  $-190.0 \text{ J}/(\text{K}\cdot\text{mol})$  and the activation enthalpy ( $\Delta H^\ddagger$ ) was  $37.39 \text{ kJ}/\text{mol}$ . The activation entropy is a large negative value which suggests a substantial reduction of the translational and rotational degrees of freedom, typical of a combination of two molecules. In addition the  $T\Delta S^\ddagger$  value is much bigger than the  $\Delta H^\ddagger$  value, which means that the reaction is entropy controlled<sup>103-105</sup>.

In order to obtain more information on the reaction mechanism, a study of the substituent effect was carried out.

#### 4.4.2 Substituents effect

Monitoring how the reactivity of a molecule changes for different substituents is a powerful tool to investigate the nature of the activated complex. A common method used to quantify the substituent effect is the Hammett plot, however in some cases this linear relationship does not hold. Commonly, substituents affect a reaction by polar or steric effects, however they have to be close to the reaction site. If these substituents are located at a certain distance, so that the polar and steric effects can be considered small, the rate of reaction becomes dependent on the mass of the substituents. This effect is called *ponderal effect*<sup>106</sup>. In the transition state theory, reactants and transition state are in pre-equilibrium and the rate of reaction depends

on the Gibbs energy difference between starting material and transition state. The addition of an inert mass to one of the reactants will affect the entropy of that starting material and the transition state, with a consequent change of the reaction rate. In particular, the entropy of a system corresponds to the sum of the translational, vibrational and rotational entropies, which are mass dependent, as reported by De La Mare<sup>106</sup>. Therefore, an additional mass will cause an increase in the initial entropy compared to the compound with no substituents, but the entropy of the transition state will be lowered, as a change of mass in the transition state is proportionally smaller than in the initial state. Since a change of entropy in the system is given by the difference between the entropy of the transition state and that of the initial state, an additional mass corresponds to an overall decreasing of the entropy of the system, with a consequent slowing down of the rate of reaction. This effect was invoked by Church<sup>107</sup> to explain the deviation from the linear correlation between the Hammett parameters and the hyperfine splitting constant of substituted phenyl spin adducts of DMPO. Electron donating substituents showed larger hyperfine splitting constants than the electron withdrawing and all values nicely correlated to the Hammett parameters, except for the unsubstituted phenyl.

In this section, the substituent effect on the rate of reaction between DBHA and 2,5-DTBBQ was monitored. Electron donating and withdrawing substituents were introduced in para position on both aromatic rings of DBHA.

*N,N*-bis(*p*-methylbenzyl)hydroxylamine (DBHA-CH<sub>3</sub>), *N,N*-bis(*p*-chlorobenzyl)hydroxylamine (DBHA-Cl), and *N,N*-bis(*p*-trifluoromethylbenzyl)hydroxylamine (DBHA-CF<sub>3</sub>) were synthesised by nucleophilic substitution of hydroxylamine hydrochloride and *p*-substituted benzyl bromide (Figure 4.15). A detailed description of the reaction conditions is reported in the Experimental section.

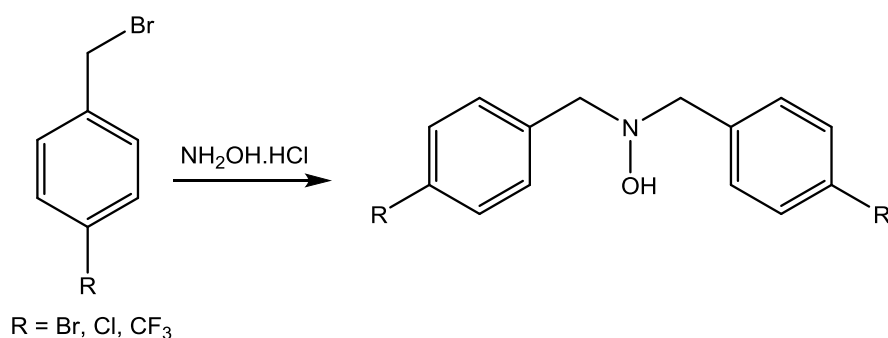


**Figure 4.15** General scheme for the synthesis of *p*-substituted hydroxylamines

The following is the general procedure of a kinetic experiment. DBHA-R (0.1 mmol) and 2,5-di-*tert*-butyl-1,4-benzoquinone (0.1 mmol) were dissolved in toluene-*d*<sub>8</sub> (1 mL). 1,4-Dioxane (0.04 mmol) was added as an internal standard. The analysis was monitored under nitrogen atmosphere at 70 °C for 11 h, recording a spectrum every 17 min. The experimental concentrations of reagents and products were then fitted to a second order kinetic to establish the rate constants (Figure 4.16, Figure 4.17 and Figure 4.18).

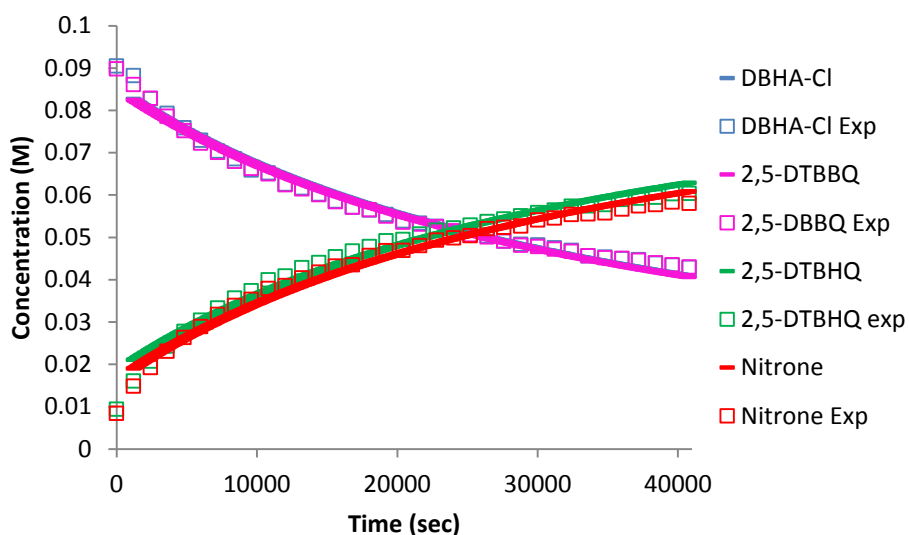


**Figure 4.16** Fitting of Dynafit data (lines) to experimental data (empty squares) for the reaction between 2,5-DTBBQ and DBHA-Cl in toluene-*d*<sub>8</sub> at 70 °C

The rate constant for the reaction between DBHA-Cl and 2,5-DTBBQ at 70 °C is  $(3.1 \pm 0.4) \times 10^{-4} \text{ M}^{-1} \text{ s}^{-1}$ . As shown by Figure 4.16, the initial experimental concentrations

were not included in the calculation to allow better fitting. The initial concentrations may not be quite accurate as the temperature is not yet equilibrated in the system.

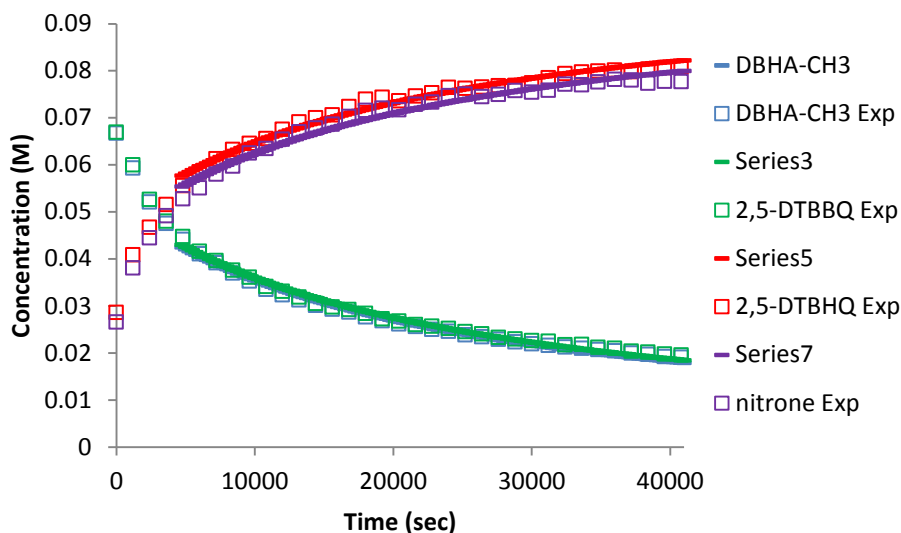


Figure 4.17 Fitting of Dynafit data (lines) to experimental data (empty squares) for the reaction between 2,5-DTBBQ and DBHA-CH<sub>3</sub> in toluene-d<sub>8</sub> at 70 °C

The rate constant for the reaction between DBHA-CH<sub>3</sub> and 2,5-DTBBQ at 70 °C is  $(8.8 \pm 0.2) \times 10^{-4} \text{ M}^{-1} \text{ s}^{-1}$ .

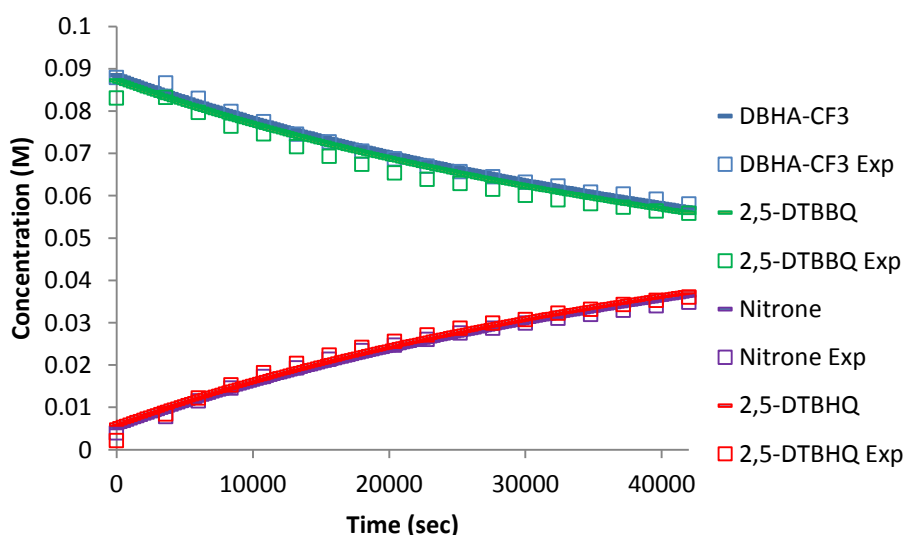


Figure 4.18 Fitting of Dynafit data (lines) to experimental data (empty squares) for the reaction between 2,5-DTBBQ and DBHA-CF<sub>3</sub> in toluene-d<sub>8</sub> at 70 °C

The rate constant for the reaction between DBHA-CF<sub>3</sub> and 2,5-DTBBQ at 70 °C is  $(1.6 \pm 0.2) \times 10^{-4} \text{ M}^{-1} \text{ s}^{-1}$ .

Table 4.1 reports the rate constant values calculated for different substituents.

**Table 4.1 Rate constants at 70 °C for the reaction of 2,5-DTBBQ with *p*-substituted DBHAs**

Reactant	k (M <sup>-1</sup> s <sup>-1</sup> )
DBHA-H	1.20x10 <sup>-3</sup>
DBHA-CH <sub>3</sub>	8.8x10 <sup>-4</sup>
DBHA-Cl	3.1x10 <sup>-4</sup>
DBHA-CF <sub>3</sub>	1.6x10 <sup>-4</sup>

The values of rate constants in Table 4.1 suggest that increasing of the substituent mass is associated with the slowing down of the rate of reaction. This can be explained by the ponderal effect.

Electronic effect was too small compared to the ponderal effect, thus we could not obtain information about the structure of the activated complex using the Hammett linear relationship. However, with the data accumulated so far the mechanism of reaction is discussed in the next section.

## 4.5 Reaction mechanism

The experiments carried out and discussed above do not allow to propose a detailed mechanism for the oxidation of DBHA by 2,5-DTBBQ. However, a combination of our results with those published by Hassan *et al*<sup>98, 108</sup> on the oxidation of *N*-benzyl-*N*-alkylhydroxylamine by benzoquinone allows some conclusions to be made. The following is the mechanism proposed in the Hassan's work (Figure 4.19).

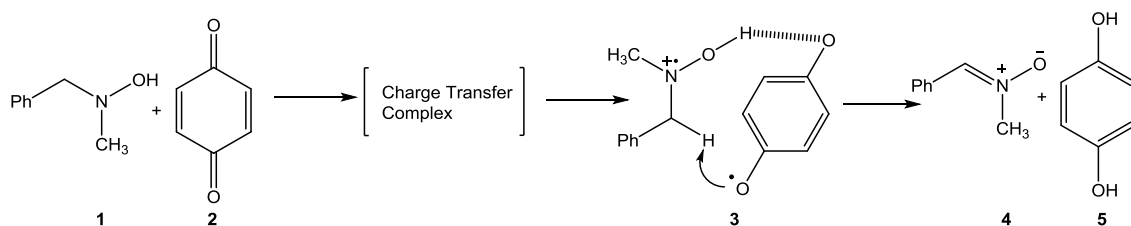


**Figure 4.19 Mechanism proposed by Hassan for the oxidation of *N*-benzyl-*N*-methylhydroxylamine by benzoquinone**

These authors observe a blue charge transfer complex upon mixing hydroxylamine (**1**) and benzoquinone (**2**) in  $\text{CDCl}_3$ . The colour disappears only when the reactants are converted to products. In addition, a strong EPR signal is associated with the radical ion formation (**3**). The formation of a positive charge on the nitrogen atom is supported by the  $\rho$  value in the Hammett plot ( $\rho = -0.483$ ). Furthermore, formation of (**3**) is the rate determining step and to explain the radical isotope effect, observed by H/D substitution on the benzylic protons of hydroxylamine (**1**), the authors suggested a reversible formation of the radical pair (**3**).

A schematic mechanism for DBHA-2,5-DTBBQ reaction is reported in Figure 4.20.

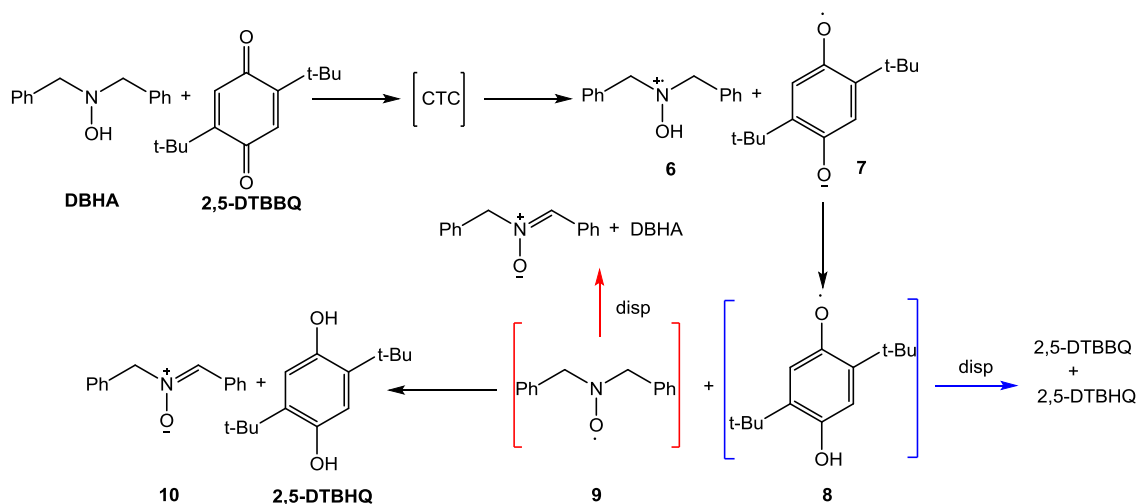


**Figure 4.20 Schematic mechanism of DBHA oxidation by 2,5-DTBBQ**

Similarly to the results of Hassan and co-workers, we observed the formation of a charge transfer complex. Although we did not estimate the molar extinction coefficient to calculate the real concentration in solution, we can speculate that the CTC does not accumulate in solution because the radical ion pair (**6**) and (**7**) rapidly undergoes

proton transfer leading to *N,N*-dibenzyl nitroxide (**9**) and semiquinone (**8**). The absence of an intense coloration of the solution characteristic of the CTC, also supports the idea that the CTC is present in a relatively low concentration. Semiquinone, then, oxidizes *N,N*-dibenzyl nitroxide (**9**) to *N,N*-benzylidenebenzylamine-*N*-oxide (**10**) reducing itself to 2,5-DTBHQ. However, the formation of *N,N*-dibenzyl nitroxide and semiquinone does not exclude their rapid disproportionation as we know from chapter 2 and 3<sup>77</sup>.

## 4.6 Conclusions

### 4.7

An investigation of potential inhibitors responsible for the excellent ability of DBHA/2,5-DTBBQ mixture to stop the auto-initiated styrene polymerisation was carried out. There are no data in the literature regarding the mechanism of oxidation of DBHA by 2,5-DTBBQ, but a similar reaction has been studied by Hassan and co-workers. We observed the formation of a charge transfer complex and even though it appears to rapidly convert to *N,N*-dibenzyl nitroxide (**9**) and semiquinone (**8**) we cannot exclude its role in the inhibition. In addition, the EPR experiment confirmed the formation of *N,N*-dibenzyl nitroxide as an intermediate in this reaction. This is an important result which establishes that during the inhibition of styrene polymerisation the reaction between DBHA and 2,5-DTBBQ also contributes to nitroxide formation. Semiquinone (**8**) was not directly observed, but the presence of the *N,N*-dibenzyl nitroxide implies its formation. The final products of DBHA/2,5-DTBBQ reaction are *N,N*-benzylidenebenzylamine-*N*-oxide and 2,5-DTBHQ whose inhibition property is tested in chapter 6.

## 5 Products analysis of inhibition of the styrene polymerisation by DBHA/2,5-DTBBQ mixture

### 5.1 Introduction

*N,N*-Dibenzylhydroxylamine (DBHA)/2,5-di-*tert*-butyl-1,4-benzoquinone (2,5-DTBBQ) mixture is an excellent inhibitor for the thermal initiated styrene polymerisation. When used separately, these two compounds show inhibition or retardation properties, however mixed together they give rise to a pronounced synergism. In the previous chapter, the reaction between 2,5-DTBBQ and DBHA was investigated in a non-polymerizable solvent in order to simplify the system. Here, an extensive analysis of the inhibition products of the styrene polymerisation is carried out. A variety of common analytical techniques are used to identify compounds responsible for the excellent inhibition properties of the mixture.

#### 5.1.1 Background

The literature reported in this section aims to direct the attention on what products are likely to be formed during the styrene polymerisation at high temperature in the presence of hydroxylamines or benzoquinones in the reaction mixture.

##### 5.1.1.1 Alkoxyamines

The reaction between nitroxide (**1**) and a carbon centred radicals (**2**) produces an alkoxyamines (**3**) (Figure 5.1).

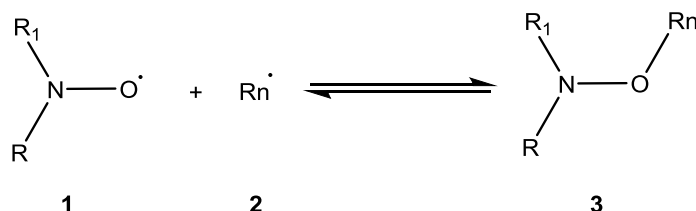


**Figure 5.1 Basic mechanism of nitroxide mediated polymerisation**

In nitroxide mediated polymerisation (NMP), the use of suitable nitroxides during the polymerisation allows control of the kinetics of the process, and hence the



characteristics of the final polymer (e.g., polydispersity, molecular weight and architecture)<sup>48</sup>. As explained in more detail in Chapter 2, NMP is based on the activation-deactivation equilibrium established between the active species (nitroxide (**1**) and propagation radicals (**2**)) and the latent species (alkoxyamines (**3**)) (Figure 5.1). Although several factors influence the above equilibrium (e.g. nitroxide stability, steric and polar effects), it is likely that alkoxyamines are formed in our reaction mixture.

### 5.1.1.2 Isoxazolidine and benzisoxazolidine

Five membered heterocycles isoxazolidine and benzisoxazolidine are conveniently synthesised via 1,3-dipolar cycloaddition, reacting a dipole and a dipolarophile via concerted mechanism. A dipole is a molecule characterised by a dipolar structure, thus it acts both as a nucleophile and electrophile, depending on whether the dipolarophile (generally a C=C double bond) is electron rich or electron poor. Nitrones (**4** and **4'**) are an example of dipoles and their reactivity towards styrene (**5**) (electron rich dipolarophile) and 2,5-DTBBQ (**6**) (electron poor dipolarophile) is well documented (Figure 5.2)<sup>109-112</sup>. In the elegant work of Shimizu and co-workers,<sup>109</sup> *N,N*-benzylidenebenzylamine-*N*-oxide (**4**) was reacted with styrene in refluxed benzene and the *endo* and *exo* diastereoisomers were obtained, with a large excess of the latter. This result is consistent with both electronic and steric effects. Indeed, electron rich dipolarophiles have higher energy HOMO compared to nitrone, thus they undergo exclusively a dipole-LUMO/dipolarophile HOMO cycloaddition with *Z*-nitrone (acyclic nitrones are stable in the *Z* configuration with respect to the *E*). However, the interaction allows both the *endo* transition state, which leads to the *trans* isoxazolidine (**trans-7**), and the *exo* transition state which gives the *cis* isoxazolidine (**cis-7**). The latter is the major product as the steric repulsions in the *exo* transition state are smaller than in the *endo*, as shown in Figure 5.3. On the other hand, the products of the cycloaddition between nitrone (**4'**) and 2,5-DTBBQ (**6**) have been investigated by Shiraishi et al.<sup>110</sup>. Though the reaction requires long time and the yield is quite poor, the benzisoxazolidine (**8**) was isolated. They found that the reaction follows the dipole-HOMO/dipolarophile LUMO and the *exo* addition is the only transition state allowed,

with the exclusive formation of the *cis* benzisoxazolidine (**8**) (Figure 5.2). Indeed, the *endo* addition is too sterically demanding to occur.

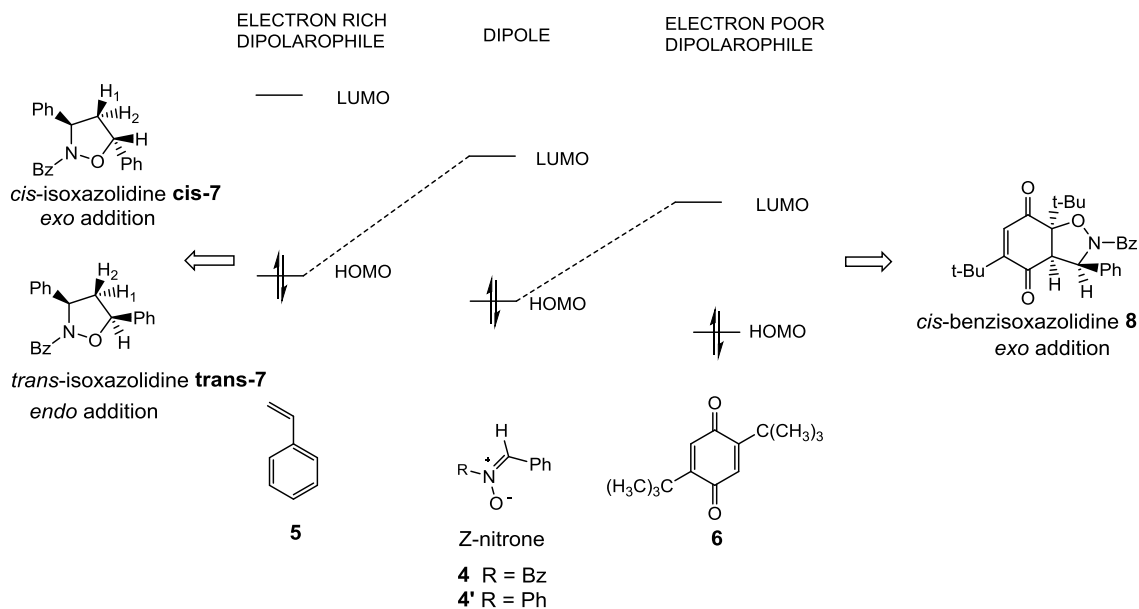


**Figure 5.2** Interaction scheme of nitrene (**4**) with an electron rich dipolarophile (styrene) and electron poor dipolarophile (2,5-DTBBQ)

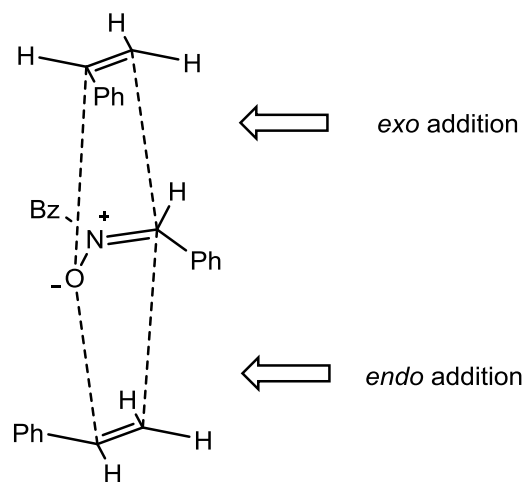


**Figure 5.3** Representation of the *exo* and *endo* addition of styrene to the nitrene **4**

Therefore, *N,N*-benzylidenebenzylamine-*N*-oxide (**4**) undergoes 1,3-dipolar cycloaddition with styrene to give isoxazolidine, but 1,3-dipolar cycloaddition with 2,5-DTBBQ is also possible. Although the latter reaction has not been specifically studied with (**4**), a similar substrate (**4'**) has been used.

## 5.1.2 Aim of the chapter

In order to unravel the mechanism of inhibition of the self-initiated styrene polymerisation by *N,N*-dibenzylhydroxylamine/2,5-di-*tert*-butyl-benzoquinone, products analysis was carried out by a range of analytical techniques. Therefore, the detection and characterisation of products (or intermediates) is the main aim of this chapter. Instead, the investigation of their inhibition properties is a concern of Chapter 6.

## 5.2 Investigation on a milligram-scale

Working with polymerizable molecules involves complex reaction mixtures which makes the isolation of all products difficult. Thus, gas chromatography and mass spectrometry are suitable analytical techniques for this particular case, as they allow analysis of the reaction mixture without prior separation. A further advantage is that both techniques require a small amount of compound for the analysis, so they allow working on a milligram-scale, reducing the quantities of reagents and solvents. On the other hand, a full characterisation of the product by these methods can only be achieved by comparison of the retention time or the fragmentation pattern to another characterised molecule. In the next sections, gas chromatography and mass spectrometry are coupled to monitor the products of DBHA/2,5-DTBBQ during reaction, in both the auto-initiated styrene polymerisation and a non-polymerizable solvent, using di-*tert*-butyl peroxide as a source of radicals.

### 5.2.1 Analysis of the styrene polymerisation inhibited by DBHA/2,5-DTBBQ

This section details the products investigation by gas chromatography coupled to mass spectrometry, followed by the structure assignment.

DBHA (0.19 mmol) and 2,5-DTBBQ (0.18 mmol) were weighted in a round bottomed flask and dissolved in styrene (10 mL). The solution was then heated at 110 °C for 15 h, under nitrogen atmosphere. The reaction mixture was analysed by gas

chromatography-mass spectroscopy using field ionisation (FI) as ionisation method (Figure 5.4).

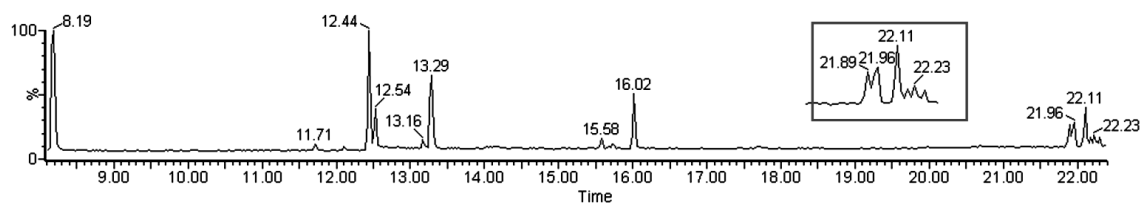


**Figure 5.4 GC chromatogram of 2,5-DTBBQ/DBHA in styrene after 15 h at 110 °C**

Figure 5.4 shows the GC chromatogram of DBHA/2,5-DTBBQ mixture in styrene after 15 h of heating. Assignment of the main peaks, based on accurate mass, is reported in Table 5.1.

**Table 5.1 Products assignment**

Retention Time (min)	Mass (g/mol)	Structure <sup>a</sup>
8.19	220.15	
12.10	197.12	
12.44	195.10	
12.54	208.12	
13.29	222.16	
16.02	222.10	Structure not assigned
21.89	315.16	
21.96/22.10/22.23	312.19	

a) in some cases the structure reported is representative of a series of possible structural isomers.

One can see from Table 5.1 that DBHA is not reported in the list, but *N*-benzylidenebenzylamine and *N,N*-dibenzylamine are present instead. These two compounds come from the decomposition of DBHA in the GC-MS spectrometer, and this was proven by injecting a DBHA solution in dichloromethane. Furthermore, the decomposition depends on the column and the instrument used, as this effect was not observed in the GC apparatus fitted with an FID detector. The main peaks were assigned to 2,5-DTBBQ, 2,5-di-*tert*-butyl-hydroquinone (2,5-DTBHQ) and styrene dimers and trimers. In addition, there is a small peak at 21.89 min, with mass 315.16  $m/z$ , which correspond to the isoxazolidine (**7**). Isoxazolidine is formed by the reaction between *N,N*-benzylidenebenzylamine-*N*-oxide (**4**) and styrene (**5**)<sup>109</sup> (Figure 5.5).

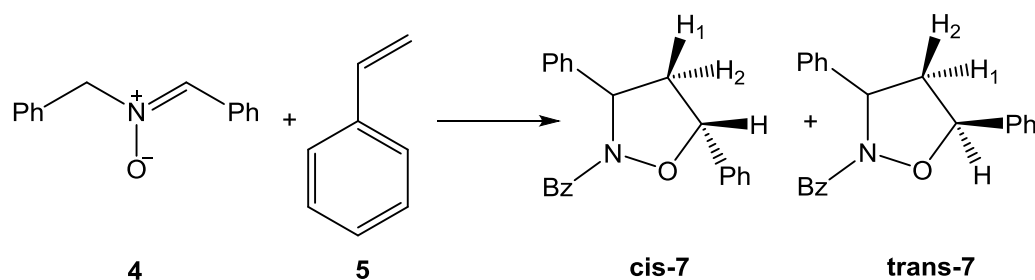


**Figure 5.5** Reaction scheme of the 1,3-dipolar cycloaddition between *N,N*-benzylidenebenzylamine-*N*-oxide (**4**) and styrene (**5**) leading to isoxazolidines (*cis*-**7**) and (*trans*-**7**)

To identify the structure, tandem mass spectrometry (MS/MS) was carried out on the crude mixture, using electrospray as ionisation method, which produces  $[M+H]^+$  ions. The MS/MS fragmentation pathway of the precursor ion  $m/z$  316, combined to the assignment of the main peaks, is shown in Figure 5.6.

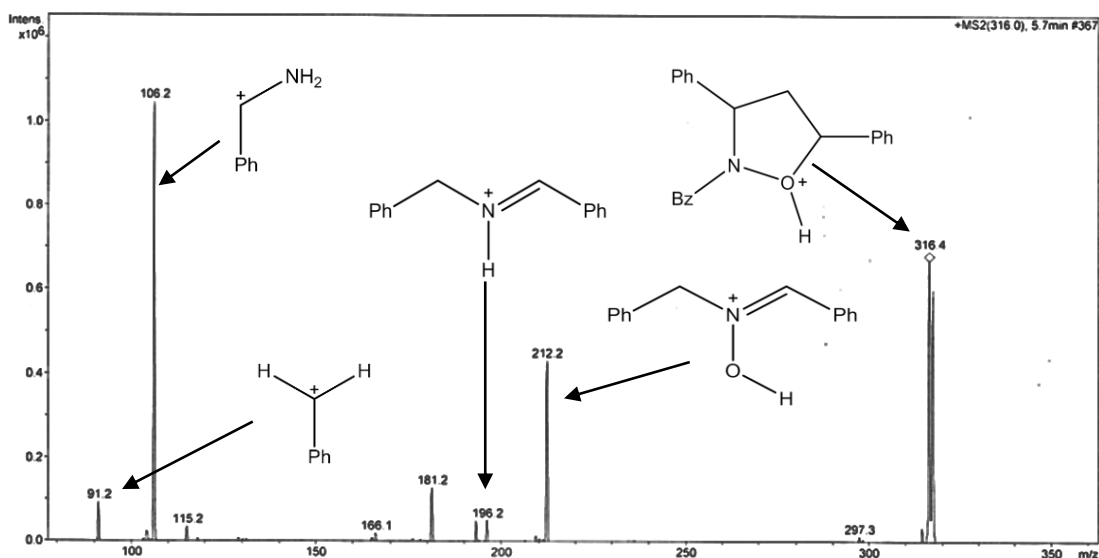


**Figure 5.6** Tandem MS-MS spectrum for the mixture 2,5-DTBBQ/DBHA in styrene after 15 h at 110 °C

To confirm the structure of the compound found in the reaction mixture, the isoxazolidine (**7**) was synthesised, and then the two mass spectra were compared.

The preparation and full characterisation of the isoxazolidine (**7**) is described in the experimental section. The following is the fragmentation pattern of (**7**) (Figure 5.7).

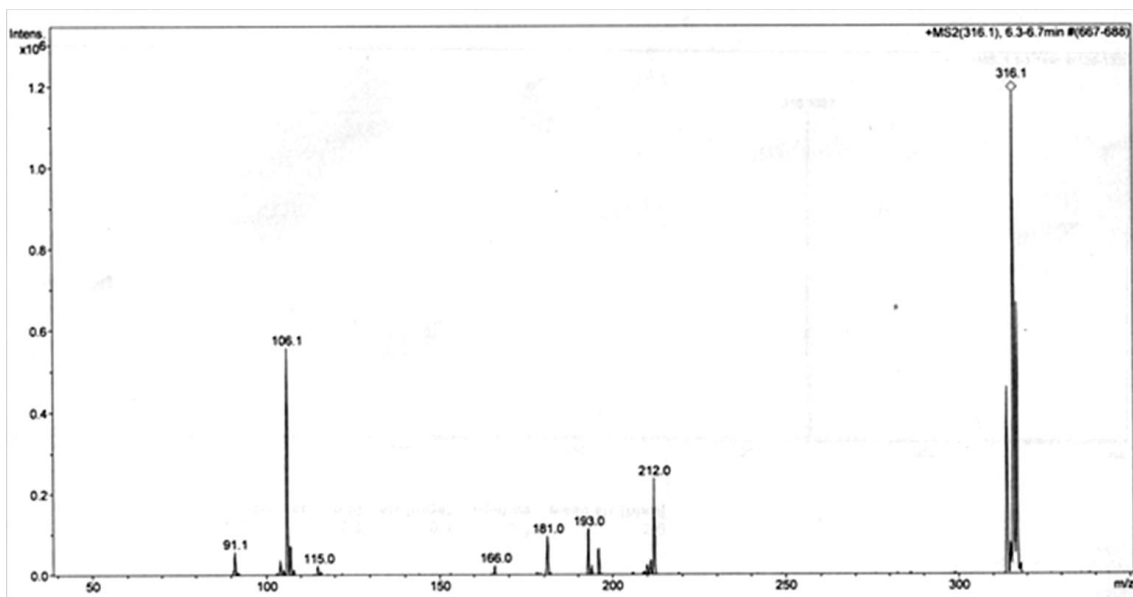


**Figure 5.7** Fragmentation pattern of isoxazolidine (**7**)

A comparison between the mass spectra in Figure 5.7 and 5.6 shows similarity between the two fragmentation patterns, confirming that the compound detected during the inhibition of polymerisation with DBHA/2,5-DTBBQ is the isoxazolidine (**7**).

### 5.2.1.1 Synthesis of three rings hydroxylamine

Looking at the previous paragraph, the assignment of the  $m/z$  316 product to isoxazolidine (**7**) seems pretty straightforward, but initially we proposed that this compound could be *N*-(1,2-diphenylpropyl)-*N*-[(*Z*)-phenylmethylidene]amine oxide (**12**) (Figure 5.8), for simplicity it is called three rings nitron (**12**). The hypothesis was that *N,N*-benzylidenebenzylamine-*N*-oxide (**4**) reacts with a styrene radical (**9**) to form the intermediate nitroxide (**10**). Indeed, nitrones commonly stop propagation chains by the addition of a carbon centred radical on the carbon of the carbon-nitrogen double bond<sup>66</sup>. Nitroxide (**10**) then could either react further to form the alkoxyamine (**11**) or decompose by disproportionation<sup>50</sup> to form nitron (**12**) and *N*-benzyl-*N*-hydroxy-1,2-diphenylpropane-1-amine (**13**), which is called three rings hydroxylamine (**13**) (Figure 5.8). Compound (**12**) has mass of 315.16 g/mol consistent with the  $m/z$  316 peak observed for the  $[M+H]^+$  ion during styrene inhibition (Table 5.1).

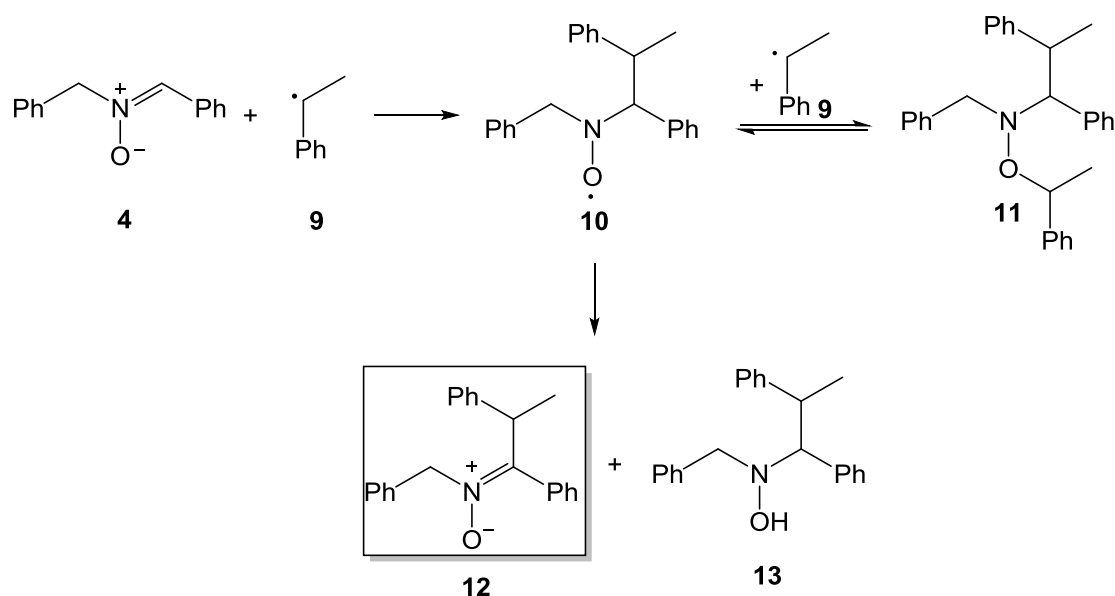
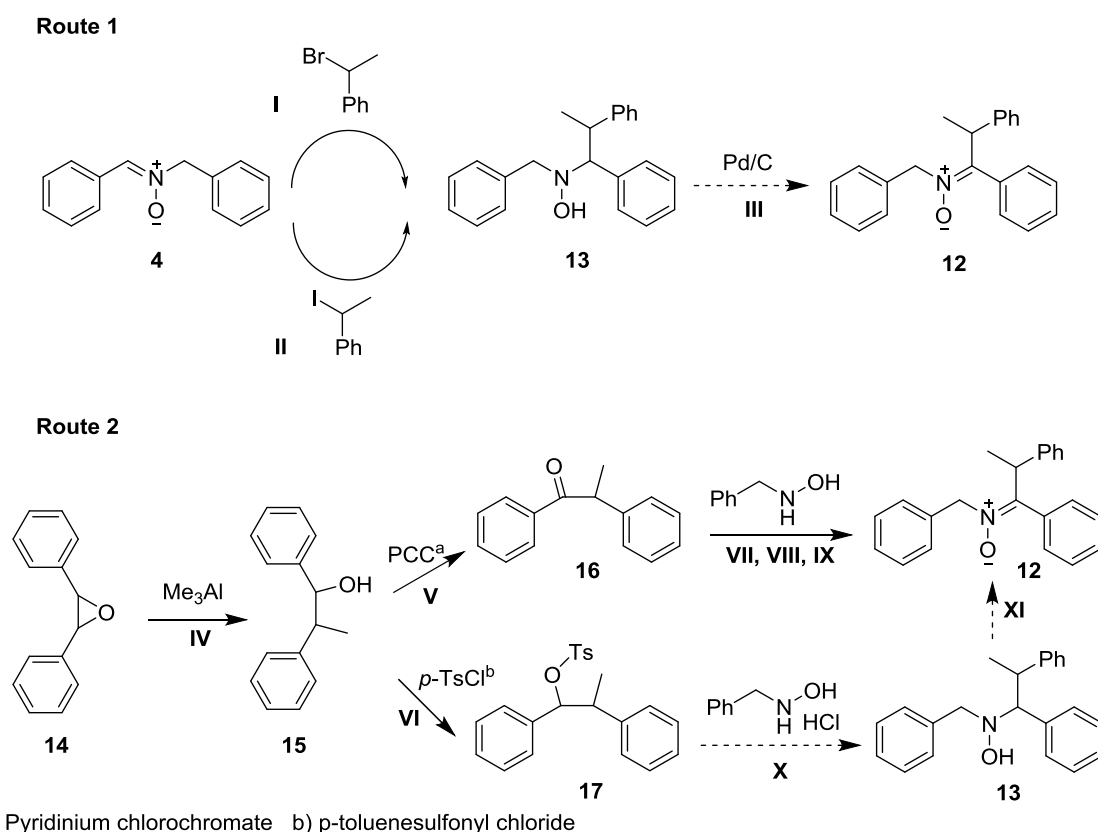


Figure 5.8 Hypothesised mechanism of formation of *N*-(1,2-diphenylpropyl)-*N*-[(*Z*)-phenylmethylidene]amine oxide (**12**)

This hypothesis was only discounted after we compared the fragmentation pattern of three rings nitron (12) with that of the compound found in the reaction mixture. Therefore, the new three rings nitron (12) had to be synthesised. The presence of highly hindered substituents confers interesting properties to the molecule.

The synthesis of (12) proved rather challenging and several alternative pathways have been tried before the desired product was obtained. Figure 5.9 reports the unsuccessful routes (dash arrows means that the reaction was not attempted, due to the failure of the previous reactions), while Figure 5.10 describes the synthetic pathway to (12).



**Figure 5.9 General scheme of the attempts for the synthesis of nitron (12)**

The first attempt (Route 1) to synthesise the three rings nitron (12) was the deprotonation of the proton on the C=N double bond of nitron (4), and the introduction of a phenylmethyl group (Reaction I and II). Route 2, instead, involves the opening of the epoxide ring of (14)<sup>113</sup> (Reaction IV), followed by the oxidation of alcohol (15) to ketone (16)<sup>114</sup> (Reaction V), and condensation reaction to give (12). The



condensation reaction was carried out in different conditions (Reaction VII, VIII and IX). A good leaving group was also introduced on (**15**) (Reaction VI) to facilitate the nucleophilic substitution of (**17**) with N-benzylhydroxylamine hydrochloride leading to (**13**) (Reaction X). Reaction conditions are reported in the experimental part.

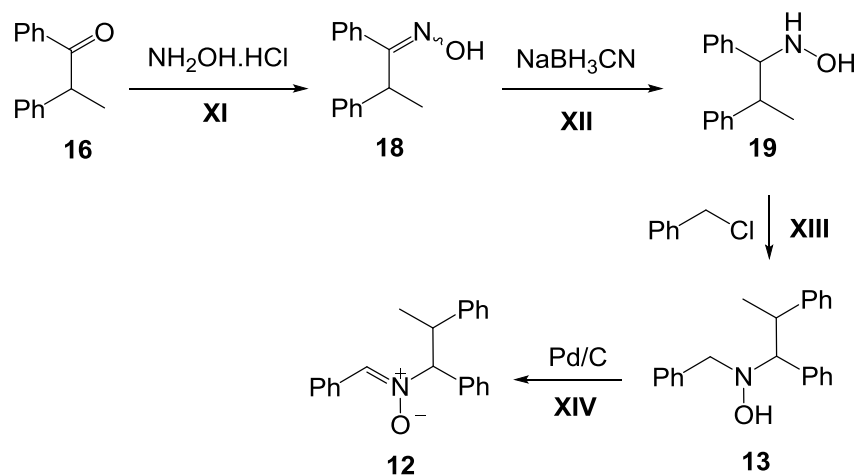


**Figure 5.10 Synthetic route to *N*-(1,2-diphenylpropyl)-*N*-[(*Z*)-phenylmethylidene]amine oxide (**12**)**

The approach shown in Figure 5.10 includes the conversion of ketone (**16**) to ketoxime (**18**)<sup>115</sup> (Reaction XI), followed by the reduction of (**18**) to hydroxylamine (**19**)<sup>116</sup> (Reaction XII). Hence, hydroxylamine (**13**) was synthesised by nucleophilic substitution on the nitrogen atom of (**19**) with benzyl chloride<sup>117, 118</sup> (Reaction XIII). The oxidation of (**13**) gave nitronium (**12**)<sup>119</sup> (Reaction XIV). Characterisations and reaction conditions are reported in the experimental part.

The  $^1\text{H-NMR}$  of the hydroxylamine (**13**) in deuterated chloroform is reported below, as its interpretation was rather challenging. The presence of sterically demanding substituents do not allow the free rotation of the bonds, leading to observation of rotamers. Indeed, protons  $\text{H}_A$ ,  $\text{H}_B$  and  $\text{H}_D$  in three rings hydroxylamine (**13**) were expected to show three doublets with integration 1, a doublet, which integrates to 3 protons for the methyl group and a doublet of quartet for  $\text{H}_E$  with integration 1. However,  $\text{H}_A$  partially overlaps with  $\text{H}_E$  and the shape of the signal is far from that of a doublet (Figure 5.11). The full signal assignment was possible by a combination of 1D and 2D-NMR methods.

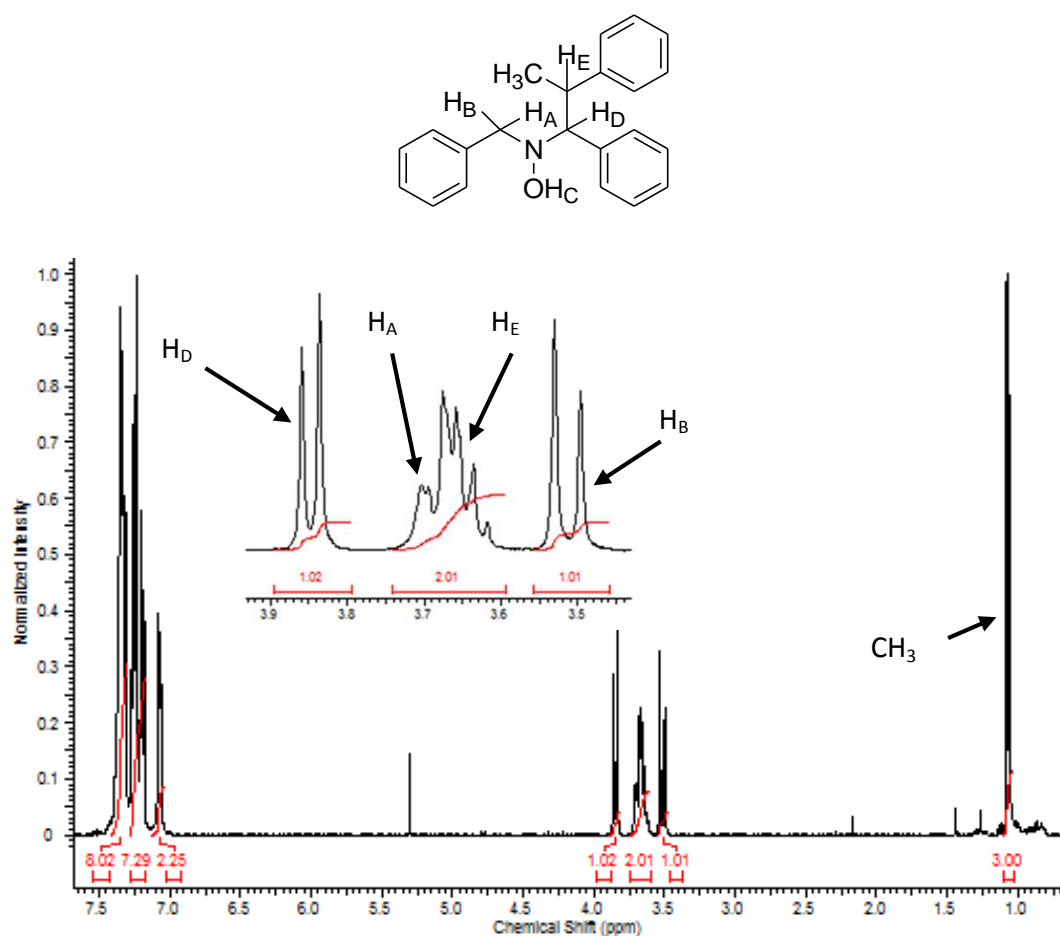


**Figure 5.11**  $^1\text{H-NMR}$  of *N*-benzyl-*N*-hydroxy-1,2-diphenylpropane-1-amine (**13**) recorded on a 700 MHz spectrometer and using  $\text{CDCl}_3$  as a solvent.

Changing the solvent from a non-polar ( $\text{CDCl}_3$ ) to a polar ( $\text{DMSO-d}_6$ ) leads to a shift in the position of the signal, and the shape of the peaks become much more resolved (Figure 5.12(a)).

In addition, when the spectra were recorded at different temperatures, we observed a sharpening of the signal going from 25 to 80 °C (Figure 5.12 (b), (c) and (d)) and a broadening at lower temperature (-30 °C, Figure 5.13 (f)). This demonstrates that the molecule assumes more than one stable conformation. Indeed, at higher temperature the fast interconversion from one conformation to another is on the time scale of the NMR experiment producing a sharp peak. In this case the J coupling constant ( $J_{\text{E-CH}_3}$ ,  $J_{\text{E-D}}$ ,  $J_{\text{A-B}}$  and  $J_{\text{D-E}}$ ) is an average for each conformation. On the other hand, at low temperature the exchange happens in a time comparable to the time scale of the experiment and the coupling constant is not averaged anymore. Furthermore, varying

the temperature (Figure 5.12) produce a pronounced movement of the CH<sub>2</sub> protons relative to others and this could be an indication of molecular association<sup>120</sup>.

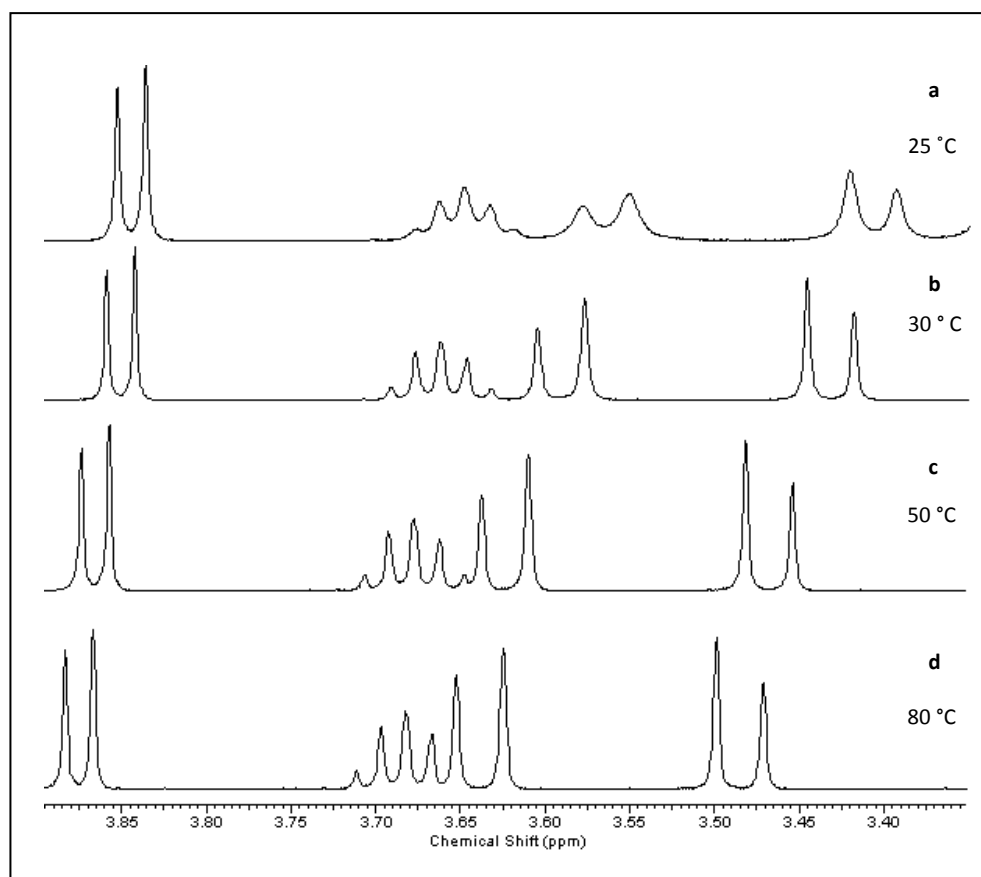


**Figure 5.12** <sup>1</sup>H-NMR spectra of *N*-benzyl-*N*-hydroxy-1,2-diphenylpropane-1-amine (13) recorded in a 400 MHz spectrometer, in DMSO-d<sub>6</sub>, at 25 °C (a), 30 °C (b), 50 °C (c) and 80 °C (d).

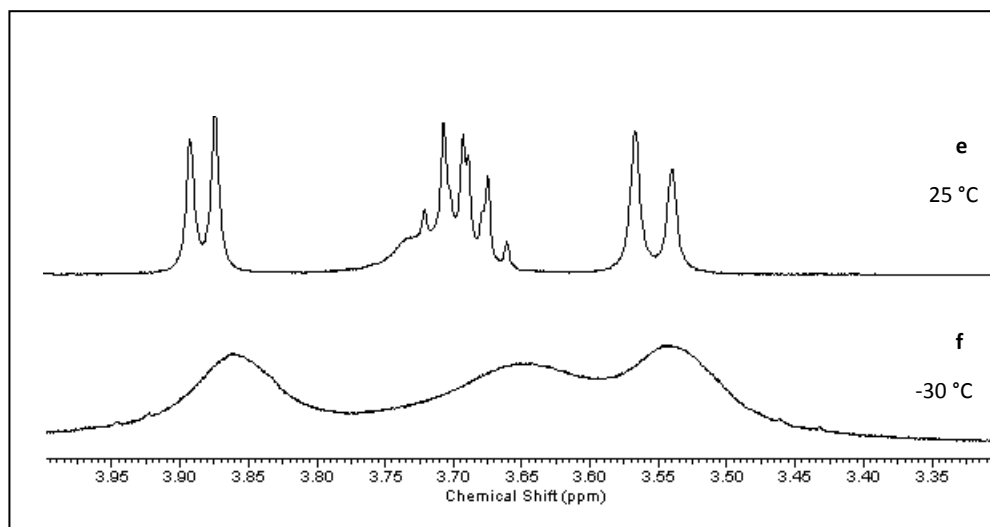


**Figure 5.13**  $^1\text{H}$ -NMR of *N*-benzyl-*N*-hydroxy-1,2-diphenylpropane-1-amine (**13**) in  $\text{CDCl}_3$ , at 25 °C and -30 °C

For a better definition of the structure of the hydroxylamine (**13**) we recorded an EPR spectrum of the correspondent nitroxide and we analysed the hyperfine coupling constants. Nitroxide (**10**) was generated by dissolving the hydroxylamine (**13**) in styrene (100 ppm) and heating the solution in the EPR cavity at 110 ° (Figure 5.14).

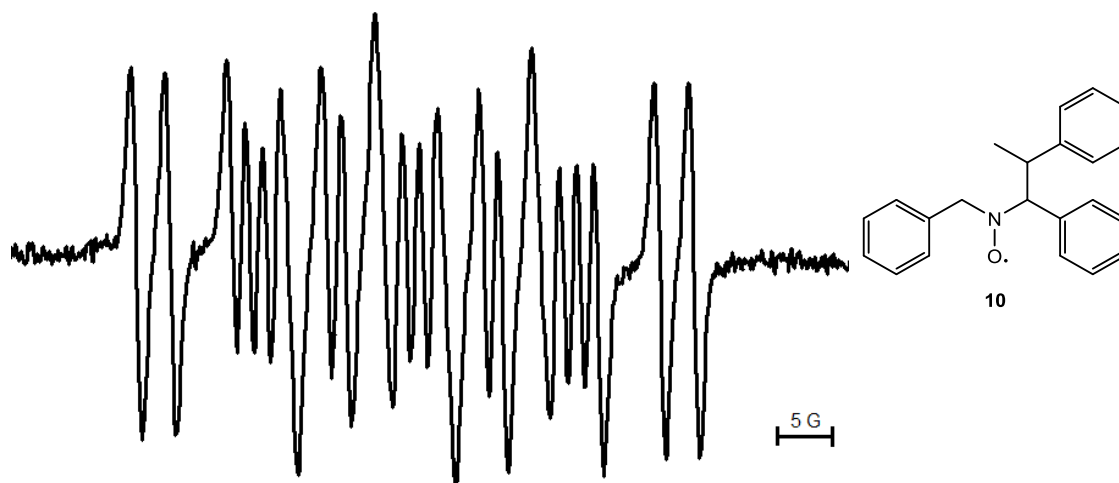


**Figure 5.14** EPR spectrum of nitroxide (**10**)

The EPR spectrum of (**10**) in Figure 15.14 shows 20 lines, however for a  $^{14}\text{N}$  (spin angular moment  $I=1$ ) next to three non-equivalent protons ( $I=1/2$ ) you would expect 24 lines, in this case some of them overlap. The hyperfines were estimated by using WinSim, a software which simulates experimental EPR spectra providing spectral parameters. The estimated hyperfines are  $a_{\text{N}} = 14.96$  G,  $a_{\text{H}_1} = 3.29$  G,  $a_{\text{H}_2} = 10.83$  G and

$a_{\text{H3}} = 9.17 \text{ G}$ . The hyperfine of one of the protons is significantly smaller than the others, meaning that one of the C-H bonds should be almost perpendicular to the  $p_z$  orbital of the nitrogen atom<sup>121</sup>. Contrary to the  $^1\text{H}$ -NMR spectrum, the EPR spectrum shows only one rotamer (the most abundant), and this is because NMR transition occurs at much lower frequency (Hz) than EPR (MHz)<sup>53, 120</sup>.

The presence of demanding substituents also influences the reactivity of this hydroxylamine. Indeed, the dehydrogenation reaction of **(13)** to give the corresponding nitron **(12)** eliminates the hydrogen on the less substituted carbon, contrary to the stability rules (Figure 5.15).

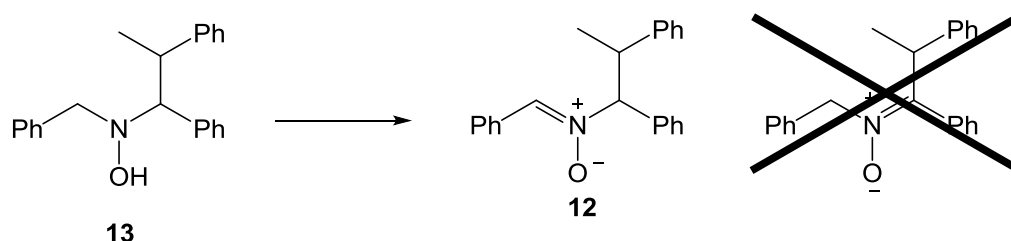


**Figure 5.15 Oxidation 3 rings hydroxylamine (13) to 3 rings nitron (12)**

As mentioned earlier, two compounds **(12)** and **(13)** were synthesised because **(12)** was incorrectly believed to be an inhibition product, but they revealed interesting properties, and were therefore included in this thesis. Coming back to our main task of determining the inhibition products formed during the inhibition of styrene polymerisation with DBHA/2,5-DTBBQ, the possibility of detecting benzisoxazolidine is considered in the next section.

### 5.2.1.2 *Synthesis of benzisoxazolidine (8)*

The analysis of the inhibition of the styrene polymerisation with a DBHA/2,5-DTBBQ mixture by GC-MS revealed *N,N*-benzylidenebenzylamine-*N*-oxide **(4)** and isoxazolidine **(7)** as the only products derived from DBHA (Table 5.1). But, as already mentioned in the introduction, nitron **(4)** could also undergo 1,3-dipolar cycloaddition to the C=C double bond of 2,5-DTBBQ leading to a benzisoxazolidine **(8)**<sup>110</sup> (Figure 5.2). Thus, the feasibility of formation of **(8)** was tested under polymerisation conditions. This indirect route was exploited to investigate the presence of benzisoxazolidine in the real

system, and in the case of its characterisation we would have taken advantage of knowing its retention time to identify it in the reaction mixture.

A solution of *N,N*-benzylidenebenzylamine-*N*-oxide (**4**) and 2,5-DTBBQ in toluene was refluxed at 110 °C, but only starting material was recovered, suggesting that the reactivity of nitron (**4**) is quite poor towards 2,5-DTBBQ.

This experiment suggests that it is unlikely that during the inhibition of styrene polymerisation *N,N*-benzylidenebenzylamine-*N*-oxide (**4**) reacts with 2,5-DTBBQ. An alternative to facilitate the detection of other inhibition products is described in the next paragraph.

## 5.2.2 Products analysis in a non-polymerizable solvent

The approach used so far was to search for the inhibition products in the real system, including styrene heated at 110 °C, however the formation of polymeric chains may impede the identification of the products. Thus, styrene was replaced with a non-polymerizable solvent and di-*tert*-butyl peroxide was used as a source of radicals (the half-life at 130 °C is approximately 6 h)<sup>96</sup>.

To a 5 mM solution of 2,5-DTBBQ ( $7.5 \times 10^{-2}$  mmol) and DBHA ( $7.5 \times 10^{-2}$  mmol) in toluene (15 mL), di-*tert*-butyl peroxide (0.75 mmol) was added. The solution was left at 120 °C for 24 h under nitrogen atmosphere. Gas chromatography and gas chromatography with electron impact mass spectrometry (GC-EI) were used to investigate new products (Figure 5.16 and 5.17).

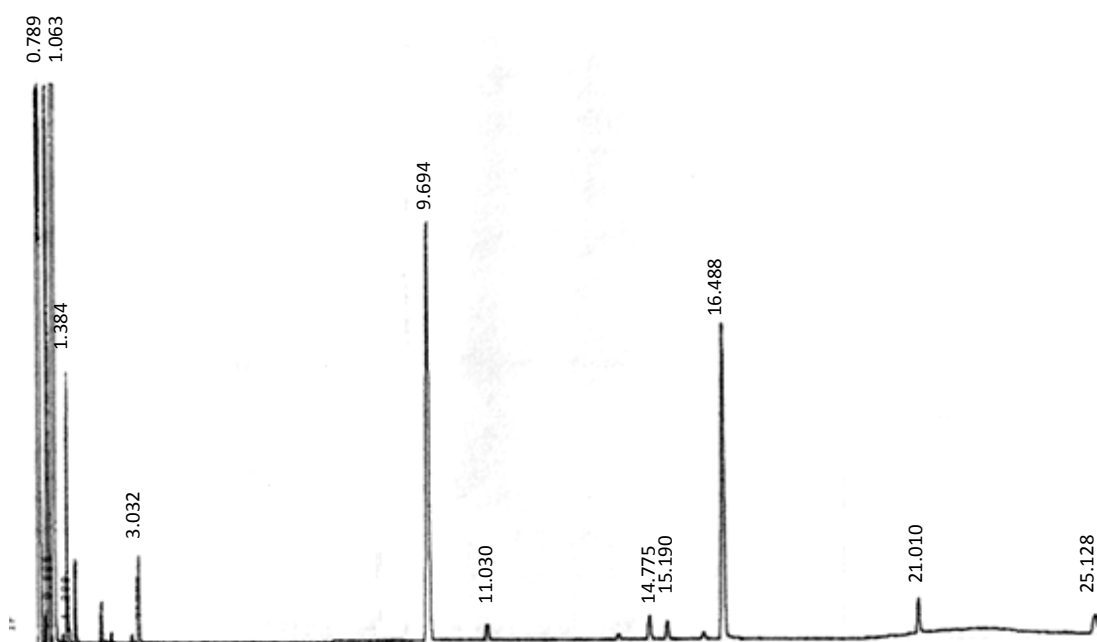


**Figure 5.16 Chromatogram of DBHA/2,5-DTBBQ and di-*tert*-butyl-benzoquinone in toluene at time 0**

The peaks at 0.79 and 0.99 min (Figure 5.16) correspond to di-*tert*-butyl peroxide and one of its decomposition products (*tert*-butyl alcohol and acetone are commonly observed as major degradation products<sup>122</sup>), while at 1.06 min is toluene. 2,5-DTBBQ and DBHA, instead, elute at 9.69 and 16.49 min, respectively.

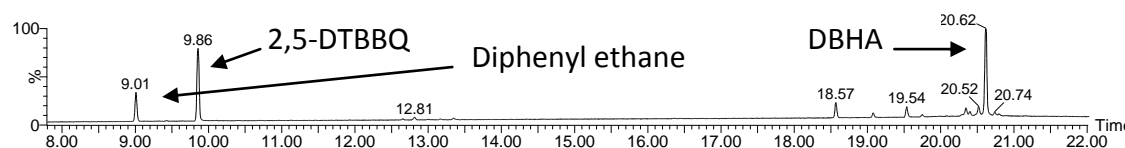


**Figure 5.17 GC-chromatogram of DBHA/2,5-DTBBQ and di-*tert*-butyl peroxide in toluene after 24 h at 110 °C**

The chromatogram in Figure 5.17 shows three main peaks. The peak at 20.62 min is DBHA, the peak at 9.86 min is 2,5-DTBBQ and the peak at 9.01 min corresponds to diphenyl ethane. *Tert*-butoxyl radical is indeed able to abstract one hydrogen from the solvent which then combine with another benzyl radical leading to diphenyl ethane<sup>122</sup>. Its structure has been also confirmed comparing the fragmentation pattern with standard spectra in NIST (National Institute of Standards and Technology) (Figure 5.18).

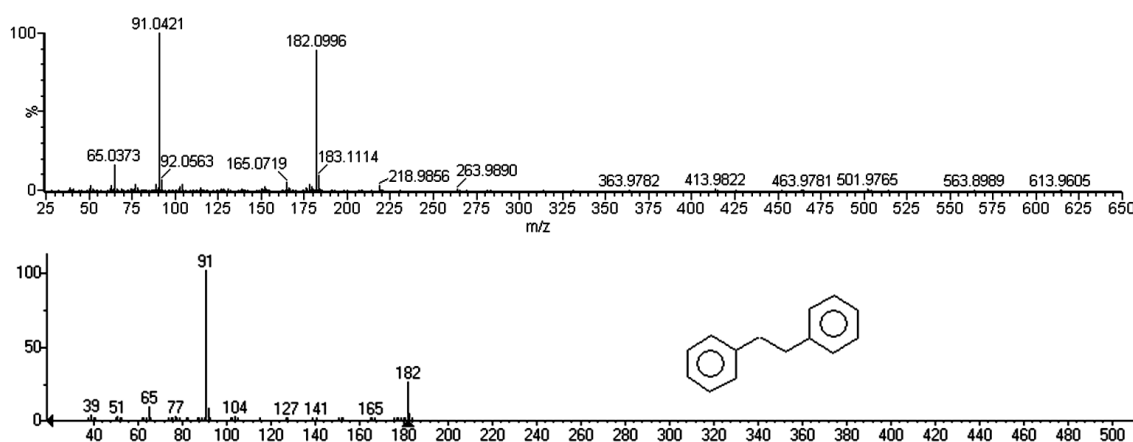


**Figure 5.18 Top MS spectrum: fragmentation of compound at retention time 9.1 min. Bottom MS spectrum: fragmentation of diphenyl ethane found in NIST**

The matching probability between the two spectra in Figure 5.18 is 91.4%.

This experiment did not allow detection of new products. DBHA and 2,5-DTBBQ are consumed during the reaction, but no evident formation of new peak was observed. Thus, in order to identify more compounds, the inhibition of styrene polymerisation by DBHA/2,5DTBBQ was investigated on grams scale.

### 5.3 Investigation of the inhibition products in reactions carried out on a large scale

The inhibition of styrene polymerisation was investigated on a large scale. Working with grams of starting material, even the isolation and characterisation of minor products is feasible. In this section, a combination of different techniques (e.g., NMR spectroscopy, elemental analysis and mass spectroscopy) was used for the detection and quantification of inhibition products.

#### 5.3.1 DBHA/2,5-DTBBQ mixture

The aim of this section is to characterise the products isolated from the inhibition of the auto-initiated styrene polymerisation with DBHA/2,5-DTBBQ. The nitrogen containing compounds were also quantified in order to verify that all the products derived from DBHA decomposition were recovered.

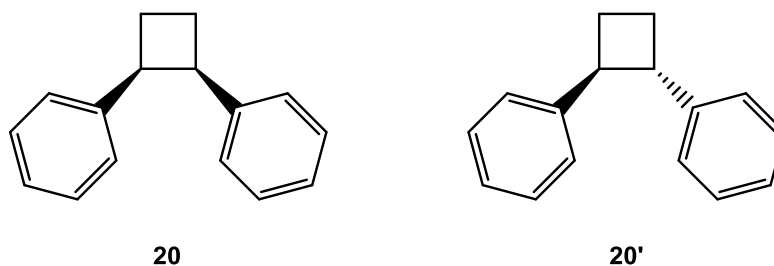


DBHA (10 mmol) and 2,5-DTBBQ (2.5 mmol) were dissolved in styrene and left stirring at 140 °C in a nitrogen atmosphere. A full description of the reaction and purification conditions is reported in the experimental section.

The following is a list of the products (or product mixtures) isolated. In some cases the structure is fully assigned, in others the identification of certain functional groups is attempted. The necessity of purifying the products several times made accurate quantification of each product difficult, therefore no amounts are associated to the compounds in this analysis. However, quantitative data are given in the next experiment.

2,5-DTBHQ, DBHA and *N,N*-benzylidenebenzylamine-*N*-oxide and traces of 2,5-DTBBQ were isolated from the reaction mixture.

#### **Cis and trans 1,2-diphenylcyclobutane**



The  $^1\text{H-NMR}$  spectra of *cis* and *trans* 1,2-diphenylcyclobutane (**20** and **20'** respectively) are reported in Figure 5.19 and 5.20. Their characterisation has been published before by other researchers and the spectra match those found in the literature<sup>123</sup>.

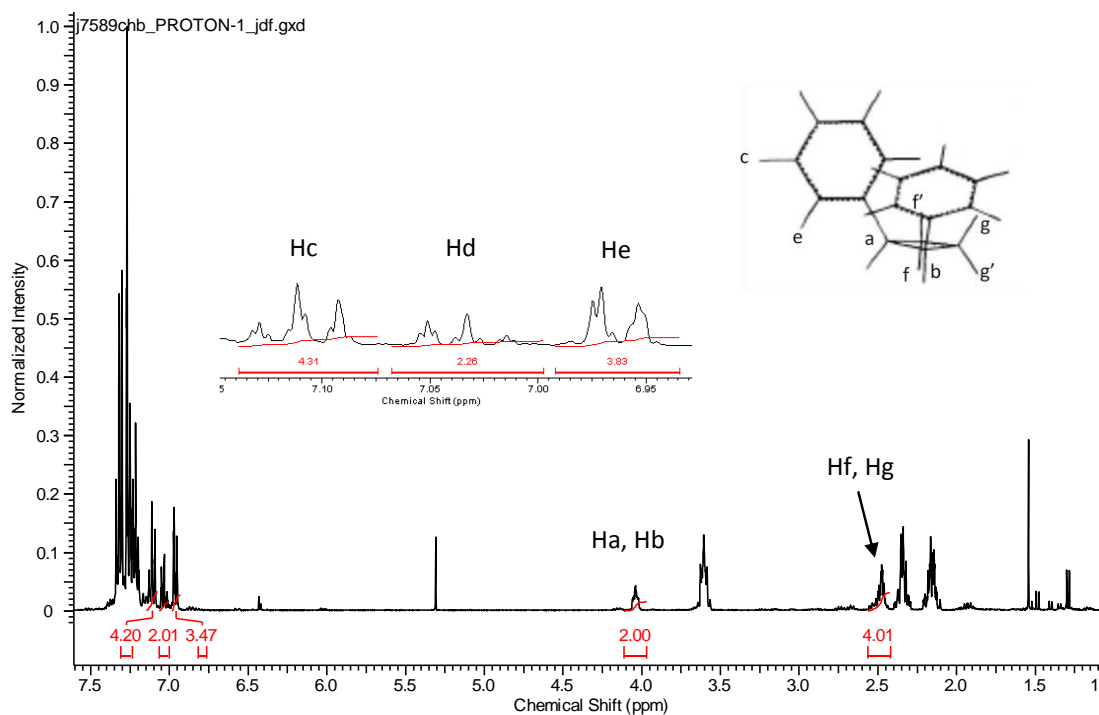


Figure 5.19  $^1\text{H-NMR}$  spectrum of *cis*-1,2-diphenylcyclobutane

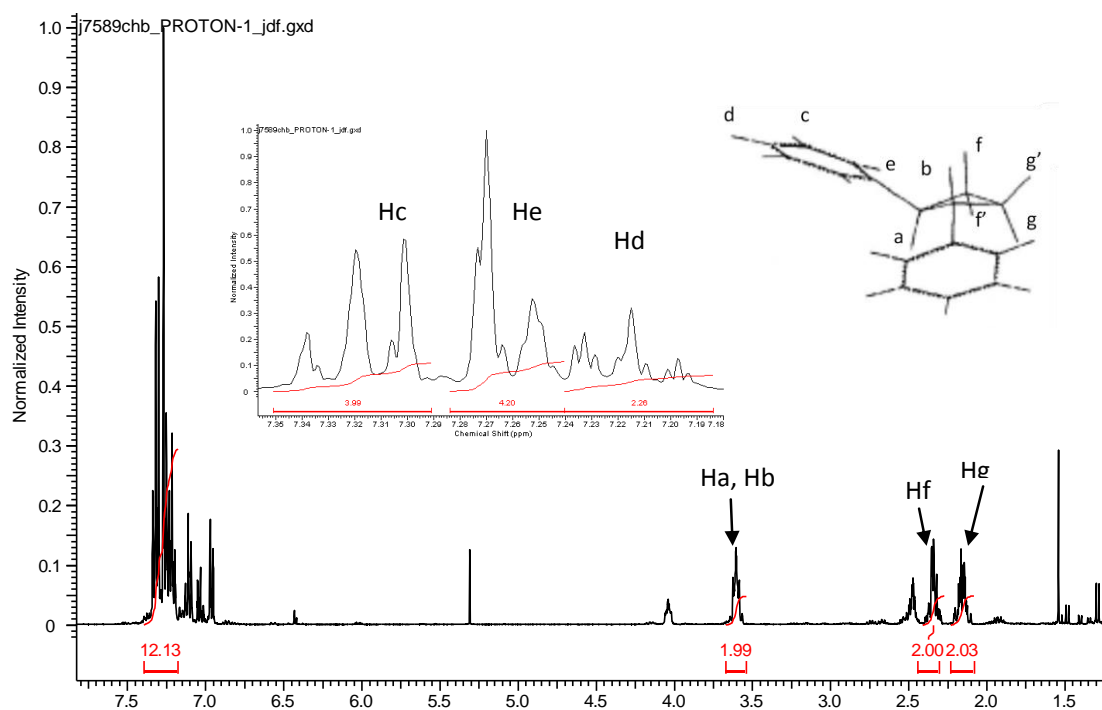
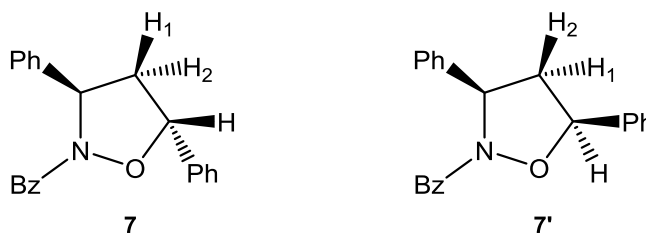
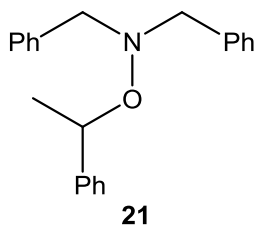


Figure 5.20  $^1\text{H-NMR}$  spectrum of the *trans* 1,2-diphenylcyclobutane

(20) and (20') are the termination products of two styrene radicals<sup>11</sup>.

***Cis* isoxazolidine (*cis-7*) and *trans* isoxazolidine (*trans-7*)**

Full characterisation of (*cis-7*) and (*trans-7*) is reported in the experimental section.

***O*-(1-phenylethyl)-*N,N*-dibenzylhydroxylamine**

*O*-(1-phenylethyl)-*N,N*-dibenzylhydroxylamine (**21**) is an alkoxyamine formed by the coupling between *N,N*-dibenzylnitroxide and a styrene radical. Compound (**21**) is a new molecule and the full characterisation is reported in the Experimental section.

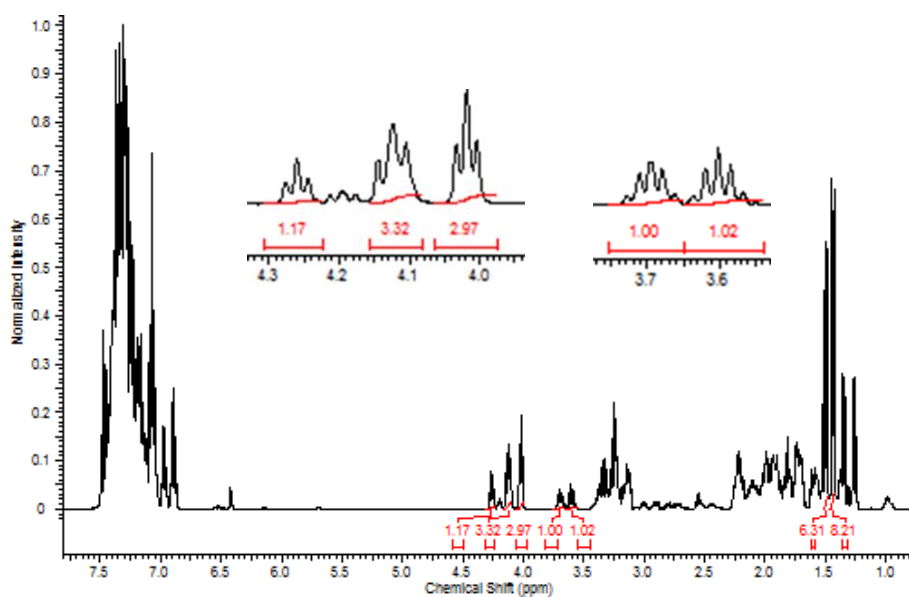
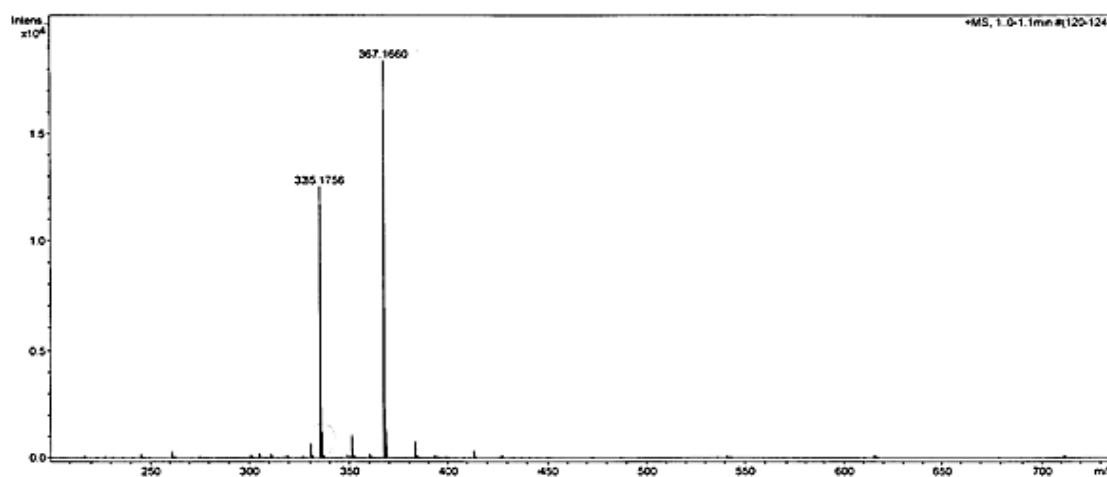
**Fraction 1**

Figure 5.21  $^1\text{H}$ -NMR spectrum of the fraction 1

The  $^1\text{H}$ -NMR spectrum of fraction **1** is shown in Figure 5.21. This fraction is a mixture of several compounds which cannot be separated by flash chromatography. The elemental analysis (CHN) does not show any evidence of nitrogen in the mixture, suggesting that it contains only styrene polymerisation products. Analysis of fraction **1** by mass spectrometry with positive electrospray ion source (ESI) (Figure 5.22) reveals two main peaks at  $m/z$  335.1756 and 367.1660 which correspond to the  $[\text{M}+\text{H}]^+$  ions. Both peaks have even nominal masses, thus an even or null number of nitrogen atoms should be present. For the former peak, the most likely molecular formulas are  $\text{C}_{21}\text{H}_{23}\text{N}_2\text{O}_2$  and  $\text{C}_{26}\text{H}_{23}$  (referred to  $[\text{M}+\text{H}]^+$ ), instead for the latter peak are  $\text{C}_{29}\text{H}_{18}$ ,  $\text{C}_{21}\text{H}_{23}\text{N}_2\text{O}_4$  and  $\text{C}_{26}\text{H}_{23}\text{O}_2$ , but CHN analysis rules out the formulas containing nitrogen.



**Figure 5.22** ESI mass spectrum of Fraction **1**

It is likely that these molecules are polymeric chains, thus our experimental data were compared with those of the products of the styrene polymerisation available in the literature<sup>7, 124-129</sup>. The NMR spectrum in Figure 5.21 does not match any spectra of the most typical dimers and trimers. The spectrum in Figure 5.21 shows four doublets in the region between 1 and 1.5 ppm, and these signals are consistent with three equivalent protons of a methyl group next to a CH. In addition, there are two distinct quintets in the region between 3.3-3.6 ppm and other two quintets between 3.1 and 3.4 ppm, but those at 3.1-3.4 ppm overlap other signals. TOCSY (Total correlation spectroscopy) analysis revealed that each doublet is correlated to the corresponding pentet, suggesting that there are 4 different compounds in the mixture. So, in each

molecule a proton ( $H^2$ ) must be next to a methyl ( $H^1$ ) and a CH ( $H^3$ ) (Figure 5.23). Further information derive from the correlation between  $H^2$  and  $H^1$  observed in the 2D-COSY experiment (hydrogen-hydrogen correlation) and the signals integrations on the  $^1H$ -NMR spectrum, which gives a 1:3  $H^2:H^1$  ratio. Also, based on the chemical shift we can assume that  $H^2$  is connected to a phenyl group, which gives the signal in the expected region of 3-3.5 ppm.

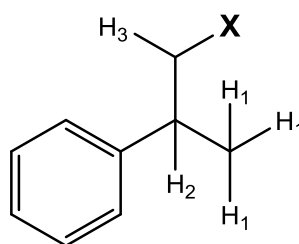


Figure 5.23 Possible fragment present in Fraction 1

### Fraction 2

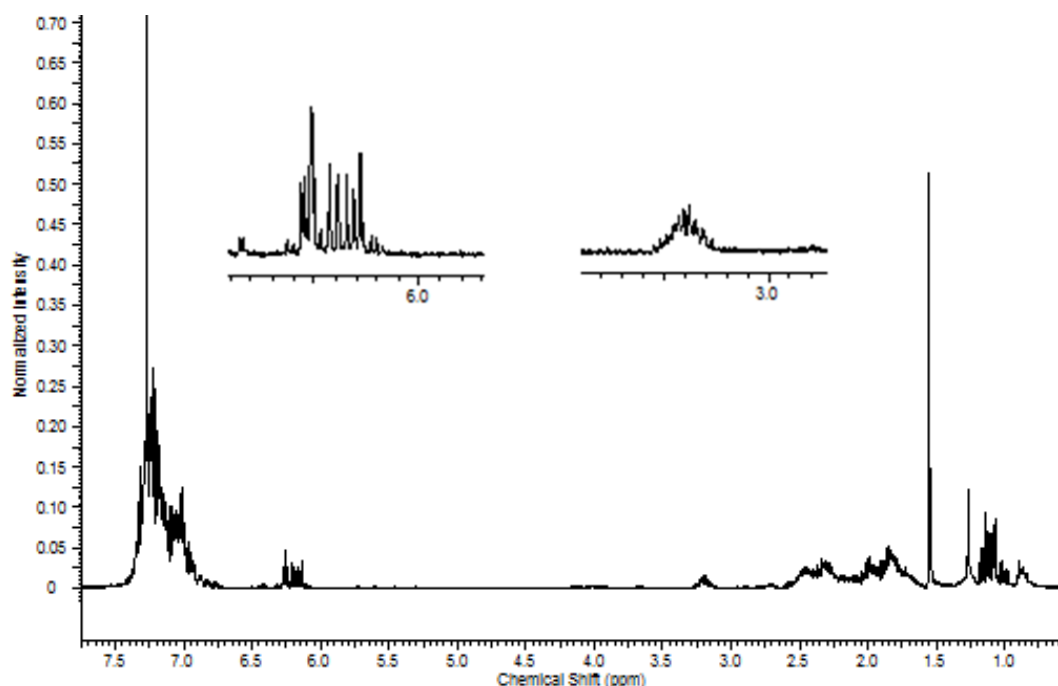
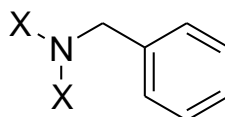


Figure 5.24  $^1H$ -NMR of Fraction 2

The absence of peaks around 4 ppm in the  $^1H$ -NMR spectrum of Fraction 2 (Figure 5.24) gives a strong indication that this sample does not contain any fragment of DBHA inhibitor, but only polystyrene. Since it is quite likely that the fragment of DBHA shown

in Figure 5.25 remains unchanged after inhibited polymerisation, the CHN protons are expected to be in the region between 3.8 and 4ppm and there is no trace of them in the  $^1\text{H}$  NMR spectrum.



**Figure 5.25** Fragment of DBHA

The spectrum, also, shows complex multiplets characteristic of aliphatic (1-2.5 ppm) and aromatic protons (7-7.5 ppm) of polymeric chains. In addition, a signal at 3.1-3.2 ppm could be associated with a proton next to a vinylic group ( $\text{H}^1$ , Figure 5.26), even though its position is slightly lower than that expected<sup>124</sup>. Instead, the protons that resonate at 6.1-6.3 ppm are related to vinylic protons next to a phenyl group ( $\text{H}^2$ ). Furthermore, the ESI spectrum in Figure 5.27 shows the main peak at  $m/z$  439.24 ( $[\text{M}+\text{Na}]^+$ ), which confirms the absence of nitrogen atoms in the molecule and supports  $\text{C}_{32}\text{H}_{32}$  as molecular formula. Here, it is shown the structure (or structural isomers) proposed for the above formula:

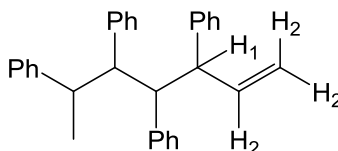


**Figure 5.26** Proposed fragment of Fraction 2

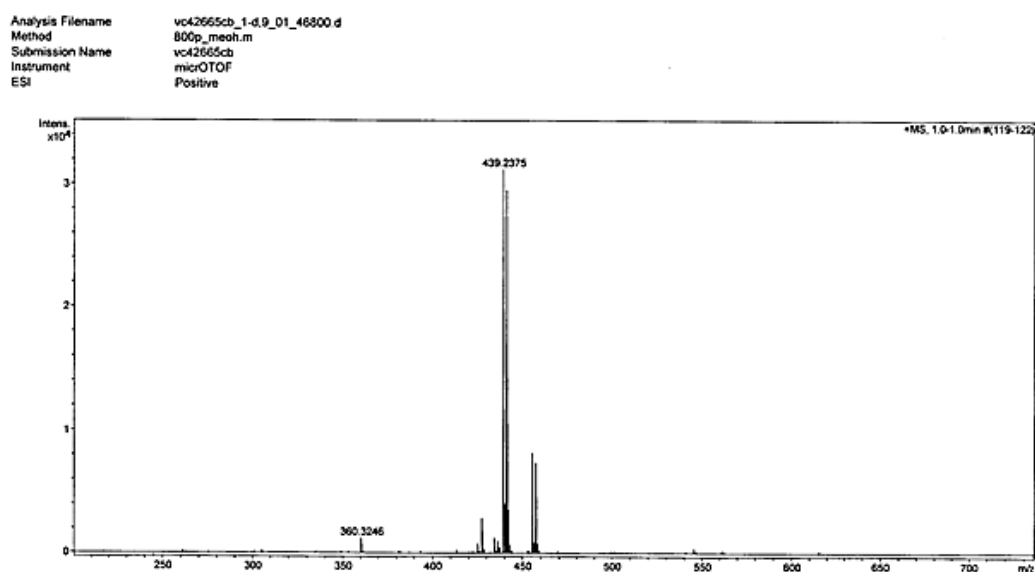


Figure 5.27 MS-ESI spectrum of Fraction 2

Even though the proposed structure contains protons which chemical shift could, in principle, match those reported in the NMR spectrum, the integral of the signals do not justify that structure. Thus, it is reasonable to conclude that the compound proposed in Figure 2.26 does not represent the whole molecule, but only a fragment of it.

### Unknown compound 3

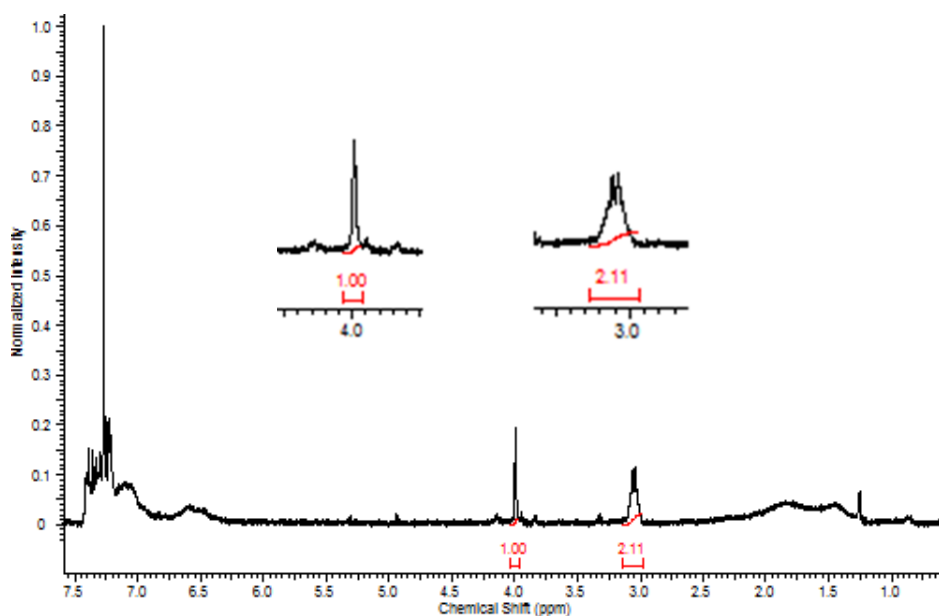


Figure 5.28  $^1\text{H-NMR}$  of Fraction 3

Only *ca* 2 mg of this compound were isolated, which makes the characterisation difficult. The actual yield of this compound is hard to quantify, due to its instability and the similar retention time to DBHA (which is in large excess). The purification was thus very difficult.

The  $^1\text{H-NMR}$  in Figure 5.28 shows a singlet at 3.99 ppm and a doublet at 3.1 ppm. The shape of the doublet makes us believe that it overlaps another signal, which is probably due to a polymer. The presence of a polymer is indeed confirmed by the characteristic broad peaks in the aromatic and aliphatic regions. The singlet at 3.99 ppm shows a chemical shift expected for protons in a  $\text{CHNAr}$  group, which indicates that this compound may have a structure similar to DBHA. In addition, the ESI spectrum shows a peak at  $m/z$  228.13 ( $[\text{M}+\text{H}]^+$ ) (Figure 5.29), which means that the molecule should have an odd number of nitrogen atoms, thus the molecular formula could be  $\text{C}_{15}\text{H}_{18}\text{NO}$ . However it is quite hard to find a plausible structure for that formula, which would also match the  $^1\text{H-NMR}$  spectrum.

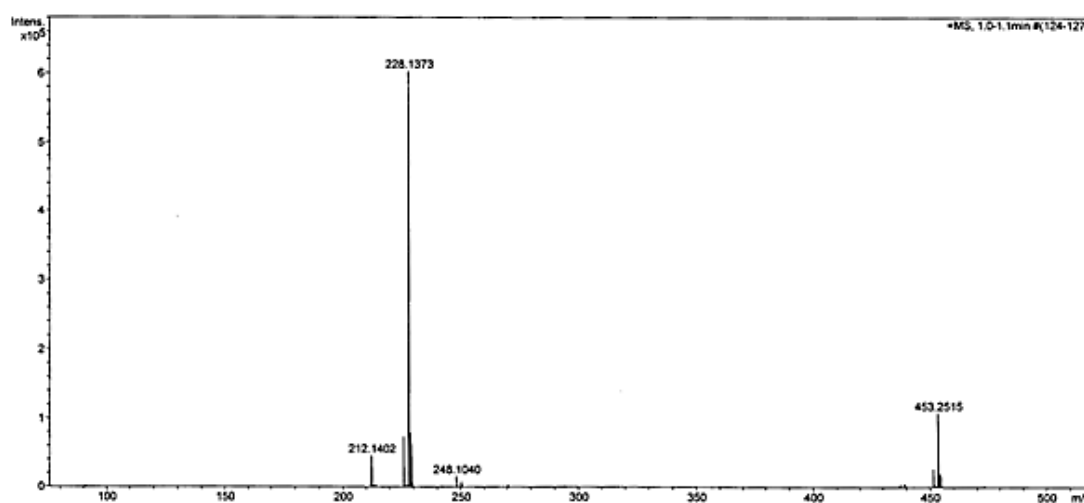


Figure 5.29 MS-ESI spectrum of Fraction 3

#### Unknown compound 4

This sample, about 200 mg, was analysed by elemental analysis which suggested that the carbon, hydrogen and nitrogen content are 82.49%, 7.20% and 1.13%, respectively. In addition, the ESI-MS spectrum (Figure 5.30) shows the presence of a peak at  $m/z$  318.16 ( $[\text{M}+\text{H}]^+$ ). Assuming that  $\text{C}_{22}\text{H}_{24}\text{NO}$  is the molecular formula, the percentages of



carbon and hydrogen fit the CHN result, however the percentage of nitrogen is too low to support this molecular formula. A combination of formulae were tried to match the results of mass spectroscopy and elemental analysis, but it was not possible to find a suitable one. It is likely that Fraction 4 is a mixture of 2 compounds.

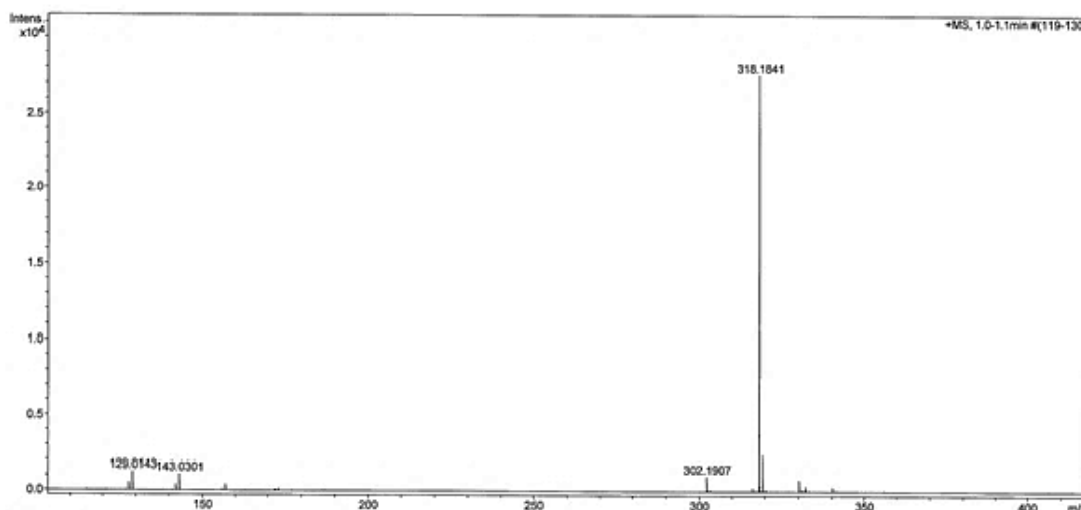


**Figure 5.30 MS-ESI spectrum of Fraction 4**

The  $^1\text{H-NMR}$  (Figure 5.31) shows broad peaks in the aromatic regions (6.4-7.3 ppm) and  $\text{CH/CH}_2$  region (0.9-2.4 ppm) typical of a long chain polymer. In addition, the multiplet at 3.55-3.75 ppm is consistent with a proton next to a double bond and a benzyl group (fragment 2,  $\text{H}^2$ , Figure 5.32). Indeed, the  $\text{H}^3$  protons would be expected in the region between 6.3-6.5<sup>124</sup>, confirming the proposed structure in Figure 5.32 (right structure). On the other hand, the signals between 3.8-4.1 ppm are in the region expected for protons next to a nitrogen atom and a phenyl ring. Thus, if we assume that Fraction 4 is a mixture of 2 compounds, and the main product is a polymer, the ESI peak may correspond to a fragment of the second product, which contains the structure on the left in Figure 5.32.

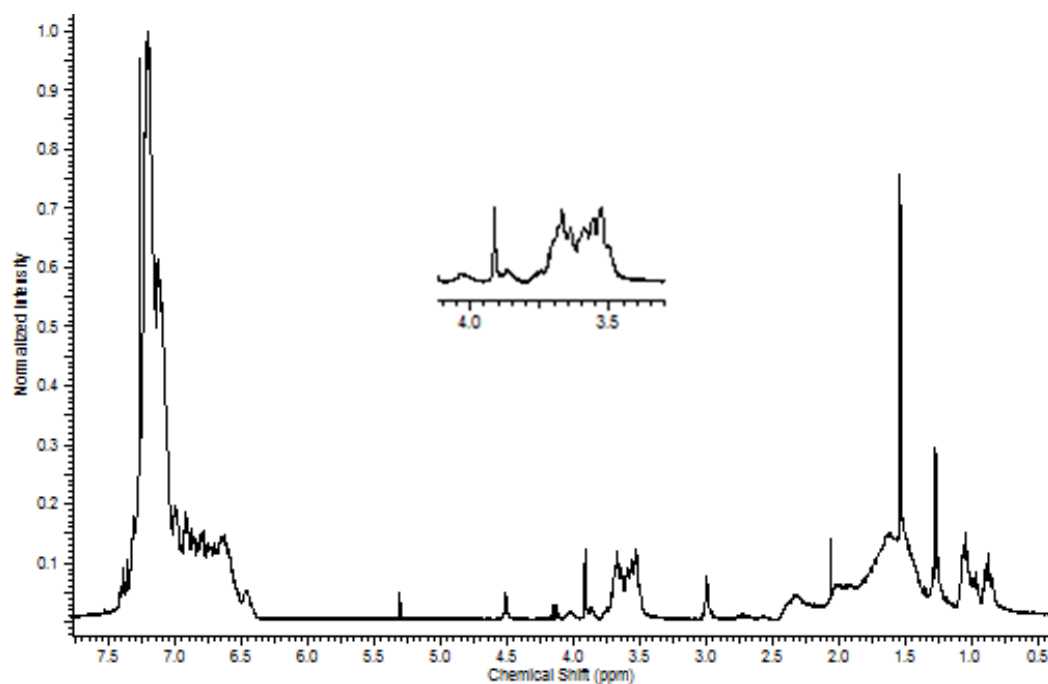


Figure 5.31  $^1\text{H-NMR}$  of Fraction 4

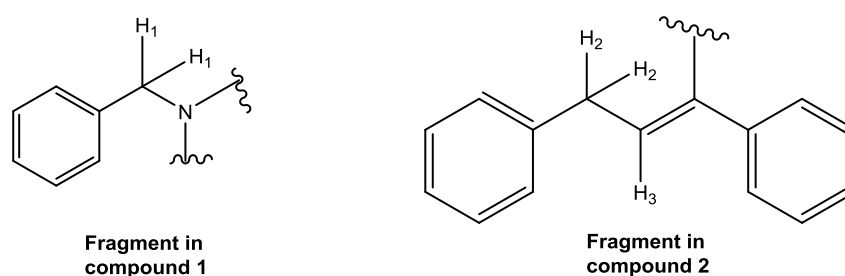
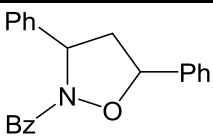
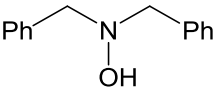
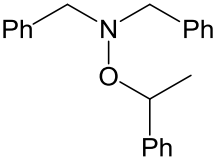
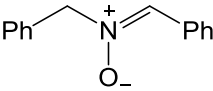


Figure 5.32 Possible fragments present in Fraction 4

Carrying out inhibited polymerisation on a gram scale and combining different analytical techniques allowed us to characterise new products and establish which of them contain nitrogen. Hence, the next step was to quantify those molecules. To do that, the inhibited polymerisation was repeated under similar conditions as the previous experiment. In this case methanol was added to precipitate polystyrene, as removing the polymer facilitates both quantification and purification of the products. The products isolated by column chromatography were quantified using DCM as an internal standard, and elemental analysis was carried out to establish the amount of nitrogen in the polymer. Although dichloromethane (DCM) has a low boiling point, it was used as an internal standard, because its signal falls in a suitable region in the  $^1\text{H-NMR}$

NMR spectrum. Reaction conditions and sample preparation are reported in the experimental section. Table 5.2 summarises the amount of nitrogen in each product.

**Table 5.2 Nitrogen content in the products isolated by column chromatography**

Product	nitrogen (mmol)
	2.6
	3.0
	1.8
	0.1
Fraction 4	0.2
polymer	1.6
Total	9.3

In conclusion, during the inhibition 2,5-DTBBQ is reduced into 2,5-DTBHQ and the latter is quantitatively recovered. On the other hand, from the initial amount of nitrogen contained in DBHA, only 93% has been recovered. It is possible that the laborious purification process affected the yield, however formation of volatile compounds cannot be excluded. Thus, in the following section the gas phase analysis by IR spectroscopy is detailed.

### 5.3.1.1 Investigation of volatile products

Approximately 90% of the initial nitrogen contained in DBHA was recovered from the products after column chromatography, and the reason for this discrepancy could be attributed to hydroxylamine decomposition to volatile nitrogen-containing products. Since the formation of CO<sub>2</sub> and N<sub>2</sub>O is expected from previous works<sup>130, 131</sup> and since

these two molecules possess characteristic IR spectra, IR spectroscopy was used as an investigation technique.

### *Sensitivity of the IR instrument*

Before the samples analysis, sensitivity of the instrument was estimated to ensure that the minimum concentration detectable is well below the expected products concentration. Since the amount of CO<sub>2</sub> in the air is known, the intensity of the IR signal of CO<sub>2</sub> contained in the air was used to work out the sensitivity of the instrument.

The gas phase IR cell was evacuated and the background was recorded. After that, the tap of the IR cell was opened, the air was let coming in, and the second spectrum was recorded. The peak at 2330 cm<sup>-1</sup> is due to the presence of CO<sub>2</sub> in the air (Figure 5.33).

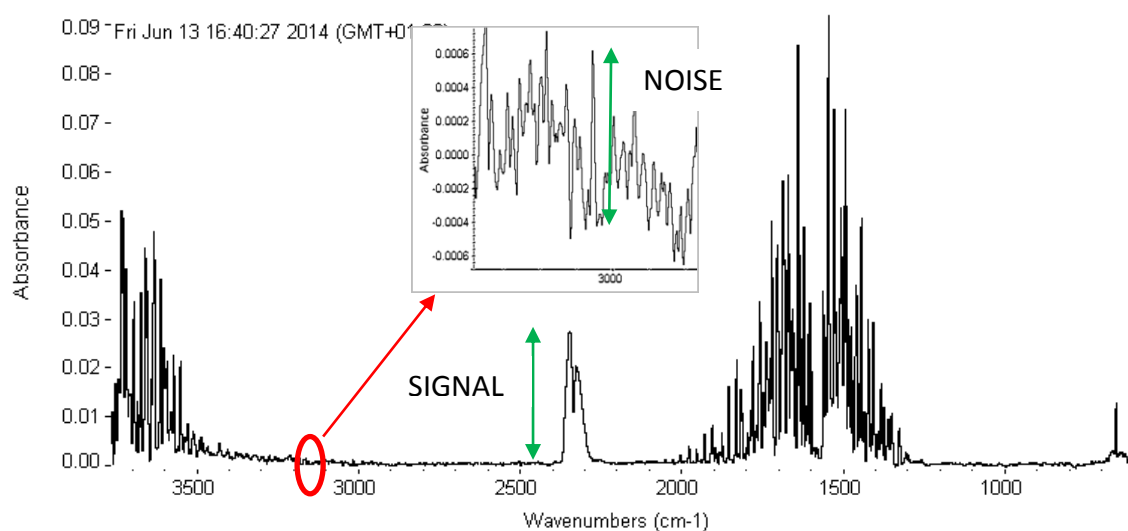


**Figure 5.33 IR spectrum of CO<sub>2</sub> in the air**

The signal/noise ratio = absorbance CO<sub>2</sub>/height of noise signal = 0.03/0.003 = 10

The amount of CO<sub>2</sub> in air is 397 ppm, it is a known value<sup>132</sup>.

The limit of CO<sub>2</sub> detection = CO<sub>2</sub> in air/(S/N ratio) = 397/10 = 39.7 ppm.

The detection limit of the IR method is 39.7 ppm of CO<sub>2</sub> which corresponds to a concentration  $8 \times 10^{-4}$  mol/L. This value is much lower than the expected products concentration.

### Sample analysis

A solution of DBHA and 2,5-DTBBQ in styrene was deoxygenated and heated at 140°C under nitrogen atmosphere for 3 days. The IR spectra of the head space were recorded at time 0 (before heating the reaction mixture), after 4 hours and after 3 days (Figure 5.34). A detailed analysis procedure is reported in the experimental part.

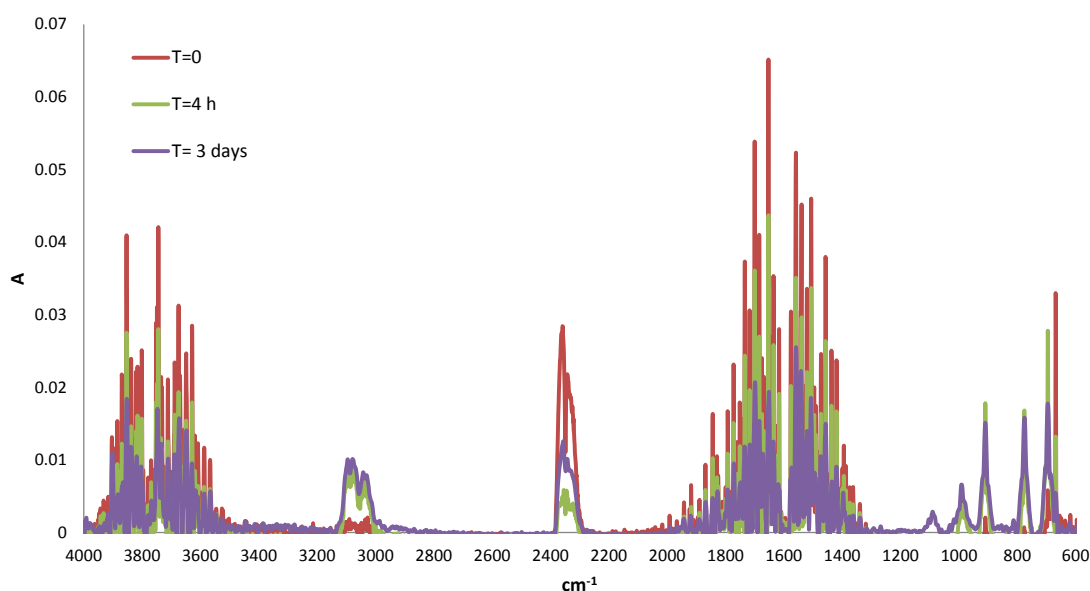


**Figure 5.34** IR spectra of the head space of the styrene polymerisation inhibition by DBHA-2,5-DTBBQ

The spectrum in Figure 5.34 shows a peak at *ca.*  $2330 \text{ cm}^{-1}$ , characteristic of the CO<sub>2</sub> stretching, but also the stretching and bending bands of water are observed. The intensity of the CO<sub>2</sub> signal varies from one sample to the other probably due to either natural variation of CO<sub>2</sub> concentration in the air or leaks. However, there are no N<sub>2</sub>O peaks at 2212-2236 and 1272-1299  $\text{cm}^{-1}$ <sup>46</sup>. The IR extinction coefficients of N<sub>2</sub>O and CO<sub>2</sub> are similar, therefore if any N<sub>2</sub>O was formed in a comparable or higher concentration to CO<sub>2</sub> we were able to detect it. In addition, a typical signal of the aromatic C-H stretching of styrene is observed at 3075-2985  $\text{cm}^{-1}$ .

The analysis of the head space during the inhibition of the styrene polymerisation with DBHA/2,5-DTBBQ did not reveal any trace of volatile nitrogen-containing compound such as N<sub>2</sub>O. Thus, the discrepancy observed between the initial and recovered moles of nitrogen in the previous experiment cannot be attributed to the formation of volatile products. In the next section, a characterization of the polymer formed after heating styrene in the presence of DBHA/2,5-DTBBQ mixture is attempted. The analysis was carried out to obtain information about the structure of the inhibitor contained in the polymer.

### **5.3.1.2 Investigation of the polymer structure**

Elemental analysis revealed that a substantial amount of nitrogen is contained in the polymer. Thus, unravelling the structure of the polymer would be extremely useful for understanding how DBHA/2,5-DTBBQ works. As mentioned previously, the <sup>1</sup>H-NMR spectrum of a solution of the polymer is too complex to be interpreted, thus matrix assisted laser desorption ionization-mass spectrometry (MALDI-MS) and pyrolysis gas chromatography-mass spectroscopy (Pyr-GC-MS) were used as alternative techniques.

#### **MALDI technique**

MALDI, a soft-ionization technique, is commonly used in mass spectrometry analyses of polymers<sup>133</sup>. The sample, mixed with a salt and a large excess of a matrix, is irradiated with a laser beam. The radiation causes the evaporation of the matrix, which brings indirectly the analyte in the gas phase. The key is that non-volatile compounds can be vaporized without degradation. In addition, the matrix ionises the analyte acting either as a proton donor (positive mode) or acceptor (negative mode). In the presence of a time-of-flight analyser, the separation of the ions is based on the time necessary to reach the detector, which depends on the m/z ratio. The choice of the matrix and the salt for cationisation are extremely important for the success of the analysis. In our case, the polymer was mixed with silver trifluoroacetate and a solution of dithranol (1,8,9-trihydroxyanthracene) in THF. The preparation of the sample was carried out following literature procedure<sup>134</sup>. The spectrum is shown in Figure 5.35 and 5.36.

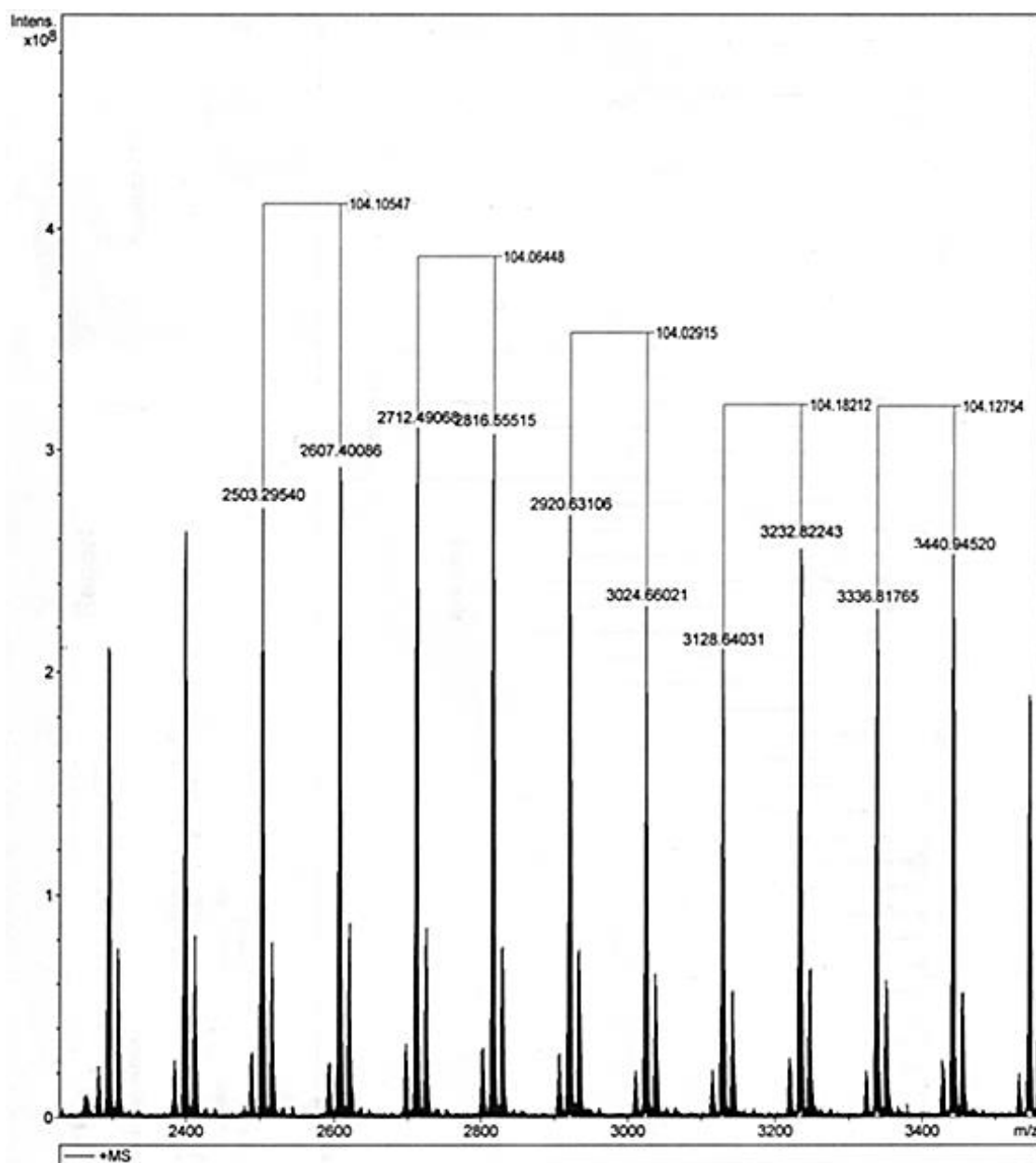


Figure 5.35 MALDI-MS spectrum of the polymer

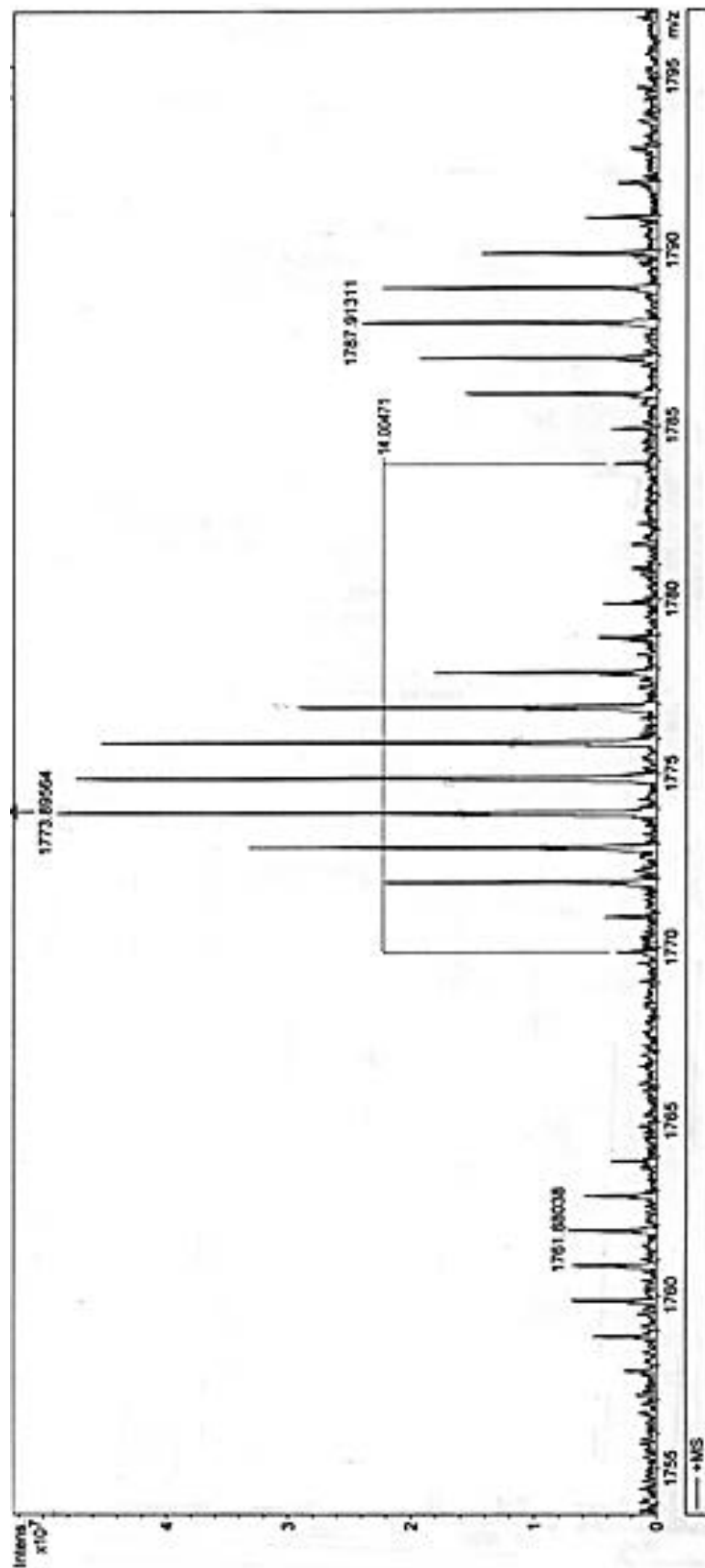


Figure 5.36 Enlargement of the MALDI-MS spectrum in Figure 5.35



The mass spectrum in Figure 5.35 shows only a section of the  $m/z$  range, as the sample has a large polydispersity. The main intense peaks differ by  $m/z$   $104.10 \pm 0.05$ , which corresponds to the mass of styrene monomer. The expansion of the spectrum in the region between  $m/z$  1755-1795 (Figure 5.36) shows three bands of peaks with different isotopic distribution. The central band shows the first peak at  $m/z$  1771.91 which corresponds to  $[(C_8H_8)_{16}+Ag]^+$  ion, and the isotopic distribution is consistent with the molecular formula proposed. Although many combinations of molecular formulas were tried, the peaks at  $m/z$  1757 and 1785 could not be assigned.

The MALDI analysis of the polymer thus did not clarify the polymer structure.

### Pyrolysis-gas chromatography-mass spectrometry

During the pyrolysis process, the heat leads to the breaking of the covalent bonds of the sample with formation of stable fragments. The fragmentation depends on the type of bonding and on the stability of the fragment. There are three different mechanisms of fragmentation: random scission, side-group scission and monomer revision (Figure 5.37)<sup>135</sup>.

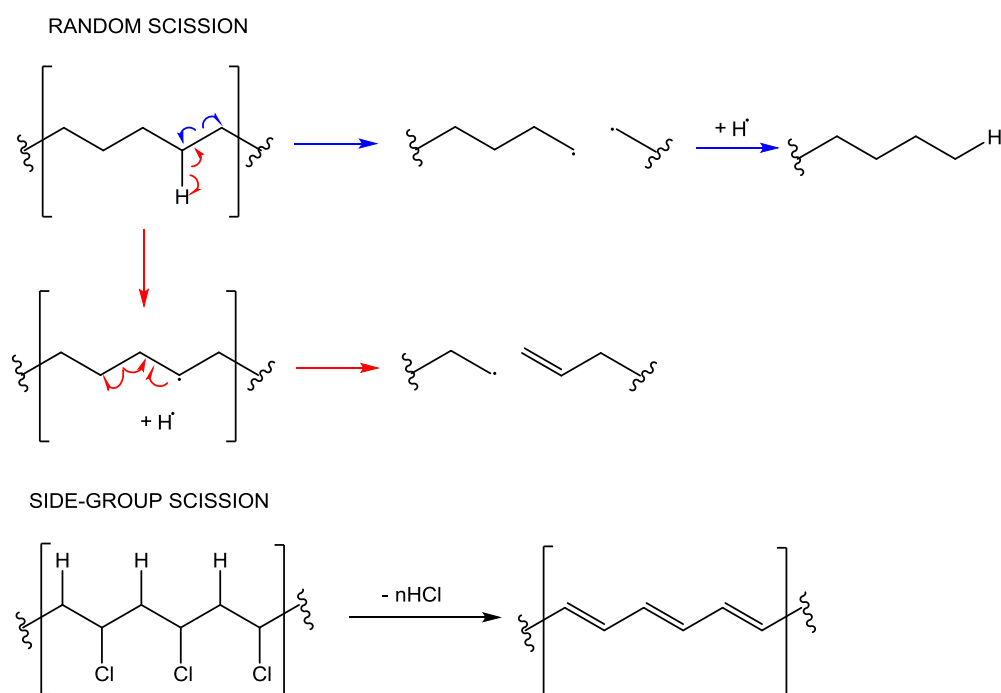


**Figure 5.37** Mechanism of fragmentation during pyrolysis degradation

The random scission is the mechanism preferred by polyolefins, such as polystyrene<sup>135</sup>. It involves the breaking of the C-C bonded backbone leading to the formation of smaller alkanes and alkenes. The side-group scission comports the elimination of the side groups to form an unsaturated molecule (Figure 5.37). Once the fragments are formed, they enter the gas chromatograph-mass spectrometer for the usual analysis. The spectrum reporting the abundance of each fragment vs the retention time is called pyrogram. Since a GC-Pyr-MS instrument was not available in ours laboratories, the sample was sent to Nufarm Ltd. for the analysis. In Figure 5.38 the pyrogram is reported.

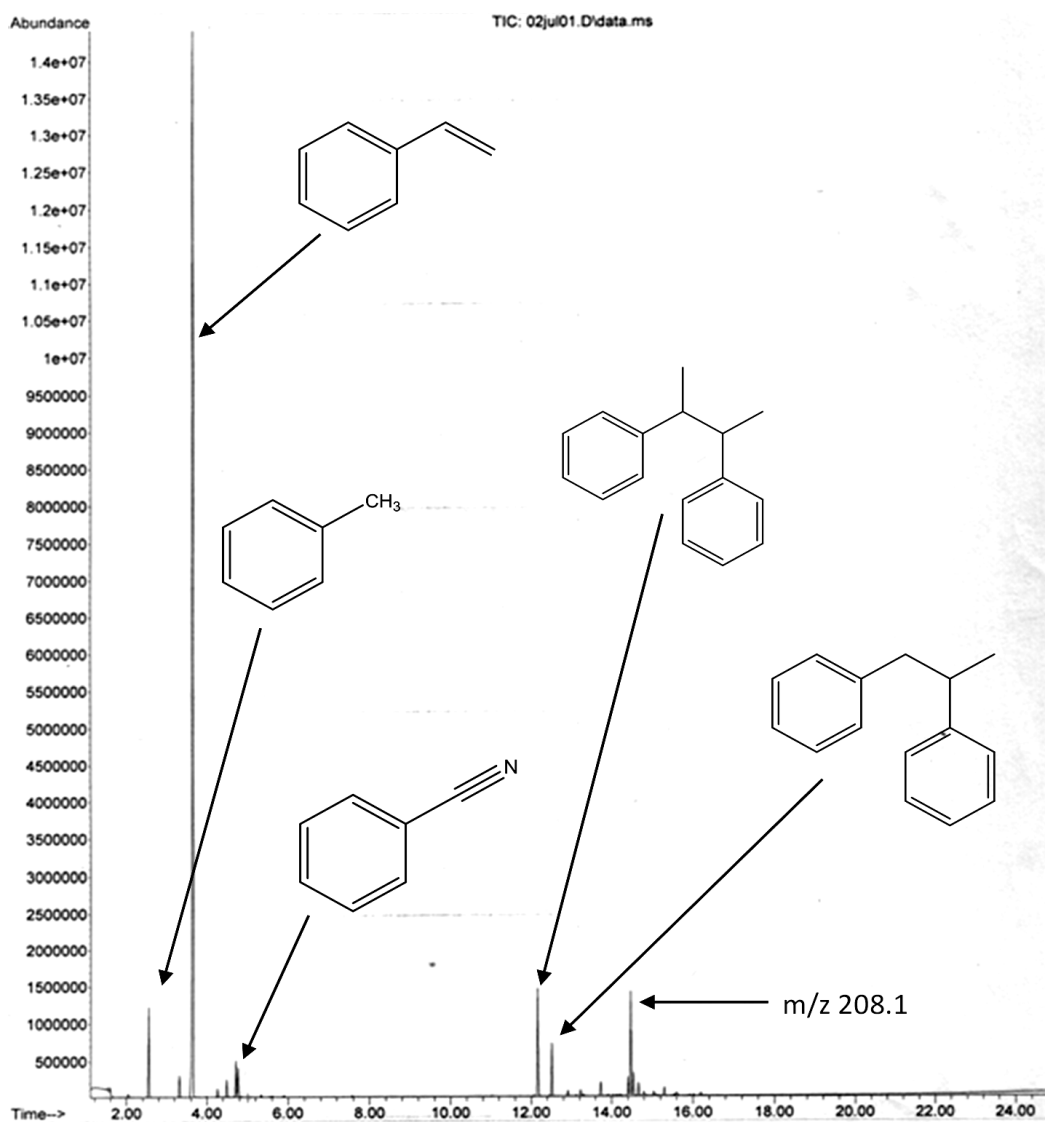
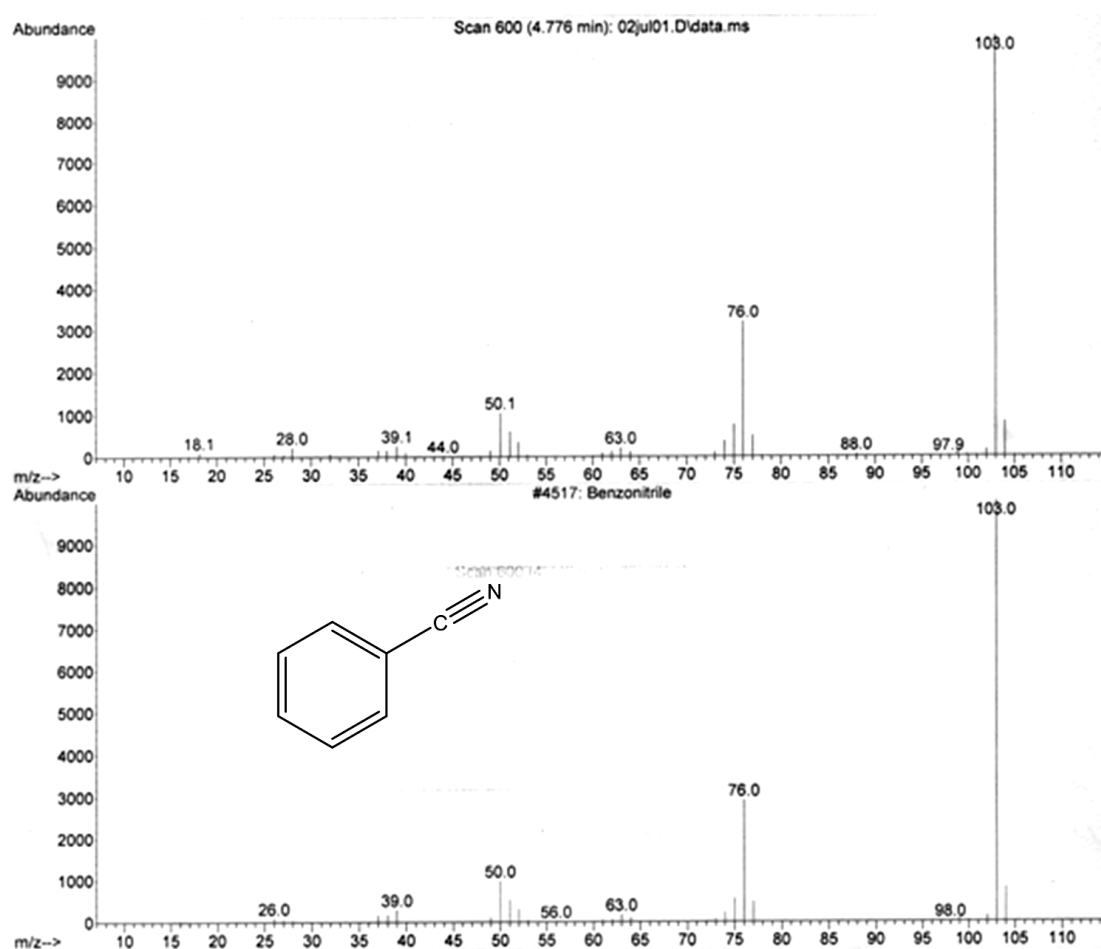


Figure 5.38 Pyrogram of the polymer

To assign a structure to each fragmentation pattern, the experimental data were compared with standard spectra in NIST (National Institute of Standards and Technology) database. Most of the peaks are related to the polystyrene fragmentation. Styrene represents the most abundant component at 3.6 min (5.38). Toluene, 2,3-diphenylbutane and 1,2-diphenylpropane elute at 2.5, 12.2 and 12.5 min, respectively. The peak at 14.5 min corresponds to a  $m/z$  208.1, typical mass of a styrene dimer, however its mass fragmentation pattern could not be linked to any of the common dimer structures. The only fragment containing nitrogen has a retention time of 4.8 min and corresponds to benzonitrile (Figure 5.39).



**Figure 5.39** Top spectrum: fragmentation of our sample. Bottom spectrum: spectrum of benzonitrile found in the NIST library

The presence of benzonitrile confirms that the benzylaminy fragment of DBHA is combined with the polymer (Figure 5.40 left). It is likely that benzonitrile is formed from the imine, which eliminates a proton and a benzyl group (Figure 5.40, right),

however there is not enough information to determine if the whole structure of DBHA is contained in the polymer.

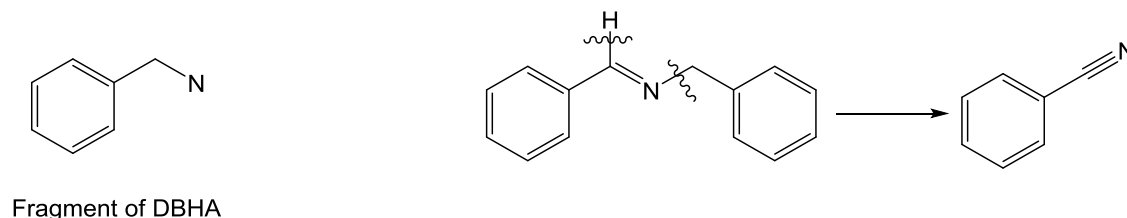


**Figure 5.40** Fragment of DBHA found in the polymer (on the right). Formation of benzonitrile fragment (on the left)

Neither MALDI nor Pyrolysis gas chromatography allowed determination of the structure of DBHA products attached to the polymer.

### 5.3.1.3 Conclusion

The product analysis of the inhibited styrene polymerisation in the presence of DBHA and 2,5-DTBBQ on a large scale, revealed that 2,5-DTBBQ is quantitatively recovered as 2,5-DTBHQ, DBHA instead, reacts giving several products. DBHA is oxidized to *N,N*-benzylidenebenzylamine-*N*-oxide (**4**), which reacts with styrene via 1,3-dipolar cycloaddition yielding to the isoxazolidine (**7**). DBHA is also converted into *N,N*-dibenzylnitroxide which reacts with propagation radicals producing the alkoxyamine (**21**). Nitrogen atoms are also contained in the polymer, but the structure could not be determined. In order to simplify the system, the next section describes products analysis of the styrene polymerisation inhibited with either DBHA or *N,N*-benzylidenebenzylamine-*N*-oxide (**4**).

## 5.3.2 Product analysis in the presence of either DBHA or *N,N*-benzylidenebenzylamine-*N*-oxide

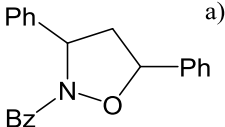
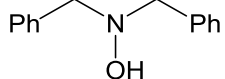
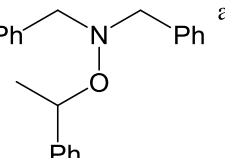
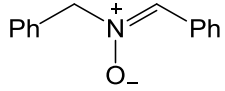
Unlike 2,5-DTBBQ, during the inhibition, DBHA reacts with propagation radicals and is converted to other products which then react further. To unravel the complex mechanism we decided to simplify the system using pure DBHA or *N,N*-benzylidenebenzylamine-*N*-oxide (**4**) as an inhibitor. We wanted to see the effect of the absence of 2,5-DTBBQ on the products distribution and if *N,N*-

benzylidenebenzylamine-*N*-oxide (**4**) can form other products apart from isoxazolidine (**7**).

### 5.3.2.1 Product analysis in the presence of DBHA

*N,N*-Dibenzylhydroxylamine (10 mmol) was dissolved in styrene and the solution was stirred under nitrogen atmosphere at 140°C for 24 h. A list of the products separated by column chromatography is reported in Table 5.3.

**Table 5.3** List of the products isolated from the styrene polymerisation inhibited with DBHA

Product	nitrogen (mmol)
 <chem>C1CN(C1c2ccccc2)c3ccccc3</chem>	1.4
 <chem>Oc1ccc(cc1)CN(c2ccccc2)c3ccccc3</chem>	1.9
 <chem>CC(Oc1ccc(cc1)CN(c2ccccc2)c3ccccc3)c4ccccc4</chem>	1.5
 <chem>[O-]N(=C(c1ccccc1)C2=CC=CC=C2)CC3=CC=CC=C3</chem>	0.1
polymer	1.8
Total	6.7

<sup>a</sup>The product was mixed to the polymer. The number of moles reported, which were calculated by the CHN analysis, refers to the mixture.

Overall, the 33% of nitrogen was lost compared to the initial amount (Table 5.3), which is probably related to the purification process. Inhibition with DBHA gives the same products as in the presence of DBHA/2,5-DTBBQ (Table 5.2 and 5.3). The quantitative analysis suggests that DBHA was consumed quicker compared to the DBHA/2,5-DTBBQ mixture; in the presence of DBHA, 1.9 mmol of inhibitor are recovered after 24 h, instead 3 mmol of DBHA unreacted were found after 48 h of inhibition with DBHA/2,5-

DTBBQ (Table 5.2). The hypothesis that this effect is due to DBHA regeneration during the inhibition by DBHA/2,5-DTBBQ needs to be confirmed (Chapter 6).

### 5.3.2.2 *N,N*-benzylidenebenzylamine-*N*-oxide as an inhibitor

*N,N*-benzylidenebenzylamine-*N*-oxide (**4**) (1.42 mmol) was dissolved in styrene. The reaction was stirred for 2 hours at 140 °C under nitrogen atmosphere. The only product isolated from the column (except styrene dimers) was the cycloadduct (**7**) (Figure 5.5, pag 117). An overall 80% of the initial nitrogen was recovered, and no trace of nitrogen was found in the polymer (the polymer was analysed by CHN analysis). This suggests that once nitrene is formed, it reacts with styrene nearly quantitatively to give 1,3-dipolar cycloaddition.

Two main conclusions can be made for this section. Alkoxyamine (**21**), isoxazolidine (**7**), *N,N*-benzylidenebenzylamine-*N*-oxide (**4**) and nitrogen-containing polymer are formed both in the presence and absence of 2,5-DTBBQ. However, DBHA seems to be consumed quicker than in the DBHA/2,5-DTBBQ inhibited mixture. The second conclusion is that *N,N*-benzylidenebenzylamine-*N*-oxide (**4**) reacts quantitatively via 1,3-dipolar cycloaddition. In those experiments it was not possible to recover the total amount of initial nitrogen, which could be caused by the purification processes or instability of products/intermediates. In the case of unstable compounds (e.g., air sensitive compounds), it would be ideal to work in a sealed system, such as in an NMR tube. However, using <sup>1</sup>H as nuclide of investigation is not useful, as the spectrum is too complex to be interpreted. Thus, we decided to introduce fluorine atoms on DBHA and monitor the reaction by <sup>19</sup>F-NMR technique, which generate more accessible spectra. This new strategy is reported in the next section.

## 5.3.3 Investigation of fluorine containing compounds

An alternative method to trace DBHA products formed during the inhibition of the styrene polymerisation is to introduce fluorine in the DBHA structure and monitor the



*Synthesis of N,N-bis(p-trifluoromethylbenzyl)hydroxylamine (22):*

*N,N-bis(p-trifluoromethylbenzyl)hydroxylamine (22)* was synthesised mixing hydroxylamine hydrochloride and 1-(bromomethyl)-4-(trifluoromethyl)benzene in ethanol. After the product was characterized using common analytical techniques, a  $^{19}\text{F}$ -NMR spectrum was recorded at 110 °C in styrene and 1-bromo-4-fluoro-benzene was used as an internal standard, Figure 5.42.

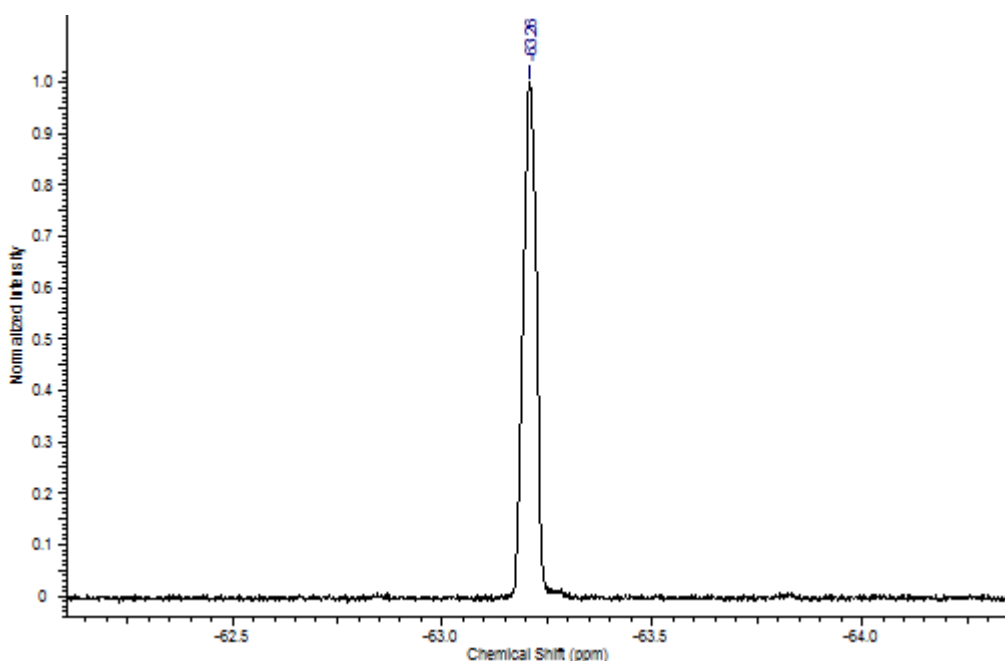


**Figure 5.42**  $^{19}\text{F}$ -NMR spectrum of DBHA- $\text{CF}_3$  (**22**) in styrene at 110 °C

DBHA- $\text{CF}_3$  (**22**) produces a singlet at chemical shift -63.26 ppm (Figure 5.42).

*Synthesis of N-(p-trifluoromethylbenzyl)-N-(p-trifluorophenyl) nitron (23) (nitron- $\text{CF}_3$  (23)):*

*N-(p-trifluoromethylbenzyl)-N-(p-trifluorophenyl) nitron (23) (nitron- $\text{CF}_3$  (23))* was synthesised mixing DBHA- $\text{CF}_3$  (**22**) and Pd/C in toluene. The reaction was stirred at 110 °C for 2 days under nitrogen atmosphere.  $^{19}\text{F}$ -NMR spectrum was recorded at 110 °C in styrene, Figure 5.43.



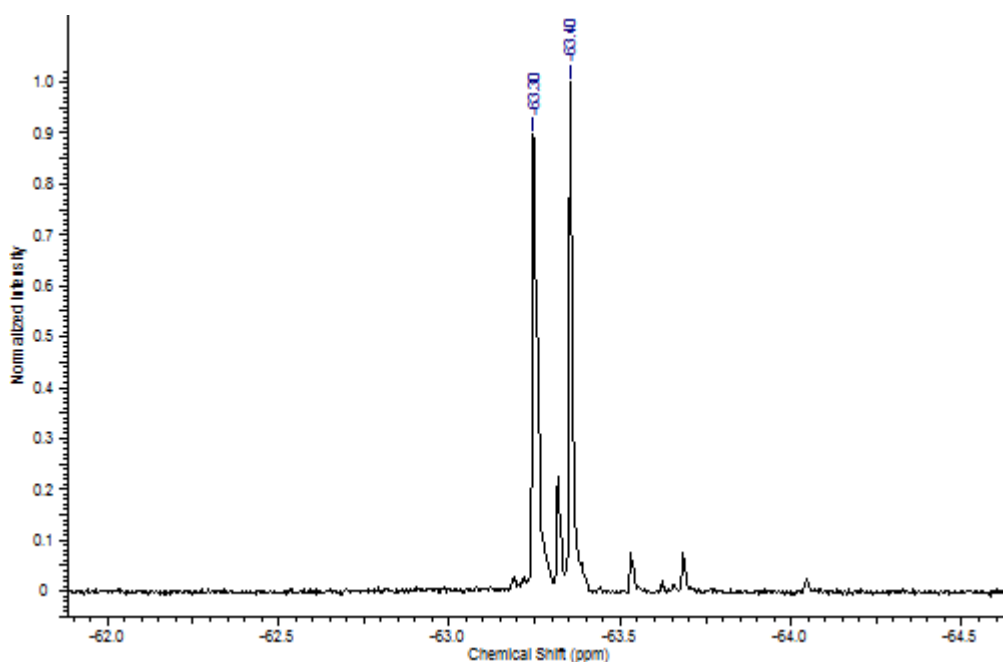


**Figure 5.43**  $^{19}\text{F}$ -NMR spectrum of nitrone- $\text{CF}_3$  (**23**) recorded at 110 °C in styrene

Nitron- $\text{CF}_3$  (**23**) gives two singlets at -63.30 and -63.40 ppm, respectively. The small peaks are due to the rapid formation of products between nitron- $\text{CF}_3$  and styrene, as they were not observed in the spectrum at room temperature.

*Synthesis of 2-(p-trifluoromethylbenzyl)-3-(p-trifluoromethylphenyl)-5-phenyl isoxazolidine (**24**) (isoxazolidine- $\text{CF}_3$  (**24**)):*

Stirring nitron- $\text{CF}_3$  (**23**) in styrene at 140 °C, isoxazolidine- $\text{CF}_3$  (**24**) was formed. A  $^{19}\text{F}$ -NMR of (**24**) was recorded in styrene at 110 °C, Figure 5.44.

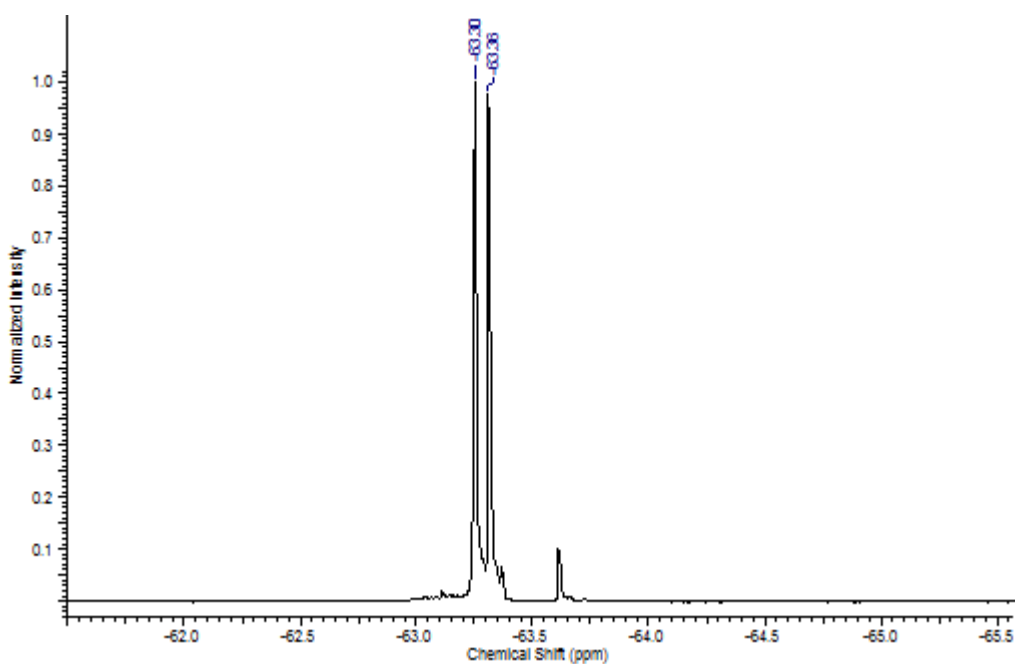


**Figure 5.44** <sup>19</sup>F-NMR spectrum of isoxazolidine-CF<sub>3</sub> (**24**) recorded at 110 °C in styrene  
Isoxazolidine-CF<sub>3</sub> (**24**) gives two singlets at -63.30 and -63.36 ppm, (Figure 5.44).

*Synthesis of o-(1-phenylethyl)-N,N-bis(p-trifluoromethylbenzyl)hydroxyl amine (25) (alkoxyamine-CF<sub>3</sub> (25)):*

DBHA-CF<sub>3</sub> (**22**) and 2,5-DTBBQ were dissolved in styrene. The reaction was heated at 140 °C in a nitrogen atmosphere for 24 h. A <sup>19</sup>F-NMR spectrum of (**25**) was recorded in styrene at 110 °C, Figure 5.45.

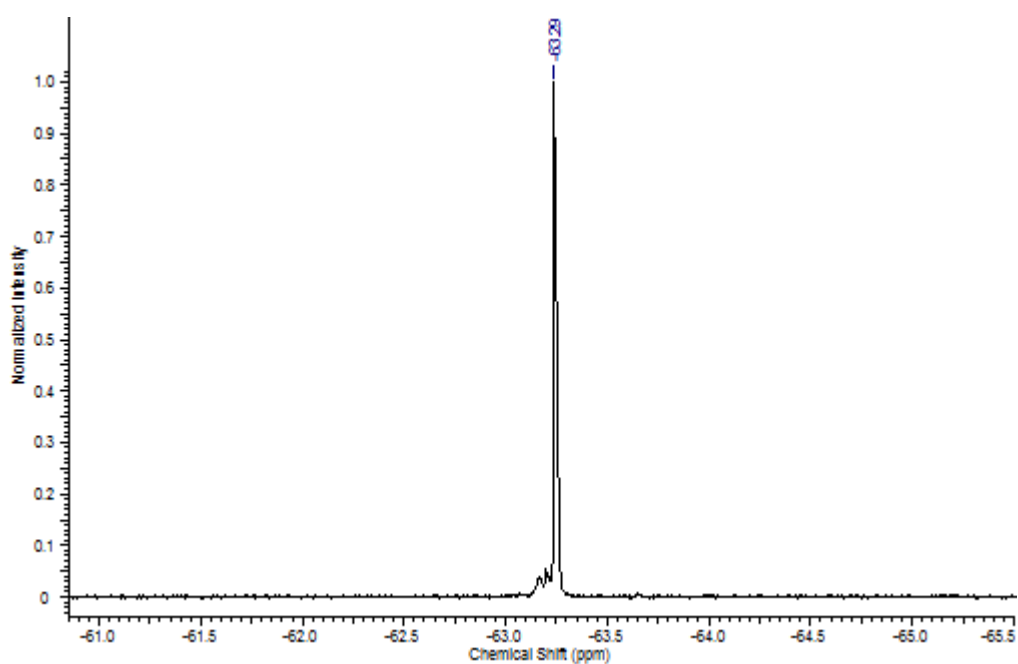


**Figure 5.45**  $^{19}\text{F}$ -NMR spectrum of the alkoxyamine- $\text{CF}_3$  (**25**) recorded at 110 °C in styrene

Alkoxyamine- $\text{CF}_3$  (**25**) produces a singlet at -63.29 ppm (Figure 5.45).

*Synthesis of polymer:*

During the reaction to synthesise alkoxyamine- $\text{CF}_3$  (**25**), the polymer was formed as well. Thus, it was precipitated from the solution using methanol and analysed by  $^{19}\text{F}$ -NMR (Figure 5.46).

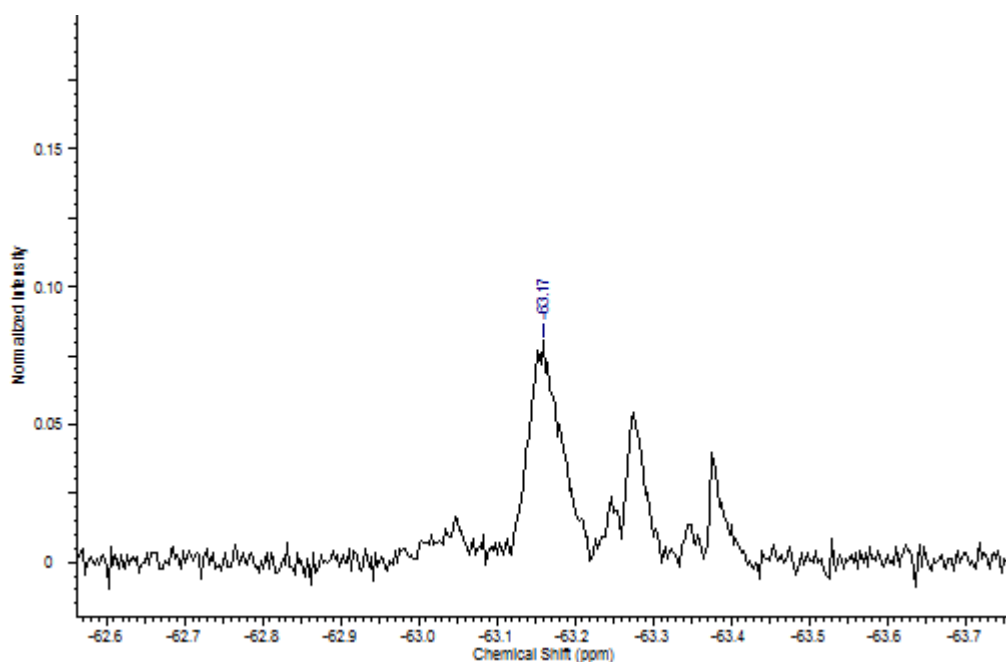


**Figure 5.46**  $^{19}\text{F}$ -NMR spectrum of the polymer recorded in styrene at 110 °C

The polymer shows a signal at -63.17 ppm, confirming that it incorporates some inhibitor (Figure 5.46). The spectrum also shows two minor peaks which correspond to alkoxyamine- $\text{CF}_3$  (**25**) and isoxazolidine- $\text{CF}_3$  (**24**). It was not possible to obtain the polymer in high purity due to solubility problems.

Once the all products were characterised, inhibition of the styrene polymerisation was monitored *in situ*.

DBHA- $\text{CF}_3$  (**22**) and 2,5-DTBBQ were dissolved in styrene and 1-bromo-4-fluorobenzene was added as a reference. The reaction was monitored *in situ* at 110 °C, recording  $^{19}\text{F}$ -NMR spectra every 20 min for 8 hours (Figure 5.47).

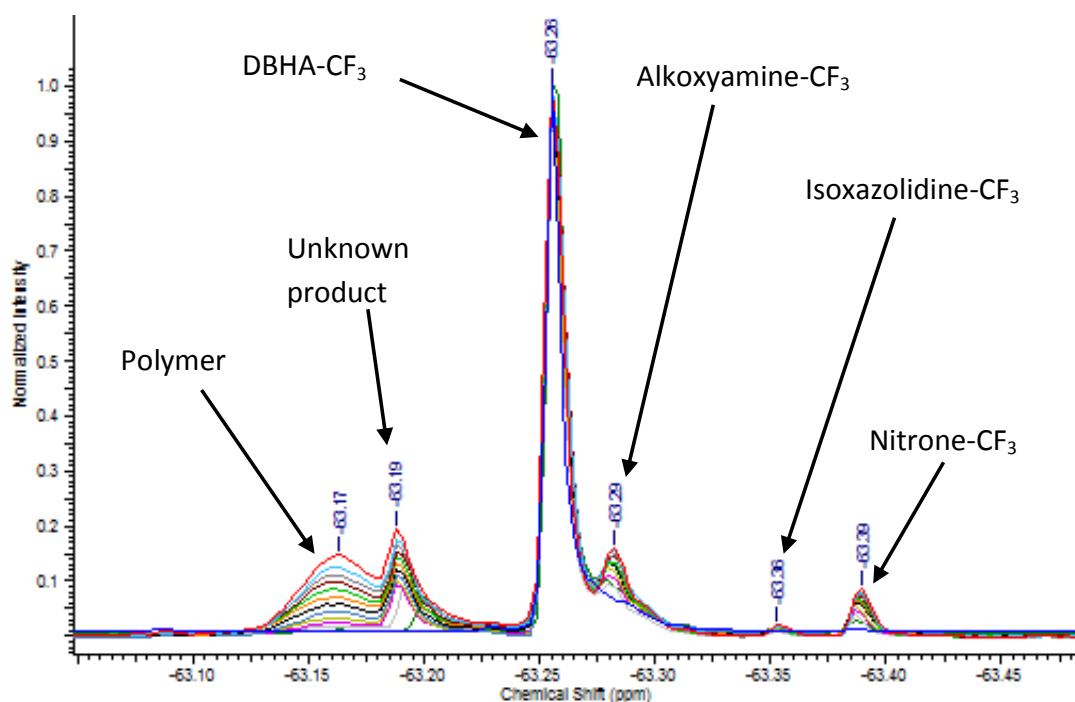


**Figure 5.47**  $^{19}\text{F}$ -NMR spectra of the styrene polymerisation inhibited by DBHA- $\text{CF}_3$  (**22**)/2,5-DTBBQ at 110 °C

Figure 5.47 confirms the formation of nitron- $\text{CF}_3$  (**23**) (-63.39 ppm), isoxazolidine- $\text{CF}_3$  (**24**) (-63.36 ppm) and alkoxyamine- $\text{CF}_3$  (**25**) (-63.29 ppm). The broad signal at -63.17 ppm is the polymer, however there is quite an intense peak at -63.19 ppm which could not be associated to any of the products synthesised. Thus, it was decided to scale-up the reaction and attempt the isolation of that product.

DBHA- $\text{CF}_3$  (**22**) and 2,5-DTBBQ were dissolved in styrene. The reaction mixture was heated at 110 °C for 72 h, under nitrogen atmosphere. During that time, the reaction was monitored by  $^{19}\text{F}$ -NMR in order to stop the reaction at the point of the highest concentration of the unknown compound (-63.19 ppm). The reaction mixture was monitored at 5 h, 24 h and 72 h (Figure 5.48 and 5.49).

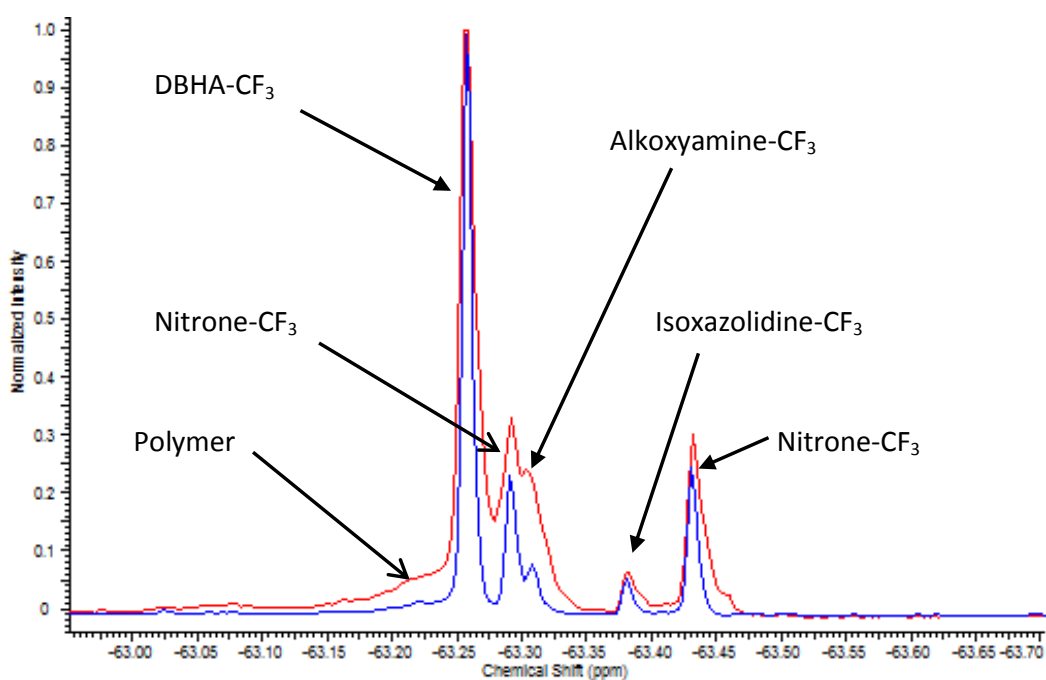
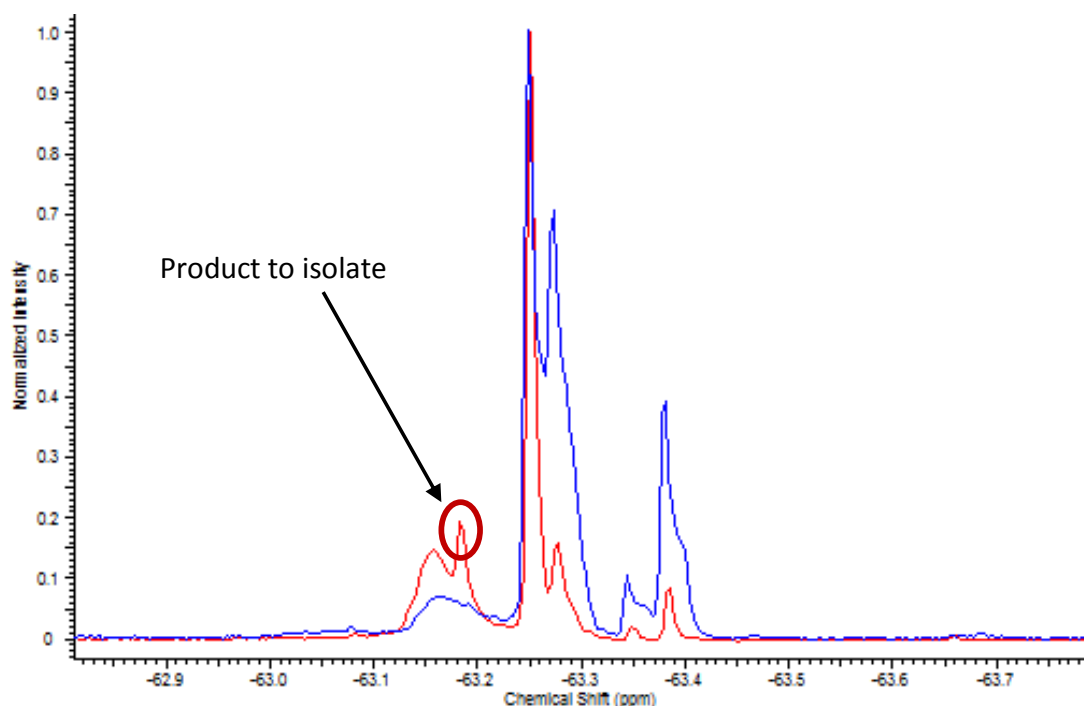


Figure 5.48  $^{19}\text{F}$ -NMR spectra recorded after 5 h and 24 h (the spectra were recorded at 25 °C, in a 400 MHz spectrometer) of styrene polymerisation inhibited with DBHA- $\text{CF}_3$  (**22**)/2,5-DTBBQ

The spectra in Figure 5.48 shows clearly the signals of nitron- $\text{CF}_3$  (**23**), isoxazolidine- $\text{CF}_3$  (**24**), alkoxyamine- $\text{CF}_3$  (**25**) and a rather weak signal of the polymer, however there is no trace of the unknown compound, and prolonging the reaction time did not improve the result (Figure 5.49).



**Figure 5.49** Comparison of the spectrum of the reaction mixture carried out in the NMR tube (blue line) and the spectrum recorded after 72 hours of the large scale reaction. The spectra were recorded at 110 °C, at a 400 MHz spectrometer

Figure 5.49 compares the spectrum after 72 hours with that recorded in the sealed system, which confirms that the only signal missing is the unknown compound. A plausible explanation could be that the unknown compound is highly unstable, so once it is removed from the reaction system it quickly degrades.

Since we wanted to see if this product is also formed when DBHA-CF<sub>3</sub> is used on its own, a products analysis was carried out on the inhibition of styrene polymerisation with DBHA-CF<sub>3</sub>, as reported in the next section.

### **5.3.3.1** *Product analysis in the presence of DBHA-CF<sub>3</sub> as an inhibitor*

The unknown product detected during the inhibition with DBHA-CF<sub>3</sub>/2,5-DTBBQ could be responsible for the synergism, thus, if this is the case, we expect it to be absent (or formed in little concentration) in the absence of 2,5-DTBBQ. Hence, the products distribution during the styrene polymerisation inhibited by DBHA-CF<sub>3</sub> was monitored.

DBHA-CF<sub>3</sub> was dissolved in styrene, in the presence of 1-bromo-4-fluorobenzene as an internal standard. The solution was heated, under nitrogen atmosphere, in the NMR cavity at 110 °C. <sup>19</sup>F-NMR spectra were recorded every 20 min for 4 h (Figure 5.50).

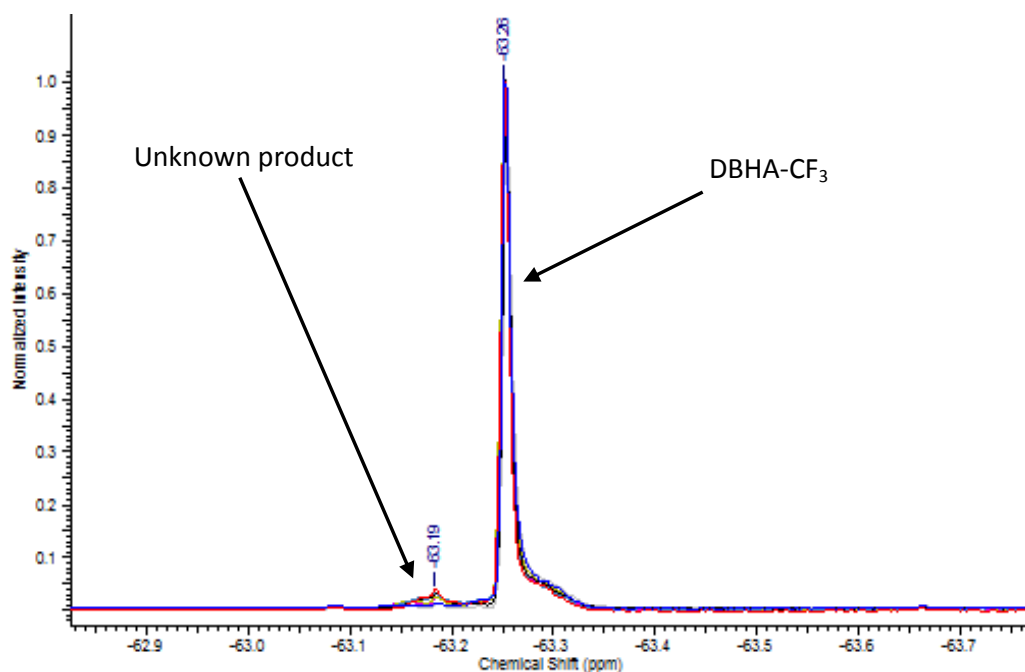


**Figure 5.50** <sup>19</sup>F-NMR spectra recorded at 110 °C during the styrene polymerisation inhibited by DBHA-CF<sub>3</sub>

The spectrum in Figure 5.50 shows that after 4 hours only a small amount of fluorinated products is formed. However, notwithstanding DBHA-CF<sub>3</sub> is quite inert, a weak signal at -63.19 ppm is observed, which resonates at the same position as the unknown product detected in the mixture DBHA-CF<sub>3</sub>/2,5-DTBBQ. The reactivity of DBHA-CF<sub>3</sub> seems quite different from DBHA (Paragraph 5.3.2.1), in fact most of DBHA is consumed during the inhibition, while for DBHA-CF<sub>3</sub>, 2,5-DTBBQ seems vital to increase its reactivity. This may be attributed to the presence of CF<sub>3</sub> groups, which increase the BDE of DBHA-CF<sub>3</sub>. The above experiment does not confirm if the unknown compound is responsible for the synergism, however, one possibility could be that in the case of DBHA-CF<sub>3</sub>/2,5-DTBBQ mixture, the reactivity of DBHA-CF<sub>3</sub> is intensified with a consequent higher formation of the unknown product. This enhances the inhibition property of the mixture.



## 5.4 Conclusions

An extensive product analysis was carried out for the inhibited styrene polymerisation in the presence of DBHA/2,5-DTBBQ. By combining different analytical techniques, we determined that 2,5-DTBBQ is reduced to 2,5-DTBHQ. A few products derived from DBHA were isolated, such as *N,N*-benzylidenebenzylamine-*N*-oxide (**4**), isoxazolidine (**7**) and alkoxyamine (**21**). In addition, some DBHA got incorporated into polystyrene. The structure of this polymer was investigated by pyrolysis gas chromatography and MALDI mass spectrometry. Although full structure assignment was not possible, we demonstrated that a fragment of DBHA is incorporated into the polymer structure. In addition, the DBHA/2,5-DTBBQ inhibited polymerisation was monitored by  $^{19}\text{F}$ -NMR, in situ, following the introduction of fluorine atoms in the hydroxylamine structure. The results suggested the formation of an unstable product, which could not be isolated. Inhibition of styrene polymerisation was also monitored by  $^{19}\text{F}$ -NMR in the absence of 2,5-DTBBQ; significantly lower reactivity of the hydroxylamine was observed in this case. The  $\text{CF}_3$  groups in *para* position decreases the reactivity of DBHA- $\text{CF}_3$ , compared to DBHA. Indeed, the BDE of RNO-H bond is higher in the case of DBHA- $\text{CF}_3$ <sup>45</sup>, which contrarily to DBHA, needs 2,5-DTBBQ to react at least to some extent. This suggests that the mechanism may proceed via concerted proton electron transfer.

## 6 A new inhibitor composition for the auto-initiated styrene polymerisation

### 6.1 Aim of the chapter

The two previous chapters were focussed on the detection of reaction products generated during self-polymerization of styrene inhibited by the mixture of 2,5-di-*tert*-butyl-1,4-benzoquinone (2,5-DTBBQ) and *N,N*-dibenzylhydroxylamine (DBHA). Here, their inhibition properties are tested, in order to decipher the mechanism of action of the DBHA/2,5-DTBBQ mixture in the auto-initiated styrene polymerization. The attention is focussed on the role of *N,N*-dibenzylnitroxide which is examined by carrying out a series of dilatometry and EPR experiments.

### 6.2 Inhibition efficiency of the DBHA/2,5-DTBBQ mixture

As mentioned in the introduction in chapter 1, Nufarm Ltd identified a composition that allows controlling the auto-initiated styrene polymerisation for hours<sup>13</sup>. However, conditions under which they tested the composition may be different (e.g., oxygen concentration, temperature, inhibitor/retarder concentration etc.) from our system, hence dilatometry experiments were carried out to establish the ability of DBHA/2,5-DTBBQ mixture to stop the auto-initiated styrene polymerisation under our conditions.

Styrene solutions containing individually DBHA (4.7 mM) or 2,5-DTBBQ (4.5 mM) or their mixture (DBHA/2,5-DTBBQ, 1.2/0.9 mM) were prepared. The analysis was carried out at 110 °C, and the percentage of conversion of styrene to polystyrene was plotted against the time (Figure 6.1 and 6.2).

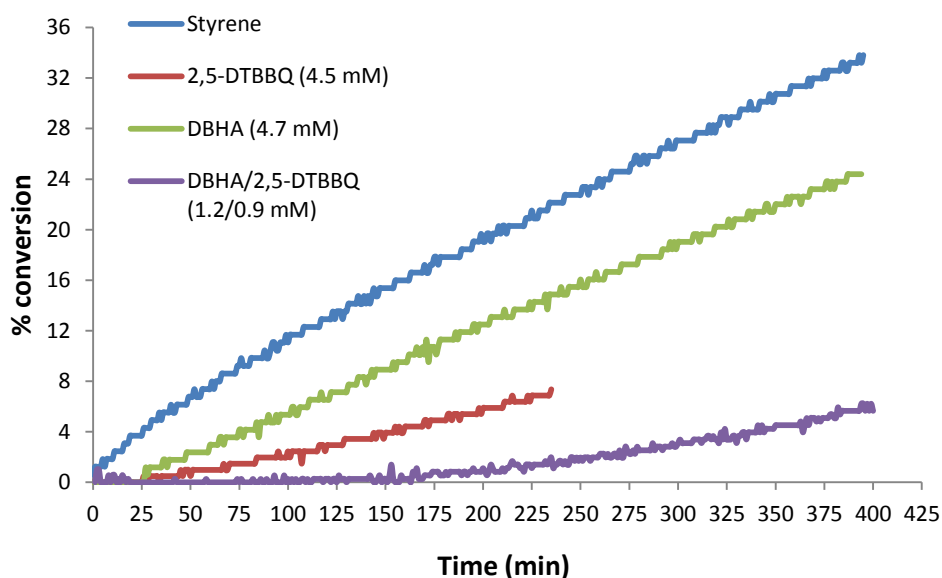


**Figure 6.1 Dilatometry traces for the inhibition of the auto-initiated styrene polymerisation by DBHA, 2,5-DTBBQ and DBHA/2,5-DTBBQ mixture**

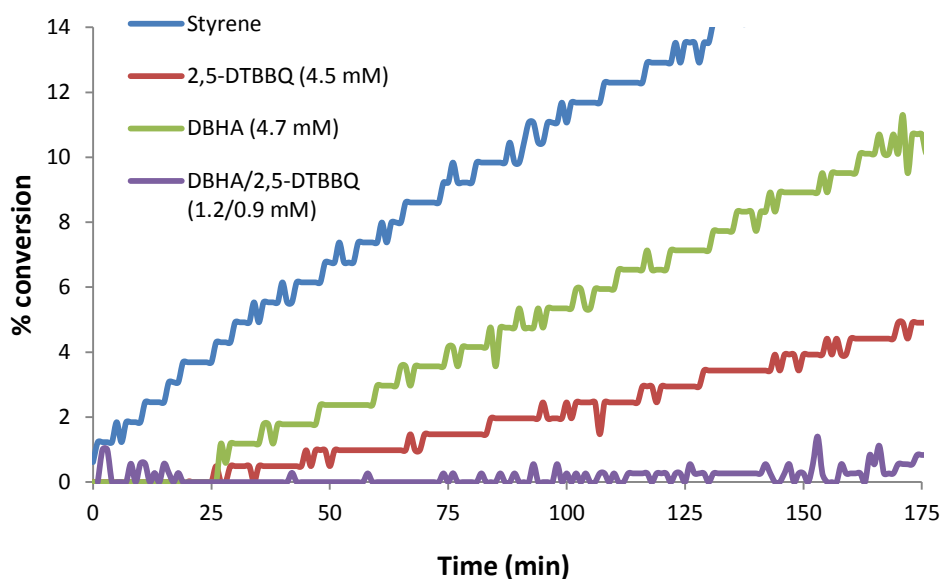


**Figure 6.2 Enlargement of Figure 6.1**

Figure 6.1 and 6.2 show that the DBHA/2,5-DTBBQ mixture is far more effective (inhibition time  $165 \pm 6$  min) in inhibiting styrene polymerisation compared to DBHA (inhibition time  $28 \pm 3$  min) and even more with respect to 2,5-DTBBQ, which is only a retarder (a detailed explanation of how the inhibition time and error are estimated is reported in the experimental part). Clearly, there is synergism between the two

components, because although the concentration in the mixture is much lower than that of the single components, the inhibition time is considerably longer than the sum of the inhibition time of DBHA and 2,5-DTBBQ taken separately. In addition, the mixture maintains its efficiency even in deoxygenated conditions. Indeed, in paragraph 6.4.1 is demonstrated, by an oximetry experiment, that oxygen is rapidly consumed in the system.

Dilatometry traces confirmed the synergism in the DBHA/2,5-DTBBQ mixture. In order to establish if the synergism is a consequence of regeneration of the inhibitors during the process, their concentrations were monitored, as explained in the next section.

### **6.3 Concentrations monitoring by gas chromatography**

In chapter 4 (section 4.4.1) we learnt that DBHA and 2,5-DTBBQ in toluene react as a second order process, however during the polymerisation the mechanism may be different. One possibility is that one of the two inhibitors maybe regenerated during the inhibition and this could be the reason of the excellent ability of DBHA/2,5-DTBBQ mixture to stop polymerisation. In order to probe that, we decided to compare concentration trends during the polymerisation with those in toluene. A considerably slower inhibitor consumption in the case of polymerisation would be a good indication that it is reformed during the process. Thus, styrene polymerisation in the presence of DBHA/2,5-DTBBQ was monitored by gas chromatography (GC).

A mixture of DBHA (0.058 M) and 2,5-DTBBQ (0.029 M) in a N<sub>2</sub> saturated styrene solution (15 mL) was heated at 110 °C for 5 h. Samples were taken at different times and before the analysis, each of them was diluted and the internal standard was added. The concentration of reagents and products in Figure 6.3 refers to the sample before dilution. For more detailed conditions and sample preparation see the experimental section.

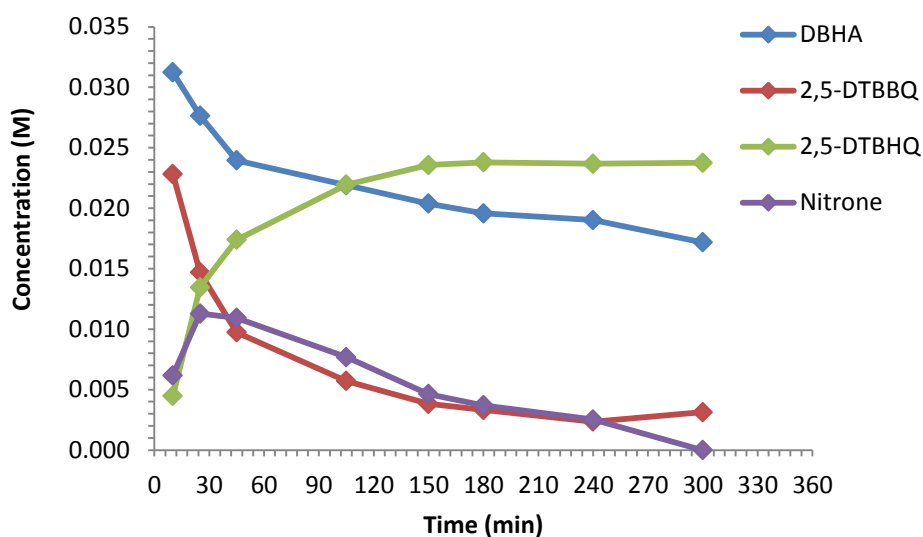


**Figure 6.3** Reagents concentrations trend during the styrene polymerisation inhibited by 2,5-DTBBQ and DBHA at 110 °C

Figure 6.3 confirms what was observed previously in chapter 4. 2,5-DTBBQ plays the role of an oxidizing agent. Indeed, 2,5-DTBBQ is reduced to 2,5-DTBHQ during the reaction, therefore it is likely that it oxidizes DBHA. In addition, Figure 6.3 shows that the sum of 2,5-DTBBQ and 2,5-DTBHQ concentrations remains constant throughout the entire analysis. This means that even though 2,5-DTBBQ/2,5-DTBHQ couple is involved in the inhibition, it does it only by hydrogen abstraction (or redox reaction)<sup>27, 77</sup> as shown in Figure 6.4.

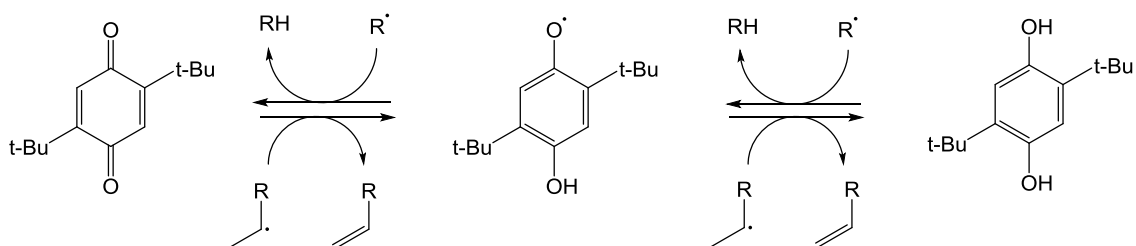


**Figure 6.4** Hydrogen abstraction mechanism

DBHA, instead, is only partially converted into *N,N*-benzylidenebenzylamine-*N*-oxide. *N,N*-benzylidenebenzylamine-*N*-oxide is likely to be mainly consumed via 1,3-dipolar cycloaddition reaction. The evidence for this is that the only product recovered, almost quantitatively, from the reaction of *N,N*-benzylidenebenzylamine-*N*-oxide in styrene, was the cycloadduct (section 5.3.2.2). Since the aim of this investigation was to find

evidence of inhibitor regeneration, we compared the above reaction (Figure 6.3) with that in toluene (chapter 4, section 4.4.1) as they should be similar. The rate constant for the reaction DBHA/2,5-DTBBQ in toluene at 110 °C ( $k = 0.0051 \text{ M}^{-1}\text{s}^{-1}$ ) can be used to calculate the expected half-life of DBHA and 2,5-DTBBQ in styrene and see if they match the data in Figure 6.3. Assuming that the initial concentrations of 2,5-DTBBQ and DBHA (the initial concentration in this case refers to the first sample analysed by gas chromatography) are 0.023 M and 0.031 M, the expected half-life times are 143 min and 105 min, respectively. The half-life in styrene is 45 min for 2,5-DTBBQ, which seems to be converted to 2,5-DTBHQ faster than in a non-polymerizable solvent. Therefore, 2,5-DTBBQ in styrene reacts with something else faster (e.g., propagation chains as shown in Figure 6.4) than it reacts with DBHA. On the other hand, the concentration of DBHA in styrene does not halve even after 300 min. This result suggests that it is likely that DBHA is regenerated during the inhibition.

Kinetic data thus support the suggestion that regeneration of DBHA may be the explanation for the synergistic inhibition of the polymerisation by the DBHA/2,5-DTBBQ mixture, however the species directly involved in the inhibition still have to be identified. The most promising candidate is *N,N*-dibenzyl nitroxide.

## 6.4 Role of *N,N*-dibenzyl nitroxide in the inhibition mechanism

*N,N*-Dibenzyl nitroxide is formed during the inhibition of styrene polymerisation by the DBHA/2,5-DTBBQ mixture, thus a combination of EPR and dilatometry experiments were carried out to establish its role in the inhibition mechanism.

### 6.4.1 *N,N*-Dibenzyl nitroxide formation in the presence of DBHA and 2,5-DTBBQ/DBHA

Nitroxides, as already mentioned in the previous chapters, can trap propagation chains leading to alkoxyamines, however, the labile NO-R bond of alkoxyamine may break regenerating both the carbon centred radical and the nitroxide<sup>136</sup>. Moreover, it has

been proved that nitroxides may initiate the polymerisation through hydrogen abstraction from the Mayo dimer or by addition to the double bond of styrene<sup>11</sup>. Thus, nitroxides may act both as an inhibitor and an initiator<sup>10</sup>. If *N,N*-dibenzyl nitroxide acts predominantly as an initiator, it would be reasonable to assume that the role of 2,5-DTBBQ is to remove it from the reaction mixture by oxidizing it to a more stable compound (e.g., *N,N*-benzylidenebenzylamine-*N*-oxide). If this were true, the concentration of *N,N*-dibenzyl nitroxide in the presence of DBHA/2,5-DTBBQ mixture would be lower compared to the case where DBHA is the only inhibitor. Thus, EPR data for the inhibition of styrene polymerisation in the presence of DBHA and 2,5-DTBBQ/DBHA were compared.

DBHA (9.4 mM) and 2,5-DTBBQ (9.0 mM) were dissolved in styrene. The solution (in air) was sealed in a capillary tube and analysed in the EPR cavity at 110 °C for 2 h. The same conditions were used for a 9.4 mM solution of DBHA in styrene. The relative nitroxide and oxygen concentrations were estimated by EWVoigt software<sup>60</sup> (procedure for normalization of the relative nitroxide concentrations provided by EWVoigt is reported in the experimental part) and plotted against the time (Figure 6.5 and 6.6).

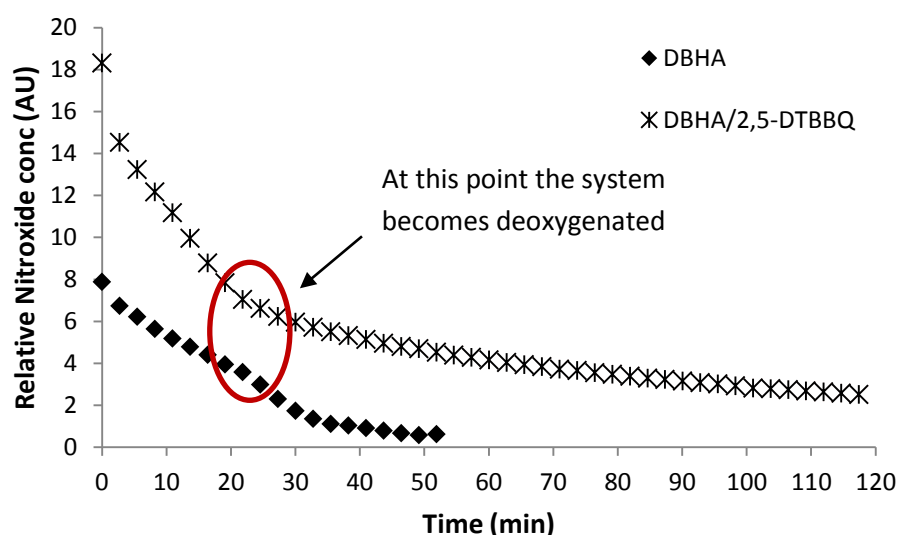
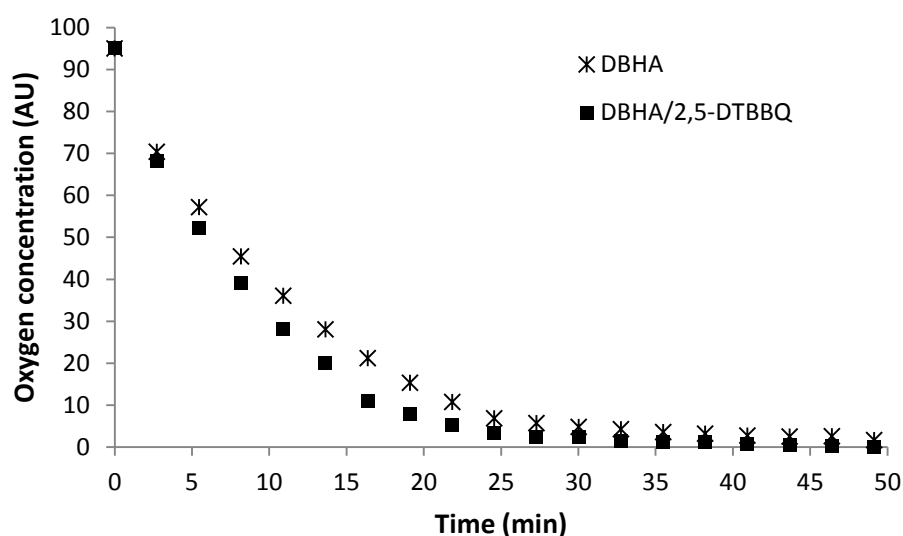


Figure 6.5 Evolution of *N,N*-dibenzyl nitroxide in the inhibition of styrene polymerisation with DBHA (diamonds) and 2,5-DTBBQ/DBHA mixture (stars)

Figure 6.5 shows that the nitroxide concentration is higher in the DBHA/2,5-DTBBQ mixture than in DBHA alone and that in both samples the maximum nitroxide concentration is observed at time zero. In section 2.3.2 it was established that the oxygen dissolved in solution contributes to the initial *N,N*-dibenzyl nitroxide formation, by oxidizing DBHA. A similar scenario is plausible for the DBHA/2,5-DTBBQ mixture. This is confirmed by the oximetry experiment shown in Figure 6.6.



**Figure 6.6 Oxygen consumption in the inhibition of styrene polymerisation with DBHA (stars) and 2,5-DTBBQ/DBHA mixture (diamonds)**

Figure 6.6 shows that oxygen consumption is similar in DBHA and DBHA/2,5-DTBBQ and that at approximately 28 min both systems become deoxygenated. Comparison of Figure 6.6 with 6.5 shows that in DBHA and DBHA/2,5-DTBBQ samples, *N,N*-dibenzyl nitroxide concentration decreases in parallel with the oxygen concentration. Therefore, even for the DBHA/2,5-DTBBQ mixture, the initial higher nitroxide concentration is due to the oxygen in solution. Unlike DBHA, however, DBHA/2,5-DTBBQ mixture maintains a reasonable amount of *N,N*-dibenzyl nitroxide even in a deoxygenated system. This is due to the contribution of the reaction between DBHA and 2,5-DTBBQ to the *N,N*-dibenzyl nitroxide formation, as observed in section 4.3. The persistence of *N,N*-dibenzyl nitroxide for longer time in the DBHA/2,5-DTBBQ mixture, combined with the fact that *N,N*-dibenzyl nitroxide is formed in higher concentration in



the DBHA/2,5-DTBBQ mixture, suggests that the role of 2,5-DTBBQ is not to oxidize *N,N*-dibenzyl nitroxide, but rather to promote its formation.

Contrary to our hypothesis, this experiment indicates that *N,N*-dibenzyl nitroxide may be involved in the process as an inhibitor rather than an initiator, and we decided to investigate it further.

## 6.4.2 Electronic effect of substituents in dibenzylhydroxylamines

The tendency of hydroxylamines to form the corresponding nitroxides is correlated with the energy required to break the  $R_2NO-H$  bond, e.g., the higher the bond dissociation energy, the lower the tendency to form nitroxide. The value of the bond dissociation energy increases with the increased stability of the hydroxylamine and with the decreased radical stability<sup>45</sup>. The stability of nitroxide is affected by polar and steric effects. The introduction of electron donating groups is expected to stabilize nitroxide by positive inductive effect, the electron withdrawing substituents should destabilise it. Thus, we decided to take advantage of this effect to change *N,N*-dibenzyl nitroxide concentration in solution. Our idea was to add a series of electron donating and withdrawing substituents to the aromatic ring of DBHA and monitor the change in nitroxide concentration by EPR spectroscopy. At the same time, a dilatometry experiment was carried out to observe the effect on the inhibition properties of the mixture.

*N,N*-Bis-(*p*-methylbenzyl)hydroxylamine (DBHA-CH<sub>3</sub>), *N,N*-bis-(*p*-chlorobenzyl)-hydroxylamine (DBHA-Cl), *N,N*-bis-(*p*-trifluoromethylbenzyl)hydroxylamine (DBHA-CF<sub>3</sub>) and *N,N*-bis-(*p*-cyanobenzyl)hydroxylamine (DBHA-CN) (Figure 6.8, left side) were used in this experiment. The synthetic procedure is reported in the experimental part.

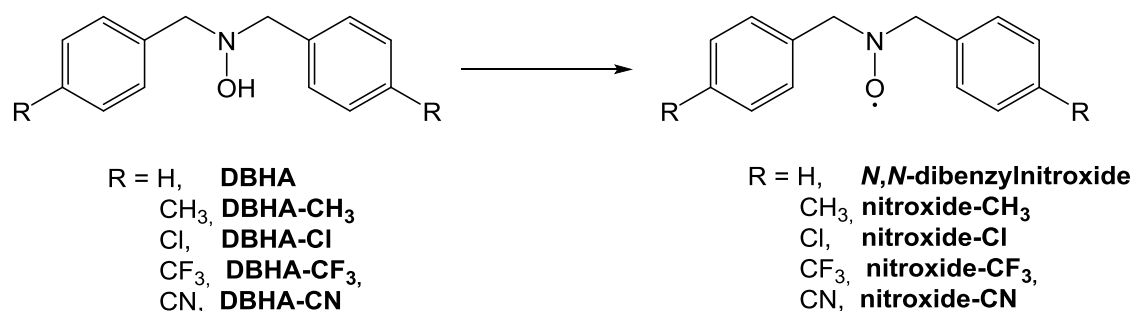


**Figure 6.7** *p*-Substituted *N,N*-dibenzylhydroxylamines synthesised and the corresponding nitroxides

The hydroxylamines ( $9.3 \times 10^{-3}$  M) were mixed with 2,5-DTBBQ ( $4.6 \times 10^{-3}$  M) and dissolved in styrene (2.5 mL). The EPR experiment was carried at 110 °C for 5 h. The absolute nitroxide concentration was plotted against the time, as reported in Figure 6.8.

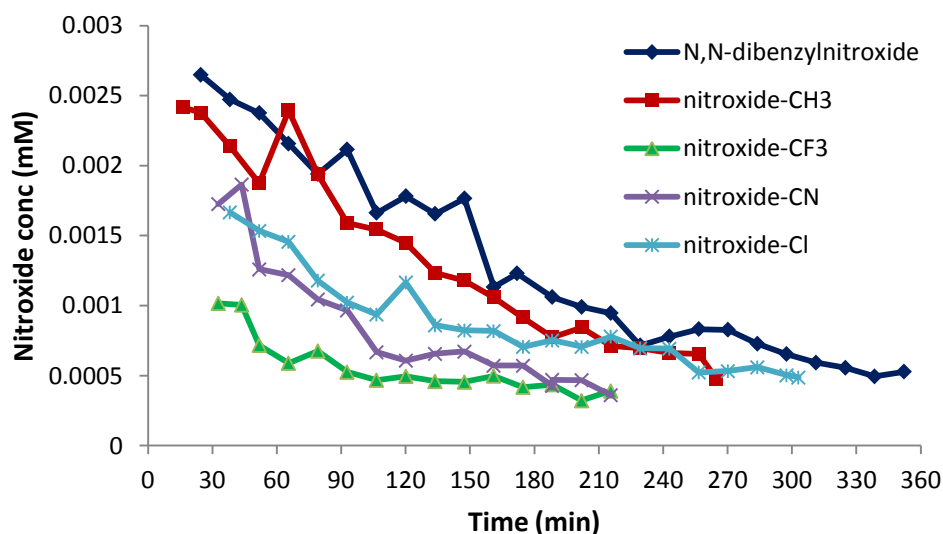


**Figure 6.8** Evolution of nitroxide concentration during the inhibition of styrene using *p*-substituted hydroxylamines and 2,5-DTBBQ

Figure 6.8 shows that nitroxide concentration in solution decreases in the following order: *N,N*-dibenzylnitroxide > nitroxide-CH<sub>3</sub> > nitroxide-Cl > nitroxide-CN > nitroxide-CF<sub>3</sub>. Clearly this trend does not correlate with the electronic properties of the substituents, as it should be in the decreasing order nitroxide-CH<sub>3</sub> > *N,N*-dibenzylnitroxide > nitroxide-Cl > nitroxide-CF<sub>3</sub> > nitroxide-CN<sup>103</sup>. There is a relationship, instead, between nitroxide concentration and mass of the substituent.

Hence, as in the case of the effect of electron donating and withdrawing substituents on the rate constant of hydroxylamines oxidation by 2,5-DTBBQ (section 4.4.2), the ponderal effect can be invoked. The only exception is for DBHA-CN and DBHA-Cl, where the trend is reversed, however they are quite close to each other so it is reasonable to assume that they are within experimental error.

The effect of nitroxide concentration in solution on the inhibition time was then observed in a dilatometry experiment. Solutions of *p*-substituted hydroxylamines ( $1.9 \times 10^{-3}$  M) with 2,5-DTBBQ ( $9 \times 10^{-4}$  M) in styrene were analysed at 110 °C. Percentage of styrene conversion was plotted against the time (Figure 6.9).

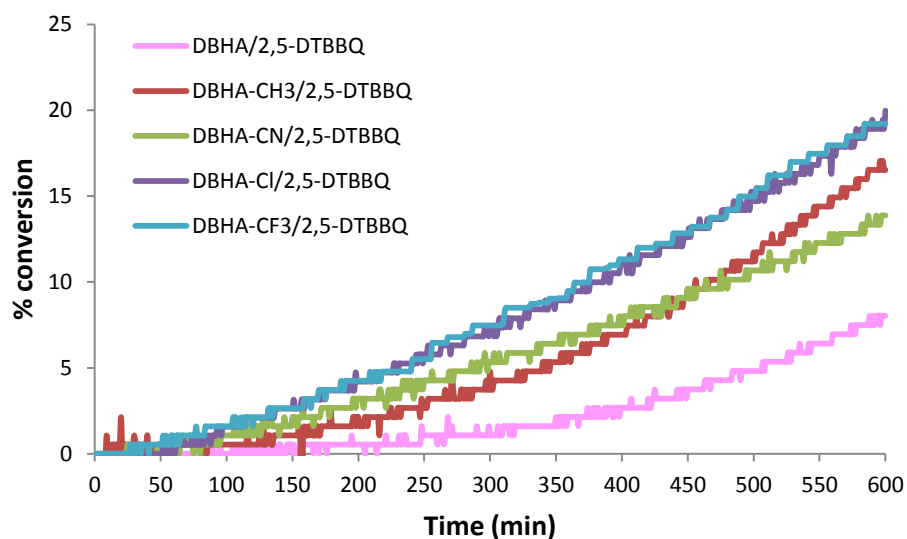
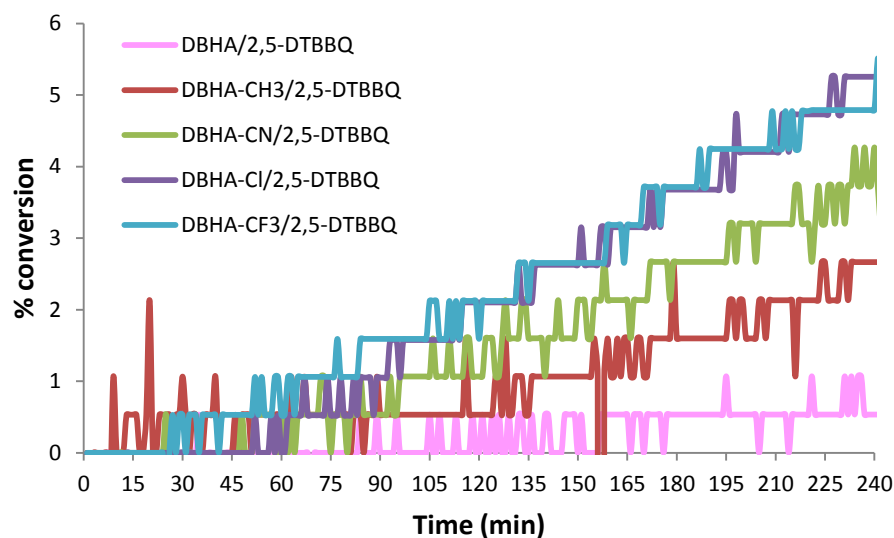


Figure 6.9 Dilatometry trace of *p*-substituted hydroxylamines and 2,5-DTBBQ mixture during the inhibition of styrene polymerisation at 110 °C



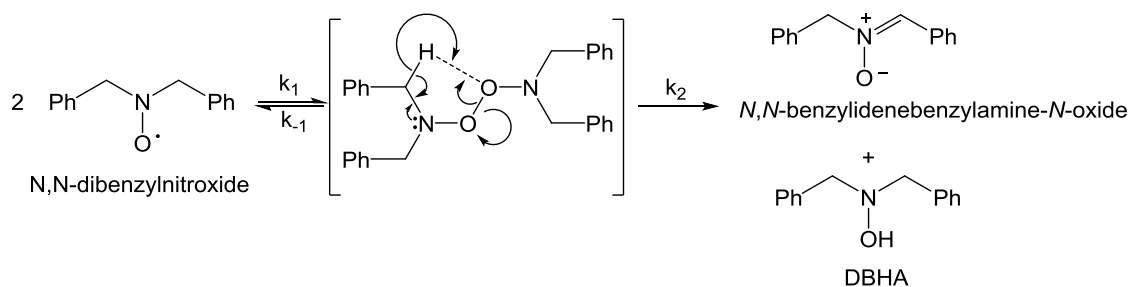
**Figure 6.10 Enlargement of Figure 6.9**

Figure 6.9 and 6.10 show that the DBHA/2,5-DTBBQ mixture possesses the best inhibition profile, followed by the mixture containing DBHA-CH<sub>3</sub>, DBHA-CN, DBHA-Cl and DBHA-CF<sub>3</sub>. The trend matches that of the nitroxide concentrations in Fig. 6.8, e.g., the higher nitroxide concentration corresponds to a longer inhibition time.

This experiment proved that the inhibition time is correlated with the concentration of nitroxide in solution. In the next paragraph, the effect of more hindered hydroxylamine is be evaluated.

### 6.4.3 Steric effect of substituents in dibenzylhydroxylamines

Nitroxides bearing at least one H atom on the carbon  $\alpha$  to the nitrogen are not stable (they have a finite life-time) and disproportionate to the corresponding nitron and hydroxylamine. The mechanism of decomposition has been a matter of debate and two possible pathways were suggested by Ingold and Nilsen. In the mechanism proposed by Ingold<sup>5</sup>, two nitroxide molecules reversibly dimerize forming an O-O  $\sigma$  bond, and then the intermediate is converted to products by the concerted hydrogen atom transfer, as shown in Figure 6.11.



**Figure 6.11 Mechanism proposed by Ingold and co-workers for the *N,N*-dibenzyl nitroxide decomposition**

On the other hand, even though Nilsen and co-workers agree on a two-step mechanism, they believe that the dimerization involves a head to tail dipolar interaction, which is then followed by a single electron transfer (Figure 6.12)<sup>50</sup>.

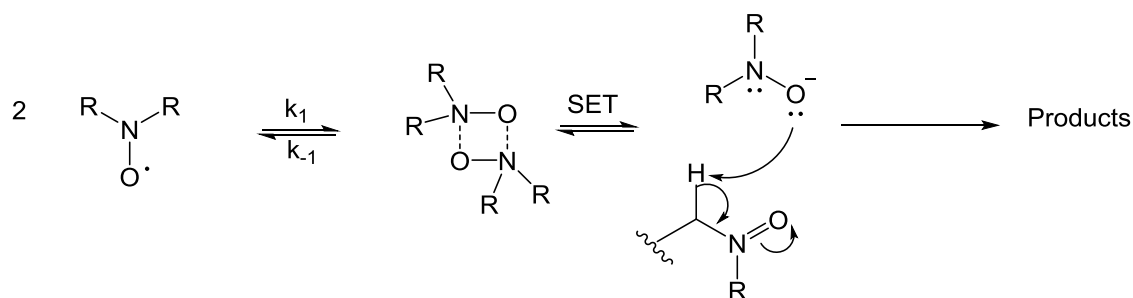


**Figure 6.12 Mechanism proposed by Nilsen and co-workers for nitroxide decomposition**

The key step in both mechanisms is the dimerization, which is dependent on the size of the substituents. Therefore, sterically demanding substituents will tend to hamper the dimer formation consequently slowing down the rate of nitroxide decomposition, and increasing nitroxide stability. For example, dimethyl nitroxide decomposes 3900 times faster than diisopropyl nitroxide<sup>50</sup>.

A series of hydroxylamines with different substituents was thus synthesised (Figure 6.13) aiming to generate nitroxides with different stability. By doing so, we were able to change transient nitroxide concentration in solution and hence monitor its effect on the inhibition time. Detailed synthetic procedures are reported in the experimental section.

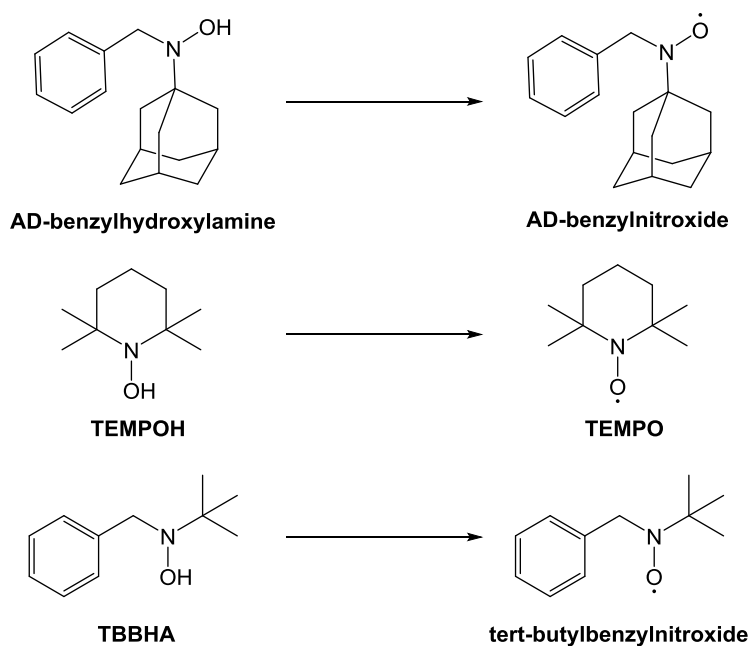


**Figure 6.13 Hydroxylamines synthesised and the corresponding nitroxides**

AD-benzylhydroxylamine, TEMPOH, TBBHA and DBHA ( $9.3 \times 10^{-3}$  M) were individually mixed with 2,5-DTBBQ ( $4.6 \times 10^{-3}$  M) and dissolved in styrene. Each solution was monitored by EPR spectroscopy at 110 °C. Absolute nitroxide concentration is plotted against the time (Figure 6.14).

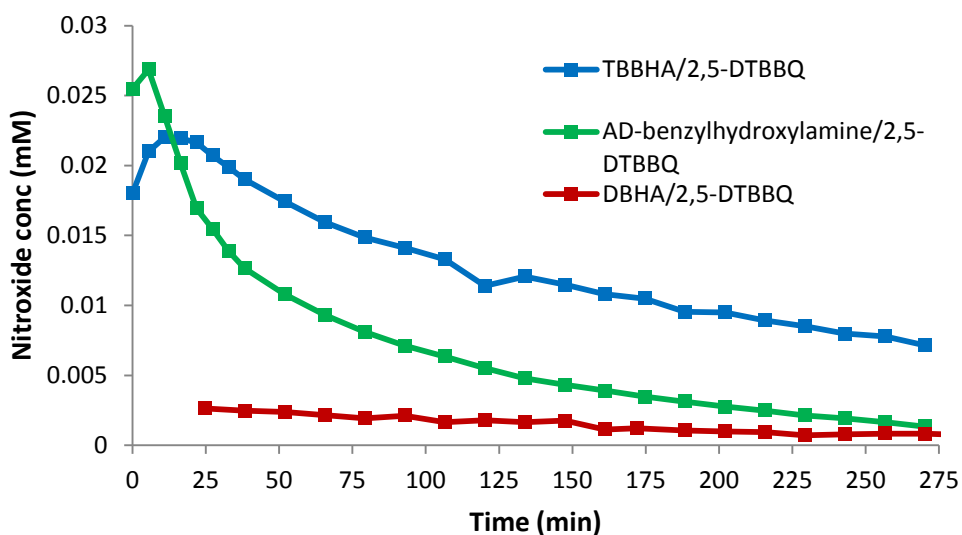


**Figure 6.14 Evolution of nitroxide concentration during the inhibition of styrene at 110 °C using hindered hydroxylamines/2,5-DTBBQ mixture**

Figure 6.14 shows that AD-benzylhydroxylamine and TBBHA produce significantly higher nitroxide concentration as compared to DBHA. AD-benzylnitroxide is less stable than *tert*-butylbenzylnitroxide; the concentration of the latter is relatively high even at long reaction times. Nitroxide generated by TEMPOH is not included in the graph as the concentration is much higher than for the other nitroxides. TEMPOH produces a nitroxide concentration of approximately  $1.8 \times 10^{-3}$  M.

Samples for dilatometry analysis were prepared by dissolving AD-benzylhydroxylamine, TBBHA, TEMPOH and DBHA ( $1.9 \times 10^{-3}$  M) in styrene containing 2,5-DTBBQ ( $9 \times 10^{-4}$  M). The experiment was carried out at 110 °C. Percentage of styrene conversion is plotted against time (Figure 6.15).

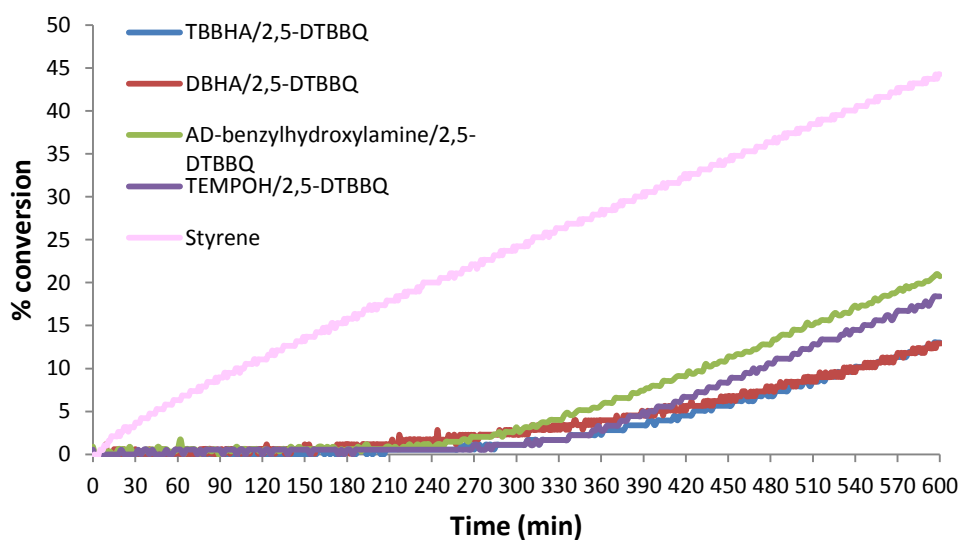
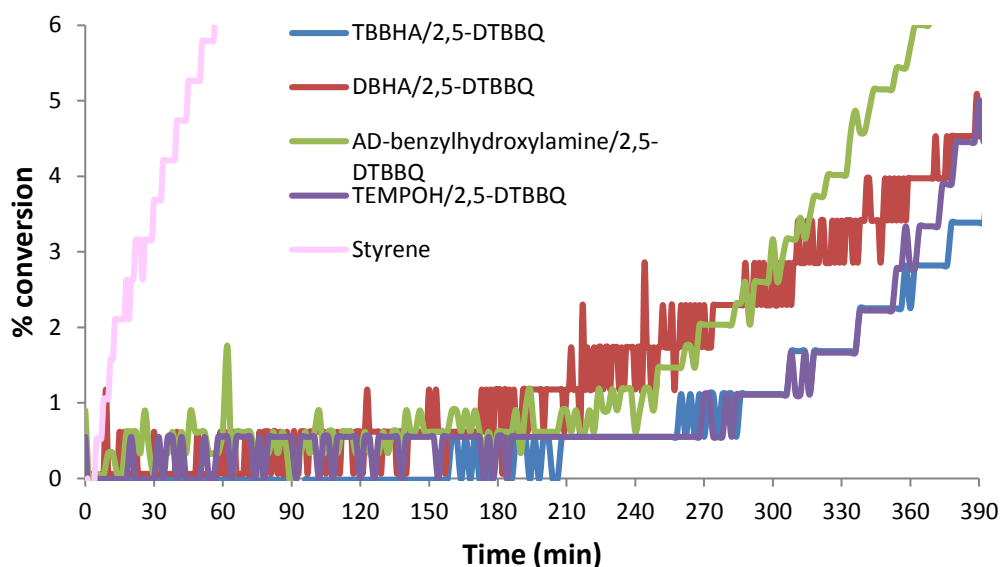


Figure 6.15 Dilatometry trace of hindered hydroxylamines/2,5-DTBBQ mixture during the inhibition of styrene polymerisation at 110 °C



**Figure 6.16 Enlargement of Figure 6.15**

Figure 6.16 shows that TEMPOH/2,5-DTBBQ and TBBHA/2,5-DTBBQ mixtures show longer inhibition times than AD-benzylhydroxylamine/2,5-DTBBQ and DBHA/2,5-DTBBQ mixtures. This is consistent with the EPR trend shown in Figure 6.14. Indeed, TEMPO and *tert*-butylbenzyl nitroxide are more stable than *N,N*-dibenzyl nitroxide and AD-benzyl nitroxide. Even though the dilatometry and EPR show similar trends, the effect of the more stable nitroxide on the inhibition of the correspondent hydroxylamine is quite restricted. For instance, there is a substantial difference in concentration between TEMPO and *N,N*-dibenzyl nitroxide, but this does not produce the same pronounced effect on the inhibition time as shown in Figure 6.16. The effect of increasing nitroxide concentration, however, may be cushioned by the slower rate of coupling between nitroxide and propagation chains<sup>137</sup>. Hence, even though more sterically hindered hydroxylamines produce higher concentration of nitroxide in solution during inhibition, this may not be very effective due to the steric hindrance of the substituents. On the other hand, styrene polymerisation at long reaction times proceeds unretarded in the presence of TEMPOH/2,5-DTBBQ and AD-hydroxylamine/2,5-DTBBQ. Comparison of data in Figure 6.15 and 6.14 shows that, in the case of AD-hydroxylamine, the inhibitor loses its efficacy after AD-nitroxide concentration reaches a sufficiently low concentration. Thus, TEMPO and AD-nitroxide



are good at inhibiting at short reaction times, but once they are consumed, the polymerization proceeds unchecked. TEMPO and AD-hydroxylamine react mainly by coupling reaction<sup>24</sup>. Therefore the mechanism of reaction involves the oxidation of the hydroxylamine either by 2,5-DTBBQ or molecular oxygen dissolved in solution leading to nitroxide (Equation 3). Nitroxide then stop propagation chains by coupling reaction (Equation 4). However, in the presence of oxygen they may also stop propagation chains by hydrogen abstraction (Equation 1 and 2) (Figure 6.17).

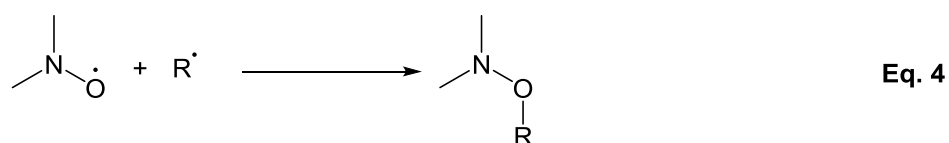
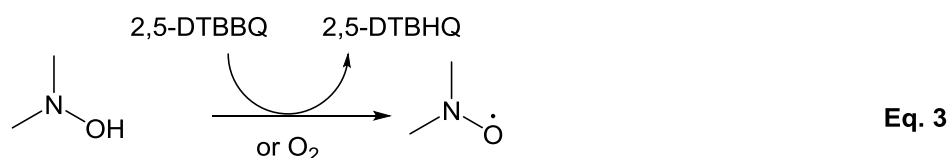
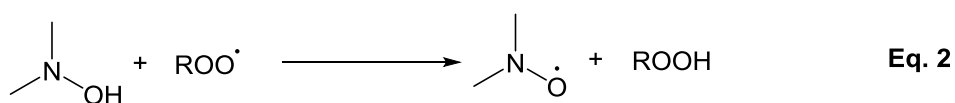
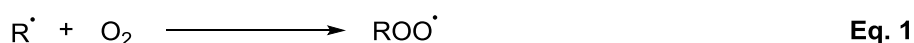


**Figure 6.17 Mechanism of inhibition of TEMPOH and AD-hydroxylamine**

On the contrary, DBHA and TBBHA are capable of retarding the polymerization for much longer.

Nitroxide seems to be involved in the inhibition mechanism, in particular the data suggest a correlation between inhibition time and nitroxide concentration. However, at longer time things become confusing. With TEMPOH and AD-hydroxylamine it appears that the absence of nitroxide in solution corresponds to an un-retarded polymerisation, and with TBBHA during retardation there is always a reasonable high concentration of nitroxide. However, for DBHA there is retardation even at extremely low nitroxide concentration. Therefore the above data do not allow us to establish if there is a correlation between nitroxide concentration and inhibition. Thus, we decided to change nitroxide concentration by simply changing reactants

concentrations. In this case we overcome the problem of different reactivity due to the steric hindrance of the substituents.

#### 6.4.4 Varying reactants concentration

The above results suggest that a change in nitroxide concentration affects the inhibition time. It is therefore possible that the nitroxide is the main inhibiting species in the DBHA/2,5-DTBBQ mixture. In order to test this hypothesis further, we investigated the inhibition of styrene polymerisation by using different DBHA/2,5-DTBBQ ratios.

In the first experiment, the concentration of DBHA in styrene was kept constant at 200 ppm, while the concentration of 2,5-DTBBQ was varied in the range 50 - 250 ppm. An EPR experiment was carried out in a sealed capillary tube at 110 °C for 5 h. Absolute nitroxide concentration was plotted against time (Figure 6.18).

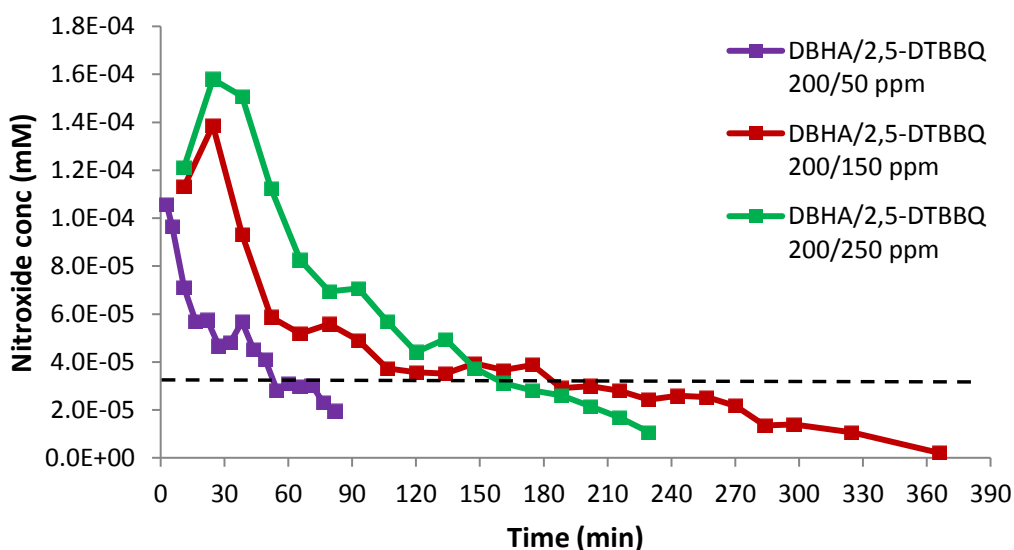
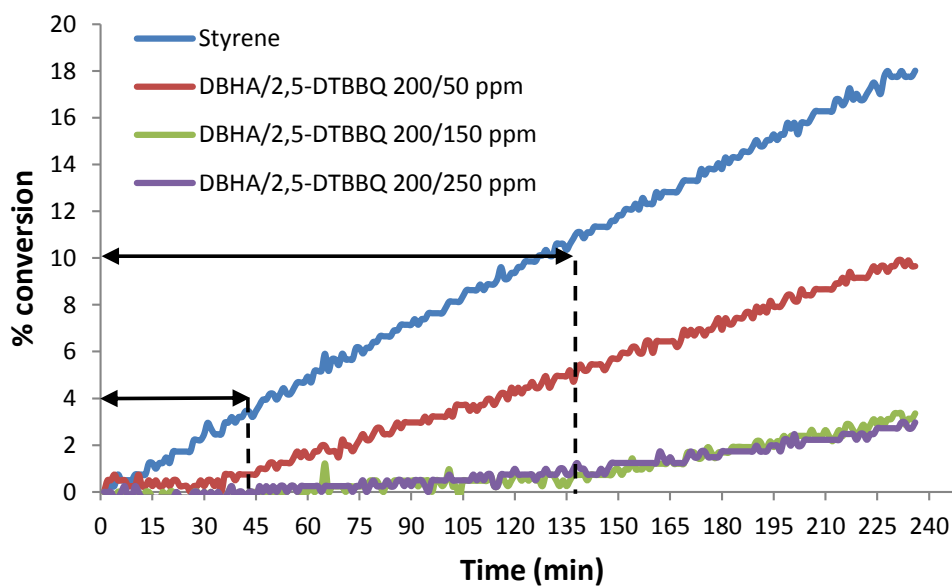


**Figure 6.18** Evolution of *N,N*-dibenzyl nitroxide concentration for a series of DBHA/2,5-DTBBQ ratios during the inhibition of styrene polymerisation at 110 °C

Figure 6.18 shows that the initial *N,N*-dibenzyl nitroxide concentration in solution increases with the increased 2,5-DTBBQ concentration. In addition, on increasing the concentration from 50 ppm to 150 ppm, *N,N*-dibenzyl nitroxide remains detectable in

solution for considerably longer time. This positive effect, however is not observed at 250 ppm, with the nitroxide consumed in 240 min.

The same solutions used for the EPR experiment were analysed by dilatometry at 110 °C (Figure 6.19).



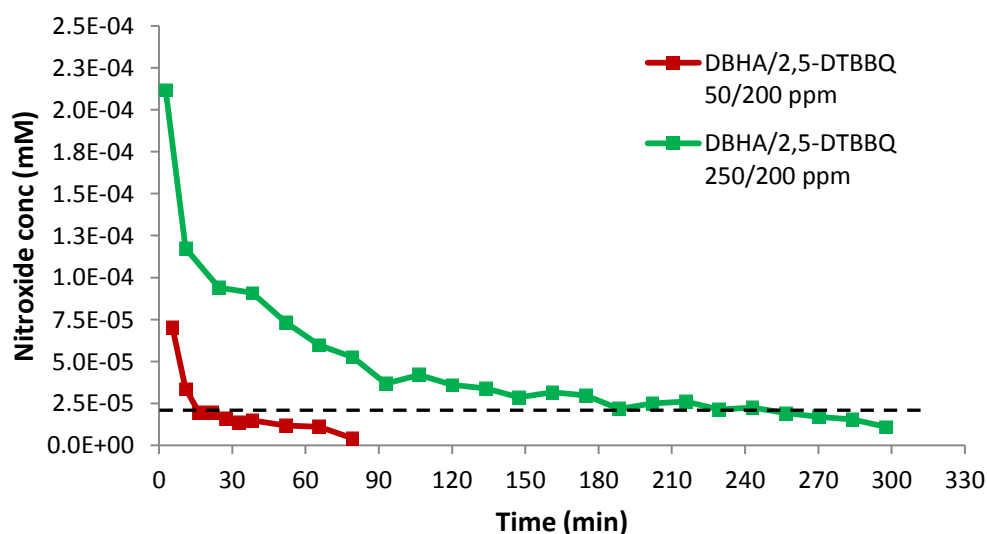
**Figure 6.19 Dilatometry traces for the inhibition of the auto-initiated styrene polymerisation in the presence of different DBHA/2,5-DTBBQ ratios**

Figure 6.19 shows that the mixture DBHA/2,5-DTBBQ produces two effects, inhibition and retardation, however, here we are focussing only on inhibition as it is known that nitroxides completely inhibit polymerisation<sup>138, 139</sup>, also we have seen in the previous experiment that nitroxide appears to affect inhibition time rather than retardation. So, increasing concentration of 2,5-DTBBQ from 50 to 150 ppm leads to longer inhibition time (inhibition time increases from  $40 \pm 6$  min to  $135 \pm 6$  min). However, further increase in 2,5-DTBBQ concentration does not affect the inhibition time.

If we assume that the inhibition is controlled by nitroxide concentration, then by comparing the figure 6.18 and 6.19, one can calculate the limiting concentration of nitroxide that can provide inhibition. This concentration can be assumed being approximately  $3 \times 10^{-5}$  M. In the case of DBHA/2,5-DTBBQ 200/50 ppm, nitroxide concentration drops below  $3 \times 10^{-5}$  M after about 40 min (Figure 6.18), and this time

corresponds approximately to the inhibition time (Figure 6.19). The same correlation can be observed for the other mixtures. However, this correlation is not valid for the retardation period, as the 200/150 ppm DBHA/2,5-DTBBQ mixture shows that *N,N*-dibenzyl nitroxide is consumed after 240 min (Figure 6.18), however a very good retardation is still observed at that time (Figure 6.19). This suggests that during retardation other species must be involved.

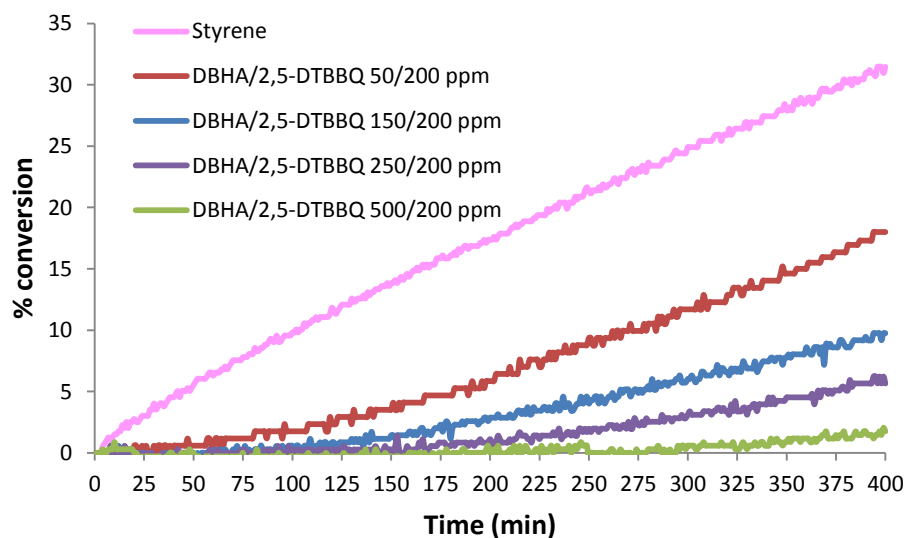
The fact that the nitroxide limiting concentration (about  $3 \times 10^{-5}$  M) seems to be consistent for different compositions, supports the hypothesis that the inhibition is controlled by the nitroxide. In the next experiments, the inhibition of styrene polymerisation was carried out with constant concentration of 2,5-DTBBQ (200 ppm), but varying concentration of DBHA (50-250 ppm) at 110 °C (Figure 6.20).



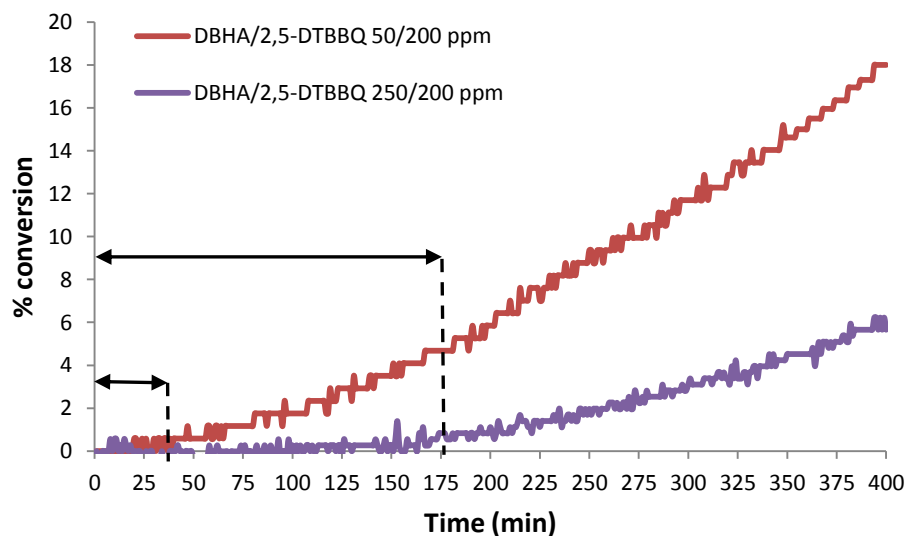
**Figure 6.20 Evolution of *N,N*-dibenzyl nitroxide concentration during the inhibition of styrene polymerisation in the presence of different ratios of DBHA/2,5-DTBBQ**

Figure 6.20 shows that increasing the DBHA concentration from 50 to 250 ppm leads to higher levels of *N,N*-dibenzyl nitroxide concentration in solution and therefore the nitroxide remains detectable in solution for a longer period of time.

A dilatometry analysis was also carried out for 50/200 ppm, 150/200 ppm, 250/200 ppm and 500/200 ppm ratios of DBHA/2,5-DTBBQ. Percentage of styrene conversion is plotted against the time in Figure 6.21 and 6.22.



**Figure 6.21** Dilatometry trace of the inhibition of styrene polymerisation using different concentrations of DBHA and constant 2,5-DTBBQ concentration.



**Figure 6.22** Dilatometry trace of DBHA/2,5-DTBBQ 50/200 ppm and 250/200 ppm, for the inhibition of the styrene polymerisation at 110 °C

Figure 6.21 shows that increasing DBHA concentration leads to a significant increase in the inhibition efficiency of the mixture. The induction times are  $28 \pm 6$  min,  $105 \pm 6$  min,  $175 \pm 6$  min and  $325 \pm 6$  min for 50 ppm, 150 ppm, 250 ppm and 500 ppm of DBHA, respectively. In addition, comparison of Figure 6.19 and 6.21 shows that the most efficient inhibition is observed in mixtures containing excess of DBHA with respect to 2,5-DTBBQ.

We assume, as before, that nitroxide determines inhibition time, and by comparing Figure 6.20 and Figure 6.22, we estimate that the limiting concentration at which nitroxide provides inhibition is approximately  $3 \times 10^{-5}$  M. DBHA/2,5-DTBBQ 50/200 ppm mixture shows inhibition time of about 28 min (Figure 6.22), and this time corresponds to that necessary for nitroxide to decay at a concentration below  $3 \times 10^{-5}$  M (Figure 6.20). Similarly, DBHA/2,5-DTBBQ 250/200 ppm inhibits polymerisation for 175 min and nitroxide drops below the limiting concentration at approximately the same time. These data confirm that the limiting concentration is approximately  $3 \times 10^{-5}$  mM, and support the idea that the inhibition time is correlated with the concentration of nitroxide in solution. On the other hand, by comparing Figure 6.20 and 6.21 we observe no correlation between retardation and nitroxide concentration. For example, EPR data for the 250/200 ppm DBHA/2,5-DTBBQ mixture show that nitroxide concentration drops below the detection limit at 300 min (Figure 6.20), but the DBHA/2,5-DTBBQ mixture is still capable of retarding polymerisation (Figure 6.21).

To summarise, there is a correlation between the nitroxide concentration in solution and the inhibition efficiency of the mixture, hence nitroxide may be responsible for the inhibition but not for retardation. Isolation of alkoxyamine (section 5.3.1) proves that *N,N*-dibenzyl nitroxide can trap propagation chains at least to some extent. Therefore, it supports the hypothesis that *N,N*-dibenzyl nitroxide is capable of controlling the polymerisation. However, other potential inhibitors are tested in the next section.

## 6.5 Other potential inhibitors of styrene polymerisation

A screening of the inhibition properties of the compounds formed during the inhibition was carried out. In the cases where a reaction between two compounds could form a new potential inhibitor, their mixture was tested too.

### 6.5.1 *N,N*-Benzylidenebenzylamine-*N*-oxide

Nitrones are well known to act as spin traps<sup>140</sup>, but they may also give dipolar cycloaddition with 2,5-DTBBQ leading to benzisoxazolidine (**1**). Benzisoxazolidine is a

cyclic alkoxyamine with a weak C-O bond, which at high temperature may break regenerating a nitroxide and a carbon centred radical (Figure 6.23).

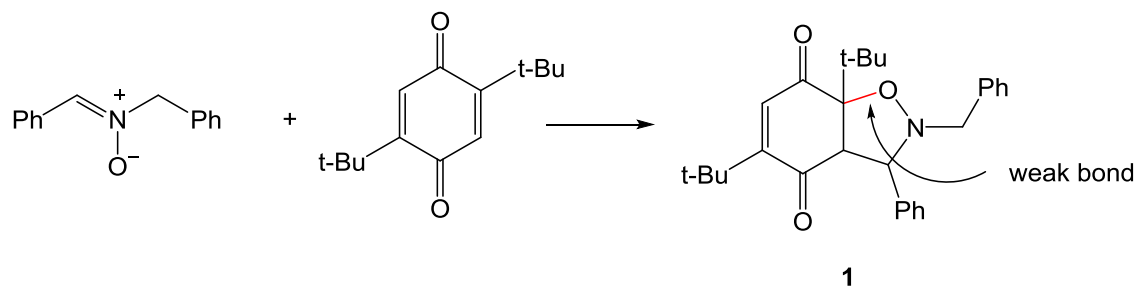


**Figure 6.23 Benzisoxazolidine formation**

Two solutions were prepared, a mixture of *N,N*-benzylidenebenzylamine-*N*-oxide ( $1.9 \times 10^{-3}$  M) with 2,5-DTBBQ ( $9 \times 10^{-4}$  M) and *N,N*-benzylidenebenzylamine-*N*-oxide ( $9.3 \times 10^{-4}$  M) in styrene. The two samples were then analysed at 110 °C by dilatometry (Figure 6.24).

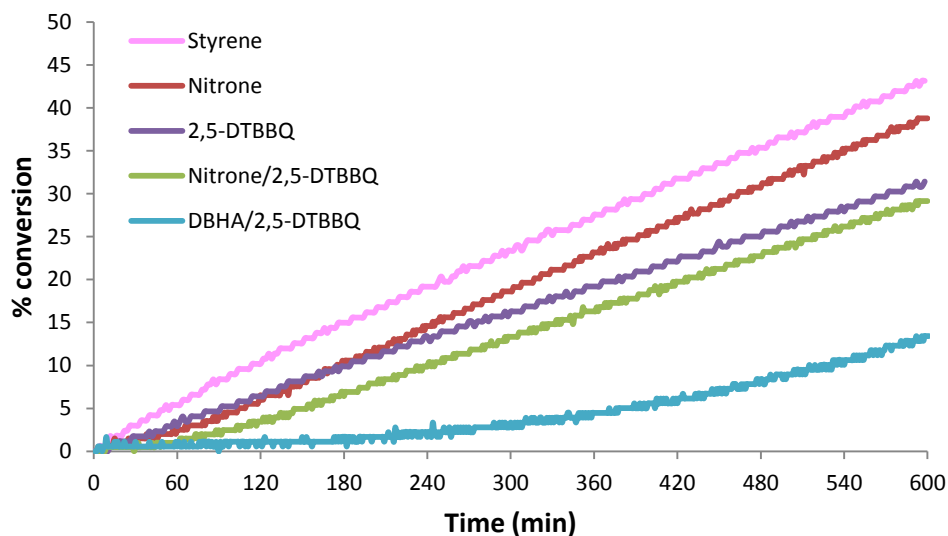


**Figure 6.24 Dilatometry trace for the inhibition of the styrene polymerisation at 110 °C by *N,N*-benzylidenebenzylamine-*N*-oxide/2,5-DTBBQ mixture and *N,N*-benzylidenebenzylamine-*N*-oxide.**

Figure 6.24 shows the inhibition/retardation profile of *N,N*-benzylidenebenzylamine-*N*-oxide (red line) and of the *N,N*-benzylidenebenzylamine-*N*-oxide/2,5-DTBBQ mixture (green line). These data were compared to 2,5-DTBBQ ( $9.3 \times 10^{-4}$  M) and DBHA/2,5-DTBBQ ( $[DBHA] = 1.9 \times 10^{-3}$  M and  $[2,5-DTBBQ] = 9 \times 10^{-4}$  M) in styrene. It is evident that

neither *N,N*-benzylidenebenzylamine-*N*-oxide nor its mixture with 2,5-DTBBQ can compete with DBHA/2,5-DTBBQ, however, they both retard the polymerisation at least to some extent. In addition, the *N,N*-benzylidenebenzylamine-*N*-oxide/2,5-DTBBQ mixture shows a better profile than the single components, however it is unlikely that there is synergism between *N,N*-benzylidenebenzylamine-*N*-oxide and 2,5-DTBBQ. The *N,N*-benzylidenebenzylamine-*N*-oxide/2,5-DTBBQ profile is probably due by the additive effect of the single components. However, this effect seems too small to contribute to the overall inhibition.

Dilatometry results showed that neither *N,N*-benzylidenebenzylamine-*N*-oxide nor *N,N*-benzylidenebenzylamine-*N*-oxide/2,5-DTBBQ mixture are likely to be responsible for the synergism between DBHA and 2,5-DTBBQ. However, the product analysis revealed that *N,N*-benzylidenebenzylamine-*N*-oxide is converted into other products, which are tested in the next section.

## 6.5.2 Isoxazolidine and isoxazoline

We have learnt from chapter 5 that *N,N*-benzylidenebenzylamine-*N*-oxide reacts with styrene to give isoxazolidine (**2**) (section 5.2.1). These compounds have a weak C-O bond, which may lead to some inhibition properties, thus they were analysed by dilatometry. In addition, isoxazolidines may be oxidized to isoxazoline (**3**)<sup>141</sup>, which could also act as inhibitors as it retains the weak C-O bond (Figure 6.25). Even though isoxazoline was not detected in the reaction mixtures, a mixture of isoxazolidine and 2,5-DTBBQ was tested to probe this hypothesis.

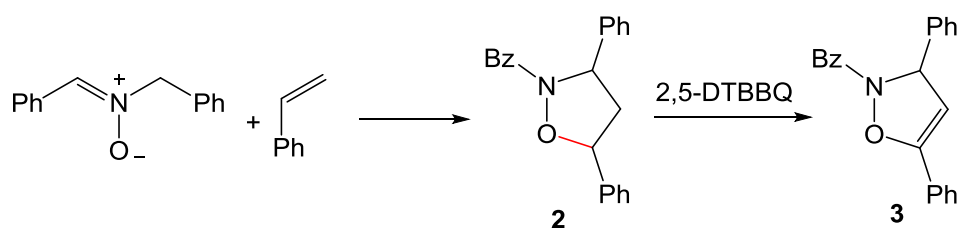


**Figure 6.25** Isoxazolidine and isoxazoline formation

Isoxazolidine (**2**) was synthesised by heating *N,N*-benzylidenebenzylamine-*N*-oxide with styrene, as reported in the experimental section.



A dilatometry experiment was carried out at 110 °C for a solution of isoxazolidine ( $1.9 \times 10^{-3}$  M) in neat styrene and for a mixture of isoxazolidine ( $1.9 \times 10^{-3}$  M) with 2,5-DTBBQ ( $9 \times 10^{-4}$  M). Dilatometry trace is reported in Figure 6.26.

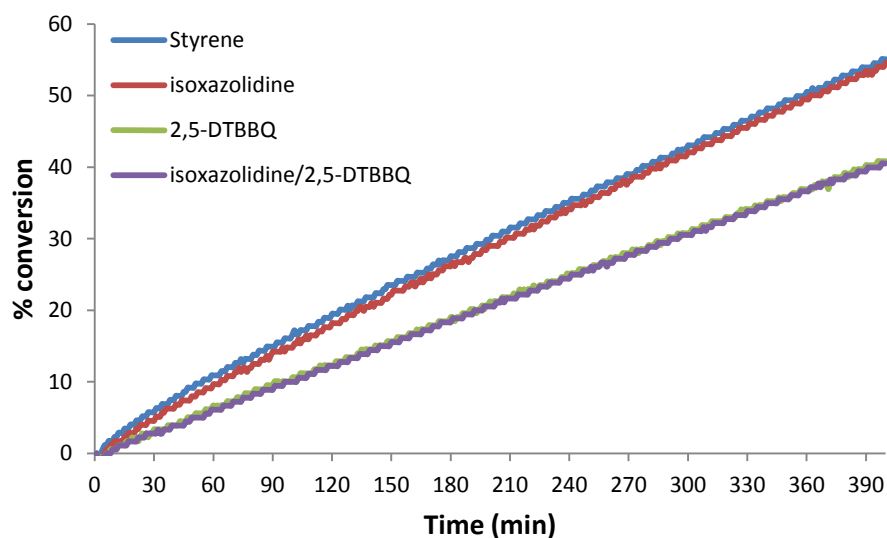


**Figure 6.26 Dilatometry trace for the inhibition of the styrene polymerisation at 110 °C by isoxazolidine and isoxazolidine/2,5-DTBBQ mixture.**

Figure 6.26 shows that the isoxazolidines (red line) do not have any effect on the inhibition of styrene polymerisation, and the dilatometry trace is identical to that of neat styrene (blue line). Similarly, if any isoxazoline (**3**) is formed in the mixture isoxazolidine/2,5-DTBBQ, it is not able to interact with the propagation chains, as the inhibition properties of the mixture are identical to those of 2,5-DTBBQ.

The conclusion from the above experiments is that neither the isoxazolidine nor the isoxazoline play a role in the inhibition of styrene polymerisation. In the next section, a dilatometry experiment is carried out on the mixture of *N,N*-benzylidenebenzylamine-*N*-oxide and 2,5-di-*tert*-butyl-hydroquinone (2,5-DTBHQ).

### 6.5.3 Mixture of *N,N*-benzylidenebenzylamine-*N*-oxide and 2,5-DTBHQ

The GC study of the inhibition of styrene polymerisation by the DBHA/2,5-DTBBQ mixture (Figure 6.3) revealed that most of 2,5-DTBBQ is quickly converted to 2,5-

DTBHQ, while some DBHA is converted to *N,N*-benzylidenebenzylamine-*N*-oxide. Even though there are no data related to the use of nitrono-hydroquinone compositions as polymerisation inhibitor, it was worth investigating the inhibition property of the mixture, which could be responsible for the synergism between DBHA/2,5-DTBBQ.

A solution of *N,N*-benzylidenebenzylamine-*N*-oxide ( $1.9 \times 10^{-3}$  M) and 2,5-DTBHQ ( $9 \times 10^{-4}$  M) in styrene was analysed at 110 °C. In addition, 2,5-DTBHQ ( $9 \times 10^{-4}$  M), *N,N*-benzylidenebenzylamine-*N*-oxide ( $1.9 \times 10^{-3}$  M), DBHA/2,5-DTBBQ (DBHA  $1.9 \times 10^{-3}$  M and 2,5-DTBBQ  $9 \times 10^{-4}$  M) and neat styrene were monitored as a reference (Figure 6.27).

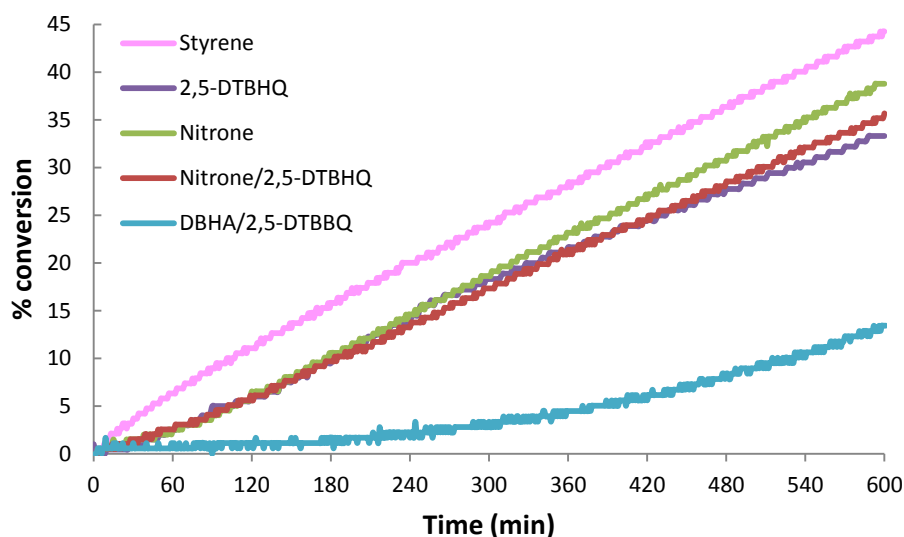


**Figure 6.27** Dilatometry trace for the inhibition of the styrene polymerisation at 110 °C by *N,N*-benzylidenebenzylamine-*N*-oxide and *N,N*-benzylidenebenzylamine-*N*-oxide/2,5-DTBHQ mixture.

Figure 6.27 shows that *N,N*-benzylidenebenzylamine-*N*-oxide/2,5-DTBHQ mixture (red line) acts as a weak retarder of the styrene polymerisation. However, the mixture has a similar retardation profile to that of single components (green line and purple line). Hence, the mixture does not show any synergism, and in addition its inhibition properties are far less effective than those of the DBHA/2,5-DTBBQ mixture (light blue line).

A series of dilatometry experiments were carried out using the products (or their mixture) identified during the inhibition of styrene polymerisation in the presence of DBHA/2,5-DTBBQ. Those experiments help to rule out some possible reactions that may be involved in the inhibition mechanism. A discussion of the mechanism is detailed in the next section.

## 6.6 Mechanism of inhibition

This section aims to provide a plausible explanation of the synergism shown by the DBHA/2,5-DTBBQ mixture towards in the inhibition of the auto-initiated styrene polymerization. Since a complex set of reactions occurs during the inhibition, to simplify the discussion this section is divided into two main sections. Initially, the overall set of reactions that takes place during the inhibition is described. The second part is focussed on the inhibition properties of each component present in the mixture, so that the role of certain molecules in the synergism can be ruled out or confirmed.

### Overall reaction mechanism

A combination of experiments (e.g., products analysis) and analytical techniques allowed us to identify products and intermediates formed during the inhibition, and also to establish which reactions occur during the inhibition. In Figure 6.28 the overall reaction mechanism is described.

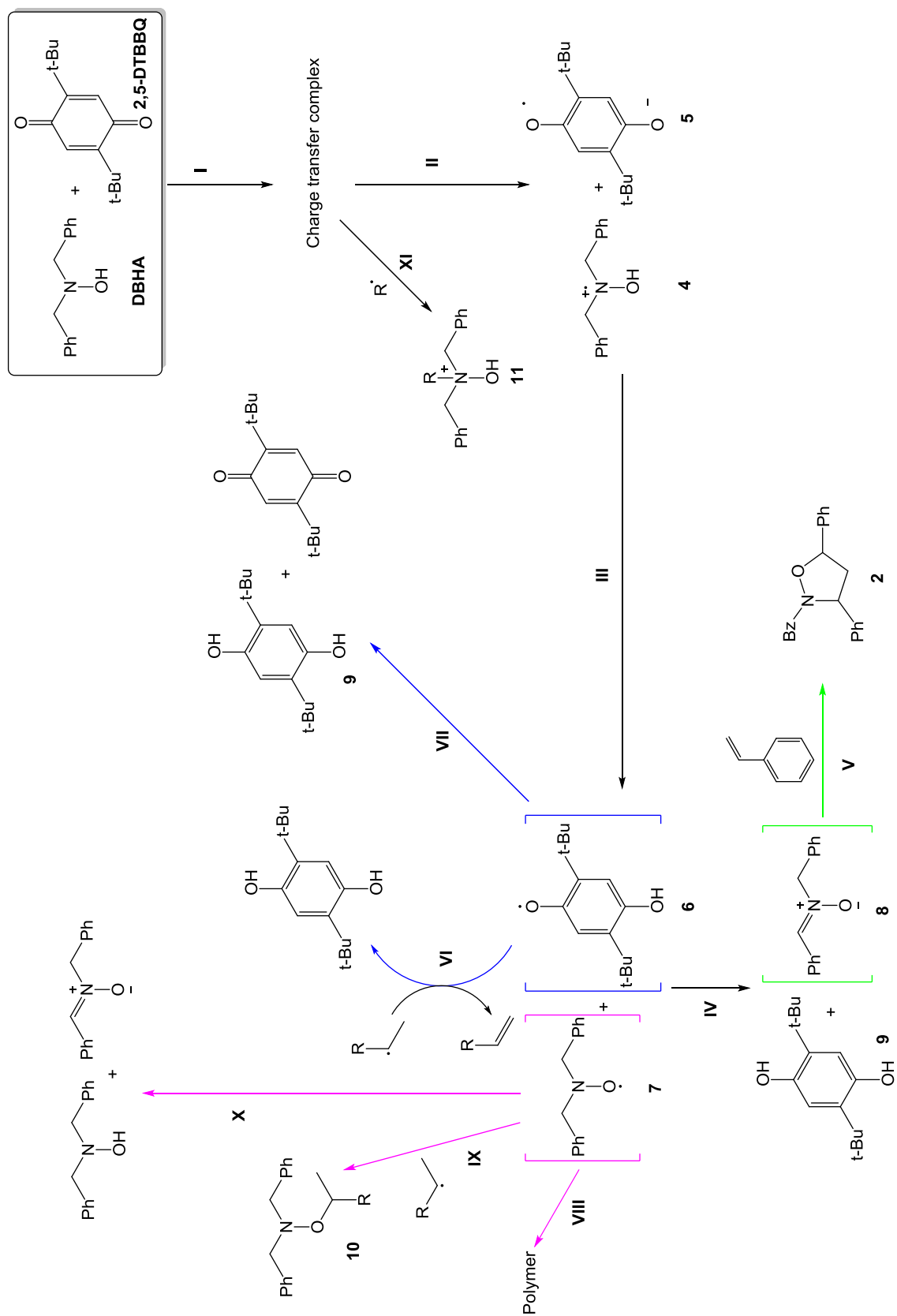


Figure 6.28 Overall mechanism of reaction

The 2,5-DTBBQ/DBHA mixture in styrene at 110 °C is rapidly converted to several products. The detection of 2,5-DTBHQ (**9**) and *N,N*-benzylidenebenzylamine-*N*-oxide (**8**) in the reaction mixture shows that DBHA is oxidized while 2,5-DTBBQ is reduced. The electronic spectrum of a solution of DBHA and 2,5-DTBBQ in toluene showed a band characteristic of a charge transfer complex, therefore it is likely that during the polymerization the charge transfer complex is also formed (**I**). The charge transfer complex then breaks down into radicals ion (**4**) and (**5**) (**II**), which undergo proton transfer to generate *N,N*-dibenzyl nitroxide (**7**) and semiquinone (**6**) (**III**). The radicals (**7**) can be further oxidized to *N,N*-benzylidenebenzylamine-*N*-oxide (**8**), while semiquinone (**6**) is reduced to 2,5-DTBHQ (**9**).

*N,N*-Benzylidenebenzylamine-*N*-oxide (**8**) reacts quantitatively with styrene via 1,3-dipolar cycloaddition leading to a mixture of *cis* and *trans* isoxazolidine (**2**) (**V**). Indeed, isoxazolidine (**2**) was isolated from the reaction mixture during the inhibition of styrene with DBHA/2,5-DTBBQ. In addition, the complete conversion of *N,N*-benzylidenebenzylamine-*N*-oxide to isoxazolidine (**2**) was confirmed by reacting *N,N*-benzylidenebenzylamine-*N*-oxide in styrene; the reaction goes to completion leading to isoxazolidine (**2**) as the only product.

*N,N*-Dibenzyl nitroxide (**7**) can undergo several reactions. Isolation of the alkoxyamine (**10**) during the inhibition demonstrates that *N,N*-dibenzyl nitroxide is capable of trapping styrene radicals (**IX**). In addition, it is likely that *N,N*-dibenzyl nitroxide also traps longer propagation chains (**VIII**), as the elemental analysis of the polymer indicated high nitrogen content. However this needs to be confirmed, since we do not have full characterization of the polymer structure. In addition, as we learnt from chapter 2, nitroxide (**7**) disproportionates to *N,N*-benzylidenebenzylamine-*N*-oxide and DBHA (**X**).

Even though semiquinone (**6**) was not detected, it must be formed during the mechanism. Indeed, dissociation of the charge transfer complex formed during the inhibition, leads to (**4**) and (**5**) (**II**) and (**III**), and since we were able to detect nitroxide (**7**), semiquinone (**6**) also has to be formed. However, due to the high instability of

semiquinone (**6**), its concentration in solution is always below the detection limit. It is likely that the main reaction of semiquinone is the disproportionation to 2,5-DTBBQ and 2,5-DTBHQ (**9**)<sup>77</sup> (**VII**). Semiquinone could also abstract a hydrogen atom from a styrene radical leading to an alkene and 2,5-DTBHQ (**VI**). The addition reactions of semiquinone (**9**) to carbon centred radicals was excluded, as addition products were not found in the reaction mixture of styrene with either 2,5-DTBBQ or 2,5-DTBHQ (chapter 3). Therefore, disproportionation of semiquinone to 2,5-DTBBQ and 2,5-DTBHQ seems to be the main pathway.

### **Synergism in the DBHA/2,5-DTBBQ mixture**

The previous section described the reactions occurring during the inhibition. In this section, the most plausible explanation for the synergism between DBHA and 2,5-DTBBQ will be discussed.

The first possibility that can be ruled out is that DBHA and 2,5-DTBBQ are good inhibitors, and that the synergism was caused by the regeneration of these two components, which keep polymerization under control for a long time. Dilatometry experiments confirmed that 2,5-DTBBQ is only a retarder which becomes effective only at high concentration. On the other hand, DBHA is a good inhibitor only in oxygenated conditions, but we know that the efficiency of DBHA/2,5-DTBBQ is oxygen independent. However a comparison of DBHA concentration during the oxidation with 2,5-DTBBQ in styrene and in toluene, suggests that DBHA is regenerated during the inhibition, therefore it is likely that DBHA formation is correlated with regeneration of other components in the mixture that can give synergism (e.g., *N,N*-dibenzyl nitroxide, charge transfer complex).

The reaction between 2,5-DTBBQ and DBHA leads to *N,N*-benzylidenebenzylamine-*N*-oxide and 2,5-DTBHQ, and the efficiency of a mixture of these two compounds was tested by dilatometry. The *N,N*-benzylidenebenzylamine-*N*-oxide/2,5-DTBHQ mixture is not capable of inhibiting the polymerization, and only a limited retardation of the polymerization is observed (Section 6.5.3). This result rules out the formation of the *N,N*-benzylidenebenzylamine-*N*-oxide/2,5-DTBHQ as the reason for the synergism.

As mentioned earlier, *N,N*-benzylidenebenzylamine-*N*-oxide reacts with styrene via 1,3-dipolar cycloaddition leading to isoxazolidine (**2**) (Figure 6.25). Isoxazolidine is a cyclic alkoxyamine with a labile C-O bond; the breaking of this bond generates a nitroxide<sup>141</sup>. The inhibition efficiency of isoxazolidine was investigated, but it did not affect the rate of polymerization (Figure 6.26). Hence, isoxazolidine is not involved in the inhibition. Isoxazolidine was also tested in a mixture with 2,5-DTBBQ, as it can oxidize isoxazolidine to isoxazoline, which could also act as an inhibitor. However, 2,5-DTBBQ/isoxazolidine mixture showed no inhibition.

Previous reports confirmed<sup>112</sup> the feasibility of the reaction between *N,N*-benzylidenebenzylamine-*N*-oxide and 2,5-DTBBQ, which leads to benzisoxazolidine (**1**) (Section 6.5.1). Benzisoxazolidine is a cyclic alkoxyamine with a weak C-O bond, hence, could be a good inhibitor. Therefore, it was not unreasonable to suggest that the *N,N*-benzylidenebenzylamine-*N*-oxide/2,5-DTBBQ mixture could be responsible for the synergism as it yields benzisoxazolidine. However, the mixture does not show a good inhibition profile suggesting that even if isoxazoline is formed, it does not stop the polymerisation.

The role of *N,N*-dibenzyl nitroxide has been thoroughly investigated (Section 6.4). The presence of the alkoxyamine (**10**) in the reaction mixture shows that *N,N*-dibenzyl nitroxide is able to trap propagation radicals to some extent. In addition, a combination of dilatometry and EPR experiments revealed that there is a correlation between *N,N*-dibenzyl nitroxide concentration in solution and the inhibition time. Indeed, we observed that only mixtures containing at least  $3 \times 10^{-5}$  M *N,N*-dibenzyl nitroxide show inhibition. It is likely that *N,N*-dibenzyl nitroxide traps propagation chains by a coupling reaction, but its interaction with 2,5-DTBBQ cannot be excluded, as it is known that nitroxides form charge transfer complexes with benzoquinones<sup>142</sup>. Since in a charge transfer complex there is a partial donation of one electron from the donor to the acceptor due to orbital overlapping, there is a formation of a localized charge that may enhance the reactivity of *N,N*-dibenzyl nitroxide towards styrene radicals, resulting in long inhibition times.

Our results suggest that *N,N*-dibenzyl nitroxide can only be responsible for the inhibition but not retardation process. Indeed, DBHA/2,5-DTBBQ mixture still shows good retardation at *N,N*-dibenzyl nitroxide concentrations below the detection limit (Figure 6.18, Figure 6.19, Figure 6.20 and Figure 6.22). One possibility could be that at concentrations below  $3 \times 10^{-5}$  M (minimum concentration of *N,N*-dibenzyl nitroxide at which inhibition was observed) *N,N*-dibenzyl nitroxide can only trap some propagating chains thus leading to the retardation of the polymerisation. However, this hypothesis seems unlikely as our studies on the inhibition mechanism of DBHA (chapter 2) revealed that for *N,N*-dibenzyl nitroxide concentrations below  $3 \times 10^{-5}$  M, the polymerization proceeds unretarded. Therefore, our conclusion is that *N,N*-dibenzyl nitroxide is only involved in the inhibition process, but not in the retardation.

As mentioned earlier in this section, DBHA and 2,5-DTBBQ form a charge transfer complex. It is not easy to test the inhibition properties of the charge transfer complex, as in our case it is not stable enough to be isolated. However, a paper published by Yassin demonstrates<sup>97</sup> that a charge transfer complex can be an inhibitor for the styrene polymerization. They observed that the charge transfer complex formed from the interaction between *N,N*-dimethylaniline and chloranil enhances the ability of *N,N*-dimethylaniline to trap propagation chains (Figure 6.29).

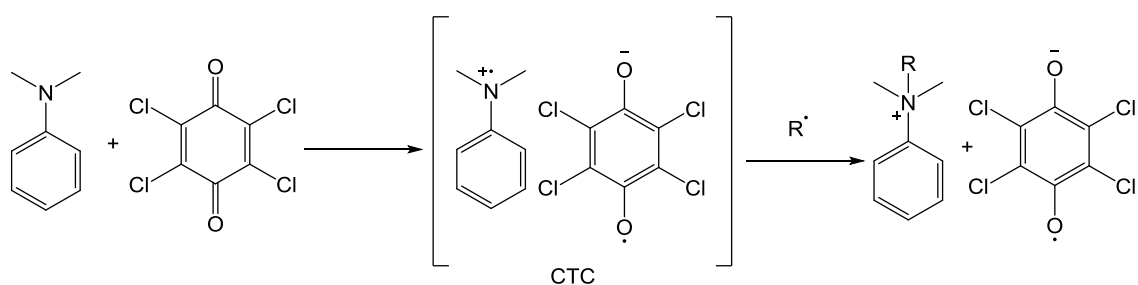


**Figure 6.29** Inhibition of styrene polymerization by *N,N*-dimethylaniline/chloranil charge transfer complex

The orbital overlap between an electron donor and an electron acceptor in the charge transfer complex results in electron-rich *N,N*-dimethylaniline partially donating an electron to the electron poor chloranil. This interaction creates localized charges in the complex that favours the addition of propagation radicals to the nitrogen atom of *N,N*-



dimethylaniline (Figure 6.29). Similarly to the *N,N*-dimethylaniline/benzoquinone system, the formation of the charge transfer complex between DBHA and 2,5-DTBBQ may enhance the reactivity of DBHA with carbon centred radicals (Figure 6.28, **XI**). In this case DBHA may interact with carbon centred radical via electron transfer, instead of by hydrogen abstraction. The efficiency of the reaction of carbon centred radicals to the nitrogen atom of DBHA would be oxygen independent; therefore the charge transfer complex will be inhibiting polymerisation even in deoxygenated conditions. It is reasonable to suggest that the DBHA/2,5-DTBBQ charge transfer complex may be responsible for both inhibition and retardation.

To summarize, the *N,N*-dibenzyl nitroxide is likely to be responsible for the inhibition of the auto-initiated styrene polymerization, while charge transfer may be involved in both inhibition and retardation.

## 6.7 Conclusions

DBHA/2,5-DTBBQ is a new inhibitor composition for the thermal styrene polymerisation. Dilatometry analysis revealed a pronounced synergism between these two compounds, thus an investigation was carried out to shed some light on the mechanism of action. This chapter was focused on exploring the inhibition properties of the products and intermediates detected during the inhibition process, in order to compare dilatometry traces of these components (or their mixture) with that of the DBHA/2,5-DTBBQ mixture. The general idea was to find the components that give an inhibition profile similar to that of DBHA/2,5-DTBBQ. We exclude that synergism is due to regeneration of 2,5-DTBBQ and DBHA, because 2,5-DTBBQ is only a retarder and DBHA works only in the presence of oxygen. Dilatometry traces exclude also, *N,N*-benzylidenebenzylamine-*N*-oxide, 2,5-DTBHQ and their mixture as responsible for the synergism. The 2,5-DTBBQ/ *N,N*-benzylidenebenzylamine-*N*-oxide mixture, benisoxazolidine and isoxazolidine have been ruled out as inhibitors. Our data suggests that *N,N*-dibenzyl nitroxide may be responsible for the synergism, as we observe inhibition only above a certain *N,N*-dibenzyl nitroxide concentration, but

charge transfer complex formed by the interaction of DBHA with 2,5-DTBBQ could also be responsible for both inhibition and retardation.

## 7 General conclusion and future work

A study of a new retarder composition of the auto-initiated styrene polymerisation was carried out. DBHA/2,5-DTBBQ mixture represents a non-toxic alternative to the commercial harmful retarders on the market. The mechanism of action of inhibition/retardation of DBHA/2,5-DTBBQ mixture was investigated. The mechanism of action is quite complex, therefore the inhibitors were first investigated individually and then together.

DBHA is a commercial antioxidant, however the information available in the literature about its mechanism of action is rather limited, and lacks in kinetic data. A dilatometry study reveals that DBHA works only in the presence of oxygen. Hence, the main mechanism of inhibition is the quenching of peroxy radicals at the end of the propagating chains by hydrogen abstraction from DBHA. On the contrary, in the absence of oxygen, the hydrogen abstraction from DBHA by carbon-centred radicals is quite inefficient, therefore the polymerisation proceeds unchecked. EPR analysis revealed the formation of *N,N*-dibenzyl nitroxide in oxygenated conditions. By monitoring nitroxide formation in styrene and in a non-polymerizable solvent, we established that most of the nitroxide is generated by the oxidation of DBHA by molecular oxygen. The role of the nitroxide as a radical trap was investigated as no information was available in the literature. The conclusion is that *N,N*-dibenzyl nitroxide contributes to some extent to the inhibition as a radical trap. This was proven by the isolation of an alkoxyamine formed by the coupling between *N,N*-dibenzyl nitroxide and styrene radical. In addition, a kinetic study of the stability of nitroxide was carried out and we established that *N,N*-dibenzyl nitroxide is approximately 900 times more stable than what was reported in previous experiments.

Analysis of the styrene polymerisation in the presence of the 2,5-DTBBQ/DBHA mixture showed that 2,5-DTBBQ is reduced to 2,5-DTBHQ. We investigated the ability of 2,5-DTBBQ and 2,5-DTBHQ to stop propagation chains by addition reaction. This was ruled out as we could not detect any addition products. The rather limited

retardation of styrene polymerization by 2,5-DTBBQ/2,5-DTBHQ was attributed to the ability of the couple to interact with propagation chains by redox reactions or hydrogen abstraction. It is likely that the contribute of 2,5-DTBBQ/2,5-DTBHQ mixture during the inhibition of styrene polymerization with DBHA/2,5-DTBBQ is quite limited.

In order to shed some light on the mechanism of action of DBHA/2,5-DTBBQ mixture, product analysis was carried out in a non-polymerizable solvent, which confirmed that DBHA and 2,5-DTBBQ are converted to 2,5-DTBHQ and *N,N*-benzylidenebenzylamine-*N*-oxide. 2,5-DTBHQ and *N,N*-benzylidenebenzylamine-*N*-oxide do not show good inhibition either in a mixture or as separate components. A mixture of DBHA and 2,5-DTBBQ in toluene shows charge transfer complex formation, thus it is likely that a similar process occurs in styrene. Inhibition of styrene polymerisation has been attributed to charge transfer complexes of quinones in the past, however in our case this needs to be proven. If the charge transfer complex is responsible for the inhibition, any change of the electron donating/withdrawing ability of the substituents should affect the inhibition efficiency of the mixture, as in a charge transfer complex localised charges are formed, so it would be quite sensitive to electronic effects. Introduction of electron donating and withdrawing substituents in the para position of the aromatic ring of DBHA showed only a small electronic effect. The reason for the limited electronic effect probably is that the substituents were too distant from the reaction centre to influence the reactivity of the charge transfer complex. Thus we observed ponderal effect rather than electronic effect. In the future, it would be interesting to modify the 2,5-DTBBQ structure and see how electronic effect influences the inhibition property of the mixture. Since the reactivity of 2,5-DTBBQ would also be strongly dependent on the steric environment, *t*-butyl needs to be replaced with a substituent that provides similar steric hindrance (e.g. CF<sub>3</sub>). Product analysis of styrene polymerization with DBHA/2,5-DTBBQ revealed that *N,N*-benzylidenebenzylamine-*N*-oxide reacts with styrene leading to isoxazolidine. Dilatometry study demonstrated that isoxazolidine, either on its own or in the mixture with 2,5-DTBBQ is a poor inhibitor. Dilatometry also excludes any synergism between *N,N*-benzylidenebenzylamine-*N*-oxide and 2,5-DTBBQ, since a mixture of them shows

limited inhibition. By comparing concentration trends of DBHA and 2,5-DTBBQ in styrene and in toluene, we observe that DBHA consumption is significantly slower in styrene with respect to toluene. This may suggest that DBHA is regenerated during the inhibition. The role of DBHA as a main inhibitor is excluded because DBHA works only in oxygenated conditions, instead the efficacy of DBHA/2,5-DTBBQ is oxygen independent.

*N,N*-dibenzyl nitroxide was detected as an intermediate by EPR analysis, and alkoxyamine is formed in the reaction mixture. Hence, the nitroxide may well be the main species responsible for the inhibition properties of the DBHA/2,5-DTBBQ mixture. By varying the concentration of *N,N*-dibenzyl nitroxide in solution, we observed a correlation between the concentration of nitroxide and the inhibition time. However, this correlation is not observed during the retardation, as DBHA/2,5-DTBBQ mixture shows good retardation even at extremely low nitroxide concentration. Therefore, our data suggest that *N,N*-dibenzyl nitroxide is likely to be involved in the inhibition, but not in the retardation of styrene polymerisation. Analysis of the polymer revealed the presence of nitrogen, thus confirming that the inhibitor is incorporated in the polymer. We believe that nitroxide may react with long chains, but this needs to be confirmed. However, the possibility that the DBHA/2,5-DTBBQ charge transfer complex allows DBHA to react with propagation chains cannot be excluded. Therefore, it would be interesting to characterise the polymer structure (e.g.,  $^1\text{H-NMR}$ ) to clarify the structure of the inhibitor in the polymer.

Products analysis of reaction mixtures containing 2,5-DTBBQ and DBHA- $\text{CF}_3$  allowed detection of a new product, however it was not possible to isolate and characterise it due to poor stability. Since it contains  $\text{CF}_3$ , this product is a derivative of hydroxylamine inhibitor. This suggests that not all inhibition products have been characterized. On a big scale reaction with unsubstituted DBHA, approximately 90% of the initial hydroxylamine was recovered. It would be good to verify that important products are not missed. A possibility would be to replace  $^{14}\text{N}$  with  $^{15}\text{N}$  in DBHA; this will allow easier monitoring of the complex reaction by  $^{15}\text{N-NMR}$  significantly reducing the purification process.

## 8 Experimental

### 8.1 General materials and methodology

Solvents and reagents were used as supplied unless stated otherwise. *N,N*-benzylidenebenzylamine-*N*-oxide was obtained from Nufarm Ltd. Thin layer chromatography was performed on commercially available Merck Silica gel 60 F254 aluminium backed silica plates. Column chromatography was carried out on a Fluka silica gel (pore size 60 Å, particle size 220-440 mesh). Preparative thin layer chromatography was performed on Analtech Inc. thin layer chromatography plates (20x20 cm, 1500 µ).

Proton and carbon NMR spectra were recorded on a Jeol JNM-ECS 400 MHz, Jeol ECX 400 MHz, Bruker AMX 300 MHz or Bruker AVII 700 MHz. All NMR experiments were performed using deuterated chloroform unless indicated otherwise. Fluorine NMR spectra were recorded at 110 °C or 20 °C on a Bruker ACS 60 500 MHz. 1-Bromo-4-fluorobenzene was used as internal reference. Chemical shifts are quoted in  $\delta$  units and were calibrated using the residual solvent peak (or the internal reference in fluorine NMR). Coupling constant values (J) are given in Hz.

Positive ion electrospray mass spectra were obtained on a Bruker micro-TOF time of flight mass spectrometer with electrospray ion source (ESI). The average mass error with respect to the exact monoisotopic mass is  $\pm 1.4$  mDa. GC-EI and GC-FI chromatograms were recorded on a Waters GCT Premier time of flight spectrometer with electrospray ionization (EI) or field ionization sources (FI) connected to an Agilent 7890A gas chromatograph system. The average mass errors with respect to the exact monoisotopic mass are  $\pm 10.0$  mDa and  $\pm 2.5$  mDa respectively. Gas chromatograms were obtained on a HP5890 gas chromatograph equipped with a flame ionization detector (FID). The GC column used is a Zebron ZB-1. The temperature program was held at 100 °C for 1 min, and then increased from 100 to 200 °C by 7 °C per min. The temperature was held for 0.5 min and then increased from 200 to 250 °C by 10 °C per min followed by an isothermal period of 250 °C for 15 min. Nitrogen was used as a

carrier gas at a flow rate of 14 mL/min. A commercial software (Clarity) was used for integrating chromatograms.

Elemental analysis was carried out on a CE-440 Exeter Analytical Inc C, H, N machine. Acetanilide was used as a standard for calibration and *S*-benzyl-thiouronium chloride as internal standard check.

Infra-red spectra were recorded on a Thermo-Nicolet AVATAR 370 FT-IR spectrometer. Using a gas-tight IR cuvette cell (KBr) for measurements. UV-vis spectra were recorded on a Hitachi U-3000 spectrophotometer.

All EPR spectra were recorded on a Bruker EMX micro spectrometer. The parameters applied for the measurements were: microwave power 5.02 mW, modulation amplitude 1 G and acquisition time 163.84 sec. The experiments were carried out at 110 °C. The reaction kinetics was monitored by recording EPR spectra automatically.

## 8.2 General procedure of EPR experiments

### 8.2.1 Sample preparation

*N,N*-Dibenzyl nitroxide and its derivatives are relatively unstable nitroxide compounds. These radicals were produced from the corresponding hydroxylamines with concentrations varied from  $1 \times 10^{-2}$  to  $2 \times 10^{-4}$  M. Typically these samples were prepared by filling a capillary tube with a solution of hydroxylamine (on its own or mixed with another reagent), approximately 1/3 of the volume. The capillary tube was flame sealed on both ends, leaving a head space of two centimetres (Figure 8.1). The capillary tube was then inserted in an NMR tube which was placed in the EPR cavity. In some experiments EPR tubes (4 mm OD) were used to improve the quality of the signal.

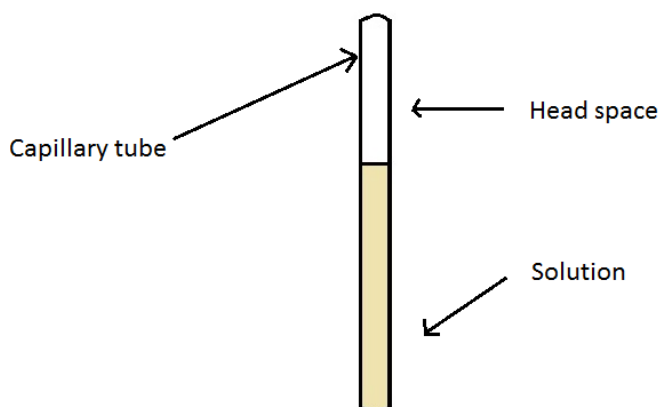


**Figure 8.1** Sample for EPR experiment

In a few cases nitroxide signal was monitored under nitrogen atmosphere, so the sample was degassed first and then filled with nitrogen using the freeze-pump-thaw method. This procedure was repeated several times until the sample was completely oxygen free.

## 8.2.2 Processing EPR data

All EPR spectra were processed using Spectrum Viewer<sup>143</sup>. This software allows viewing and manipulating spectra. In general, each spectrum was resampled, smoothed and the baseline was corrected before analysis. Two different ways were used to process the spectra:

Nitroxide concentration was estimated by comparing the double integral of the spectrum with that of a TEMPO standard solution in toluene (0.01 mM).

Due to the interaction between oxygen and nitroxide electron spins, broad spectra were processed using EWVoigt developed by Smirnov<sup>60</sup>. This program allows extracting nitroxide and oxygen concentration from a series of continuous-wave EPR spectra. The relative nitroxide concentrations provided by the software were normalised using the height of one line of a sharp spectrum (e.g., after oxygen consumption) with a reasonable intensity as a reference (Figure 8.2). So, the relative nitroxide concentrations were calculated using the following equation:

$$C_N = \left( \frac{C_i}{C_S} \right) \times h_s$$



$C_N$  is the normalised nitroxide concentration

$C_i$  is the relative nitroxide concentration provided by EWVoigt software

$C_s$  is the absolute nitroxide concentration of the reference spectrum

$h_s$  is the peak-to-peak height of the reference spectrum



**Figure 8.2 Height of a peak of a sharp *N,N*-dibenzyl nitroxide**

The heights (Figure 8.2) were used instead of double integrals in the case nitroxide concentration was too low to obtain accurate nitroxide concentration by the double integral (large signal-noise ratio).

## 8.3 General procedure of dilatometry experiments

### 8.3.1 Sample preparation

Polymerisation inhibition properties of a series of molecules were tested by dilatometry. These samples were analysed in styrene at 110 °C and the inhibitor concentration was in the range between  $2 \times 10^{-4}$  and  $2 \times 10^{-3}$  M. Before the analysis, styrene was purified by passing through an alumina column to remove any trace of other inhibitors. Generally, a capillary tube was flame sealed on one end and filled for 1/4 of the volume with a solution of the inhibitor in styrene. The remaining drops on the internal wall of the capillary tube were dried with compressed air in order to avoid non-thermal and uncontrolled styrene polymerisation. Before being immersed in the oil bath, the capillary tube was sealed on the top end leaving a head space of 2 cm. The oil bath was preheated at 114 °C and once the samples were dipped in the oil, the

temperature was changed to 110 °C. This significantly shortened the time required to equilibrate the oil bath temperature after the introduction of the samples. Images of the samples were recorded every 2 min for 10 hours.

### 8.3.2 Processing data

Data were analysed using an automation program which allows measuring the position of the meniscus inside the capillary tube. The height of the meniscus at  $T = 0$  is compared to the height of the meniscus at different times. The meniscus does not move during the inhibition period (when rate of inhibition is comparable to the rate of polymerisation), but shifts down during the retardation period or when the inhibitor stops working (when rate of polymerisation is greater than the rate of inhibition). Each sample was run twice and the height used in the analysis of the data is an average of the two heights. Heights were then converted to % of conversion (% of conversion expresses how much monomer is converted to polymer) using the following equation:

$$\% \text{ conv} = \frac{1 - \text{relative height}}{1 - 0.8} \times 100$$

Here 0.8 represents the relative height in the case styrene is all converted to polystyrene.

These data were plotted against the time in an Excel sheet obtaining the kinetics of inhibition (Figure 8.3).

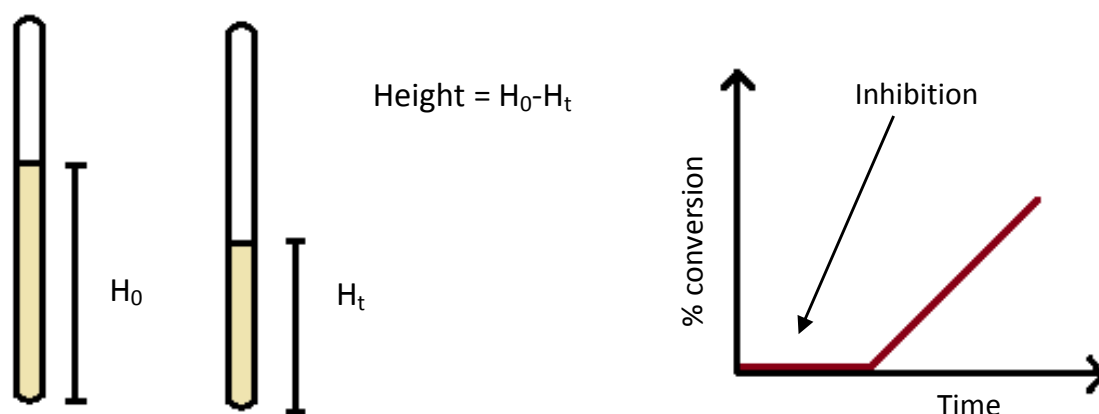


Figure 8.3 Sample preparation and analysis in dilatometry experiments

It is taken as inhibition time the time at which the percentage of conversion holds at zero. In addition, the error on the inhibition time corresponds to the deviation standard calculated on 5 values. Each value corresponds to the difference in inhibition time estimated for two samples containing the same solution and analysed during the same batch.

## 8.4 General procedure of NMR experiments

### 8.4.1 Sample preparation

NMR spectroscopy was used to monitor the kinetics of reaction between 2,5-di-*tert*-butyl-1,4-benzoquinone and *N,N*-dibenzylhydroxylamine (and *p*-substituted hydroxylamines) and for the detection of inhibition products.

For monitoring the kinetic of reaction the experiments were carried out in NMR tubes (5 mm OD) with a Teflon tap to work under deoxygenated conditions. In a general procedure, a NMR tube was filled with 0.5 mL of the solution to be analysed, which contained 1,4-dioxane as an internal standard (1-bromo-4-fluorobenzene in the case of <sup>19</sup>F-NMR analysis). The sample was degassed and filled with N<sub>2</sub> using freeze-pump-thaw cycles.

### 8.4.2 Processing NMR data

All NMR spectra were processed using ACD/NMR processor<sup>144</sup>. This software was used for manipulating the baseline and phase, referencing the spectrum and integrating peaks.

Product and reagent concentration were calculated using the following equation:

$$C_x = \frac{A_x \times C_{IS}}{A_{IS}}$$

A<sub>x</sub> (or A<sub>IS</sub>) = Normalised area of the analyte (or internal standard). C<sub>x</sub> (or C<sub>IS</sub>) = Analyte (or internal standard) concentration

The order of reaction and the kinetic data were estimated using Dynafit<sup>62</sup>. Experimental concentrations were fitted to an empirical molecular mechanisms and the best fitting was used to obtain the rate of reaction.

## 8.5 General procedures of gas chromatography and gas chromatography-mass spectrometry experiments

### 8.5.1 Qualitative analysis

Gas chromatography and gas chromatography coupled to mass spectrometry were used for the detection of intermediates and products of reaction. The analyses were carried out in either on a milligram or gram-scale.

*N,N*-Dibenzylhydroxylamine and 2,5-di-*tert*-butyl-1,4-benzoquinone were weighted in a three necks round bottomed flask and dissolved in styrene. Before the analysis, styrene was purified by passing through an alumina column to remove any trace of other inhibitors. The round bottomed flask was connected to a condenser, and once the system was sealed, oxygen was replaced with nitrogen using freeze-pump-thaw cycles. The solution was then heated at 110 °C and samples were taken at different times for the analysis. Before the analysis, methanol was added to the sample (2 parts of methanol : 3 parts of reaction mixture), as it facilitates precipitation of polystyrene. The precipitate was then filtrated off and the solution was analysed.

### 8.5.2 Quantitative analysis

#### 8.5.2.1 Calibration curve

A stock solution of DBHA was prepared dissolving DBHA (0.9 mmol) in toluene (25 mL). 0.5 mL, 2 mL, 4 mL and 6 mL of stock solution were transferred in 25 ml volumetric flasks, respectively. Before dilution, 2 mL of internal standard (n-dodecane, 2.8 mM) was added to each solution. The four samples were injected in the GC using the conditions reported in section 8.1. Calibration curves were obtained plotting the area of DBHA in the chromatogram against the concentration of the corresponding solution.

The slope represents the retention factor. The same procedure was repeated for 2,5-DTBBQ, 2,5-DTBHQ, and *N,N*-benzylidenebenzylamine-*N*-oxide. Retention factors are 0.7807, 0.9971, 0.9673 and 0.8209 for DBHA, 2,5-DTBBQ, *N,N*-benzylidenebenzylamine-*N*-oxide and 2,5-DTBHQ, respectively.

### 8.5.2.2 *Sample preparation*

Samples for the analysis were prepared taking 0.6 mL of the reaction mixture, adding 0.4 mL of internal standard (n-dodecane, 2.8 mM) and diluting with 5 mL of toluene.

## 8.6 Procedure of IR experiment

A solution of DBHA (2.13g, 10 mmol) and 2,5-DTBBQ (1.10g, 5 mmol) in styrene (20 mL) was deoxygenated and heated at 140°C under nitrogen atmosphere for 3 days. The IR spectra of the head space were recorded at different times. The head space was taken by using a 20 mL syringe and injecting the sample into the IR cell. The IR cell was previously degassed by nitrogen-vacuum cycles (3 times) and then leaving the cell under vacuum for 2 h.

## 8.7 Investigation of the reactivity of 2,5-DTBBQ and 2,5-DTBHQ (chapter 3)

### 8.7.1 Reactivity of 2,5-DTBBQ in the presence of AIBN (Section 3.4)

Reaction 1: 2,5-DTBBQ ( $5 \times 10^{-3}$  mmol) and AIBN ( $1.5 \times 10^{-2}$  mmol) were dissolved in toluene (0.5 mL). After purging nitrogen through the solution for 5 min, the reaction was left stirring at reflux for 4.5 h. Thin Layer Chromatography (TLC) [DCM / hexane (4:6)] was used to check the presence of inhibition products.

Reaction 2: 2,5-DTBBQ (0.15 mmol) and AIBN (0.23 mmol) were dissolved in toluene (15 mL). After purging nitrogen through the solution for 15 min, the reaction was refluxed for 4.5 h. TLC [DCM / hexane (4:6)].

## 8.7.2 Reactivity of 2,6-DTBBQ in the presence of AIBN

2,6-DTBBQ ( $1.5 \times 10^{-1}$  mmol, 33 mg) and AIBN ( $2.3 \times 10^{-1}$  mmol, 39 mg) were dissolved in toluene (10 mL). After purging nitrogen through the solution for 15 min, the reaction was left at 80 °C for 12 h. Toluene was hence evaporated and the crude was purified by preparative TLC [EtOAc / Hexane (1.5:8.5)]. Yield 1%.

## 8.8 Charge transfer complex investigation (chapter 4)

Solutions of DBHA ( $3 \times 10^{-5}$  M), 2,5-DTBBQ ( $3 \times 10^{-5}$  M) and 2,5-DTBBQ/DBHA (1:1) (0.1 M) in acetonitrile were prepared. Similarly, a solution of N,N-benzylidenebenzylamine-N-oxide ( $3 \times 10^{-5}$  M) and 2,5-DTBHQ ( $3 \times 10^{-5}$  M) were prepared. The solution were analysed by ultraviolet-visible spectroscopy (UV-Vis). Acetonitrile cut-off is at 190 nm.

## 8.9 Reactions on a large scale

### 8.9.1 DBHA/2,5-DTBBQ mixture (Section 5.3.1)

DBHA (2.16 g, 10 mmol) and 2,5-DTBBQ (0.55 g, 2.5 mol, 0.25 M) were weighed in a round bottom flask and styrene (10 mL) was added. After degassing the solution by *freeze-pump-thaw* cycles, the reaction was left stirring for 24 hours at 140 °C and then the products were isolated by column chromatography. In order to avoid any loss of products (e.g., volatile products), the crude reaction mixture was subjected to column chromatography without any prior work-up. In addition, because of the complexity of the reaction mixture, in some cases, it was necessary to repeat column chromatography several times, changing the polarity of the solvent. In general, ethyl acetate-petroleum ether mixture was used as an eluent, but for very non polar compounds petroleum ether-dichloromethane mixture was used.

#### Quantitative analysis

DBHA (2.16 g, 10 mmol) and 2,5-DTBBQ (0.55 g, 2.5 mol, 0.25 M) were weighed in a round bottom flask and styrene (10 mL) was added. After degassing the solution by

*freeze-pump-thaw* cycles, the reaction was left stirring for 48 hours at 140 °C under nitrogen atmosphere. Once the solution was brought back to room temperature, methanol was added to precipitate polystyrene. The products were isolated by column chromatography [petroleum ether / diethyl ether (9.5:0.5)]. For a quantitative estimation of the sample, DCM was introduced as an internal standard. A stock solution of the internal standard was prepared diluting 30  $\mu\text{L}$  of DCM in  $\text{CDCl}_3$  (10 mL). The NMR sample was prepared dissolving 8 mg of compound in 0.7 mL of stock solution.

### 8.9.2 DBHA (Section 5.3.2.1)

*N,N*-Dibenzylhydroxylamine (2.16 g, 10 mmol) was dissolved in styrene (10 mL) and the solution was degassed using *freeze-pump-thaw* cycles and refilled with nitrogen. The reaction mixture was heated at 140°C for 24 h. The polymer was separated by precipitation with methanol and the remaining solvent was removed under reduced pressure. Column chromatography [petroleum ether / diethyl ether (9.5:0.5)] was used to separate the products.

### 8.9.3 *N,N*-Benzylidenebenzylamine-*N*-oxide (Section 5.3.2.2)

*N,N*-Benzylidenebenzylamine-*N*-oxide (300 mg, 1.42 mmol) was dissolved in styrene (5 mL). The reaction mixture was degassed by using the *freeze-pump-thaw* procedure and refilled with nitrogen gas. The system was stirred for 2 hours at 140 °C. At this stage the solution was visibly viscous suggesting that long polystyrene chains were formed. After cooling, methanol was added to the reaction mixture to precipitate the polymer. The solid was then washed several times with methanol. The combined mother liquors were evaporated and a column chromatography [petroleum ether / diethyl ether (8:2)] was carried out to isolate the products.

## 8.9.4 Procedure of fluorine-containing compounds (Section 5.3.3)

### 8.9.4.1 *DBHA-CF<sub>3</sub>/2,5-DTBBQ mixture monitored in-situ*

DBHA-CF<sub>3</sub> (2.67 mg,  $8 \times 10^{-3}$  mmol) and 2,5-DTBBQ (0.8 mg,  $4 \times 10^{-3}$  mmol) were dissolved in styrene (1 mL) and 1-bromo-4-fluoro-benzene (5  $\mu$ L) was added as an internal standard. The solution was then transferred in a NMR tube equipped with a Young's cap, degassed (using the *freeze-pump-thaw* procedure) and then refilled with nitrogen gas. <sup>19</sup>F-NMR spectra were recorded at 110 °C every 20 min for 8 hours.

### 8.9.4.2 *DBHA-CF<sub>3</sub>/2,5-DTBBQ mixture monitored on a large scale*

DBHA-CF<sub>3</sub> (1 g, 2.86 mmol) and 2,5-DTBBQ (0.22 g, 0.99 mmol) were dissolved in styrene (5 mL). The solution was degassed using *freeze-pump-thaw* cycles and refilled with nitrogen. The reaction mixture was heated at 110 °C for 3 days.

### 8.9.4.3 *DBHA-CF<sub>3</sub> as an inhibitor*

DBHA-CF<sub>3</sub> (2.67 mg,  $7.64 \times 10^{-3}$  mmol) was dissolved in styrene (1 mL) and 1-bromo-4-fluorobenzene (5  $\mu$ L) was added as an internal standard. The solution was degassed using *freeze-pump-thaw* cycles and refilled with nitrogen. The reaction was heated in the NMR cavity at 110 °C for 4 h and NMR spectra were recorded every 20 min.

## 8.10 Synthetic procedures

### 8.10.1 *N,N*-Dibenzylnitroxide generation (Chapter 2)

DBHA (0.47 mmol), Ag<sub>2</sub>O (0.099 mmol) and MgSO<sub>4</sub> were mixed in dichloromethane (25 mL) and left under vigorous stirring at room temperature for 15 min. Yield 1.2 %. EPR (9.75 GHz): triplet of quintet,  $a_N$  17.0 G,  $a_H$  10.0 G.

Purification-attempt 1: a pH 4.65 buffer solution sodium acetate/acetic acid (2  $\times$  10 mL) was added to the reaction mixture to protonate DBHA. After the acidification the solution was neutralized with water (2  $\times$  10 mL) and then dried over MgSO<sub>4</sub> and filtered.



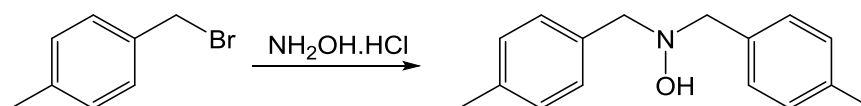
Purification-attempt 2: The purification was carried out by using a silver-loaded sulfonic acid resin (Dowex<sup>®</sup> DR 2030). The resin was prepared following literature procedure<sup>75</sup>.

### 8.10.2 Synthesis of benisoxazolidine

A solution of *N,N*-benzylidenebenzylamine-*N*-oxide (0.44 mmol) and 2,5-DTBBQ (1.78 mmol) in toluene (10 mL) was refluxed in toluene for 15 h at 110 °C. Only starting material was recovered.

### 8.10.3 Synthesis of substituted hydroxylamines

#### *N,N*-bis(*p*-methylbenzyl)hydroxylamine

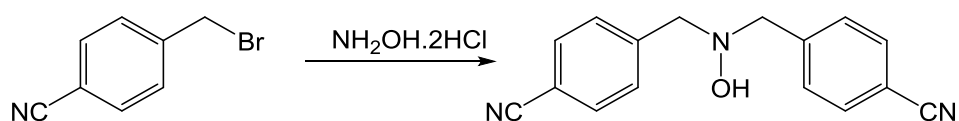


Preparation of *N,N*-bis(*p*-methylbenzyl)hydroxylamine was carried out following literature procedure<sup>145</sup>. To a suspension of anhydrous sodium carbonate (33 mmol, 3.53 g) in dry DMF (17 mL) was added hydroxylamine hydrochloride (8.34 mmol, 0.58 g) followed by of *p*-methylbenzyl bromide (21.9 mmol, 3.08 g). The reaction was stirred at room temperature for 15 h.

The reaction mixture was filtered to remove sodium carbonate and then diluted with DCM (25 mL). The organic phase was washed with water to remove DMF (15 mL x 3) and dried over  $\text{MgSO}_4$ . Solvent was evaporated under vacuum to obtain a white solid. Trituration with ethanol gave the pure product. Yield: 0.50 g, 25%.

M.P. 105.4-106.6 °C.  $R_f$  0.3 (PET ether:Et<sub>2</sub>O 8:2). <sup>1</sup>H NMR (400 MHz, CDCl<sub>3</sub>)  $\delta$  7.3-7.2 (m, 4H, CH<sub>2</sub>C=CH x 4), 7.2-7.1 (m, 4H, CH<sub>3</sub>C=CH x 4), 3.8 (s, 4H, NCH<sub>2</sub> x 2), 2.3 (s, 6H, CH<sub>3</sub>C=CH). ESI-MS ( $m/z$ ):  $[\text{M} + \text{H}]^+$  calcd for C<sub>16</sub>H<sub>20</sub>NO 242.1545; found, 242.1538.

#### *N,N*-bis(*p*-cyanobenzyl)hydroxylamine

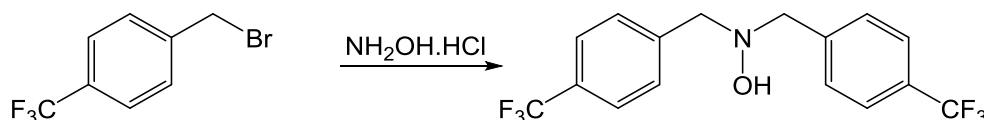


Preparation of *N,N*-bis(*p*-cyanobenzyl)hydroxylamine was carried out following literature procedure<sup>117, 118</sup>. To a solution of hydroxylamine hydrochloride (2.6 mmol, 0.18 g) and 4-bromomethyl-benzonitrile (5.1 mmol, 1.00 g) in 70% ethanol (3 mL), Na<sub>2</sub>CO<sub>3</sub> (9.5 mmol, 0.78 g) was added. The solution was then refluxed at 78 °C for 3 h.

The reaction mixture was concentrated under reduced pressure to remove ethanol and then diluted with water (25 mL). The reaction product was extracted with DCM (30 mL x 3). The combined organic phases were dried over MgSO<sub>4</sub>, filtered and concentrated under reduced pressure. The product was purified by column chromatography on silica [petroleum ether / diethyl ether (8:2)]. White solid. Yield: 0.10 g, 14%.

M.P. 174.6-175.2 °C. R<sub>f</sub> 0.4 (PET ether:Et<sub>2</sub>O 7:3). <sup>1</sup>H NMR (400 MHz, CDCl<sub>3</sub>) δ 7.7-7.6 (d br, J = 8.2 Hz, 4H, CNC=CH x 4), 7.6-7.5 (d br, J = 7.9 Hz, 4H, CH<sub>2</sub>C=CH x 4), 4.0 (s, 4H, NCH<sub>2</sub> x 2). ESI-MS (*m/z*): [M + H]<sup>+</sup> calcd for C<sub>16</sub>H<sub>14</sub>N<sub>3</sub>O, 264.1137; found, 264.1131.

#### ***N,N*-bis(*p*-trifluoromethylbenzyl)hydroxylamine**

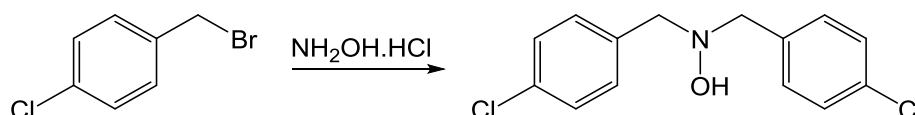


Preparation of *N,N*-bis(*p*-trifluoromethylbenzyl)hydroxylamine was carried out following literature procedure<sup>117, 118</sup>. To a solution of hydroxylamine hydrochloride (2.1 mmol, 0.15 g) and 1-(bromomethyl)-4-(trifluoromethyl)benzene (4.2 mmol, 1.00 g) in 70% ethanol (3 mL), Na<sub>2</sub>CO<sub>3</sub> (6.0 mmol, 0.64 g) was added. The solution was then refluxed at 78 °C for 3 h.

The reaction mixture was concentrated under reduced pressure to remove ethanol and then diluted with water (15 mL). The reaction product was extracted with DCM (30 mL x 3). The combined organic phases were dried over MgSO<sub>4</sub>, filtered and concentrated under vacuum. The product was purified by column chromatography on silica [petroleum ether / diethyl ether (8:2)]. White solid. Yield: 0.40 g, 54%.

M.P. 108.2-109.0 °C. R<sub>f</sub> 0.3 (PET ether:Et<sub>2</sub>O 7:3). <sup>1</sup>H NMR (400 MHz, CDCl<sub>3</sub>) δ 7.7-7.6 (d br, J = 8.2 Hz, 4H, CF<sub>3</sub>C=CH x 4), 7.6-7.5 (d br, J = 8.2 Hz, 4H, CH<sub>2</sub>C=CH x 4), 4.0 (s, 4H, NCH<sub>2</sub> x 2). <sup>19</sup>F NMR (500 MHz, neat, 110 °C) δ -63.26 (s, 6F, CF<sub>3</sub> x 2). ESI-MS (*m/z*): [M + H]<sup>+</sup> calcd for C<sub>16</sub>H<sub>14</sub>F<sub>6</sub>NO, 350.0979; found, 350.0953.

### *N,N*-bis(*p*-chlorobenzyl)hydroxylamine



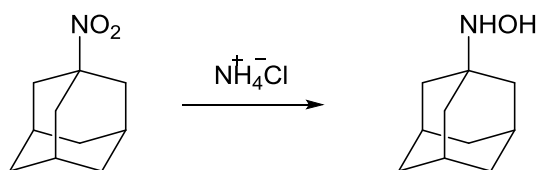
Preparation of *N,N*-bis(*p*-chlorobenzyl)hydroxylamine was carried out following literature procedure<sup>117, 118</sup>. To a solution of hydroxylamine hydrochloride (3.2 mmol, 0.22 g) and 4-chloro-benzyl chloride (6.2 mmol, 1.00 g) in 70% ethanol (3 mL), Na<sub>2</sub>CO<sub>3</sub> (9.0 mmol, 0.95 g) was added. The solution was then refluxed at 78 °C for 3 h.

The reaction mixture was concentrated under reduced vacuum to remove ethanol and then diluted with water (15 mL). The reaction product was extracted with DCM (30 mL x 3). The combined organic phases were dried over MgSO<sub>4</sub>, filtered and concentrated under vacuum. The product was purified by column chromatography on silica [petroleum ether / diethyl ether (7:3)]. White solid. Yield: 0.30 g, 34%.

M.P. 114.8-116.0 °C. R<sub>f</sub> 0.4 (PET ether:Et<sub>2</sub>O 6:4) <sup>1</sup>H NMR (400 MHz, CDCl<sub>3</sub>) δ 7.6-7.5 (m, 4H, ClC=CH x 4), 7.5-7.4 (m, 4H, CH<sub>2</sub>C=CH x 4), 4.0 (s, 4H, NCH<sub>2</sub> x 2). ESI-MS (*m/z*): [M + H]<sup>+</sup> calcd for C<sub>14</sub>H<sub>14</sub>Cl<sub>2</sub>NO, 282.0452; found, 282.0456.

### *N*-adamantyl-*N*-benzylhydroxylamine and its precursors

#### *N*-adamantylhydroxylamine



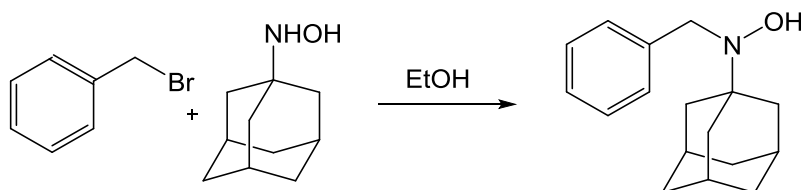
Preparation of *N*-adamantylhydroxylamine was carried out following literature procedure<sup>146</sup>. A suspension of 1-nitro-adamantane (11 mmol, 2.00 g) and NH<sub>4</sub>Cl (22

mmol, 1.18 g), in a 50% ethanol solution (200 mL) was stirred at 0° C. To the suspension, zinc powder (33 mmol, 2.15 g) was added over 1.5 h. The reaction mixture was then stirred for 3 h at room temperature.

The suspension was filtered and the collected solid was washed with ethanol (10 mL x 3). The combined filtrates were adjusted to pH 2 with conc HCl and solvent was evaporated. The residue was neutralised with Na<sub>2</sub>CO<sub>3</sub> and extracted with DCM (15 mL x 3). The extract was dried over MgSO<sub>4</sub> and evaporated to give a white solid. Yield: 1.05 g, 50%.

M.P 166.3-168 °C. R<sub>f</sub> 0.4 (PET ether:Et<sub>2</sub>O 8:2). <sup>1</sup>H NMR (400 MHz, CDCl<sub>3</sub>) δ 2.1 (s br, 3H, CH<sub>2</sub>CHCH<sub>2</sub> x 3), 1.8-1.6 (m, 12H, CCH<sub>2</sub>CH x 3, CHCH<sub>2</sub>CH x 3). ESI-MS (*m/z*): [M + H]<sup>+</sup> calcd for C<sub>10</sub>H<sub>18</sub>NO, 168.1388; found, 168.1382.

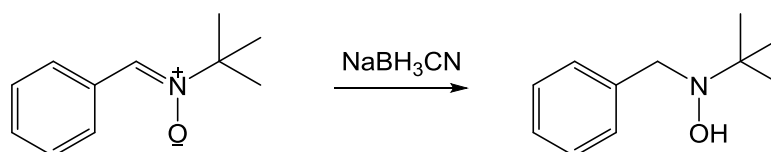
#### ***N*-adamantyl-*N*-benzylhydroxylamine**



*N*-adamantylhydroxylamine (5.3 mmol, 0.88 g) was dissolved in ethanol (16 mL) and benzylbromide (21 mmol, 2.5 mL) was added. The solution was deoxygenated and heated at 78 °C for 2.5 h.

The solvent was evaporated and the product was purified by column chromatography on silica [petroleum ether / ethyl acetate (9:1)]. White solid. Yield: 0.60 g, 44%.

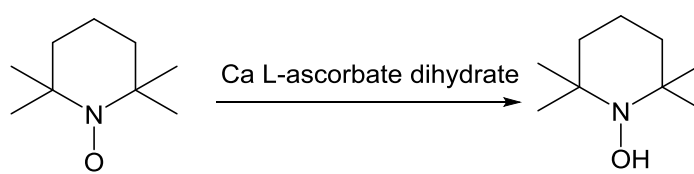
M.P. 106.6-108.7 °C. R<sub>f</sub> 0.4 (PET ether:EtOAc 8:2). <sup>1</sup>H NMR (400 MHz, CDCl<sub>3</sub>) δ 7.4-7.2 (m, 5H, CH Ar x 5), 3.8 (s, 2H, OHNCH<sub>2</sub>) 2.1 (s br, 3H, CH<sub>2</sub>CHCH<sub>2</sub> x 3), 1.9-1.6 (m, 12H, CCH<sub>2</sub>CH x 3, CHCH<sub>2</sub>CH x 3). <sup>13</sup>C NMR (100 MHz, CDCl<sub>3</sub>) 140.0 (C Ar), 129.4 (CH Ar x 2), 128.3 (CH Ar x 2), 126.9 (CH Ar), 59.1 (NC), 54.7 (NCH<sub>2</sub>), 38.3 (NCCH<sub>2</sub> x 3), 37.0 (CH<sub>2</sub>CHCH<sub>2</sub> x 3), 29.6 (CH<sub>2</sub>CHCH<sub>2</sub> x 3). IR (neat) 3276, 3029, 2908, 2846, 1493, 1450, 746, 718, 695 cm<sup>-1</sup>. ESI-MS (*m/z*): [M + H]<sup>+</sup> calcd for C<sub>17</sub>H<sub>24</sub>NO, 258.1858; found, 258.1856.

**N-benzyl-N-tert-butylhydroxylamine**

Preparation of *N*-benzyl-*N*-*tert*-butylhydroxylamine was carried out following literature procedure<sup>147</sup>. To a solution of  $\alpha$ -(phenyl)-*N*-*tert*-butyl nitron (2.8 mmol, 0.50 g) and NaBH<sub>3</sub>CN (4.8 mmol, 0.30 g) in methanol (50 mL) at 0 °C, HCl (12 N) was added drop wise until pH  $\sim$  3. The reaction mixture was allowed to stir at 65 °C for 4 h.

NaOH (2N) was added until pH  $\sim$  9. The reaction mixture was concentrated under vacuum and the product was extracted with DCM (15 mL x 3), washed with brine (15 mL), dried over MgSO<sub>4</sub> and concentrated under reduced pressure. The crude product was purified by column chromatography on silica [petroleum ether / diethyl ether (7:3)]. White solid. Yield: 0.20 g, 40%.

M.P. 71.9-74.3 °C. R<sub>f</sub> 0.4 (PET ether:Et<sub>2</sub>O 6:4). <sup>1</sup>H NMR (400 MHz, CDCl<sub>3</sub>)  $\delta$  7.4-7.2 (m, 5H, CH Ar x 5), 3.8 (s, 2H, OHNCH<sub>2</sub>), 1.2 (s, 9H, CH<sub>3</sub> x 3). ESI-MS (*m/z*): [M + H]<sup>+</sup> calcd for C<sub>11</sub>H<sub>18</sub>NO, 180.1389; found, 180.1388.

**TEMPO hydroxylamine**

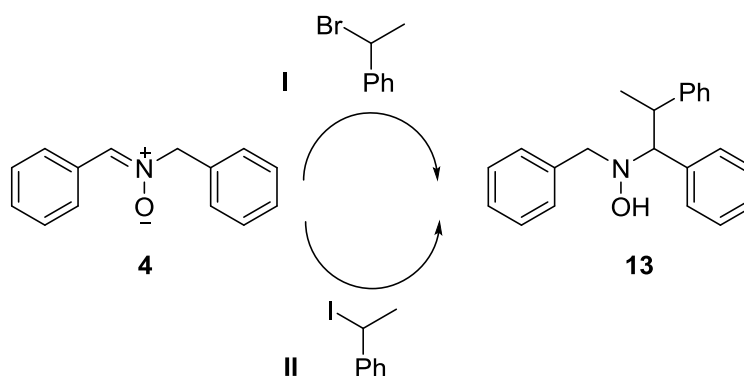
Preparation of TEMPO hydroxylamine (TEMPOH) was carried out following literature procedure<sup>46</sup>. To a suspension of TEMPO (3.2 mmol, 0.50 g) in water (21 mL), calcium L-ascorbate dihydrate (1.26 g, 2.9 mmol) was added. The mixture was stirred at room temperature for 30 min until solution turned light yellow (residual TEMPO level was less than 10%).

TEMPOH was extracted by diethyl ether (20 mL x 2). The combined organic phases were washed with water (10 mL), dried with MgSO<sub>4</sub> and concentrated under vacuum. TEMPOH was stored at 0 °C under nitrogen. Yield: 0.05 g, 10%.

White solid. <sup>1</sup>H NMR (400 MHz, toluene-d<sub>8</sub>) δ 1.5-1.3 (m, 6H, CH<sub>2</sub> x 3), 1.2 (s, 12H, CH<sub>3</sub>).

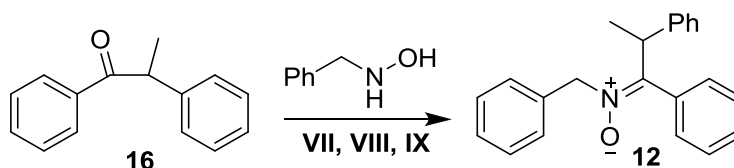
## 8.10.4 Attempts to the synthesis of three rings hydroxylamine

### 8.10.4.1 Route 1



Reaction I: Preparation of (**13**) was carried out following literature procedure<sup>148</sup>. To a solution of *N,N*-benzylidenebenzylamine-*N*-oxide (**4**) (0.95 mmol) in THF (7 mL) at 0 °C *n*-butyllithium (0.95 mmol) was added. The solution was stirred for 1 h and then cooled down to -78 °C. Keeping the temperature constant at -78 °C, 1-bromo-1-phenylethane (0.48 mmol) in THF (0.5 mL) was added. After the addition, the reaction was stirred at room temperature for 10 min.

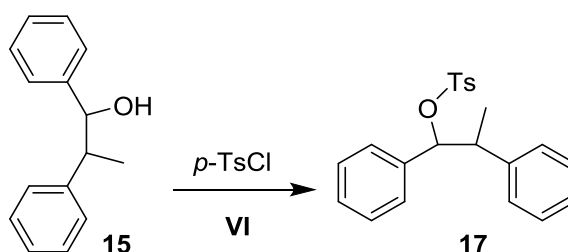
Reaction II: Preparation of (**13**) was carried out following literature procedure<sup>149, 150</sup>. A suspension of *N,N*-benzylidenebenzylamine-*N*-oxide (**4**) (0.71 mmol), Zn (2.84 mmol), CuI (1.42 mmol) and 2-iodoethylbenzene (2.84 mmol) was stirred at room temperature for a day.

**8.10.4.2 Route 2**

Reaction VII: Preparation of (**12**) was carried out following literature procedure<sup>151</sup>. Ketone (**16**) (0.48 mmol), zinc chloride (0.48 mmol), *N*-benzylhydroxylamine (0.48 mmol) and MgSO<sub>4</sub> (0.48 mmol) were stirred in DCM (3 mL) at room temperature for 24 h.

Reaction VIII: Preparation of (**12**) was carried out following literature procedure<sup>152</sup>. Ketone (**16**) (0.65 mmol) and *N*-benzylhydroxylamine (0.33 mmol) were dissolved in *tert*-butanol (1 mL). The argon saturated solution was refluxed at 110 °C for 15 h.

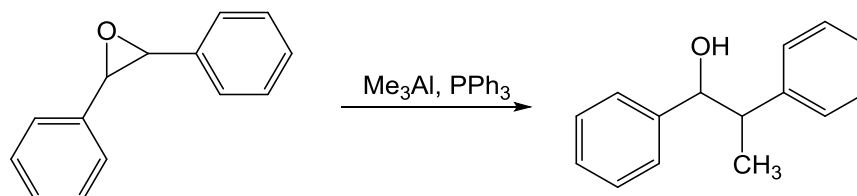
Reaction IX: Preparation of (**12**) was carried out following literature procedure<sup>117, 118</sup>. Ketone (**16**) (0.71 mmol), *N*-benzylhydroxylamine (0.71 mmol) and Na<sub>2</sub>CO<sub>3</sub> (0.71 mmol) were stirred in dry DCM (1 mL) for 24 h.



Reaction VI: Preparation of (**17**) was carried out following literature procedure<sup>153</sup>. A solution of (**15**) (1.8 mmol) and pyridine (2 mL) in DCM (1 mL) was cooled to 0 °C. *p*-Toluenesulfonyl chloride (2.7 mL) was added, and the reaction was stirred at room temperature for 2 h.

## 8.10.5 Synthesis of three rings nitrone (12) and its precursors

### 1,2-Diphenylpropane-1-ol (mixture of diastereoisomers)

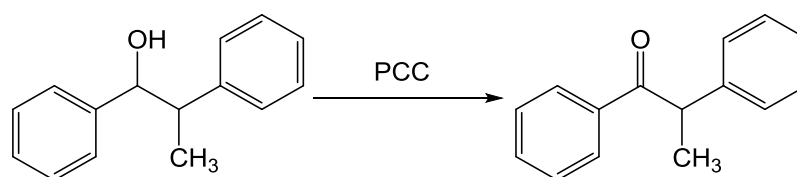


Preparation of a mixture of *syn*- and *anti*-1,2-diphenylpropan-1-ol was carried out following literature procedure<sup>154</sup>. Triphenylphosphine (1.4 mmol, 0.36 g) was added to a solution of *trans*-2,3-diphenyloxirane (27.3 mmol, 5.35 g) in toluene (55 mL) and subsequently 2.0 M trimethylaluminium in hexane (27.3 mmol, 13.6 mL) was added and the reaction was stirred for 24 h at room temperature under a nitrogen atmosphere.

The reaction mixture was cooled to  $-78\text{ }^\circ\text{C}$  and then quenched with HCl (1M, 46 mL) solution. The phases were separated and the aqueous layer was extracted with diethyl ether (15 mL x 2). The combined organic extracts were dried over  $\text{MgSO}_4$  and the solvent was evaporated in *vacuo*. The crude product was purified by column chromatography on silica [petroleum ether / ethyl acetate (9:1)],  $R_f = 0.2$ . White solid. Yield: 1.64 g, 29%.

M.P.  $94.3\text{--}96.1\text{ }^\circ\text{C}$ .  $R_f$  0.4 (PET ether:EtOAc 7:3)  $^1\text{H}$  NMR (400 MHz,  $\text{CDCl}_3$ )  $\delta$  *anti* diastereoisomer 7.4-7.1 (m, 10H, CH Ar x 10), 4.7 (d,  $J = 8.0\text{ Hz}$ , OHCHPh), 3.0 (m, 1H,  $\text{CH}_3\text{CHPh}$ ), 1.0 (d,  $J = 8.0\text{ Hz}$ , 3H,  $\text{CH}_3$ ); *syn* diastereoisomer 7.4-7.0 (m, 10H, CH Ar x 10), 4.7 (d,  $J = 8.0\text{ Hz}$ , 1H, OHCHPh), 3.0 (m, 1H,  $\text{CH}_3\text{CHPh}$ ), 1.4 (d,  $J = 8.0\text{ Hz}$ , 3H,  $\text{CH}_3$ ). ESI-MS ( $m/z$ ):  $[\text{M} + \text{H}]^+$  calcd for  $\text{C}_{15}\text{H}_{17}\text{O}$ , 213.1279; found, 213.1274.

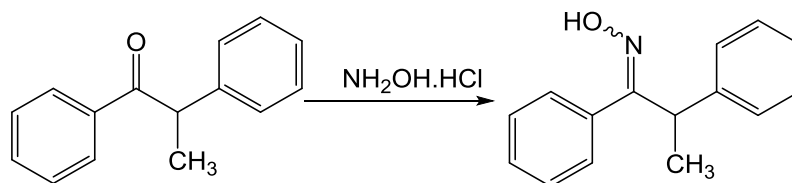


**1,2-Diphenylpropan-1-one**

Preparation of 1,2-diphenylpropan-1-one was carried out following literature procedure<sup>114</sup>. In a flame-dried 25 mL round-bottom flask, pyridinium chlorochromate (11.2 mmol, 2.41 g) was suspended in DCM (8 mL) and 1,2-diphenylpropan-1-ol (7.4 mmol, 1.57 g) in DCM (8 mL) was rapidly added at room temperature. The solution briefly became homogeneous before depositing the black insoluble reduced reagent. After 3 h the oxidation was completed.

The black reaction mixture was diluted with diethyl ether (20 mL), the solvent was decanted, and the black solid was washed with diethyl ether (20 mL x 4). The combined organic phases were dried over MgSO<sub>4</sub> and the solvent evaporated under vacuum. The crude product was purified by column chromatography on silica [petroleum ether / diethyl ether (9:1)]. White solid. Yield: 1.7 g, 96%.

M.P. 51.7-53.2 °C. *R*<sub>f</sub> 0.5 (PET ether:Et<sub>2</sub>O 9:1). <sup>1</sup>H NMR (400 MHz, CDCl<sub>3</sub>) δ 8.0-8.0 (m, 2H, CH Ar x 2), 7.5-7.1 (m, 8H, CH Ar x 2), 4.7 (q, *J* = 7.0 Hz, 1H, CH<sub>3</sub>CHCO), 1.5 (d, *J* = 7.0 Hz, 3H, CH<sub>3</sub>). ESI-MS (*m/z*): [M + H]<sup>+</sup> calcd for C<sub>15</sub>H<sub>15</sub>O, 211.1123; found, 211.1120.

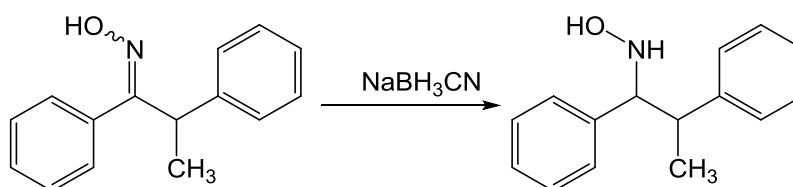
**1-*N*-hydroxy-1,2-diphenylpropane-1-imine**

Preparation of 1-*N*-hydroxy-1,2-diphenylpropane-1-imine was carried out following literature procedure<sup>115</sup>. A solution of hydroxylamine hydrochloride (20.2 mmol, 1.40 g) and 1,2-diphenylpropan-1-one (8.1 mmol, 1.7 g) in pyridine/ethanol (50 mL, 1:1) was stirred for 15 h at 40 °C under a nitrogen atmosphere.

The solvent was evaporated in *vacuum* and the product was extracted with DCM (15 mL x 3). The combined organic phases were washed with water (10 mL x 4) to remove pyridine. The product was purified by column chromatography on silica [petroleum ether / diethyl ether (8:2)]. White solid, mixture of *cis* and *trans* diastereoisomers. Yield: 1.7 g, 95%.

M.P. 96.3-98.5 °C.  $R_f$  0.5 (PET ether:Et<sub>2</sub>O 8:2). <sup>1</sup>H NMR (400 MHz, CDCl<sub>3</sub>)  $\delta$  minor isomer 7.4-7.1 (m, 10H, CH Ar), 5.2 (q, J = 8.0 Hz, 1H, CH<sub>3</sub>CH), 1.5 (d, J = 8.0 Hz, 3H, CH<sub>3</sub>); major isomer 7.4-7.1 (m, 10H, CH Ar x 10), 4.0 (q, J = 4.0 Hz, 1H, CH<sub>3</sub>CH), 1.6 (d, J = 4.0 Hz, 3H, CH<sub>3</sub>). ESI-MS ( $m/z$ ): [M + H]<sup>+</sup> calcd for C<sub>15</sub>H<sub>16</sub>NO, 226.1232; found, 226.1236.

### N-hydroxy-1,2-diphenylpropane-1-amine



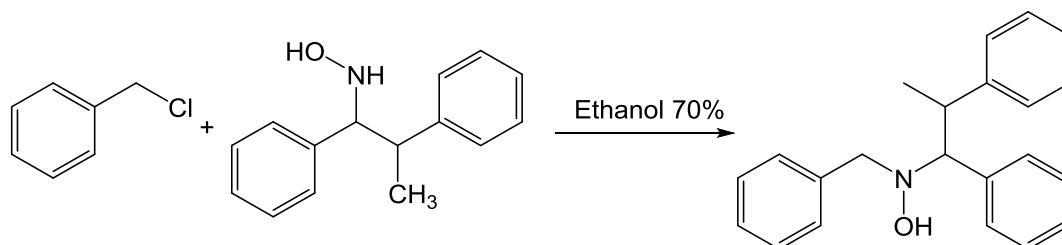
Preparation of N-hydroxy-1,2-diphenylpropane-1-amine was carried out following literature procedure<sup>147</sup>. To a solution of 1-N-hydroxy-1,2-diphenylpropan-1-amine (7.5 mmol, 1.68 g) and NaBH<sub>3</sub>CN (14.8 mmol, 0.93 g) in methanol (73 mL) at 0 °C, HCl (12N) was added drop wise until pH ~ 3. After addition the reaction mixture was allowed to stir at 60 °C for 6 h.

NaOH (2N) was added until pH ~ 9. The reaction mixture was concentrated in vacuum and the product was extracted with DCM (15 mL x 3), washed with brine (15 mL), dried over MgSO<sub>4</sub> and concentrated under reduced pressure. The crude product was purified by column chromatography on silica [petroleum ether / diethyl ether (8:2)]. White solid. Yield: 0.70 g, 41%.

M.P. 112.2-113.9 °C.  $R_f$  0.4 (PET ether:Et<sub>2</sub>O 7:3). <sup>1</sup>H NMR (400 MHz, CDCl<sub>3</sub>)  $\delta$  7.5-7.2 (m, 10H, CH Ar x 10), 4.6 (s br, 1H, NOH), 4.0 (d, J = 12.0 Hz, 1H, HONCHPh), 3.0 (m, 1H, CH<sub>3</sub>CHPh), 1.0 (d, J = 4.1 Hz, 3H, CH<sub>3</sub>). <sup>13</sup>C NMR (100 MHz, CDCl<sub>3</sub>) 143.8 (NHCHC), 140.9

(CH<sub>3</sub>CH(R)C), 129.0-127.1 (CH Ar x 10), 72.9 (NHCH), 43.4 (CH<sub>3</sub>CH), 19.6 (CH<sub>3</sub>CH). ESI-MS (*m/z*): [M + H]<sup>+</sup> calcd for C<sub>15</sub>H<sub>18</sub>NO, 228.1388; found, 228.1388.

**N-benzyl-N-hydroxy-1,2-diphenylpropane-1-amine**

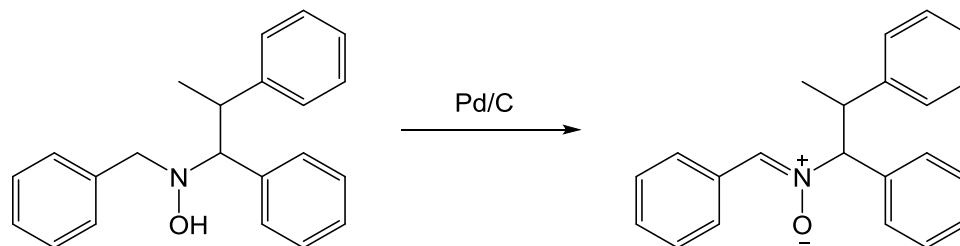


A solution of N-hydroxy-1,2-diphenylpropan-1-amine (0.9 mmol, 0.20 g) and benzyl chloride (3.5 mmol, 0.4 mL) in 70% ethanol (4 mL), was refluxed at 50 °C for 15 h.

The reaction mixture was concentrated under vacuum to remove ethanol. The crude mixture was diluted with water (15 mL) and the product was extracted with DCM (30 mL x 3). The combined organic phases were dried over MgSO<sub>4</sub>, filtered and evaporated. The product was purified by column chromatography on silica [petroleum ether / ethyl acetate (9:1)]. White solid. Yield: 0.92 g, 33%.

M.P. 99.7-101.2 °C. R<sub>f</sub> 0.4 (PET ether:EtOAc 9:1). <sup>1</sup>H NMR (400 MHz, DMSO-d<sub>6</sub>) δ 7.3-7.1 (m, 13H, CH Ar x 13), 7.0 (d br, J = 6.8 Hz, 2H, CH Ar x2), 3.8 (d, J = 8.3 Hz, 1H, HONCH(Ph)CH), 3.6 (m, 1H, CH<sub>3</sub>CH(Ph)CH), 3.5 (d, J = 14.2 Hz, 1H, HONCHH'), 3.4 (d, J = 14.2 Hz, 1H, NHCHH'), 1.00 (d, J = 7.1 Hz, 3H, CH<sub>3</sub>). <sup>13</sup>C NMR (100 MHz, CDCl<sub>3</sub>) 145.8 (C Ar), 138.4 (C Ar), 137.4 (C Ar), 130.2 (CH Ar), 129.1 (CH Ar), 128.4 (CH Ar), 128.2 (CH Ar), 128.0 (CH Ar), 127.8 (CH Ar), 127.26 (CH Ar), 126.3 (CH Ar), 75.9 (CH<sub>3</sub>CH(R)CH(R)), 61.39 (OHNCH<sub>2</sub>(R)), 41.9 (CH<sub>3</sub>CH(R)), 18.3 (CH<sub>3</sub>). IR (neat) 3499, 3060-2867, 1489, 1451, 766, 737, 697 cm<sup>-1</sup>. ESI-MS (*m/z*): [M + H]<sup>+</sup> calcd for C<sub>22</sub>H<sub>24</sub>NO, 318.1858; found, 318.1858.

### 8.10.6 Synthesis of *N*-(1,2-diphenylpropyl)-*N*-[(*Z*)-phenylmethylidene]amine oxide



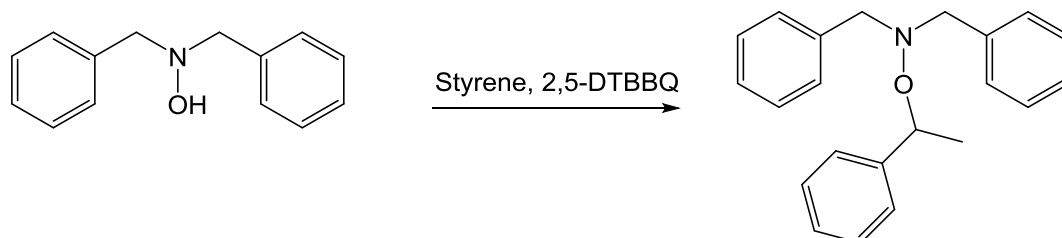
To a solution of *N*-benzyl-*N*-hydroxy-1,2-diphenylpropan-1-amine (0.1 mmol, 0.03 g) in toluene (2 mL) Pd/C (0.005 mmol,  $6 \times 10^{-4}$  g) was added. The reaction system was degassed, filled with argon and refluxed for 24 h.

The solution was filtered to remove palladium and the solvent was concentrated under vacuum. The product was purified by column chromatography on silica [petroleum ether / diethyl ether (8:2)]. White solid. Yield:  $5 \times 10^{-3}$  g, 15%.

M.P. 191.5-193.4 °C.  $R_f$  0.4 (PET ether:Et<sub>2</sub>O 6:4). <sup>1</sup>H NMR (400 MHz, CDCl<sub>3</sub>)  $\delta$  8.0-7.9 (m, 2H, CH Ar x 2), 7.8-7.7 (m, 2H, CH Ar x 2), 7.5-7.4 (m, 5H, CH Ar x 5), 7.3-7.2 (m, 5H, CH Ar), 7.2-7.1 (m, 1H, CH Ar x 5), 7.1 (s, 1H, PhCH=N<sup>+</sup>O<sup>-</sup>(R)), 4.8 (d,  $J = 12.0$  Hz, 1H, N<sup>+</sup>O<sup>-</sup>CHPh), 4.1 (dq,  $J = 8.2, 12.0$  Hz, 1H, CH<sub>3</sub>CH), 1.1 (d,  $J = 8.2$  Hz, CH<sub>3</sub>). <sup>13</sup>C NMR (100 MHz, CDCl<sub>3</sub>) 143.3 (C Ar), 136.3 (C Ar), 133.3 (<sup>-</sup>O-N<sup>+</sup>=CH(R)), 130.4 (C Ar), 129.9 (CH Ar), 129.0 (CH Ar), 128.8 (CH Ar), 128.6 (CH Ar), 128.5 (CH Ar), 128.4 (CH Ar), 128.2 (CH Ar), 127.2 (CH Ar), 127.0 (CH Ar), 87.1 (CH<sub>3</sub>CH(R)CH(R)), 41.5 (CH<sub>3</sub>CH(R)), 18.5 (CH<sub>3</sub>). IR (neat) 3060-2968, 1491, 1453, 1145, 701, 692 cm<sup>-1</sup>. ESI-MS ( $m/z$ ): [M + H]<sup>+</sup> calcd for C<sub>22</sub>H<sub>22</sub>NO, 316.1701; found, 316.1684.

## 8.10.7 Synthesis of inhibition products

### *O*-(1-phenylethyl)-*N,N*-dibenzylhydroxylamine

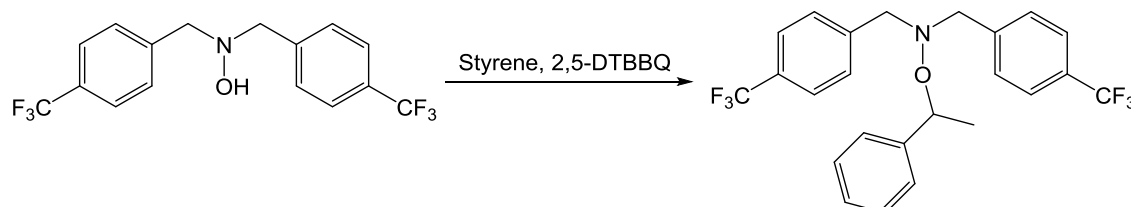


*N,N*-dibenzylhydroxylamine (2.16 g, 10.1 mmol) was dissolved in styrene (10 mL) and the solution was degassed using *freeze-pump-thaw* cycles and refilled with nitrogen. The reaction mixture was heated at 140°C for 24 h.

The polymer was separated by precipitation with methanol and the remaining solvent was removed under reduced pressure. The products were isolated by chromatography on silica [petroleum ether/ ethyl acetate (9.5:0.5)]. Colourless oil. Yield: 0.41 g 13%

$R_f$  0.6 (PET ether:EtOAc 9.5:0.5).  $^1\text{H}$  NMR (400 MHz,  $\text{CDCl}_3$ )  $\delta$  7.3-7.2 (m, 15H, CH Ar x 15), 4.2 (q,  $J = 6.4$  Hz, 1H, OCHCH<sub>3</sub>), 3.8 (d,  $J = 12.8$  Hz, 2H, CHNO x 2), 3.7 (d,  $J = 12.8$  Hz, 2H, CHNO x 2), 1.2 (d,  $J = 6.4$  Hz, 3H, CH<sub>3</sub>).  $^{13}\text{C}$  NMR (100 MHz,  $\text{CDCl}_3$ ) 143.5 (OCH<sub>2</sub>C), 138.2 (NCH<sub>2</sub>C x 2), 130.0 (CH Ar), 128.4 (CH Ar), 127.7 (CH Ar), 127.5 (CH Ar), 127.4 (CH Ar), 80.7 (CH<sub>3</sub>CH), 62.9 (NCH<sub>2</sub> x 2), 21.0 (CH<sub>3</sub>). IR (neat) 3085-2838, 1493, 1453, 748, 695  $\text{cm}^{-1}$ . (ESI-MS ( $m/z$ ):  $[\text{M} + \text{H}]^+$  calcd for C<sub>22</sub>H<sub>24</sub>NO, 318.1858; found, 318.1855.

### *o*-(1-phenylethyl)-*N,N*-bis(*p*-trifluoromethylbenzyl)hydroxyl amine



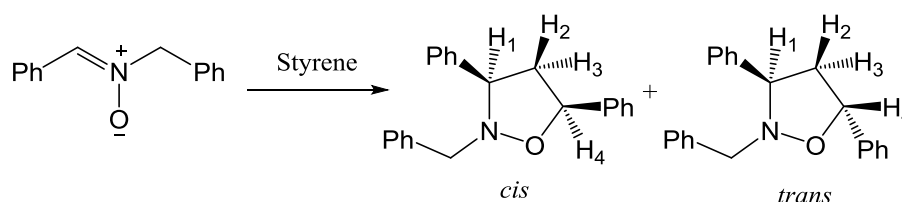
*N,N*-bis(*p*-trifluoromethylbenzyl)hydroxylamine (2.86 mmol, 1.00 g) and 2,5-di-*tert*-butyl-1,4-benzoquinone (0.99 mmol, 0.22 g) were dissolved in styrene (5 mL). The

solution was degassed using *freeze-pump-thaw* cycles and the flask was refilled with nitrogen. The reaction mixture was heated at 140 °C for 24 h.

The polymer was separated by precipitation with methanol and the solvent was removed under reduced pressure. The product was isolated by chromatography using petroleum ether/ ethyl acetate (9:1) as eluent. White solid. Yield: 0.30 g, 23%.

$R_f$  0.5 (PET ether:EtOAc 9:1).  $^1\text{H}$  NMR (400 MHz,  $\text{CDCl}_3$ )  $\delta$  7.5-7.1 (m, 13H, CH Ar x 13), 4.2 (q,  $J = 6.8$  Hz, 1H, OCHCH<sub>3</sub>), 3.8-3.7 (m, 4H, CH<sub>2</sub>NO x 2), 1.2 (d,  $J = 6.8$  Hz, 3H, CH<sub>3</sub>).  $^{13}\text{C}$  NMR (100 MHz,  $\text{CDCl}_3$ ) 143.1 (OCHC Ar), 141.8 (NCH<sub>2</sub>C x 2), 130.2 (CH Ar), 128.5 (CH Ar), 128.0 (CH Ar), 127.3 (CH Ar), 125.4 (q,  $J_{\text{CF}} = 3.1$ , CF<sub>3</sub> x 2), 81.0 (CH<sub>3</sub>CH), 62.5 (NCH<sub>2</sub> x 2), 21.2 (CH<sub>3</sub>).  $^{19}\text{F}$  NMR (500 MHz, no solvent, 110 °C)  $\delta$  -63.26 (s br, 6F). IR (neat) 2904-2854, 1619, 1419, 1321, 1021, 1064  $\text{cm}^{-1}$ . ESI-MS ( $m/z$ ):  $[\text{M} + \text{H}]^+$  calcd for C<sub>24</sub>H<sub>22</sub>F<sub>6</sub>NO, 454.1605; found, 454.1588.

### **2-benzyl-3,5-diphenylisoxazolidine**



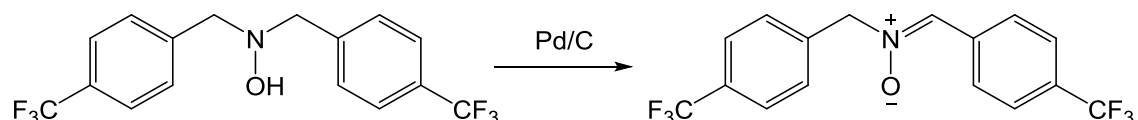
*N*-benzyl-*N*-phenylnitronium (1.24 mmol, 0.26 g), and styrene (12.4 mmol, 1.4 mL) were mixed in toluene (6 mL). The reaction was refluxed for 3 days.

Styrene and toluene were evaporated and the product was purified by column chromatography on silica [petroleum ether / ethyl acetate (9:1)]. Colourless oil. Yield: 40 mg, 10%.

$R_f$  0.4 (PET ether:EtOAc 7:3). Data compared to the work of Shimizu<sup>109</sup>.  $^1\text{H}$  NMR (400 MHz,  $\text{CDCl}_3$ )  $\delta$  *cis* diastereoisomer 7.5 (m, 15 H, CH Ar x 15), 5.2 (t,  $J = 7.7$  Hz, 1H, OCHPh), 4.0 (d,  $J = 14.6$  Hz, 1H, PhCH<sub>2</sub>), 4.0 (dd,  $J = 9.1, 7.3$  Hz, 1H, NCHPh(R)), 3.8 (d,  $J = 14.6$  Hz, 1H, PhCH<sub>2</sub>), 3.1 (dt,  $J = 12.4, 7.3$  Hz, 1H, OCH(Ph)CHH), 2.3 (ddd,  $J = 7.7, 9.1, 12.4$  Hz, 1H, OCH(Ph)CHH). *trans* diastereoisomer 7.5 (m, 15 H, CH Ar x 15), 5.2-5.1 (m,

1H, OCHPh), 4.1-3.9 (m, 3H, CH<sub>2</sub>Ph, NCHPh), 2.7 (dt, J = 8.4, 12.4 Hz, 1H, OCH(Ph)CHH), 2.5 (ddd, J = 8.4, 12.4, 6.7 Hz, 1H, OCH(Ph)CHH). MS (*m/e*) (rel intensity) 315 (10), 284 (10), 256 (15), 195 (100), 165 (21), 117 (50), 91 (80), 77 (30) 43 (40). ESI-MS (*m/z*): [M + H]<sup>+</sup> calcd for C<sub>22</sub>H<sub>22</sub>NO, 316.1701; found, 316.1694.

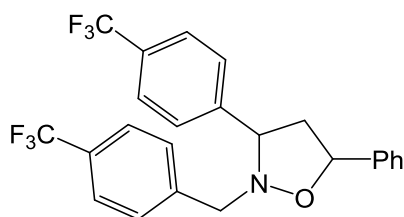
**N-(p-trifluoromethylbenzyl)-N-(p-trifluorophenyl) nitron**



To *N,N*-bis(*p*-trifluoromethylbenzyl)hydroxylamine (0.86 mmol, 0.30 g) and Pd/C (0.07 mmol, 7x10<sup>-3</sup> g) toluene (3 mL) was added. The reaction mixture was degassed by using the procedure *freeze-pump-thaw* cycles and refilled with nitrogen gas. The reaction was stirred at 110 °C for 2 days.

The catalyst was removed by filtration and the filtrate was concentrated by rotary evaporation. The product was purified by column chromatography [petroleum ether / ethyl acetate (8:2)]. White solid. Yield: 0.90 g, 30%.

M.P. 104.5-105.5 °C. R<sub>f</sub> 0.4 (PET ether:EtOAc 7:3). <sup>1</sup>H NMR (400 MHz, CDCl<sub>3</sub>) δ 8.3 (d, J = 8.2 Hz, 2H, N=CHCCH x 2), 7.7-7.6 (m, 6H, CH Ar x 6), 7.6 (s, 1H, <sup>-</sup>O<sup>+</sup>N=CH), 5.1 (s, 2H, <sup>-</sup>O<sup>+</sup>NCH<sub>2</sub>). <sup>13</sup>C NMR (100 MHz, CDCl<sub>3</sub>) δ 144.5 (C Ar), 142.2 (C Ar), 141.5 (C Ar), 135.2 (N=CH(Ph)), 128.1 (CH Ar), 127.9 (CH Ar), 127.6 (CH Ar), 127.5 (CH Ar), 127.3 (CH Ar), 126.5 (q, J<sub>C-F</sub> = 3.8 Hz, CF<sub>3</sub>), 125.9 (q, J<sub>C-F</sub> = 3.8 Hz, CF<sub>3</sub>), 65.4, (PhCH<sub>2</sub>N). <sup>19</sup>F NMR (500 MHz, neat, 110 °C) δ -63.30 (s, 6F, CF<sub>3</sub>), -63.40 (s, 6F, CF<sub>3</sub>). ESI-MS (*m/z*): [M + H]<sup>1+</sup> calcd for C<sub>22</sub>H<sub>22</sub>NO, 348.0823; found, 348.0811.

**2-(*p*-trifluoromethylbenzyl)-3-(*p*-trifluorophenyl)-5-phenylisoxazolidine**

*N*-(*p*-trifluoromethylbenzyl)-*N*-(*p*-trifluorophenyl) nitronone (0.08 mmol, 0.035 g) was dissolved in styrene (2 mL) and left stirring at 140 °C for 2 h.

The solvent was removed by rotary evaporator and the product was purified by column chromatography on silica [petroleum ether / ethyl acetate (9:1)]. Colourless oil. Yield: 0.01 g, 27%.

$R_f$  0.4 (PET:EtOAc 9:1).  $^1\text{H}$  NMR (400 MHz,  $\text{CDCl}_3$ )  $\delta$  7.7-7.2 (m, 13H, CH Ar), 5.2 (t,  $J = 7.7$  Hz, 1H, PhCHO), 4.1 (t,  $J = 8.0$  Hz, 1H, PhCHN), 4.0 (s br, 2H, NCH<sub>2</sub>Ph), 2.7-2.6 (m, 2H, OCH(Ph)CH<sub>2</sub>).  $^{13}\text{C}$  NMR (100 MHz,  $\text{CDCl}_3$ )  $\delta$  144.1 (C Ar), 141.7 (C Ar), 141.5 (C Ar), 129.3 (CH Ar), 128.9 (CH Ar), 128.8 (CH Ar), 128.7 (CH Ar), 128.6 (CH Ar), 128.3 (CH Ar), 126.8 (CH Ar), 126.2 (q,  $J_{\text{C-F}} = 3.84$  Hz, CF<sub>3</sub>), 125.5 (q,  $J_{\text{C-F}} = 3.84$  Hz, CF<sub>3</sub>), 79.3 (OCH(Ph)), 70.5 (NCH(Ph)) 60.1, (PhCH<sub>2</sub>N), 47.8 (NCH(Ph)CH<sub>2</sub>).  $^{19}\text{F}$  NMR (500 MHz, neat, 100°C)  $\delta$  -63.3 (s, 6F, CF<sub>3</sub>), -63.4 (s, 6F, CF<sub>3</sub>). ESI-MS ( $m/z$ ):  $[\text{M} + \text{H}]^+$  calcd for C<sub>24</sub>H<sub>20</sub>F<sub>6</sub>NO, 452.1449; found, 452.1430.





## List of abbreviations

$\mu$	Micron
2,5-DTBBQ	2,5-Di- <i>tert</i> -butyl-1,4-benzoquinone
2,5-DTBHQ	2,5-Di- <i>tert</i> -butyl-hydroquinone
Å	Angstrom
AIBN	Azobisisobutyronitrile
Ar	Aromatic ring
AU	Arbitrary units
BDE	Bond dissociation energy
br	Broad
Bz	Benzyl
CTC	Charge transfer complex
d	Doublet
DBHA	<i>N,N</i> -Dibenzylhydroxylamine
DCM	Dichloromethane
dd	Doublet of doublets
dt	Doublet of triplets
ESI MS	Electrospray mass spectrometry
Et	Ethyl
EtOAc	Ethyl acetate
FDI	Flame ionisation detector
G	Gauss
GC-EI	Gas chromatography with electron impact
GC-FI	Gas chromatography with field ionization
h	Hours
J	Coupling constant (Hertz)
M	Molarity (mol/L)
m	Multiplet
mDa	Milli Dalton
M.P.	Melting point

MHz	Megahertz
Min	Minute
NMP	Nitroxide mediated polymerization
OD	Outside diameter
PET ether	petroleum ether
ppm	Parts per million
s	Singlet
sec	Seconds
t	Triplet
t-Bu	<i>tert</i> -Butyl
THF	Tetrahydrofuran
$\delta$	Chemical shift for NMR spectra

---

## References

1. PRINCIPLES OF POLYMERIZATION, Odian, G., Second ed.; John Wiley & Sons: Canada, **1981**; p 731.
2. Styrene Monomer: Environmental, Health & Safety Guidelines Home Page <http://www.styrenemonomer.org/> (accessed October 10, 2011).
3. Li, X.-R.; Wang, X.-L.; Koseki, H., STUDY ON THERMAL DECOMPOSITION CHARACTERISTICS OF AIBN. *JOURNAL OF HAZARDOUS MATERIALS* **2008**, *159* (1), 13-18.
4. Chetia, P. D.; Dass, N. N., EFFECTS OF TRIS (PHENANTHROLINE)-IRON(III) COMPLEX ON POLYMERIZATION OF STYRENE. *European Polymer Journal* **1976**, *12* (3), 165-168.
5. Bowman, D. F.; Gillan, T.; Ingold, K. U., KINETIC APPLICATIONS OF ELECTRON PARAMAGNETIC RESONANCE SPECTROSCOPY .3. SELF-REACTIONS OF DIALKYL NITROXIDE RADICALS. *Journal of the American Chemical Society* **1971**, *93* (24), 6555-6561.
6. Mayo, F. R., CHAIN TRANSFER IN THE POLYMERIZATION OF STYRENE .8. CHAIN TRANSFER WITH BROMOBENZENE AND MECHANISM OF THERMAL INITIATION. *Journal of the American Chemical Society* **1953**, *75* (24), 6133-6141.
7. Mayo, F. R., DIMERIZATION OF STYRENE. *Journal of the American Chemical Society* **1968**, *90* (5), 1289-1295.
8. Kopecky, K. R.; Evani, S., MECHANISM OF INITIATION IN THERMAL POLYMERIZATION OF STYRENE . KINETIC DEUTERIUM ISOTOPE EFFECTS IN INITIATION STEP OF THERMAL POLYMERIZATION OF SOME DEUTERATED STYRENES. *Canadian Journal of Chemistry* **1969**, *47* (21), 4049-4058.
9. Flory, P. J., THE MECHANISM OF VINYL POLYMERIZATIONS. *Journal of the American Chemical Society* **1937**, (59), 241-253.

10. Greszta, D.; Matyjaszewski, K., MECHANISM OF CONTROLLED/"LIVING" RADICAL POLYMERIZATION OF STYRENE IN THE PRESENCE OF NITROXYL RADICALS. KINETICS AND SIMULATIONS. *Macromolecules* **1996**, *29* (24), 7661-7670.
11. Khuong, K. S.; Jones, W. H.; Pryor, W. A.; Houk, K. N., THE MECHANISM OF THE SELF-INITIATED THERMAL POLYMERIZATION OF STYRENE. THEORETICAL SOLUTION OF A CLASSIC PROBLEM. *Journal of the American Chemical Society* **2005**, *127* (4), 1265-1277.
12. Styrene monomer-Chevron Phillips <http://www.cpchem.com/bl/aromatics/en-us/Pages/StyreneMonomer.aspx> (accessed October 2012).
13. Conte, M.; Ma, Y.; Loyns, C.; Price, P.; Rippon, D.; Chechik, V., MECHANISTIC INSIGHT INTO TEMPO-INHIBITED POLYMERISATION: SIMULTANEOUS DETERMINATION OF OXYGEN AND INHIBITOR CONCENTRATIONS BY EPR. *Organic & Biomolecular Chemistry* **2009**, *7* (13), 2685-2687.
14. Kende, I.; Sumegi, L.; Tudos, F., INVESTIGATION OF EFFECT OF NITROSO-COMPOUNDS ON FREE-RADICAL POLYMERIZATION. *European Polymer Journal* **1972**, *8* (11), 1281-1289.
15. Tudos, F.; Foldesberezsnich, T., FREE-RADICAL POLYMERIZATION - INHIBITION AND RETARDATION. *Progress in Polymer Science* **1989**, *14* (6), 717-761.
16. Bowry, V. W.; Ingold, K. U., KINETICS OF NITROXIDE RADICAL TRAPPING .2. STRUCTURAL EFFECTS. *Journal of the American Chemical Society* **1992**, *114* (13), 4992-4996.
17. Mardare, D.; Matyjaszewski, K., THERMAL POLYMERIZATION OF STYRENE IN THE PRESENCE OF STABLE RADICALS AND INHIBITORS. *Abstracts of Papers of the American Chemical Society* **1994**, *207*, 267-270.
18. Hodgson, J. L.; Roskop, L. B.; Gordon, M. S.; Lin, C. Y.; Coote, M. L., SIDE REACTIONS OF NITROXIDE-MEDIATED POLYMERIZATION: N-O VERSUS O-C CLEAVAGE OF ALKOXYAMINES. *Journal of Physical Chemistry A* **2010**, *114* (38), 10458-10466.

- 
19. Maillard, B.; Ingold, K. U.; Scaiano, J. C., RATE CONSTANTS FOR THE REACTIONS OF FREE-RADICALS WITH OXYGEN IN SOLUTION. *Journal of the American Chemical Society* **1983**, *105* (15), 5095-5099.
20. OXIDATION AND ANTIOXIDANTS IN ORGANIC CHEMISTRY AND BIOLOGY, Denisov, E. T.; I.B.Afanas'ev,. Taylor & Francis: Amsterdam, **2005**; p 1024.
21. Goldstein, S.; Samuni, A., KINETICS AND MECHANISM OF PEROXYL RADICAL REACTIONS WITH NITROXIDES. *Journal of Physical Chemistry A* **2007**, *111* (6), 1066-1072.
22. Batch, G. L.; Macosko, C. W., OXYGEN INHIBITION IN DIFFERENTIAL SCANNING CALORIMETRY OF FREE-RADICAL POLYMERIZATION. *Thermochimica Acta* **1990**, *166*, 185-198.
23. Stepin, S. G.; Dikumar, E. A., POLYMERIZATION OF STYRENE INITIATED BY ACETYLENIC PEROXIDES. *Russian Journal of Applied Chemistry* **2009**, *82* (1), 128-131.
24. Gridnev, A. A., HYDROGEN TRANSFER REACTIONS OF NITROXIDES IN FREE RADICAL POLYMERIZATIONS. *Macromolecules* **1997**, *30* (25), 7651-7654.
25. Kurland, J. J., QUANTITATIVE ASPECTS OF SYNERGISTIC INHIBITION OF OXYGEN AND PARA-METHOXYPHENOL IN ACRYLIC-ACID POLYMERIZATION. *Journal of Polymer Science: Polymer Chemistry* **1980**, *18* (3), 1139-1145.
26. Safe Handling and Storage of Styrene Monomer [http://www.cpchem.com/bl/aromatics/en-us/Documents/Safe Handling and Storage of Styrene Monomer.pdf](http://www.cpchem.com/bl/aromatics/en-us/Documents/Safe_Handling_and_Storage_of_Styrene_Monomer.pdf) (accessed 14 February, 2014).
27. Franchi, P.; Lucarini, M.; Pedulli, G. F.; Valgimigli, L.; Lunelli, B., REACTIVITY OF SUBSTITUTED PHENOLS TOWARD ALKYL RADICALS. *Journal of the American Chemical Society* **1999**, *121* (3), 507-514.

28. Burton, G. W.; Ingold, K. U., AUTOXIDATION OF BIOLOGICAL MOLECULES .1. THE ANTIOXIDANT ACTIVITY OF VITAMIN-E AND RELATED CHAIN-BREAKING PHENOLIC ANTIOXIDANTS INVITRO. *Journal of the American Chemical Society* **1981**, *103* (21), 6472-6477.
29. Levy, L. B., INHIBITION OF ACRYLIC-ACID POLYMERIZATION BY PHENOTHIAZINE AND PARA-METHOXYPHENOL .2. CATALYTIC INHIBITION BY PHENOTHIAZINE. *Journal of Polymer Science: Polymer Chemistry* **1992**, *30* (4), 569-576.
30. Levy, L. B., INHIBITION OF ACRYLIC-ACID POLYMERIZATION BY PHENOTHIAZINE AND PARA-METHOXYPHENOL. *Journal of Polymer Science: Polymer Chemistry* **1985**, *23* (5), 1505-1515.
31. Weyler, S.; James, P.; Erpeldinger, O.; Neumann, M.; Kraushaar, F. PROCESS FOR STABILIZING OLEFINICALLY UNSATURATED MONOMERS. Unites States patent 8128804 B2, **2012**.
32. Loyns, C.; Fawbert, A. N.; Glossop, A. J.; Price, P. M. RETARDER COMPOSITION. World intellectual property organization WO 2012/004605 A1, **2012**.
33. Arhancet, G. B.; Henrici, I. K. TREATMENTS FOR INHIBITING VINIYL AROMATIC MONOMER POLYMERIZATION. World intellectual property organization WO/1996/041783, **1996**.
34. Arhancet, G. B. METHODS FOR INHIBITING VINYL AROMATIC MONOMER POLYMERIZATION. United States patents 5446220 A, **1995**.
35. Denisov, E. T.; Khudyakov, I. V., MECHANISMS OF ACTION AND REACTIVITIES OF THE FREE-RADICALS OF INHIBITORS. *Chemical Reviews* **1987**, *87* (6), 1313-1357.
36. Pospisil, J.; Nespurek, S., CHAIN-BREAKING STABILIZERS IN POLYMERS - THE CURRENT STATUS. *Polymer Degradation and Stability*. **1995**, *49* (1), 99-110.
37. Sigma-Aldrich Co.- Dinoseb  
<http://www.sigmaaldrich.com/catalog/search?interface=All&term=dinoseb&N=0&mo>

- [de=match%20partialmax&focus=product&lang=en&region=GB](#) (accessed 25 August, 2014).
38. ECHA European Chemicals Agency <http://echa.europa.eu/> (accessed 14 August, 2014).
39. European Chemicals Agency <http://echa.europa.eu/regulations> (accessed 25 August, 2014).
40. European Commission-Enterprise and Industry [http://ec.europa.eu/enterprise/sectors/chemicals/documents/classification/index\\_en.htm](http://ec.europa.eu/enterprise/sectors/chemicals/documents/classification/index_en.htm) (accessed 14 August, 2014 ).
41. REACH legislation, nanomaterials, guidance, archives [http://ec.europa.eu/enterprise/sectors/chemicals/documents/reach/index\\_en.htm#h2-1](http://ec.europa.eu/enterprise/sectors/chemicals/documents/reach/index_en.htm#h2-1) (accessed 25 August, 2014).
42. Perez, V. V. INHIBITING POLYMERIZATION OF VINYL AROMATIC COMPOUNDS. European patents EP0240297, **1987**.
43. Klemchuk, P.; Heights, Y. SUBSTITUTED HYDROXYLAMINE ANTI-OXIDANTS. United States Patent 3,867,445, **1975**.
44. Amorati, R.; Lucarini, M.; Mugnaini, V.; Pedulli, G. F.; Minisci, F.; Recupero, F.; Fontana, F.; Astolfi, P.; Greci, L., HYDROXYLAMINES AS OXIDATION CATALYSTS: THERMOCHEMICAL AND KINETIC STUDIES. *Journal of Organic Chemistry* **2003**, *68* (5), 1747-1754.
45. HANDBOOK OF BOND DISSOCIATION ENERGIES IN ORGANIC COMPOUNDS. Luo, Y.-R., 1st ed.; CRC Press: Boca Raton, Florida, **2002**, p. 381.
46. Ma, Y., NITROXIDES IN MECHANISTIC STUDIES: AGEING OF GOLD NANOPARTICLES AND NITROXIDE TRANSFORMATION IN ACIDS. PhD Thesis, White Rose eTheses Online, **2010**.



- 
47. Blanksby, S. J.; Ellison, G. B., BOND DISSOCIATION ENERGIES OF ORGANIC MOLECULES. *Accounts of Chemical Research* **2003**, *36* (4), 255-263.
48. Bertin, D.; Gigmes, D.; Marque, S. R. A.; Tordo, P., KINETIC SUBTLETIES OF NITROXIDE MEDIATED POLYMERIZATION. *Chemical Society Reviews* **2011**, *40* (5), 2189-2198.
49. Lagrille, O.; Cameron, N. R.; Lovell, P. A.; Blanchard, R.; Goeta, A. E.; Koch, R., NOVEL ACYCLIC NITROXIDES FOR NITROXIDE-MEDIATED POLYMERIZATION: KINETIC, ELECTRON PARAMAGNETIC RESONANCE SPECTROSCOPIC, X-RAY DIFFRACTION, AND MOLECULAR MODELING INVESTIGATIONS. *Journal of Polymer Science: Polymer Chemistry* **2006**, *44* (6), 1926-1940.
50. Nilsen, A.; Braslau, R., NITROXIDE DECOMPOSITION: IMPLICATIONS TOWARD NITROXIDE DESIGN FOR APPLICATIONS IN LIVING FREE-RADICAL POLYMERIZATION. *Journal of Polymer Science: Polymer Chemistry* **2006**, *44* (2), 697-717.
51. Chauvin, F.; Dufils, P.-E.; Gigmes, D.; Guillaneuf, Y.; Marque, S. R. A.; Tordo, P.; Bertin, D., NITROXIDE-MEDIATED POLYMERIZATION: THE PIVOTAL ROLE OF THE K(D) VALUE OF THE INITIATING ALKOXYAMINE AND THE IMPORTANCE OF THE EXPERIMENTAL CONDITIONS. *Macromolecules* **2006**, *39* (16), 5238-5250.
52. Ohkatsu, Y.; Baba, R.; Watanabe, K., RADICAL SCAVEGING MECHANISM OF DISTEARYL HYDROXYLAMINE ANTIOXIDANT. *Journal of the Japan Petroleum Institute* **2011**, *54* (1), 15-21.
53. Brustolon, M.; Giamello, E., ELECTRON PARAMAGNETIC RESONANCE-A PRACTITIONER'S TOOLKIT John Wiley & Sons: New Jersey, **2009**, p.608.
54. Stoneham, A. M., LINEWIDTHS WITH GAUSSIAN AND LORENTZIAN BROADENING. *Journal of Physics D-Applied Physics* **1972**, *5* (3), 670-681.
55. Flore-Llamas, H.; Yee-Madeira, H., THE DECONVOLUTION AND EVALUATION OF THE AREA UNDER THE ESR LINES. *Journal of Physics D: Applied Physics* **1992**, *25*, 970-973.

- 
56. Bales, B. L.; Peric, M.; Lamy-Freund, M. T., CONTRIBUTIONS TO THE GAUSSIAN LINE BROADENING OF THE PROXYL SPIN PROBE EPR SPECTRUM DUE TO MAGNETIC-FIELD MODULATION AND UNRESOLVED PROTON HYPERFINE STRUCTURE. *Journal of Magnetic Resonance* **1998**, *132* (2), 279-286.
57. Poole, C. P.; Farach, H., A., LINE SHAPES IN ELECTRON SPIN RESONANCE. *Bulletin of Magnetic Resonance*. **1978**, *1* (4), 162-194.
58. Smirnov, A. I., EWVOIGT AND EWVOIGTN: INHOMOGENEOUS LINE SHAPE SIMULATION AND FITTING PROGRAMS. *ESR Spectroscopy in Membrane Biophysics*. **2007**, *27*, 289-297.
59. Smirnov, A. I.; Clarkson, R. B.; Belford, R. L., EPR LINEWIDTH (T-2) METHOD TO MEASURE OXYGEN PERMEABILITY OF PHOSPHOLIPID BILAYERS AND ITS USE TO STUDY THE EFFECT OF LOW ETHANOL CONCENTRATIONS. *Journal of Magnetic Resonance Series B* **1996**, *111* (2), 149-157.
60. BIOLOGICAL MAGNETIC RESONANCE. Hemminga, M. A.; Berliner, L. J., Kluwer Academic, Plenum Publ: New York, **2007**; Vol. 27, p. 380.
61. Geng, M.; Duan, Z., PREDICTION OF OXYGEN SOLUBILITY IN PURE WATER AND BRINES UP TO HIGH TEMPERATURES AND PRESSURES. *Geochimica Et Cosmochimica Acta* **2010**, *74* (19), 5631-5640.
62. Kuzmic, P., PROGRAM DYNAFIT FOR THE ANALYSIS OF ENZYME KINETIC DATA: APPLICATION TO HIV PROTEINASE. *Analytical Biochemistry* **1996**, *237* (2), 260-273.
63. Marque, S., INFLUENCE OF THE NITROXIDE STRUCTURE ON THE HOMOLYSIS RATE CONSTANT OF ALKOXYAMINES: A TAFT-INGOLD ANALYSIS. *Journal of Organic Chemistry* **2003**, *68* (20), 7582-7590.
64. Braslau, R.; O'Bryan, G.; Nilsen, A.; Henise, J.; Thongpaisanwong, T.; Murphy, E.; Mueller, L.; Ruehl, J., THE SYNTHESIS AND EVALUATION OF NEW ALPHA-HYDROGEN NITROXIDES FOR 'LIVING' FREE RADICAL POLYMERIZATION. *Synthesis* **2005**, (9), 1496-1506.

65. Reznikov, V. A.; Volodarsky, L. B., STABLE NITROXIDES WITH HYDROGEN AT ALPHA-CARBON OF THE NITROXYL GROUP. *Tetrahedron Letters* **1994**, *35* (14), 2239-2240.
66. Adeleke, B. B.; Wong, S. K.; Wan, J. K. S., ELECTRON-SPIN RESONANCE STUDY OF ARYLSILYL ADDUCTS OF PHENYL TERT-BUTYL NITRONE AND THEIR DECOMPOSITION KINETICS. *Canadian Journal of Chemistry-Revue Canadienne De Chimie* **1974**, *52* (16), 2901-2905.
67. Alewood, P. F.; Hussain, S. A.; Jenkins, T. C.; Perkins, M. J.; Sharma, A. H.; Siew, N. P. Y.; Ward, P., ACYL NITROXIDES .1. SYNTHESIS AND ISOLATION. *Journal of the Chemical Society-Perkin Transactions 1* **1978**, (9), 1066-1076.
68. Sen, V. D.; Golubev, V. A.; Efremova, N. N., KINETICS AND MECHANISM OF THE WO<sub>4</sub><sup>2-</sup>-CATALYZED OXIDATION OF DI-TERT-ALKYLAMINES AND DI-TERT-ALKYLHYDROXYLAMINES TO NITROXYL RADICALS BY HYDROGEN-PEROXIDE. *Bulletin of the Academy of Sciences of the Ussr Division of Chemical Science* **1982**, *31* (1), 53-63.
69. Kirilyuk, I. A.; Bobko, A. A.; Grigorev, I. A.; Khramtsov, V. V., SYNTHESIS OF THE TETRAETHYL SUBSTITUTED PH-SENSITIVE NITROXIDES OF IMIDAZOLE SERIES WITH ENHANCED STABILITY TOWARDS REDUCTION. *Organic & Biomolecular Chemistry* **2004**, *2* (7), 1025-1030.
70. Couet, W. R.; Brasch, R. C.; Sosnovsky, G.; Lukszo, J.; Prakash, I.; Gnewuch, C. T.; Tozer, T. N., INFLUENCE OF CHEMICAL-STRUCTURE OF NITROXYL SPIN LABELS ON THEIR REDUCTION BY ASCORBIC-ACID. *Tetrahedron* **1985**, *41* (7), 1165-1172.
71. Mezzina, E.; Cruciani, F.; Pedulli, G. F.; Lucarini, M., NITROXIDE RADICALS AS PROBES FOR EXPLORING THE BINDING PROPERTIES OF THE CUCURBIT 7 URIL HOST. *Chemistry-a European Journal* **2007**, *13* (25), 7223-7233.
72. Gutch, C. J. W.; Waters, W. A., ELECTRON SPIN RESONANCE SPECTRA OF SOME HYDROXYLAMINE FREE RADICALS. *Journal of the Chemical Society* **1965**, (JAN), 751-755.

73. Serianz, A.; Shelton, J. R.; Urbach, F. L.; Dunbar, R. C.; Kopczewski, R. F., 2 ESR SYSTEMS FOR ADVANCED UNDERGRADUATE LABORATORY. *Journal of Chemical Education* **1976**, *53* (6), 394-395.
74. Cowley, D. J.; Waters, W. A., KINETIC STUDY BY USE OF ELECTRON SPIN RESONANCE OF AUTOXIDATION OF NN-DIBENZYLHYDROXYLAMINE. *Journal of the Chemical Society B-Physical Organic* **1970**, (1), 96-101.
75. Kurland, J. J., PROCESS FOR PREPARING SILVER(I)-EXCHANGED RESINS. United States patents 5,139,981, **1992**.
76. Aleksandrov, A. L., METHYL- AND TERT-BUTYL-SUBSTITUTED HYDROQUINONES AND SEMIQUINONE RADICALS: BOND STRENGTH ESTIMATES, ENTHALPY OF FORMATION, AND THE RATE CONSTANTS OF THEIR REACTIONS WITH PEROXY RADICALS. *Kinetics and Catalysis* **2006**, *47* (5), 672-676.
77. Valgimigli, L.; Amorati, R.; Fumo, M. G.; DiLabio, G. A.; Pedulli, G. F.; Ingold, K. U.; Pratt, D. A., THE UNUSUAL REACTION OF SEMIQUINONE RADICALS WITH MOLECULAR OXYGEN. *Journal of Organic Chemistry* **2008**, *73* (5), 1830-1841.
78. Loshadkin, D.; Roginsky, V.; Pliss, E., SUBSTITUTED P-HYDROQUINONES AS A CHAIN-BREAKING ANTIOXIDANT DURING THE OXIDATION OF STYRENE. *International Journal of Chemical Kinetics* **2002**, *34* (3), 162-171.
79. Maslovskaya, L. A.; Polyakov, Y. S.; Savchenko, A. I., INTERACTION OF ALKYL RADICALS WITH DIHYDRIC PHENOL DERIVATIVES IN HEXANE SOLUTIONS UNDER GAMMA-RADIOLYSIS. *High Energy Chemistry* **2002**, *36* (4), 213-216.
80. Engel, P. S.; Park, H. J.; Mo, H.; Duan, S., THE REACTION OF ALPHA-PHENETHYL RADICALS WITH 1,4-BENZOQUINONE AND 2,6-DI-TERT-BUTYL-1,4-BENZOQUINONE. *Tetrahedron* **2010**, *66* (46), 8805-8814.
81. Yassin, A. A.; Elreedy, A. M., MECHANISMS OF RETARDATION AND INHIBITION IN RADICAL POLYMERIZATIONS BY QUINONES. *European Polymer Journal* **1973**, *9* (7), 657-667.

82. Cohen, S. G., INHIBITION AND RETARDATION OF THE PEROXIDE INITIATED POLYMERIZATION OF STYRENE. *Journal of the American Chemical Society* **1947**, *69* (5), 1057-1064.
83. Hageman, H. J., THE THERMAL DECOMPOSITION OF 2,2'-AZOBIS(2-METHYLPROPIONITRILE) IN THE PRESENCE OF 2,6-DI-T-BUTYL AND 2,6-DIPHENYL-1,4-BENZOQUINONE. *European Polymer Journal* **2000**, *36* (2), 345-350.
84. Simandi, T. L.; Tudos, F., KINETICS OF RADICAL POLYMERIZATION .45. STERIC EFFECTS IN THE RADICAL REACTIVITY OF QUINONES. *European Polymer Journal* **1985**, *21* (10), 865-869.
85. Adams, R. D.; Miao, S. B., METAL CARBONYL DERIVATIVES OF 1,4-QUINONE AND 1,4-HYDROQUINONE. *Journal of the American Chemical Society* **2004**, *126* (16), 5056-5057.
86. Parker, V. D., HYDROQUINONE-QUINONE REDOX BEHAVIOUR IN ACETONITRILE. *Journal of the Chemical Society D-Chemical Communications* **1969**, (13), 716-717.
87. Eggins, B. R., INTERPRETATION OF ELECTROCHEMICAL REDUCTION AND OXIDATION WAVES OF QUINONE-HYDROQUINONE SYSTEM IN ACETONITRILE. *Journal of the Chemical Society D-Chemical Communications* **1969**, (21), 1267-1268.
88. Mayer, J. M.; Rhile, I. J., THERMODYNAMICS AND KINETICS OF PROTON-COUPLED ELECTRON TRANSFER: STEPWISE VS. CONCERTED PATHWAYS. *Biochimica et Biophysica Acta-Bioenergetics* **2004**, *1655* (1-3), 51-58.
89. Song, N.; Gagliardi, C. J.; Binstead, R. A.; Zhang, M.-T.; Thorp, H.; Meyer, T. J., ROLE OF PROTON-COUPLED ELECTRON TRANSFER IN THE REDOX INTERCONVERSION BETWEEN BENZOQUINONE AND HYDROQUINONE. *Journal of the American Chemical Society* **2012**, *134* (45), 18538-18541.
90. Graige, M. S.; Paddock, M. L.; Bruce, J. M.; Feher, G.; Okamura, M. Y., MECHANISM OF PROTON-COUPLED ELECTRON TRANSFER FOR QUINONE (Q(B))

REDUCTION IN REACTION CENTERS OF RB-SPHAEROIDES. *Journal of the American Chemical Society* **1996**, *118* (38), 9005-9016.

91. Zhu, X. Q.; Wang, C. H.; Liang, H., SCALES OF OXIDATION POTENTIALS, PK(A), AND BDE OF VARIOUS HYDROQUINONES AND CATECHOLS IN DMSO. *Journal of Organic Chemistry* **2010**, *75* (21), 7240-7257.

92. Klein, E.; Lukes, V., DFT/B3LYP STUDY OF THE SUBSTITUENT EFFECT ON THE REACTION ENTHALPIES OF THE INDIVIDUAL STEPS OF SINGLE ELECTRON TRANSFER-PROTON TRANSFER AND SEQUENTIAL PROTON LOSS ELECTRON TRANSFER MECHANISMS OF PHENOLS ANTIOXIDANT ACTION. *Journal of Physical Chemistry A* **2006**, *110* (44), 12312-12320.

93. Miller, A. A.; Mayo, F. R., OXIDATION OF UNSATURATED COMPOUNDS .1. THE OXIDATION OF STYRENE. *Journal of the American Chemical Society* **1956**, *78* (5), 1017-1023.

94. Mayo, F. R.; Miller, A. A., OXIDATION OF UNSATURATED COMPOUNDS .2. REACTIONS OF STYRENE PEROXIDE. *Journal of the American Chemical Society* **1956**, *78* (5), 1023-1034.

95. Krstina, J.; Moad, G.; Willing, R. I.; Danek, S. K.; Kelly, D. P.; Jones, S. L.; Solomon, D. H., FURTHER-STUDIES ON THE THERMAL-DECOMPOSITION OF AIBN IMPLICATIONS CONCERNING THE MECHANISM OF TERMINATION IN METHACRYLONITRILE POLYMERIZATION. *European Polymer Journal* **1993**, *29* (2-3), 379-388.

96. Free radical initiators <http://www.sigmaaldrich.com/materials-science/material-science-products.html?TablePage=16374963> (accessed 4 January 2012).

97. Yassin, A. A.; Rizk, N. A., CHARGE-TRANSFER COMPLEXES AS POLYMERIZATION INHIBITORS .3. STUDIES ON MECHANISM OF INHIBITION AND RETARDATION OF

STYRENE POLYMERIZATION BY N, N-DIMETHYLANILINE-CHLORANIL COMPLEXES. *British Polymer Journal* **1977**, *9* (4), 322-325.

98. Hassan, A.; Wazeer, M. I. M.; Ali, S. A., OXIDATION OF N-BENZYL-N-METHYLHYDROXYLAMINES TO NITRONES. A MECHANISTIC STUDY. *Journal of the Chemical Society-Perkin Transactions 2* **1998**, (2), 393-399.

99. ORGANIC CHARGE-TRANSFER COMPLEXES. Foster, R., Academic Press: London, New York, **1969**, 470 p.

100. Mulliken, R. S., MOLECULAR COMPOUNDS AND THEIR SPECTRA .2. *Journal of the American Chemical Society* **1952**, *74* (3), 811-824.

101. Al-Ahmary, K. M.; Habeeb, M. M.; Al-Solmy, E. A., SPECTROPHOTOMETRIC STUDY ON THE CHARGE-TRANSFER REACTION BETWEEN 4-AMINOPYRIDINE WITH 2,5-DIHYDROXY-P-BENZOQUINONE IN METHANOL AND THE BINARY MIXTURE 50% ACETONITRILE+50% 1,4-DIOXANE (V/V). *Physics and Chemistry of Liquids* **2013**, *51* (5), 621-634.

102. Subhani, M. S.; Bhatti, N. K.; Mohammad, M.; Khan, A. Y., SPECTROSCOPIC STUDIES OF CHARGE-TRANSFER COMPLEXES OF 2,3-DICHLORO-5,6-DICYANO-P-BENZOQUINONE. *Turkish Journal of Chemistry* **2000**, *24* (3), 223-230.

103. MODERN PHYSICAL ORGANIC CHEMISTRY. Anslyn, E. V.; Dougherty, D. A., University Science Books: United States, **2006**; p 1095.

104. Salama, N. N.; Abdel-Razeq, S. A.; Abdel-Atty, S., SPECTROPHOTOMETRIC DETERMINATION AND THERMODYNAMIC STUDIES OF THE CHARGE TRANSFER COMPLEXES OF AZELASTINE-HCL. *Bulletin of Faculty of Pharmacy, Cairo University* **2011**, *49*, 13-18.

105. Cohen, N., PREDICTING THE PREEXPONENTIAL TEMPERATURE-DEPENDENCE OF BIMOLECULAR METATHESIS REACTION-RATE COEFFICIENTS USING TRANSITION-STATE THEORY. *International Journal of Chemical Kinetics* **1989**, *21* (10), 909-922.

106. Delamare, P. B. D.; Fowden, L.; Hughes, E. D.; Ingold, C. K.; Mackie, J. D. H., MECHANISM OF SUBSTITUTION AT A SATURATED CARBON ATOM .159. ANALYSIS OF STERIC AND POLAR EFFECTS OF ALKYL GROUPS IN BIMOLECULAR NUCLEOPHILIC SUBSTITUTION, WITH SPECIAL REFERENCE TO HALOGEN EXCHANGES. *Journal of the Chemical Society* **1955**, 3200-3236.
107. Church, D. F., SUBSTITUENT EFFECTS ON NITROXIDE HYPERFINE SPLITTING CONSTANTS. *Journal of Organic Chemistry* **1986**, 51 (7), 1138-1140.
108. Hassan, A.; Wazeer, M. I. M.; Saeed, M. T.; Siddiqui, M. N.; Ali, S. A., REGIOCHEMISTRY AND MECHANISM OF OXIDATION OF N-BENZYL-N-ALKYLHYDROXYLAMINES TO NITRONES. *Journal of Physical Organic Chemistry* **2000**, 13 (8), 443-451.
109. Shimizu, T.; Ishizaki, M.; Nitada, N., THE EFFECTS OF LEWIS ACID ON THE 1,3-DIPOLAR CYCLOADDITION REACTION OF C-ARYLALDONITRONES WITH ALKENES. *Chemical & Pharmaceutical Bulletin* **2002**, 50 (7), 908-921.
110. Shiraishi, S.; Inoue, Y.; Imamura, K., THE CYCLOADDITION OF N,ALPHA-DIARYLNITRONES AND SUBSTITUTED PARA-BENZOQUINONES. *The Bulletin of the Chemical Society of Japan* **1991**, 64 (8), 2388-2392.
111. Demarch, P.; Escoda, M.; Figueredo, M.; Font, J., EFFICIENT MASKING OF P-BENZOQUINONE IN NITRONE CYCLOADDITION CHEMISTRY. *Tetrahedron Letters* **1995**, 36 (47), 8665-8668.
112. Paul, R. R.; Varghese, V.; Beneesh, P. B.; Sinu, C. R.; Suresh, E.; Anabha, E. R., NITRONE CYCLOADDITION TO QUINONES: A NOVEL STRATEGY FOR THE SYNTHESIS OF BENZISOXAZOLIDENES. *Journal of Heterocyclic Chemistry* **2010**, 47 (2), 396-399.
113. Schneider, C.; Brauner, J., LEWIS BASE-CATALYZED ADDITION OF TRIALKYLALUMINUM COMPOUNDS TO EPOXIDES. *European Journal of Organic Chemistry* **2001**, (23), 4445-4450.



114. Corey, E. J.; Suggs, J. W., PYRIDINIUM CHLOROCHROMATE - EFFICIENT REAGENT FOR OXIDATION OF PRIMARY AND SECONDARY ALCOHOLS TO CARBONYL-COMPOUNDS. *Tetrahedron Letters* **1975**, (31), 2647-2650.
115. Yang, S. H.; Chang, S. B., HIGHLY EFFICIENT AND CATALYTIC CONVERSION OF ALDOXIMES TO NITRILES. *Org. Lett.* **2001**, 3 (26), 4209-4211.
116. Aschwanden, P.; Frantz, D. E.; Carreira, E. M., SYNTHESIS OF 2,3-DIHYDROISOXAZOLES FROM PROPARGYLIC N-HYDROXYLAMINES VIA ZN(II)-CATALYZED RING-CLOSURE REACTION. *Organic Letters* **2000**, 2 (15), 2331-2333.
117. Jones, L. W.; Sneed, M. C., A STUDY OF BETA-BENZYLFORMHYDROXAMIC ACID. *Journal of the American Chemical Society* **1917**, 39, 674-679.
118. Andoh, F.; Kubo, K.; Sakurai, T., IMINE-FORMING RADICAL ELIMINATION REACTIONS OF O-(1-NAPHTHOYL)-N,N-BIS(P-SUBSTITUTED BENZYL)HYDROXYLAMINES ACTIVATED BY TRIPLET BENZOPHENONE. *The Bulletin of Chemical Society of Japan* **1999**, 72 (11), 2537-2542.
119. Murahashi, S. I.; Mitsui, H.; Watanabe, T.; Zenki, S. I., THE REACTION OF N-MONO AND N,N-DISUBSTITUTED HYDROXYLAMINES WITH PALLADIUM CATALYST. *Tetrahedron Letters* **1983**, 24 (10), 1049-1052.
120. Friebolin, H., BASIC ONE- AND TWO-DIMENSIONAL NMR SPECTROSCOPY, 3<sup>rd</sup> ed.; Wiley: Virginia, **2010**; p 430.
121. Ricca, A.; Tronchet, J. M. J.; Weber, J.; Ellinger, Y., CONFORMATIONAL DEPENDENCE OF BETA HYPERFINE COUPLING-CONSTANTS IN THE NITROXIDE SERIES. *Journal of Physical Chemistry* **1992**, 96 (26), 10779-10784.
122. Iizuka, Y.; Surianarayanan, M., COMPREHENSIVE KINETIC MODEL FOR ADIABATIC DECOMPOSITION OF DI-TERT-BUTYL PEROXIDE USING BATCHCAD. *Industrial & Engineering Chemistry Research* **2003**, 42 (13), 2987-2995.

123. Raza, G. H.; Bella, J.; Segre, A. L.; Ferrando, A.; Goffredi, G., STRUCTURES AND NMR PARAMETERS OF 1,2-DIPHENYLCYCLOBUTANES. *Structural Chemistry* **1998**, *9* (6), 419-427.
124. Qureshi, Z. S.; Deshmukh, K. M.; Tambade, P. J.; Dhake, K. P.; Bhanage, B. M., AMBERLYST-15 IN IONIC LIQUID: AN EFFICIENT AND RECYCLABLE REAGENT FOR NUCLEOPHILIC SUBSTITUTION OF ALCOHOLS AND HYDROAMINATION OF ALKENES. *European Journal of Organic Chemistry* **2010**, (32), 6233-6238.
125. Zaitsev, B. A.; Kiseleva, R. F.; Denisov, V. M.; Koltsov, A. I., ACID-CATALYZED DIMERIZATION AND ARALKYLATION IN DIVINYLAROMATIC COMPOUND-AROMATIC SOLVENT SYSTEMS. *Bulletin of the Academy of Sciences of the Ussr Division of Chemical Science* **1990**, *39* (11), 2323-2330.
126. Bright, S. T.; Coxon, J. M.; Steel, P. J., REACTIONS OF 2-PHENYLETHYL AND 3-PHENYLPROPYL CARBINOLS WITH FLUOROSULFURIC ACID. *Journal of Organic Chemistry* **1990**, *55* (4), 1338-1344.
127. Tsukamoto, H.; Uchiyama, T.; Suzuki, T.; Kondo, Y., PALLADIUM(0)-CATALYZED DIRECT CROSS-COUPPLING REACTION OF ALLYLIC ALCOHOLS WITH ARYL- AND ALKENYLBORONIC ACIDS. *Organic & Biomolecular Chemistry* **2008**, *6* (16), 3005-3013.
128. Gourdet, B.; Lam, H. W., CATALYTIC ASYMMETRIC DIHYDROXYLATION OF ENAMIDES AND APPLICATION TO THE TOTAL SYNTHESIS OF (+)-TANIKOLIDE. *Angewandte Chemie-International Edition* **2010**, *49* (46), 8733-8737.
129. Grealis, J. P.; Mueller-Bunz, H.; Ortin, Y.; Condell, M.; Casey, M.; McGlinchey, M. J., BIRCH REDUCTION OF HEXAPHENYL- AND PENTAPHENYLBENZENE AND AN X-RAY CRYSTALLOGRAPHY AND NMR SPECTROSCOPY STUDY OF CIS- AND EPI-1,2,3,4,5,6-HEXAPHENYLCYCLOHEXANE AND OF 2,3,5,6-TETRAPHENYL-1,1'-BICYCLOHEXYLIDENE: CANNIZZARO'S CONUNDRUM REVISITED. *Chemistry-a European Journal* **2008**, *14* (5), 1552-1560.

130. Ma, Y., NITROXIDES IN MECHANISTIC STUDIES: AGEING OF GOLD NANOPARTICLES AND NITROXIDE TRANSFORMATION IN ACIDS. PhD Thesis, White Rose eTheses Online, **2010**.
131. Murayama, K.; Yoshioka, T., STUDIES ON STABLE FREE RADICALS .4. DECOMPOSITION OF STABLE NITROXIDE RADICALS. *The Bulletin of Chemical Society of Japan* **1969**, *42* (8), 2307-2309.
132. CO2 now, <http://co2now.org/current-co2/co2-now/> (accessed 24 March, 2014).
133. Lewis, J. K.; Wei, J.; Siuzdak, G. *ENCYCLOPEDIA OF ANALYTICAL CHEMISTRY* [ONLINE], [http://masspec.scripps.edu/publications/public\\_pdf/64\\_art.pdf](http://masspec.scripps.edu/publications/public_pdf/64_art.pdf), **2000**, p. 5880 – 5894.
134. Thomson, B.; Suddaby, K.; Rudin, A.; Lajoie, G., CHARACTERISATION OF LOW MOLECULAR WEIGHT POLYMERS USING MATRIX ASSISTED LASER DESORPTION TIME-OF-FLIGHT MASS SPECTROMETRY. *European Polymer Journal* **1996**, *32* (2), 239-256.
135. Montalbani, S., PYROLISIS-GAS CHROMATOGRAPHY-MASS SPECTROMETRY AND CHEMOMETRIC ANALYSIS FOR THE CHARACTERIZATION OF COMPLEX MATRICES. Ph.D Thesis, [http://amsdottorato.unibo.it/4559/1/Montalbani\\_Simona\\_tesi.pdf](http://amsdottorato.unibo.it/4559/1/Montalbani_Simona_tesi.pdf), **2012**.
136. Moad, G.; Rizzardo, E., ALKOXYAMINE-INITIATED LIVING RADICAL POLYMERIZATION: FACTORS AFFECTING ALKOXYAMINE HOMOLYSIS RATES. *Macromolecules* **1995**, *28* (26), 8722-8728.
137. Nicolas, J.; Guillaneuf, Y.; Lefay, C.; Bertin, D.; Gimes, D.; Charleux, B., NITROXIDE-MEDIATED POLYMERIZATION. *Progress in Polymer Science* **2013**, *38* (1), 63-235.
138. Bevington, J. C.; Hunt, B. J., EFFECTS OF NITROXIDES ON RADICAL POLYMERIZATIONS. *Journal of Macromolecular Science-Pure and Applied Chemistry* **2005**, *A42* (2), 203-210.

139. Loyns, C. R.; Rippon, D. E.; Phillips, E. INHIBITION OF POLYMERIZATION. European Patents 1937726 A1, **2008**.
140. Pavlovskaya, M. V.; Kolyakina, E. V.; Polyanskova, V. V.; Semenycheva, L. L.; Grishin, D. F., POLYMERIZATION OF STYRENE IN THE PRESENCE OF NITROXYL RADICALS GENERATED DIRECTLY IN THE COURSE OF THE POLYMER SYNTHESIS (IN SITU). *Russian Journal of Applied Chemistry* **2002**, *75* (11), 1868-1872.
141. Sciannamea, V.; Jerome, R.; Detrembleur, C., IN-SITU NITROXIDE-MEDIATED RADICAL POLYMERIZATION (NMP) PROCESSES: THEIR UNDERSTANDING AND OPTIMIZATION. *Chemical Reviews* **2008**, *108* (3), 1104-1126.
142. Nakatsuji, S.; Takai, A.; Nishikawa, K.; Morimoto, Y.; Yasuoka, N.; Suzuki, K.; Enoki, T.; Anzai, H., CT COMPLEXES BASED ON TEMPO RADICALS. *Journal of Materials Chemistry* **1999**, *9* (8), 1747-1754.
143. Spectrum Viewer 2.6, <http://www.phys.tue.nl/people/etimmerman/specview/> (accessed 16 December, 2010).
144. ACD/Labs, [http://www.acdlabs.com/resources/freeware/nmr\\_proc/](http://www.acdlabs.com/resources/freeware/nmr_proc/) (accessed 20 January, 2011).
145. Winter, R. A. E.; Ravichandran, R. ALKYLATED N,N-DIBENZYLHYDROXYLAMINES AND POLYOLEFIN COMPOSITIONS STABILIZED THEREWITH. United States Patent 4,703,073, **1987**.
146. Stetter, H.; Smulders, E., COMPOUNDS WITH UROTROPIN STRUCTURE .48. MONOFUNCTIONAL NITROGENOUS DERIVATIVES OF ADAMANTANE. *Chemische Berichte-Recueil* **1971**, *104* (3), 917-923.
147. Aschwanden, P.; Kvaerno, L.; Geisser, R. W.; Kleinbeck, F.; Carreira, E. M., REDUCTION OF 2,3-DIHYDROISOXAZOLES TO BETA-AMINO KETONES AND BETA-AMINO ALCOHOLS. *Organic Letters* **2005**, *7* (25), 5741-5742.

148. Beak, P.; Pfeifer, L. A., THE REACTION OF N-BUTYLLITHIUM WITH BENZOIC ACID: IS NUCLEOPHILIC ADDITION COMPETITIVE WITH DEPROTONATION? *Journal of Physical Organic Chemistry* **1997**, *10* (7), 537-541.
149. Yang, Y.-S.; Shen, Z.-L.; Loh, T.-P., INDIUM (ZINC)-COPPER-MEDIATED BARBIER-TYPE ALKYLATION REACTION OF NITRONES IN WATER: SYNTHESIS OF AMINES AND HYDROXYLAMINES. *Organic Letters* **2009**, *11* (6), 1209-1212.
150. Barluenga, J.; Rodriguez, M. A.; Campos, P. J.; Asensio, G., A GENERAL AND USEFUL COPPER(II)-PROMOTED IODOFUNCTIONALIZATION OF UNSATURATED SYSTEMS. *Journal of the Chemical Society-Chemical Communications* **1987**, (19), 1491-1492.
151. Franco, S.; Merchan, F. L.; Merino, P.; Tejero, T., AN IMPROVED SYNTHESIS OF KETONITRONES. *Synthetic Communications* **1995**, *25* (15), 2275-2284.
152. Pfeiffer, J. Y.; Beauchemin, A. M., SIMPLE REACTION CONDITIONS FOR THE FORMATION OF KETONITRONES FROM KETONES AND HYDROXYLAMINES. *Journal of Organic Chemistry* **2009**, *74* (21), 8381-8383.
153. Moussa, I. A.; Banister, S. D.; Beinat, C.; Giboureau, N.; Reynolds, A. J.; Kassiou, M., Design, SYNTHESIS, AND STRUCTURE-AFFINITY RELATIONSHIPS OF REGIOISOMERIC N-BENZYL ALKYL ETHER PIPERAZINE DERIVATIVES AS SIGMA-1 RECEPTOR LIGANDS. *Journal of Medicinal Chemistry* **2010**, *53* (16), 6228-6239.
154. Chung, J. Y. L.; Mancheno, D.; Dormer, P. G.; Variankaval, N.; Ball, R. G.; Tsou, N. N., DIASTEREOSELECTIVE FRIEDEL-CRAFTS ALKYLATION OF INDOLES WITH CHIRAL (ALPHA-PHENYL BENZYLIC CATIONS. ASYMMETRIC SYNTHESIS OF ANTI-1,1,2-TRIARYLALKANES. *Organic Letters* **2008**, *10* (14), 3037-3040.